THE HYDROGEOCHEMISTRY OF A SALINE AQUIFER SYSTEM:

CENTRAL NEW SOUTH WALES, AUSTRALIA

A Thesis Submitted for the Degree of Doctor of Philosophy
of the Australian National University

by
Matthew James Lenahan
B.Sc.

Research School of Earth Sciences
&
Cooperative Research Centre for
Landscape Environments and Mineral Exploration

STATEMENT

I declare that, to the best of my knowledge, the work described in this thesis is original, except where due reference is made in the text, and has not been used toward the award of any other degree at any other institution.

Matthew James Lenahan

ACKNOWLEDGEMENTS

I wish to express sincere gratitude to Dr Bear McPhail and Dr Dirk Kirste for their guidance, support and patience throughout this project. I would also like to acknowledge Dr Sue Welch for her personal and academic guidance throughout my entire candidature. I extend my sincerest appreciation to Dr. Keith Fifield, Dr. Tim Barrows, Dr. Richard Cresswell and Dr. K.P. Tan for their charitable collaboration and intellectual contributions.

The Cooperative Research Centre for Landscape Environments and Mineral Exploration is gratefully acknowledged for their financial support and project funding essential to the success of this work.

I would like to especially recognize the significant contributions of Sarah O'Callaghan, Maree Coldrick, Linda McMorrow, Nigel Craddy, Brian Harold, Andy Kristie and John Spring. The accomplishments of this project owe themselves to their expertise, goodwill and excellent humour.

Special thanks to my officemates Julie Brown, Kat Fitzsimmons, Alistair Usher, Luke Wallace, Dan Wilkins, Jeremy Wykes, and Kamal Khider for their friendship and support over the past four years.

Thank you to my wonderful family for understanding the commitment required by this degree. Your love and support have been with me all the way. Thank you also to the Mikkelson family for their encouragement, love and support.

The greatest contributions to the completion of this thesis have been made by my wonderful Coalie. Her patience, understanding and sacrifices are on every page of this thesis. I owe my health, my sanity and my love to her.

ABSTRACT

Within many semi-arid regions throughout the world, secondary salinization of groundwater and surface water represents a serious environmental threat to freshwater resources. However, there exists a limited knowledge of solute dynamics in these environments, in particular subsurface solute distributions and mobility. The origin, nature and mobility of solutes were determined for 25x25 km catchment area in central New South Wales through combined hydrogeological and hydrogeochemical techniques to better understand physiochemical processes occurring in the both the unsaturated and saturate zones of saline environments. This thesis aims to address the knowledge gaps in the current understanding of the nature and mobility of solutes in the subsurface environment. At present there is a lack of understanding of (a) the processes that change the relative solute proportions in rainwater to groundwater, (b) the timeframes of solute accumulation in the unsaturated zone and saturated zones, and (c) the nature and mobility of subsurface solute stores.

Chloride concentrations of 155 unsaturated zone soil pore water solutions from four locations indicate long-term (>200,000 yrs) meteoric deposition and evapotranspiration as the dominant solute concentrating mechanism. However, meteoric water exhibits considerably different chemical and isotopic compositions compared to groundwater. Nutrient cycling is the dominant process controlling the K/Cl, Ca/Cl, Mg/Cl and NO_3/Cl ratios during vertical infiltration of rainwater through the unsaturated zone. Minor variations in Na/Cl and N/Ca ratios are the result of cation exchange. Biogeochemical processes, in particular organic adsorption and bioassimilation, influence the Br/Cl and SO_4/Cl ratios. Results from this study suggest

the commonly observed discrepancies between local meteoric water and groundwater compositions in semi-arid regions are the result of geochemical and biogeochemical processes occurring in the near surface of the unsaturated zone.

$^{36}Cl/Cl$ ratios and Cl^- and Br^- concentrations of unsaturated zone soil pore waters indicate long-term ^{36}Cl and Cl^- deposition rates, groundwater recharge rates and solute mobility in the unsaturated zone. A ~200,000 yr isotopic decay profile indicates a lack of groundwater recharge in the distal portion of the catchment. Cl^- mass balance calculations for the ^{36}Cl decay profile suggest that present day meteoric deposition of Cl^- is similar to the long-term average. At a second location, the presence of "bomb-pulse" ^{36}Cl in saline (Cl > 2,400 mg/l) pore waters at 4 metres depth indicate a high degree of vertical solute mobility proximal to the recharge zone. Furthermore, $^{36}Cl/Cl$ ratios of near surface (< 1m) pore waters appear to reflect long term (10^3 yrs) $^{36}Cl/Cl$ ratios of meteoric water. These ratios ($150\text{-}160 \times 10^{-15}$) are less than half compared to modern meteoric water.

High resolution pore water geochemical results from two diamond cores indicate highly heterogeneous saturated zone solute distributions. Pore waters within the aquifer and surrounding units exhibit greater salinity, lower $^{36}Cl/Cl$ ratios and unique element/chloride ratios compared to groundwater. Chemical and isotopic end member compositions were determined for pore water and groundwater and were incorporated into numerical models. Modelled solute and ^{36}Cl mixing trends were in good agreement with measured trends in groundwater composition. Decreases in $^{36}Cl/Cl$ ratios and increases in Cl^- concentrations along the flow path are primarily the result of mixing between older more saline pore water and younger less saline groundwater.

Flow ages corrected for "age mixing" are 50,000-75,000 years compared to uncorrected "mixed ages" of 237,000-265,000 years. The corrected flow ages were in better agreement with the hydrodynamic flow age of 65,000 years.

1 INTRODUCTION

Fundamental changes in the chemical composition of meteoric water occur during infiltration of near-surface sediments that impact freshwater resources around the world. In many arid and semi-arid regions, low annual precipitation, high degrees of evapotranspiration and low vertical infiltration rates often result in elevated solute concentrations in groundwater (i.e. Eriksson and Khunakasem 1969, Peck, 1978; . Edmunds and Wright, 1979; Thomas et al., 1989; Scanlon et al., 1991, Love et al., 1993; Zhu et al., 2003, Ewing et al., 2006). Throughout semi-arid Australia, the widespread occurrence of dryland salinity is well documented yet the nature and mobility of solutes are poorly understood. Meteoric water is often considered the dominant solute source and evapotranspiration the dominant solute concentrating mechanism (i.e., Herczeg et al., 1993; Love et al, 1993; Herczeg et al., 2001; Cartwright and Weaver, 2005; Cartwright et al., 2006). Theoretically, evapotranspiration does not change the relative solute proportions, yet groundwater typically exhibit different element ratios than its source (atmospheric precipitation). This is generally assumed to be the result unsaturated zone geochemical processes such as evaporite mineral dissolution/precipitation, cation exchange and mineral weathering (Gibbs, 1970; Love et al., 2000; Herczeg et al., 2001; Davis et al., 2004; Cartwright et al., 2006). However, most unsaturated zone studies have focused on understanding infiltration rates (i.e., Eriksson and Khunakasem, 1969; Allison and Hughes, 1978; Peck et al., 1981; Allison and Hughes, 1983; Scanlon, 1991; Wood, 1999), the timeframes of solute accumulation (Allison et al., 1985; Cook et al., 1992; Zhu et al., 2003) and on determining the effects of evapotranspiration (i.e., Peck et al.,

1981; Ullman, 1985; Johnston, 1987; Cartwright et al., 2006). These findings are based on interpretations of Cl^- and various stable and radiogenic isotope profiles. Little to no studies have performed detailed measurements of major element compositions through the entire unsaturated zone to convincingly document the processes responsible for the different element ratios measured in precipitation compared to groundwater.

Numerous studies within Australia (i.e., Macumber, 1969; Gunn and Richardson, 1979; Johnston et al., 1980; Johnston and McArthur, 1981; Mazor and George, 1992) have associated the occurrence of unsaturated zone solute "stores" with low-lying, highly weathered landscapes. In the majority of these areas, the solutes tend to be concentrated within the root zone or within low permeability clay-rich units and are regarded as immobile (Macumber, 1969; Peck, 1978; Johnston et al., 1983; Johnston, 1987). However, considering the timeframes available for solute accumulations in arid to semi-arid landscapes, far greater concentrations are expected if these solutes were progressively stored within basins over time. It is well documented that clearing of native vegetation and subsequent alteration to the hydraulic budget has resulted in the mobilization of solutes previously accumulated in the unsaturated zone (Peck and Hurle, 1973; Dimmock et al., 1974; Peck, 1978). The ratio of solute exports from catchments to solute inputs from the atmosphere was presented as a means for estimating the effects of secondary salinization by Peck and Hurle (1973). Ratios greater than 1:1 and as high as 17:1 were encountered by Peck and Hurle (1973), Evans (1994), Jolly et al. (1997) and Jolly et al. (2001), and were attributed to mobilization of unsaturated zone salt stores due to anthropogenic alternations to the hydrologic budgets of catchments in Australia. However, this concept assumes that

solutes accumulate in the unsaturated zone only by evapotranspiration and have equal mobility. The role of plants in accumulating growth limiting solutes in near-surface soils has been well documented by ecologists and biological researchers (i.e., Johnson, 1984; Foulds, 1993; Jobaggy and Jackson, 2001). Biogeochemical processes such as bioassimilation and organic adsorption can also have a large impact on solute mobility in near-surface soils (i.e. Kreitler and Jones, 1975; Boring et al., 1988; Mayer et al., 1995a; Novak et al., 2003). The significance of bio-accumulated solute stores and their potential for anthropogenic mobilization has been given very little attention by groundwater researchers (i.e. Kreitler and Jones, 1975, Gerritse and George 1988). Mass-balance calculations based on rainwater and groundwater chemistry that aim to quantify catchment solute budgets fail to account for these solute sources and sinks.

Cl- is the most conservative tracer in aqueous systems and is often used as a proxy for salinity (Herczeg and Edmunds, 2000). Simpson and Herczeg (1991) noted 2.6-4.1 times greater Cl^- is being exported from the Murray-Darling Basin than is contributed from atmospheric precipitation. This imbalance was attributed to the mobilization of unsaturated zone solutes by infiltrating irrigation water and rising groundwater tables following land clearance. Recently, Cartwright et al., 2007 demonstrated that increased recharge does not result in a rapid flushing of solutes from aquifer systems in the Murray Basin, Victoria. Recharge rates based on Cl^- mass balance calculations were up to two orders of magnitude lower than estimated from ^3H and ^{14}C reflecting the complexity of solute mobility in semi-arid areas. The authors explained that despite more than 100 years since land clearance in Northern Victoria, older saline waters are still residing in low permeability clay sediments. Despite increased

recharge, the solute stores are only slowly mobilized by the rising groundwater tables. Despite this widely documented process of secondary salinization, very few studies have interpreted unsaturated zone solute concentrations other than Cl^- to better understand the physiochemical processes occurring during vertical infiltration of meteoric water and to better understand the nature of solute stores in the unsaturated zone..

Most studies conducted in semi-arid regions of Australia have utilized Cl^- concentration and/or electrical conductivity of soil pore water and groundwater to evaluate the mechanisms contributing to groundwater salinity (e.g., Johnston, 1981; Peck et al., 1981; Simpson and Herczeg, 1994; Herczeg et al., 2001; Cartwright et al., 2004; Cartwright et al., 2006). However, the typically conservative nature of the chloride ion limits its application towards understanding geochemical and biogeochemical processes such as mineral weathering, cation exchange, bioassimilation, and nutrient cycling. These processes may have a significant influence on past and present unsaturated zone solute dynamics and exhibit considerable control on the chemical composition of regional groundwater. Furthermore, numerous hydrogeological studies have measured radiogenic tritium and chlorine-36 distributions in the unsaturated zone to understand unsaturated zone flow regimes and groundwater recharge rates (Allison et al., 1971; Allison and Hughes, 1972; Allison and Hughes, 1974; Allison and Hughes, 1978; Allison and Hughes, 1983; Walker et al., 1992; Cook et al., 1994). Measurement of major and minor element concentrations as well as radiogenic isotopes of unsaturated zone soil pore water may provide insight into past and present solute sources, timeframes of accumulation and solute mobility.

Salinity studies in Australia and overseas have traditionally considered the unsaturated zone as the dominant salt store within semi-arid landscapes (e.g., Salama et al., 1999). Less attention has been focused on saturated zone salt stores residing in lower permeable units in aquifer systems. Ortega-Guerrero et al. (1997), Timms et al. (2001), and Peck and Hatton (2003) considered isotopic and hydrochemical properties of both aquitard pore waters and aquifer groundwaters and noted appreciable degrees of mixing between the two. In the well studied Milk River Aquifer in Canada and The Great Artesian Basin in Australia, Domenico and Robbins (1985) Bentley et al. (1986) Phillips et al. (1986) and Love et al. (2000) noted higher salinity waters residing in lower permeability hydrogeologic units and attributed changes in chemical composition of groundwaters along the flow paths to mixing between the chemically heterogeneous hydrogeologic units. However, very few hydrogeochemical studies throughout the world have measured high resolution geochemical profiles of waters residing in both high and low permeability units within heterogenous aquifer systems (i.e., Ortega-Guerrero et al., 1997; Hendry and Wassenaar, 1999; Hendry and Wassenaar, 2000; Degueldre et al., 2003; Hendry et al., 2004). Considering the documented evidence within Australia (above) of higher salinity waters residing in low permeability, highly weathered regolith materials, the impact of mixing between saline pore waters and groundwater may have a significant influence on the quality of surface water and groundwater. Furthermore, flow-related mixing processes may also impact the isotopic composition of groundwater and limit the interpretive capacity of stable and radiogenic isotope data in hydrogeochemical studies. These mixing processes have been particularly problematic for ^{36}Cl-based age assessments of regional groundwater studies (i.e., Bentley et al., 1986; Phillips et al., 1986; Hendry

and Schwartz, 1988; Fabryka-Martin et al., 1991; Torgersen et al., 1991; Love et al., 2000). This study presents a detailed assessment of the chemical and isotopic composition of saturated and unsaturated zone pore fluids and groundwater in order to assess geochemical and biogeochemical processes and for understanding solute sources, mobility, and transport timeframes in the context of groundwater salinity. A thorough evaluation of the origins, nature and mobility of salt stores in one study area could prove useful for understanding the nature of other salt-affected landscapes throughout the Murray Darling Basin and other semi-arid regions of Australia.

This investigation is focused on the well studied Barmedman Creek catchment area within the Bland basin of central New South Wales.. The Barmedman Creek catchment is chosen because it is representative of low-lying, salinized landscapes in the Murray-Darling Basin, and because of an extensive physical and chemical database as a result of previous studies of the GILMORE project (i.e. Phillips et al., 2002). The GILMORE study was a multi-disciplinary approach towards quantifying the physical characteristics and subsurface distribution of regolith materials and their relationship to the distributions of subsurface salt stores (i.e. Lawrie et al., 2000). Furthermore, as a result of the GILMORE project, access to a network of permanent piezometers was available for sampling of groundwater within the Barmedman Creek catchment in the south-western portion of the Bland Basin (Figure 1.2). In addition, a comprehensive hydrogeochemical investigation was carried out for the Bland Basin (Carrara, 2005) to understand processes controlling groundwater flow and groundwater quality. Carrara (2005) sampled groundwater from bores regulated by the New South Wales Department of Infrastructure Planning and Natural Resources located to the east of Barmedman Creek Catchment. This study provides an

opportunity to compare and contrast the physical and chemical controls on groundwater quality in a small sub-catchment (25km x 25km) of the larger Bland Catchment studied by Carrara (2005). The aims of this study are to understand the

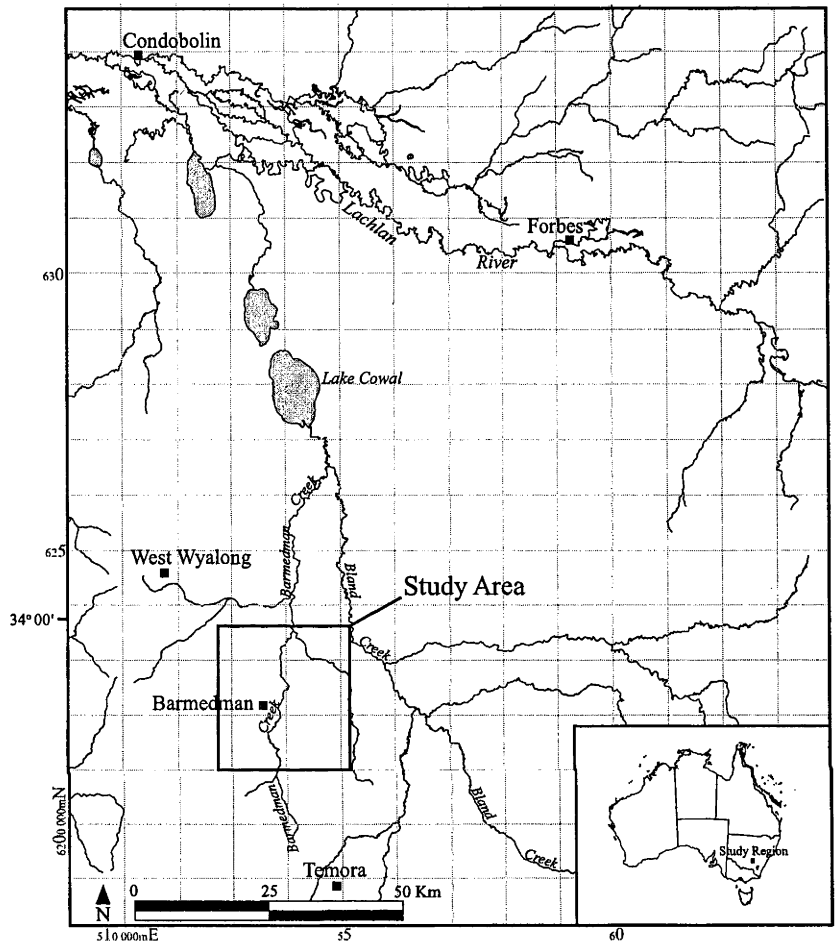

Figure 1.1: Location of study area within the Bland Basin, central New South Wales (NSW), Australia. Adapted from Forbes, NSW and Cootamundra, NSW 1:250 000 map sheets (courtesy Geoscience Australia).

mechanisms controlling the evolution of groundwater from a fresh rainwater source to salinity values approaching that of seawater, and to assess the mobility of solutes in a highly variable regolith stratigraphy. This study aims to provide additional insights into the physiochemical processes in saline semi-arid catchments that are beneficial to both the scientific community and land management authorities. The study will first consider differences in the chemical composition, stable isotopic composition, and radiogenic isotopic composition of rainwater, pore waters, and groundwater, and their

relationship to the physical and chemical characteristics of the regolith. The study will assess the mobility of solutes in the regolith by considering spatial variations ingroundwater Cl^-, Br^- and SO_4^{2-} concentrations and by interpreting pore fluid compositions from two diamond core holes. In addition to the chemical composition of pore waters from the two diamond cores, 4 shallow (< 3 m) push cores were completed within the unsaturated zone and pore water was extracted at 2 cm intervals to understand the geochemical and biogeochemical processes occurring during groundwater recharge. Finally the origin, age and mobility of solutes will be further considered via cosmogenic chlorine-36 compositions of unsaturated and saturated zone pore waters and groundwater.

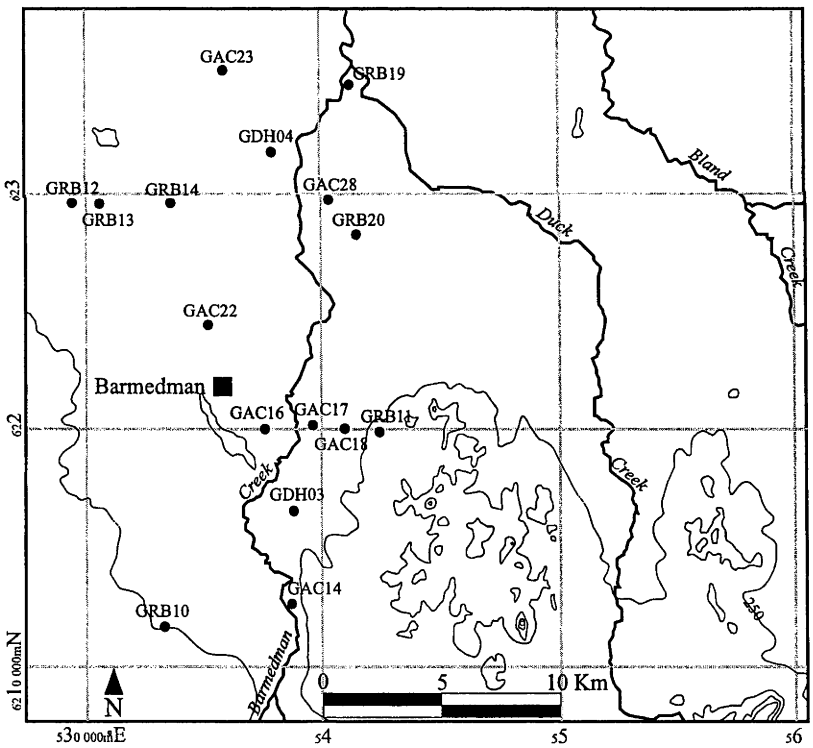

Figure 1.2: Permanent piezometer locations within the Barmedman Creek catchment of the Bland Basin. Adapted from Cootamundra 1:250 000 map sheet. (Contour interval = 50 m)

Despite the many studies published already, the processes that affect the origin, nature and mobility of solutes in low-lying semi-arid landscapes are not well understood. Without this understanding, scientists are limited in interpreting existing hydrogeochemical data, and in developing effective management strategies for remediation and land management.

The objective of this thesis is to contribute to the scientific understanding of subsurface solute sources and dynamics in salinized landscapes. The body of the thesis presents and discusses the chemical and isotopic compositions of saturated and unsaturated zone pore waters and groundwater from a heterogeneous aquifer system that hosts highly saline groundwater. The methods, results and interpretations are presented as three chapters (Chapters 3-5) in manuscript format. These chapters are written in manuscript format to ease preparation of journal submission. Chapter 3 presents chemical and isotopic compositions of pore water and groundwater and discusses saturated zone hydrogeochemical processes. Chapters 4 and 5 present chemical and isotopic compositions of unsaturated zone pore waters and discuss geochemical and biogeochemical processes occurring during groundwater recharge and their influences on the chemical composition of regional groundwater.

2 HYDROGEOCHEMICAL BACKGROUND OF GROUNDWATER SALINITY

2.0 Introduction

Numerous studies have focused on identifying the origins of solutes (i.e., Gunn and Richardson, 1979; Turner et al., 1987; Jones et al., 1994; Herczeg et al., 2001; Cartwright et al., 2004, Cartwright et al., 2007b) and the distribution and mobility of solutes in landscapes of various climates, geographic settings and land usages in Australian (i.e., Dimmock et al., 1974; Peck et al., 1981; Johnston, 1987a; Timms et al., 2001).

Mineral weathering can play an important role in the geochemical evolution of groundwater (i.e. Gunn and Richardson, 1979; Gunn, 1985; Salama et al., 1999; Harrington and Herczeg, 2003; Cartwright et al.,,2004). Salama et al. (1993) attributed the increased concentration of solutes below the root zone, where evapotranspiration was considered negligible, to the loss of water through chemical weathering reactions. Other studies evaluated the contributions of cyclic solutes to soil and water salinization throughout Australia (i.e. Hingston and Gailitis, 1976; Blackburn and McLeod, 1983; Simpson and Herczeg, 1994). Most studies have focused almost entirely on understanding the sources and nature of solutes and how rising groundwater tables have mobilized unsaturated zone solute stores. Little work has been done towards understanding saturated zone solute stores and their mobility.. A greater understanding is needed of the the timeframes of solute accumulation and the geochemical processes controlling subsurface distributions and mobility in semi-

greater depths in the profile, which the authors concluded was the result of downward leaching of the salt stored in the near surface soils prior to clearing of native vegetation. The effects of evapotranspiration on the chemical composition of groundwater in the Otway Basin, Australia were discussed by Love et al. (1993), where they noted near linear increases of SO_4, Na^+ and Mg^{2+} concentrations with increasing Cl^- concentrations. They concluded that evapotranspiration of rainwater in the unsaturated zone was responsible for the observed ion concentration trends. Ca/Cl, K/Cl and HCO_3/Cl ratios verses Cl^- plots showed more scatter which was attributed to ion exchange and calcite precipitation. In an attempt to differentiate the individual contributions of evaporation and transpiration, Love et al. (1993) considered deuterium with respect to Cl^- concentration of groundwater. A poor correlation between deuterium composition and Cl^- concentration of groundwaters led the authors to conclude that mixing of different end member waters subjected to varying degrees of evaporation and transpiration was occurring during groundwater recharge.

Turner et al. (1987) noted relatively constant values of stable isotopic compositions with increases in Cl^- concentration in groundwater sampled from highly weathered regolith material in southwest Western Australia. Based on the lack of isotopic enrichment with increasing salinity, transpiration rather than evaporation was determined as the dominant solute concentrating mechanism responsible for the measured solute concentrations in groundwater. Zimmerman et al. (1967) measured the effects of evaporation on deuterium profiles in soil profiles of constant soil moisture and steady atmospheric conditions in central Europe. The authors concluded that the rate of downward diffusion of deuterium is equal to the rate of upward evaporative flux. As a result, the observed penetration depth of deuterium-enriched

water was inversely proportional to the rate of evaporation. Although the effects of infiltration of rainwater on the stable isotope depth profile were not considered, the experiments demonstrated the depths to which evaporation is likely to occur under specific soil and atmospheric conditions. Allison and Hughes (1983) considered the depth profiles of ^{18}O and deuterium composition of soil water in a semi-arid area of southern Australia and noted isotopic enrichment trends similar to Zimmerman et al. (1967). Allison and Hughes (1983) determined that evaporation was responsible for the observed isotopic enrichment in the near surface, and depth of enrichment was dependent on the rate of evaporation. The evidence from stable isotopes of water (discussed above) indicates evapotranspiration is a dominant process in the unsaturated zone and would have a large influence on solute dynamics in semiarid areas of Australia.

2.1.2 Climate and Topography

Within Australia, subsurface solute concentrations exhibit inverse relationships to annual precipitation (i.e. Dimmock et al., 1974; Johnston and McArthur, 1981; Turner et al., 1987) and subsurface solute distributions are related to landscape morphology (i.e. Dimmock et al., 1974; Johnston et al., 1980; Johnston and McArthur, 1981; Gunn, 1985). In the Darling Range of southwest Australia, low rainfall (<800 mm/yr) catchment areas exhibited subsurface salt stores up to 5 times greater than in higher rainfall (>1000 mm/yr) catchments (Dimmock et al., 1974). They also noted the depth of peak solute concentrations was dependent on the topographic position, where peak salinity was encountered towards the bottom of profiles (~10 m) in upper landscapes and more towards the surface (~6 m) in lower landscapes. The distribution of Cl^- in soil profiles and its relationship to landscape position was further investigated by

Johnston et al. (1980). Two profile types were described; a bulge profile and a monotonic profile. Bulge profiles were characterized by a rapid increase in salinity with the maximum value at intermediate depths, followed by a marked decrease in concentration at deeper levels. The monotonic profiles were defined as those which exhibited a near linear increase in salinity to a specific depth, underneath which there were relatively uniform values. Bulge profiles correlated with lower landscape positions and exhibited unsaturated zone solute concentrations significantly greater than other topographic positions. The monotonic profiles were encountered in upper landscape positions, and in areas of higher rainfall. Johnston (1981) noted similar relationships and described locations of peak salinity in soil profiles with respect unsaturated and saturated zones salt stores. In low rainfall areas, the greatest salinity values were located within the unsaturated zone, whereas in high rainfall areas, the peak salinities were located in the saturated zone. This was attributed by Johnston (1981) to lower infiltration rates and greater degrees of evapotranspiration occurring in areas of lower rainfall.

2.1.3 Cyclic Salts

Cyclic salts are widely considered as marine sourced solutes deposited within landscapes that can be remobilized by physical and chemical weathering processes. Cyclic salts have been attributed to the occurrence of dryland salinity development throughout Australia (i.e. Blackburn and McLeod, 1983; Herczeg et al., 1993; Simpson and Herczeg, 1994; Jolly et al., 1997; Herczeg et al., 2001). Blackburn and McLeod (1983) and Simpson and Herczeg (1994) used the bulk composition and various ion ratios of rainwater to estimate the contributions of continental dust and marine aerosols to the accumulation of solutes in Australian landscapes. The studies

arid areas of Australia to better manage the risk of secondary salinization of soil and water.

2.1 Salinization Mechanisms

Solutes have been accumulating in the Australian regolith for extremely long periods of time and saline land and water are natural features of semi-arid to arid regions around the world (i.e. Allison et al., 1985, Cook et al., 1992, Tyler et al., 1996, Cartwright et al., 2007a), Salinisation of land and water results from changes in the hydrologic budget that mobilize solutes in soil and water (i.e. Salama et al., 1999). The occurrence of dryland salinity in Australia has been associated with factors such as climate, landscape, geology, mineral weathering, soil processes, hydrology, evapotranspiration, cyclic solutes, and land use. The specific mechanisms and chemical reactions related to these factors are considered individually below to assess comprehensively the origin, nature and mobility of solutes in semi-arid landscapes.

2.1.1 Evapotranspiration

More than half of all rainfall that reaches the earth's surface is returned to the atmosphere by evaporation or transpiration by plants (Drever, 1997). Within Australia, the Murray Basin experiences a mean annual loss of 90-95 vol. % of initial precipitation volume due to evapotranspiration (Simpson and Herczeg, 1991). The effects of transpiration on the concentration of solutes in the unsaturated zone were observed by Cook et al. (1989), as a marked increase in Cl^- concentration within the top 2 m of numerous soil profiles beneath mallee vegetation in the western Murray Basin. In adjacent cleared land, the peak in Cl^- concentration was encountered at

found that cyclic salts could account for up to half of the total salt deposition in the Murray-Darling Basin. Chivas et al. (1991) measured the sulfur isotopic composition of rainwater, groundwater and sulfate minerals within sediments and determined that up to 55% of sulfate in shallow saline groundwater and playa lakes in various inland areas throughout Australia consisted of marine derived cyclic salts. Based on the chemical composition of shallow saline groundwater sampled in southwest New South Wales (Murray Basin) Jones et al. (1994) determined marine-derived aerosols are the dominant source of dissolved solutes. The marine-like chemical composition and meteoric isotopic composition led Jones et al. (1994) to conclude that leaching of cyclic solutes by infiltrating rainwater was the mechanism by which the solutes were mobilized.

2.1.4 Geology and Mineral Weathering

Water-rock interactions can have a significant control on the chemical composition of groundwater and also represent a dominant source of solutes in low salinity systems (i.e. Appelo and Postma, 1993; Drever, 1997; Cartwright et al., 2004). Salama et al. (1999) proposed that mineral dissolution was a dominant process contributing solutes to groundwater in arid/semiarid areas. Gunn (1985) noted variations in groundwater composition that corresponded to variations in lithology of the underlying, weathered *in situ* regolith. The authors from both studies noted greater salinity values in groundwater in contact with highly weathered igneous and metamorphic rocks relative to weathered sedimentary rocks. Furthermore, salt-affected soils were only encountered in areas overlying weathered bedrock, despite the presence of a thick C horizons in areas overlying unweathered bedrock. These observations led the authors to conclude that mineral weathering was a significant solute source to soil water and

groundwater. More recently mineral weathering has been identified as only a minor source of solutes to groundwater systems and evidence for these processes can only be detected with major element chemistry of low salinity groundwater samples (i.e. Herczeg et al., 2001; Harrington and Herczeg, 2003; Cartwright et al., 2004, 2005, 2006, 2007b).

Surface water samples collected from the River Murray that exhibited element to chloride ratios in excess of those expected from marine derived aerosols were associated by Herczeg et al. (1993) to mineral weathering. They determined that mineral weathering was responsible for up to 98 wt. % of HCO_3-, 80 wt. % Ca, 35 wt. % K, 25 wt. % SO_4^{2-} and 20 wt. % of the Mg present in the River Murray and its tributaries. However, because the surface and groundwater samples were dominated by marine sourced Na and Cl, the authors concluded that contributions of cyclic solutes dominated those from mineral weathering reactions. Based on HCO_3^-/Cl^- ratios of groundwater from the Murray Basin, Herczeg et al. (2001) determined that < wt. 20% of total solutes present are the result of mineral weathering.

Salt output/input ratios were utilized by Peck and Hurle (1973) to evaluate the effects of land clearance on chloride balances within several catchments in southwest Western Australia. The study revealed that land cleared of vegetation exported up to 20 times more Cl/hectare than was being introduced by rainfall. The authors concluded that leaching of solutes by rising groundwater tables was responsible for the large output/input ratio.

The influence of cation exchange, silicate weathering and clay formation on groundwater composition in the Great Artesian Basin (GAB) was evaluated by (Herczeg et al., 2001). They discussed mineral weathering and exchange mechanisms responsible for $NaHCO_3$ waters in the GAB. Groundwaters were found to be in equilibrium with kaolinite-smectite minerals. Based on geochemical modelling results, the authors attributed measured concentrations of Na and HCO_3 to carbonate dissolution, cation exchange and conversion of kaolinite to Na-smectite.

2.1.5 Soil Processes

Physical and chemical reactions between natural waters and host soil media such as cation exchange and adsorption can play a significant role in controlling the chemical composition of surface water, soil water and groundwater. The role of ion exchange on the chemical composition of waters of various salinity values was investigated by Arad and Evans (1987). In this study the authors attributed measured variations in Na and Ca concentrations in low salinity waters to the exchange of Ca in groundwater for Na occupying the interlayer exchange sites on 2:1 clays. The authors found that Na was exchanged for Ca in higher salinity waters with Na concentrations in excess of 30 meq/L. Cartwright et al., 2007b indicated that cation exchange can be an important process controlling $^{87}Sr/^{86}Sr$ ratios in groundwater, however the authors highlighted that this process had only a minor impact on major element chemistry along the flow path. Berry (1969) described cation and anion exchange as a process whereby ions were selectively adsorbed to the interlayer exchange sites on clays and thus removed or filtered from solution. The author presented an adsorption sequence for halogens where Cl^- was preferentially adsorbed with respect to Br^-, which was preferentially adsorbed over I^-. Gunn (1985) sited this preferential adsorption process as a potential mechanism contributing to the elevated Cl^- levels observed in clay-rich pallid zones in

southern New South Wales. Preferential retention of SO_4^{2-} relative to Cl^- was demonstrated experimentally by Yaalon (1965) and was attributed to interactions with the soil materials. Mayer et al. (2001) conducted field experiments which irrigated various soil types with applied SO_4 tracers and noted that greater than 80 % of the applied SO_4^{2-} was retained within the soil matter. The total retention of SO_4^{2-} correlated with increasing sesquioxides content of soils and the authors concluded that adsorption onto mineral surfaces was the dominant sink for inorganic sulphate. Seaman et al. (1996) demonstrated the anion sorption capacity of iron oxide coated sediments by eluting columns of predominantly sandy materials with a range of Br^- solutions under different pH conditions. The authors found the degree of Br^- retardation correlated better with iron oxide content of sediments than with pH. Gerritse and George (1988) attributed low Br/Cl ratios relative to meteoric input in near surface soil water to biogeochemical processes and the preferential uptake of Br^- by vegetation. The authors experimentally demonstrated the sorption capacity of organic materials in sediments containing relatively low (2-7 wt. %) organic carbon. The authors proposed that oxidation of near-surface organic materials could produce elevated Br/Cl ratios in groundwater. A similar theory was proposed by Kreitler and Jones (1975), where elevated NO_3^- levels in groundwater were attributed to the oxidation of naturally occurring soil nitrate following cultivation.

2.1.6 Biogeochemical Processes and Nutrient Cycling

Solute distributions in the near surface of the unsaturated zone are often influenced by biogeochemical processes. Bioassimilation of inorganic carbon, nitrogen, sulphur and phosphorus can act as a significant sink for these elements during infiltration of rainwater through near surface sediments (i.e., McGill and Cole, 1981; Johnson, 1984;

Boring et al., 1988; Mayer et al., 1995a; Mayer et al., 1995b; Mayer et al., 2001; Novak et al., 2003; Walvoord et al., 2003). Nutrient cycling by plants can also influence unsaturated zone solute dynamics (i.e., Foulds, 1993; Jobaggy and Jackson, 2001; White et al., 2006). Little attention has been focused on the effects of biogeochemical processes and nutrient cycling on the chemical composition of regional groundwater. Kreitler and Jones (1975) and Walvoord et al. (2003) highlighted the importance of biogeochemical processes with regard to nitrogen and Mayer et al. (1995b) pointed out the importance of soil microbial processes on influencing the stable isotopic ratios of sulphur and oxygen. The effects of nutrient cycling by plants on the cation composition of groundwater have only been recently highlighted by studies in Victoria, Australia (Edwards and Webb, 2006) and in California, USA (White et al., 2006).

2.1.7 Hydrology

Unsaturated zone

Advective transport was described by Johnston et al. (1980) as the primary factor affecting the distribution of soluble solutes in soils. When considering numerous Cl^- depth profiles in soils from southwest WA, Johnston et al. (1980) associated vertical zones of uniform solute concentrations with the location of the saturated zone. Rates of recharge and preferred flow paths through lateritic soil profiles were investigated by Johnston et al. (1983). Use of fluorescent dye tracer allowed the authors to observe the vertical extent of recharge and the pathways of flow through soils of varying physical properties. The authors observed near uniform infiltration and distribution of the tracer dye in coarser grained material while in clay-rich saprolite materials, the movement of water was confined to vertical channels of coarser grained materials that

were associated with the presence tree roots. The vertical root channels were described to consist of live to variably decomposed roots surrounded by a highly permeable quartz rich material. The authors noted low permeability, unsaturated material present at the margins of the vertical channels. Minor lateral diffusion of the dye into the surrounding clay rich material was observed. The authors highlighted the significance of vertical channels for recharge of rainwater to near surface aquifers and subsequent connectivity with deeper confined aquifers.

Anthropogenic radiogenic isotopes have also been utilized as hydrogeochemical tracers to understand flow behaviour in the unsaturated zone, in particular, tritium and chlorine-36. The potential applications of radioisotopes generated from nuclear weapons testing as tracers in hydrogeologic studies were first demonstrated through measurements of tritium in spring water, well water and river water by Begemann and Libby (1957). The study was the first to recognize bomb pulse tritium in northern hemisphere rainwater in 1954. In the United States, Schmalz and Polzer (1969) used bomb-tritium measurements of unsaturated zone soil water to estimate groundwater recharge rates. Within Australia, tritium concentrations of rainwater and wine were measured to determine tritium fallout between 1950 and 1974 (Allison et al., 1971; Allison and Hughes, 1977). It was found that the peak in bomb-tritium fallout occurred from 1965-1966, which was represented by an order of magnitude greater tritium concentration in rainfall than natural background levels. This is in contrast to a three orders of magnitude peak in northern hemisphere fallout, which occurred from 1962-1963. Applying the known history of bomb-tritium fallout in southern Australia, Allison and Hughes (1972) utilized tritium concentrations of unsaturated zone soil water to assess vertical recharge dynamics in areas of differing vegetation types.

However, bomb-pulse tritium levels have since decayed (Walker et al., 1992) and therefore tritium is no longer useful as a hydrogeologic tracer. However, natural tritium concentrations in rainfall (~ 3.5 TU) are still well above the detection limits (0.1 -0.3 TU) and tritium is still used as conventional subsurface tracer (i.e. Cook et al., 2005; Cartwright et al 2007a). Chlorine-36, however, was also a product of nuclear weapons testing, and because of its longer half-life (301,000 yrs), remains a potential tracer in hydrogeologic studies. Elmore et al. (1979) conducted the first successful measurements of ^{36}Cl in natural water using a tandem accelerator mass spectrometry. The authors suggested the presence of bomb-pulse ^{36}Cl in an ephemeral river water sample believed to be of atmospheric origin. Bentley et al. (1982) also recognized bomb-pulse ^{36}Cl in natural waters. The authors stated that because bomb-pulse ^{36}Cl was generated from thermal neutron activation of ^{35}Cl, ^{36}Cl fallout pulse occurred over a relatively short period of time and could be simulated with global atmospheric circulation models. Their model was then calibrated with ^{36}Cl measurements of U.S. rainwater, river water, groundwater, and Greenland ice core samples. The fallout pulse reportedly occurred from 1953-1964 with mid-latitude fallout maximum 1000 times greater than natural background. Therefore, bomb pulse ^{36}Cl in groundwater has likely originated from meteoric deposition between the years 1953-1964 and provides a mean for recognizing relatively young recharge water and groundwater. Keywood et al. (1998) sampled rainwater over a two year period from a west-east transect and south-north transect in Australia. The study revealed large seasonal fluctuations in ^{36}Cl fallout and poor correlation between rainfall amount and fallout rate. However, they found that fallout in the southern hemisphere agreed with the predicted global fallout by Lal and Peters (1967). Considering the lag time in bomb-pulse tritium fallout between the northern hemisphere and southern hemisphere,

and peak fallout two orders magnitude less than observed in the northern hemisphere (Allison and Hughes, 1977), atmospheric fallout of bomb ^{36}Cl likely also occurred later than 1964 in the southern hemisphere. Although the magnitude of peak ^{36}Cl fallout was likely less than in the northern hemisphere, the effects of fallout of nuclear weapons generated chlorine has been highly recognizable within groundwater and soil water in Australia, although often diluted substantially through mixing with non-bomb pulse waters (i.e., Bentley et al., 1986; Fifield et al., 1987; Turner et al., 1987; Walker et al., 1992; Cook et al., 1994; Jacobson et al., 1998; Cartwright et al., 2006).

Saturated Zone

The effects of highly heterogeneous regolith materials on groundwater hydrogeology have been well studies in Australia (i.e., Johnston, 1987b; George, 1992; Mazor and George, 1992). Far less attention has been focused on the effects of highly heterogeneous aquifer systems on subsurface solute distributions and mobility. Greater salinity waters commonly reside within low permeability hydrogeologic units and have been recognized as potential solute sources to groundwater in the well studied Milk River aquifer system in Canada (i.e., Domenico and Robbins, 1985; Phillips et al., 1986) and the Great Artesian Basin in Australia (i.e., Bentley et al., 1986; Love et al., 2000). These studies recognized that mixing between different hydrogeologic units had a significant influence on the chemical composition of groundwater. The interaction between saline pore fluids in a clay rich aquitard and a freshwater aquifer was assessed by Ortega-Guerrero et al. (1997) and Degueldre et al. (2003). The authors presented saturated zone $\delta^{18}O$ profiles and noted isotopic enrichment of aquitard pore fluids relative to aquifer water. However, near the aquitard/aquifer boundary, the pore fluids were more depleted in $\delta^{18}O$, and trended

more towards those of the aquifer water. The authors concluded that the hydraulic gradient was sufficiently great enough for the isotopically depleted groundwater to flow upward through the aquitard. Love et al. (1993) noted the opposite occurring in a multi-aquifer system in South Australia. In this system, the hydraulic gradient of a lower confined aquifer was not sufficient to offset the downward leakage from an overlying unconfined aquifer. The authors' interpretation was based on stable isotope analyses, which indicated mixing of two isotopic end member waters. Similar vertical mixing between a confined and unconfined aquifers in Victoria, Australia was observed by Arad and Evans (1987) where similar ionic ratios existed between saline water of an unconfined aquifer and fresh water of a confined aquifer. The role of aquitards as osmotic membranes was evaluated by Back (1986), where osmotic flow was considered responsible for mixing of different salinity water across an aquitard membrane.

Far fewer studies have investigated the effects of physical heterogeneity of aquifer materials on solute mobility. Domenico and Robbins (1985) noted large spatial variations in Cl^- concentration in regions of the Milk River aquifer system which contained areas of greater physical heterogeneity. The authors concluded that greater salinity connate pore waters were mixing with less saline groundwater flowing through conduits of greater hydraulic conductivity. Wood et al. (1990) discovered the presence of intragranular pore spaces in course grained aquifer materials that contained waters of unique chemical composition compared to interstitial pore waters. Tracer experiments conducted on these materials revealed a high potential for diffusion between the intragranular and interstitial waters and the authors indicated a need for consideration of this process for modelling solute mobility in aquifers.

^{36}Cl based groundwater dating studies have been particularly limited by the effects of mixing between waters of different ages and geochemical origin. Well known studies from within The Great Artesian Basin (GAB) in Australia and the Milk River Aquifer in Canada have encountered uncertainties associated with "age mixing" (i.e., Bentley et al., 1986; Phillips et al., 1986; Hendry and Schwartz, 1988; Fabryka-Martin et al., 1991; Torgersen et al., 1991; Love et al., 2000). Love et al. (2000) observed an increase in Cl^- concentration and decrease in $^{36}Cl/Cl$ ratios along the flow path in the GAB that was attributed to diffusion of older, more saline waters from an overlying aquitard unit. Fabryka-Martin et al. (1991) reported Cl^- concentrations of pore waters leached from drill cuttings from within the Milk River Aquifer system that were 3 times greater than groundwater. The authors suggested that mixing between ancient connate waters and groundwater resulted in an overestimation of the groundwater residence times presented by Phillips et al. (1986) and Hendry and Schwartz (1988). The authors presented corrected ages that were half than previously estimated and that were in better agreement with the hydrodynamic age estimates.

The following four chapters (Chapters 3, 4, 5 & 6) present and discuss the chemical and isotopic composition of rainwater, surface water, soil pore water and groundwater to understand the hydrogeochemical processes resulting in a highly salinized aquifer system in central New South Wales, Australia (Figure 1). Chapters 3, 4, & 5 are presented in publication manuscript format to ease preparation of journal submission. Chapter 6 is a general discussion and summary chapter and Chapter 7 concludes the thesis.

3 EFFECTS OF MIXING ON GROUNDWATER SOLUTE CONCENTRATIONS AND ^{36}Cl BASED AGE CALCULATIONS

3.0 Introduction

Salinization of groundwater and surface water resources is a serious environmental issue in semi-arid areas of Australia. Within the Murray-Darling Basin (MDB) of south eastern Australia, it is predicted that up to 1,500,000 hectares of land will be affected by saline groundwater and surface water by the year 2010 (Starr, 1999). In this region, a considerable amount of research has focused on understanding unsaturated zone solute stores, particularly the mobilization of these solute stores by rising groundwater tables (Allison and Hughs, 1983; Calf et al., 1986; Allison et al., 1990; Cartwright and Weaver, 2005). Simpson and Herczeg (1994) estimated total Cl storage in the Murray-Darling basin to be 2×10^{15} mol, with 70% of that estimate residing within the Murray Basin. Based on current Cl deposition rates authors estimated the time-frames of accumulation to be 5×10^{4} for the Darling and 1.8×10^{5} for the Murray Basin. However, because precipitation is thought to have been significantly lower during the last glacial period, the authors estimate that the timeframes of Cl accumulation in the MDB may be an order of magnitude higher than estimated. The authors highlight the uncertainties in their estimates of subsurface solute stores and also their mobility (i.e. export from the MDB). This lack of understanding creates a difficulty in predicting short term and long term effects of land and resource management and climate change. Furthermore, heterogeneity of aquifer materials frequently results in heterogenous solute distributions, further complicating interpretations of past, present and future solute dynamics. A

fundamental difficulty faced when addressing problems relating to salinization of groundwater is quantifying the effects of mixing between waters of different chemical compositions. Groundwater dating studies have also been inhibited by the effects of mixing, particularly those which have utilized the radiogenic isotope, chlorine-36.

Mixing effects on groundwater solute concentrations

Higher salinity waters commonly reside within fine grained, low permeability materials and are identified as significant solute sources to groundwater in the well studied Milk River aquifer system in Canada (i.e., Domenico and Robbins, 1985; Phillips et al., 1986) and the Great Artesian Basin in Australia (i.e., Bentley et al., 1986b; Love et al., 2000). These studies demonstrate how mixing of waters from different hydrogeologic units can significantly influence the chemical composition of groundwater along a flow path. Far fewer studies have investigated mixing between waters residing in higher and lower permeability materials within the aquifers themselves. Domenico and Robbins (1985) noted large spatial gradients of Cl^- concentration gradients in regions of the Milk River aquifer system, which coincided with areas of greater physical heterogeneity. They attributed this to mixing of higher salinity connate pore waters with less saline groundwater flowing through preferential flow paths of greater hydraulic conductivity. More recently, Wood et al. (1990) recognized the presence of intragranular pore spaces in coarse-grained aquifer materials, and a chemical disequilibrium between interstitial and intragranular pore water. The authors experimentally demonstrated the occurrence of diffusion between the intragranular and intergranular pore spaces and suggested a need for consideration of this process for modelling solute mobility in aquifers.

Mixing effects on chlorine-36 ratios

Determination of actual groundwater ages is complicated by processes occurring in both the unsaturated and saturated zones. Mixing, filtration and halite dissolution can lower $^{36}Cl/Cl$ ratios in groundwater and result calculated ages older than actual ages (Bethke and Johnson, 2002). Furthermore, determining an appropriate input ratio for age calculations is difficult and ^{36}Cl age calculations can be inaccurate (i.e., Davis et al., 1998). However, in most cases the effects of mixing between waters of different ages and geochemical origin represent the largest uncertainty in interpreting the measured $^{36}Cl/Cl$ ratios in groundwater. The Great Artesian Basin (GAB) in Australia and the Milk River Aquifer in Canada represent well studied aquifer systems that have encountered uncertainties associated with "age mixing" (i.e., Bentley et al., 1986b; Phillips et al., 1986; Hendry and Schwartz, 1988; Fabryka-Martin et al., 1991; Torgersen et al., 1991; Love et al., 2000).

Great Artesian Basin

The GAB, along with the Milk River aquifer, were the aquifer systems chosen in early pilot studies to determine the suitability of ^{36}Cl for dating of groundwater older than the ^{14}C age limit (~ 50,000 yrs). The GAB was selected because the chloride geochemistry and hydrogeology were reasonably well constrained, and hydrodynamics suggested a potential for encountering groundwater older than 1 million years (Bentley et al., 1986b). The study focused on a section of a lower Jurassic sandstone aquifer that exhibited relatively constant Cl^- concentrations and decreasing $^{36}Cl/Cl$ along the flow path, making it an ideal system for age interpretations. However, several samples collected from the Jurassic aquifer in a different portion of the GAB exhibited greater Cl^- and lower $^{36}Cl/Cl$ than those

sampled down gradient. It was suggested that upward leakage of water from Devonian sediments containing halite produced the observed groundwater Cl^- concentrations and $^{36}Cl/Cl$ ratios. Bentley et al. (1986b) proposed an age calculation equation for these samples that corrected for the addition of the ^{36}Cl free Cl^- sourced from halite. Torgersen et al. (1991) later recognized the potential for mixing of waters of different origins, ages and chemical compositions within the GAB and offered this as a potential explanation for variability in $^{36}Cl/Cl$ ratios observed in the central portion of the basin. Love et al. (2000) observed an increase in Cl^- concentration and decrease in $^{36}Cl/Cl$ ratios along the flow path of a confined aquifer within the southwest flow system of the GAB. The authors attributed this to diffusion of older, more saline waters from an overlying aquitard unit. They corrected for this process by modifying the decay equation to account for the effects of addition of "dead" Cl^- on the measured $^{36}Cl/Cl$ ratios and presented more representative flow ages for the confined system. However, the authors noted uncertainties in their calculations due to assumptions of Cl^- concentration and $^{36}Cl/Cl$ ratios of initial input values and saline aquitard mixing endmembers.

Milk River Aquifer System

Numerous $^{36}Cl/Cl$ based groundwater dating studies have encountered similar difficulties with mixing within the Milk River aquifer system in Canada. Fabryka-Martin et al. (1991) reported Cl^- concentrations of pore waters leached from drill cuttings that were 3 times greater than those in groundwater sampled from the same unit. They attributed this difference to the heterogeneous nature of the aquifer materials and resultant displacement of connate water from larger pore spaces and lack of solute displacement from smaller, less permeable pore spaces. Diffusion of Cl^-

from these low permeability units was described as a major source of Cl^- to the aquifer waters. The connate waters were assumed to exhibit considerably lower $^{36}Cl/Cl$ ratios relative to meteoric input (i.e., $4x10^{-15}$ vs $550x10^{-15}$) and that the mixing process resulted in an overestimation of the groundwater residence times from previous studies of the same system (Phillips et al., 1986; Hendry and Schwartz, 1988). Age estimates corrected for mixing by Fabryka-Martin et al. (1991) were half those previously estimated and were in better agreement with the hydrodynamic age estimate.

The GAB and Milk River Aquifer studies demonstrate the need to understand solute distributions throughout the saturated zone in order to accurately quantify solute sources and sinks for groundwater within heterogeneous aquifer systems. In addition, there's a need to understand solute distribution and mobility in low-lying, highly salinized catchments areas typical throughout the Murray-Darling Basin. This study demonstrates how the measurements of major element concentrations and $^{36}Cl/Cl$ ratios in regional groundwater, as well as soil pore water extracted from saturated zone sediments, have provided a mean for quantifying solute mobility and mixing rates, and has allowed for reliable flow-age calculations for groundwater in a highly heterogeneous saline aquifer system. This method will prove useful for future groundwater studies focused on solute or contaminant mobility in complex hydrogeologic systems.

3.1 Regional Setting, Geology and Hydrogeology

This study focuses on the 25 x 25 km Barmedman Creek catchment located in the southwest portion of the Bland Basin in central New South Wales, Australia (Figure

3.1). The Bland Basin is a low-lying palaeo-tributary system of the Lachlan River that is located within the Murray- Darling Basin. The majority of the Barmedman creek catchment is characterized by extremely low topographic relief (<0.7 m/km) which grades from south to north. The exception is an area of low relief granite outcroppings (<50m) in the south-eastern portion of the study area (Figure 3.3).

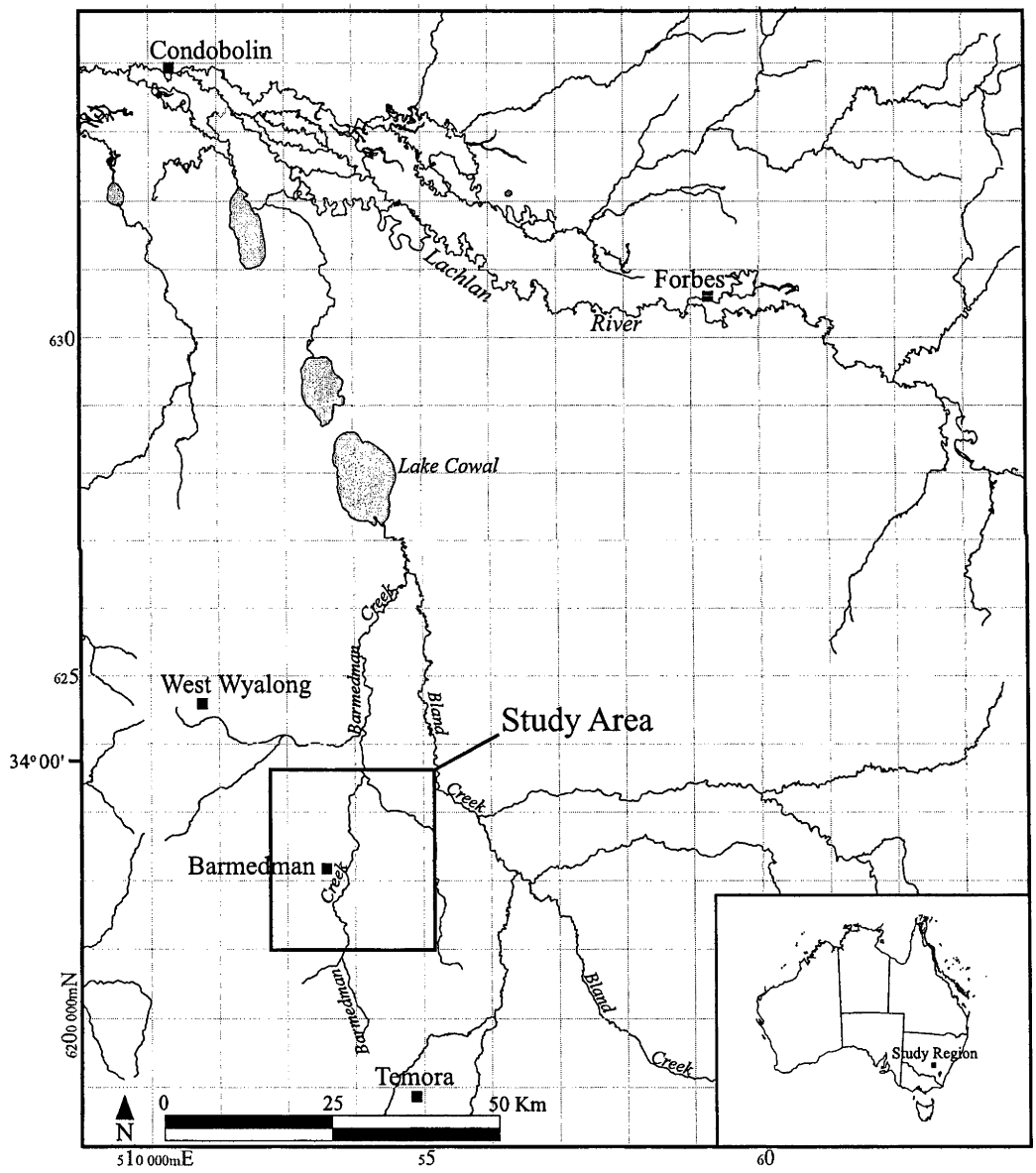

Figure 3.1: Location of study area within the Bland Basin, central New South Wales (NSW), Australia. Adapted from Forbes, NSW and Cootamundra, NSW 1:250 000 map sheets (courtesy Geoscience Australia). Grids represent geographical easting and northing plotted at 10,000 metre intervals.

3.1.1 Geology

The study area is located within the Gilmore fault zone of the Lachlan Fold Belt. The Gilmore fault zone consists of north-northwest trending, east dipping back thrust faults (Warren et al., 1995). The Gilmore fault marks the boundary between metasediments and S-type granitoids of the Wagga-Omeo metamorphic belt to the west, and to the east, Ordovician-Devonian clastic sediments and intermediate to felsic volcanics (Thompson et al., 1986; Wormald and Price, 1988; Allibone et al., 1995). The bedrock geology consists of north- northwest trending Cambro-Ordovician metasediments and granites, Ordovician intermediate volcanics and metasediments, and Silurian-Devonian clastic sediments (Warren et al., 1995).

Weathering in the Cenozoic has resulted in thick saprolite sequences (Wilford et al., 2002) followed by deposition of up to 80 metres of sediments (Gibson et al., 2002). Stratigraphic palynology of Lachlan River alluvium (~60 km northeast of the study area) suggests that regional sedimentation occurred during the Miocene and Pliocene with the most significant deposition of sediments occurring during the Pliocene (Martin, 1991). Two depositional cycles, the Lachlan and Cowra formations, are recognized within the Lachlan alluvium to the northeast (Williamson, 1986). The basal Lachlan formation was described as coarse grained materials deposited by high energy river systems and the overlying Cowra formation was characterized as silts and clays deposited by low energy river systems under semi-arid conditions.

Sediments sampled from the Barmedman Creek catchment appear to reflect this regional depositional model and classification scheme. Wilford et al. (2002) identified lithofacies within the sedimentary sequence and related them to erosional and

depositional processes. Basal sands and gravels were attributed to erosion of bedrock and deposition along palaeo-drainage lines. An overlying clay/silt unit is interpreted as colluvial transport of highly weathered bedrock within palaeo-valleys. The mid to upper sandy unit represents distally sourced sandy sediments deposited by fluvial systems. The uppermost clay and silt unit is believed to represent modern sheet flow alluvium/colluvium and possibly aeolian material. A generalized south to north cross-section of the sedimentary stratigraphy of the Barmedman Creek catchment is depicted in Figure 3.2.

3.1.2 Hydrogeology

Anderson et al. (1993) identified a large groundwater mound near present day Lake Cowal (30 km north of study area, see Figure 3.1) and a southward trending hydraulic gradient; they described the Bland Basin as a slowly filling basin no longer draining northward into the Lachlan River. This is supported by ^{14}C groundwater ages that increase along the hydraulic gradient (south to north) until reaching Lake Cowal where younger groundwater is present in both the Lachlan and Cowra Formations (Carrara, 2005). The oldest groundwater dates reported for the Lachlan and Cowra formation are 26,000 yrs and 9,500 yrs respectively.

In 1999, airborne geophysical data, including airborne electromagnetic (AEM) and aeromagnetic data were collected from the Barmedman Creek catchment, located in the southwest portion of the Bland Basin, as part of a joint project coordinated by The Australian Geological Survey Organization (now Geoscience Australia) and The Bureau of Rural Sciences (i.e., Lawrie et al., 2000). An extensive drilling program was also carried out to ground-truth the airborne geophysical data. The geophysical

surveys and drilling program revealed parallel zones of north-northwest trending shallow (~10 m) buried resistive ridges consisting of in-situ regolith materials derived from igneous and metamorphic units (Lawrie et al., 2000; Wilford et al., 2002). Adjacent to these buried ridges are palaeo-valleys containing up to 80 metres of transported sediments (Lawrie et al., 2000; Gibson et al., 2002). Preferential groundwater flow was interpreted as occurring from south to north through the more conductive sediments within the north-northwest trending buried palaeo-valleys (i.e., Lawrie et al., 2000). Furthermore, higher electromagnetic conductivity was measured in the shallow clay rich in-situ saprolite materials compared to the thicker transported

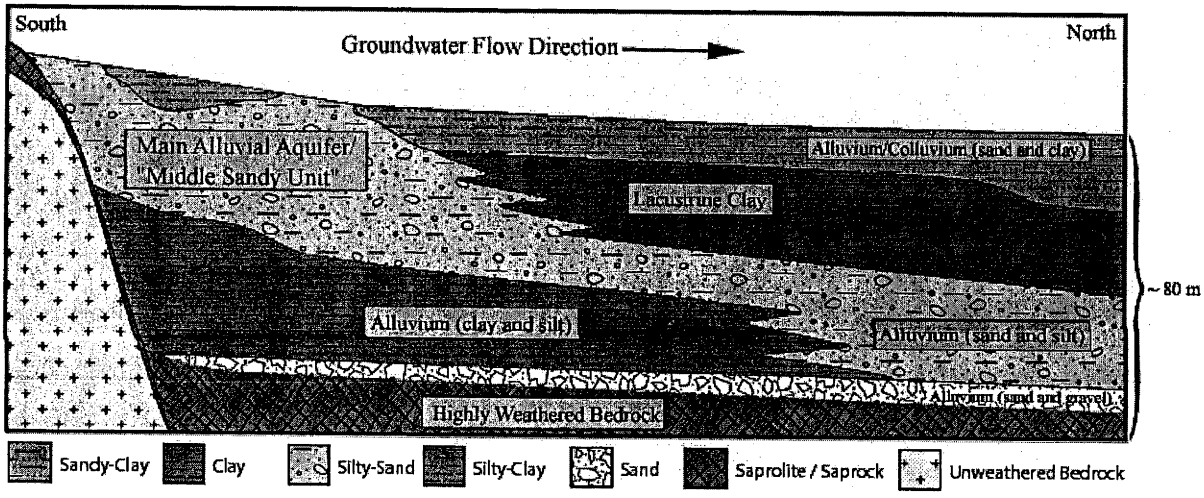

Figure 3.2: Generalized south to north cross-section of unconsolidated sedimentary stratigraphy of Barmedman Creek catchment. Adapted from (Gibson et al., 2002; Wilford et al., 2002).

sediments. The clay rich in-situ regolith materials were identified as potential salt stores to the coarser grained transported sediments that comprise the main alluvial aquifer within the Barmedman Creek catchment (Lawrie et al., 2000).

In 2000, 19 piezometers were installed within the Barmedman Creek catchment (Figure 3.3). "GAC" and "GDH" piezometers have a diameter of 12.5 cm while "GRB" piezometers have a diameter of 5.0 cm. The slotted intervals vary in length

from 1 metre to 6 metres and are situated in materials of variable hydrogeologic properties, including fine grained saprolite materials. The majority of the piezometers intersect the middle sand unit described by Wilford et al. (2002), and in the majority of the catchment, this unit is overlain by >10 m of clay and silt (Figure 3.2). However, in the vicinity of granite outcropping areas in the southern portion of the catchment, the middle sand unit outcrops the surface (Figure 3.2). This middle sandy unit seems analogous to the Cowra Formation described by Williamson (1986). The hydraulic conductivities measured by the BRS in piezometers intersecting this aquifer system

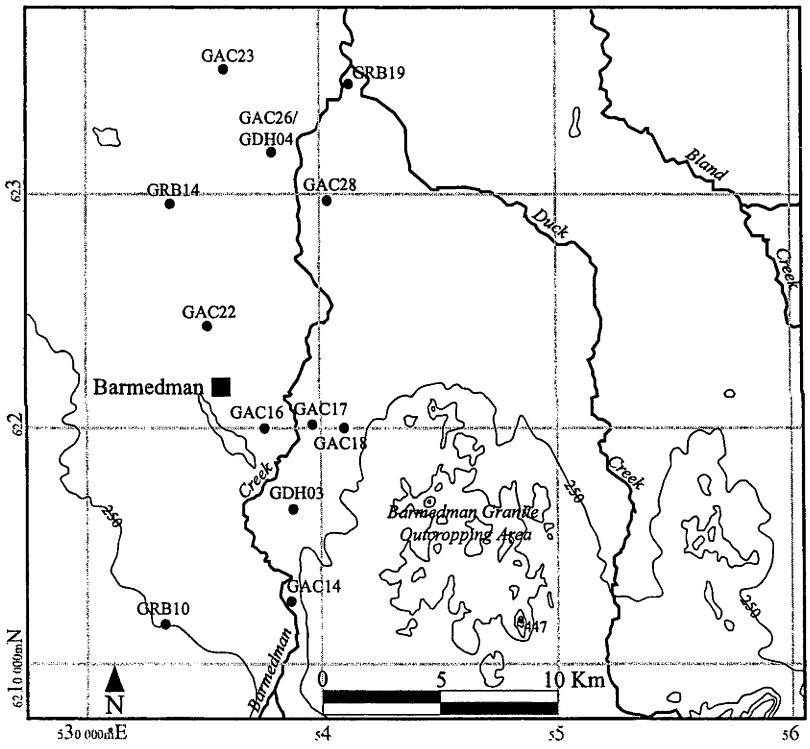

Figure 3.3: Piezometer and sediment diamond core locations within the Barmedman Creek subcatchment of the Bland Basin. Adapted from Cootamundra, NSW 1:250 000 map sheet (50 metre contour interval). Grids represent geographical easting and northing and depicted as 10,000 metre intervals.

Results of pump and slug tests conducted on piezometers intersecting the middle sandy unit by the Bureau of Rural Sciences in 2001 revealed hydraulic conductivity values of 10^{-4} - 10^{-5} m/s. Hand-held GPS water levels elevations revealed a general south to north hydraulic gradient.

3.2 Methods

Regolith materials were sampled by the Australian Bureau of Rural Sciences (BRS) in 2001 via diamond coring at two locations, GDH03 and GDH04 (Figure 3.3), to depths of 59 and 80 m respectively. Grain size analyses were performed using laser scattering by Geoscience Australia on selected 2 cm intervals of diamond core materials in 2006. Soil pore water was extracted by the BRS from saturated zone regolith materials with a uniaxial compression device at the BRS laboratories in Canberra, ACT in 2001. Pore water samples were collected in sterile 10 mL syringes then filtered through a 0.45 μm filter into sterile viles. Piezometer elevations and horizontal coordinates (GDA94 geographic coordinates) were measured with a Differential GPS in 2006 as part of Geoscience Australia's National Geospatial Reference Systems Project. Spatial data were logged for ~ 4 hrs at each location and 3-D coordinate results reported accurate to within 5 cm. Depth to the water table was measured with a graduated dip meter. Mean annual rainfall, calculated from monthly measurements by the Australian Bureau of Meteorology from 1887-2005, is 480 mm/yr. The majority of the study area has been cleared of native *Eucalypt* vegetation and is presently cultivated with canola and wheat.

Groundwater was sampled in this study from permanently installed piezometers in 2004 using a Grundfos™ electrical submersible pump equipped with a Teflon hose. HCO3 was determined in the filed by titration of known sample volume with known volume and concentration (mol/l) HCl solution. Temperature, electrical conductivity, dissolved oxygen, pH and Eh were monitored in a flow cell during pumping and

samples were collected after a minimum of three piezometer volumes had been purged and meter readings had stabilized. Samples were field filtered through 0.45 μm filter paper. High density polyethylene containers were thoroughly rinsed with respective filtered sample prior to collection. Samples for cation analysis were acidified in the field with concentrated A.R. grade nitric acid. Pore water and groundwater samples were stored in refrigerators maintained at ~10° C. Anion concentrations were measured with a Dionex DX4500i ion chromatograph using an AS14A column with $NaHCO_3/Na_2CO_3$ eluent and electrochemical detector in conductivity mode at The Australian National University (ANU) Department of Earth and Marine Sciences (DEMS). Cation concentrations were determined via ion chromatography and ICP atomic emission spectrometry at The Australian National University (ANU) Department of Earth and Marine Sciences and Australian Bureau of Rural Sciences. Results from major/minor ion analyses for groundwater samples yielded charge imbalances of less than 3%. Stable isotope (δ^2H and $\delta^{18}O$) analyses were carried out via isotope ratio mass spectrometry on a Finnigan MAT 252 MS at Monash University Data were normalised following Coplen (1988) and are expressed as per mil relative to Vienna-Standard Mean Ocean Water (V-SMOW).. Precision for δ^2H and $\delta^{18}O$ is 1.0 and 0.2 ‰ respectively. ^{36}Cl samples were prepared using a similar the method described by (Conrad et al., 1986) in clean labs at ANU Department of Nuclear Physics and Research School of Earth Sciences. $^{36}Cl/Cl$ was determined by accelerator mass spectrometry at ANU Department of Nuclear Physics (Fifield et al., 1987).

3.3 Results

Geographical location of piezometers and water level elevations are reported in Table 3.1. Major element concentrations and stable and radiogenic isotope data for 43 groundwater and pore water samples are presented in Table 3.2. Grain sizes and moisture contents for unconsolidated sediments collected from diamond cores GDH03 and GDH04 are also presented in Table 3.2.

Piezometer ID	Easting (m)	Northing (m)	Casing Height (m)	Elevation (m) (TOC)	2001 SWL (m)	2004 SWL (m)	2006 SWL (m)
GRB10	533250.89	6211652.34	N/A	N/A	25.03	25.18	N/A
GAC14	538548.55	6212443.33	1.00	N/A	18.95	18.98	18.27
GDH03_1	538627.29	6216703.24	0.89	236.06	8.35	8.83	9.13
GDH03_2	538627.29	6216703.24	1.04	N/A	19.21	19.2	19.3
GDH03_3	538627.29	6216703.24	0.96	236.00	19.23	19.81	19.29
GAC18_2	541007.72	6219902.00	0.94	238.22	N/A	N/A	27.19
GAC17_3	539695.12	6220000.69	0.95	230.18	17.69	17.62	17.63
GAC16_2	537401.12	6220036.28	1.33	231.80	18.17	18.2	18.27
GAC22	534845.85	6224527.30	1.19	226.49	16.6	16.59	16.52
GRB14	533011.93	6229614.55	1.00	N/A	N/A	13.95	N/A
GAC28	540276.38	6229677.49	0.95	220.45	9.95	9.07	9.33
GAC26_1	538078.88	6231715.04	0.92	219.77	8.79	N/A	9.26
GAC26_2	538078.88	6231715.04	1.05	219.89	8.93	9.15	9.4
GRB19	541147.62	6234673.61	1	N/A	9.77	10.52	N/A
GAC23_1	536019.55	6235120.20	0.97	222.85	12.59	12.65	12.71
GA23_2	536019.55	6235120.20	0.95	222.83	12.58	12.62	12.69

TOC = top of piezometer casing
N/A = non applicable or not measured
SWL = standing water level in piezometer reported as depth below top of piezometer casing

Table 3.1: Piezometer locations, piezometer elevations and standing water levels measured in 2001, 2004 and 2006.

3.3.1 Hydrogeology of Barmedman Creek Catchment

Groundwater levels in Barmedman Creek catchment were measured in 2001 by the Bureau of Rural Sciences and in 2004 and 2006 as part of this study. Despite a persistent drought over this period (~ 100 mm/yr less than long term average), the groundwater levels measured in 2006 were only slightly lower (<0.8m) than 2001 suggesting a relatively stagnant aquifer system. Results from differential GPS measurements of piezometer elevations and map coordinates, as well as groundwater levels measured during sampling revealed a south to north hydraulic gradient of ~0.35

m/km, consistent with the closed basin theory proposed by Anderson et al. (1993) and confirmed with ^{14}C measurements of groundwater in the Bland Basin by Carrara, 2005. Considering the hydraulic gradient and the BRS pump-test results with reported hydraulic conductivity values for the main alluvial aquifer of $\sim 10^{-5}$ m/s (unpublished data courtesy BRS), the calculated groundwater linear flow velocity is approximately 15 cm/yr. Hydraulic conductivity values reported for the Lachlan Formation Groundwater recharge to the deeper confined/semiconfined aquifers occurs via vertical infiltration of rainwater at outcropping areas and through the near surface (<5 m) sandy-silt sediments in the southern portion of the study area (Chapter 5).

											mg/L										
Sample ID	Sample Depth (m)	%Moisture	%Sand	%Clay+Silt	Cl (atom/L)	^{36}Cl (atom/L)	^{36}Cl/Cl	^{36}Cl/Cl Error	^{18}O‰	^{2}H‰	Cl^-	Br^-	NO_3^-	PO_4^{3-}	SO_4^{2-}	HCO_3^-	Si	Ca	Mg	Na	K
GDH03*	8.65	17	44	56	8.65E+22	9.79E+09	1.13E-13	6.56E-15	N/A	N/A	5090.0	16.9	BD	BD	892.0	N/A	29.5	50.0	285.0	3280.0	9.9
GDH03*	10.50	20	31	69	1.02E+23	8.69E+09	8.51E-14	8.60E-15	N/A	N/A	6010.0	29.3	BD	BD	2370.0	N/A	45.6	200.0	1260.0	4920.0	6.1
GDH03*	12.20	15	45	55	1.07E+23	1.24E+10	1.16E-13	6.90E-15	N/A	N/A	6320.0	12.1	7.8	BD	1170.0	N/A	37.0	259.0	1500.0	4850.0	9.6
GDH03*	21.10	15	77	23	1.43E+23	1.28E+10	8.97E-14	6.20E-15	N/A	N/A	8410.0	27.0	BD	BD	1610.0	N/A	14.4	228.0	978.0	5390.0	32.3
GDH03*	25.00	21	90	10	7.35E+22	7.20E+09	9.79E-14	6.10E-15	N/A	N/A	4330.0	11.8	BD	BD	997.0	N/A	18.2	216.0	984.0	5250.0	33.9
GDH03*	28.30	21	72	28	2.11E+23	1.81E+10	8.61E-14	5.50E-15	N/A	N/A	12400.0	39.4	N/A	BD	2760.0	N/A	19.0	303.0	1450.0	7030.0	42.7
GDH03*	29.65	17	88	12	1.87E+23	1.81E+10	9.70E-14	6.00E-15	N/A	N/A	11000.0	35.9	BD	BD	2380.0	N/A	19.9	239.0	1140.0	5730.0	37.8
GDH03*	32.20	16	15	85	1.15E+23	8.91E+09	7.76E-14	5.90E-15	N/A	N/A	6760.0	19.3	BD	BD	1510.0	N/A	17.9	230.0	1150.0	5040.0	26.1
GDH03*	33.20	16	5	95	1.68E+23	1.78E+10	1.06E-13	6.70E-15	N/A	N/A	9890.0	31.5	BD	BD	2180.0	N/A	24.4	255.0	1330.0	5110.0	9.9
GDH03*	34.60	17	12	88	1.87E+23	1.98E+10	1.06E-13	6.10E-15	N/A	N/A	11000.0	35.3	BD	BD	2320.0	N/A	20.2	242.0	1260.0	5200.0	23.5
GDH03*	46.30	18	36	64	1.45E+23	1.55E+10	1.04E-13	5.22E-15	N/A	N/A	8510.0	25.9	BD	BD	1890.0	N/A	7.5	190.0	915.0	4370.0	15.5
GDH03*	52.00	10	69	31	1.64E+23	1.59E+10	9.47E-14	6.05E-15	N/A	N/A	9660.0	31.1	BD	BD	2010.0	N/A	6.4	230.0	948.0	5180.0	32.7
GDH03*	53.00	N/A	90	10	1.31E+23	8.90E+09	6.78E-14	5.50E-15	N/A	N/A	7730.0	25.1	BD	BD	1620.0	N/A	6.3	189.0	750.0	4500.0	27.6
GDH03*	53.50	16	0	100	1.80E+23	1.93E+10	1.07E-13	6.40E-15	N/A	N/A	10600.0	34.7	BD	BD	2220.0	N/A	5.8	246.0	1030.0	5510.0	88.6
GDH03*	58.00	16	20	80	1.61E+23	1.69E+10	1.05E-13	5.80E-15	N/A	N/A	9490.0	31.1	8.5	BD	1950.0	N/A	4.4	237.0	985.0	5320.0	56.2
GDH04*	9.00	30	18	82	2.28E+23	2.17E+10	8.73E-14	5.99E-15	N/A	N/A	13400.0	34.2	BD	BD	3940.0	N/A	76.6	447.0	1750.0	6010.0	13.2
GDH04*	12.70	35	15	85	2.29E+23	2.01E+10	8.30E-14	6.03E-15	N/A	N/A	13500.0	32.7	BD	BD	4090.0	N/A	42.8	529.0	1660.0	6320.0	51.5
GDH04*	17.70	N/A	15	85	1.05E+23	9.35E+09	8.34E-14	5.94E-15	N/A	N/A	6170.0	17.2	BD	BD	2170.0	N/A	24.0	207.0	648.0	3520.0	20.3
GDH04*	27.90	56	25	75	8.46E+22	7.36E+09	8.26E-14	5.89E-15	N/A	N/A	4980.0	14.3	BD	BD	1480.0	N/A	15.5	168.0	437.0	2810.0	20.6
GDH04*	29.50	29	71	30	1.77E+23	1.42E+10	7.62E-14	5.46E-15	N/A	N/A	10400.0	30.1	3.5	BD	3140.0	N/A	20.8	483.0	1420.0	5010.0	13.4
GDH04*	43.00	21	65	35	2.36E+23	1.63E+10	6.90E-14	6.50E-15	N/A	N/A	13900.0	32.4	BD	BD	3180.0	N/A	18.1	991.0	1630.0	6570.0	41.2
GDH04*	44.00	23	65	35	1.40E+23	1.26E+10	9.00E-14	5.50E-15	N/A	N/A	8240.0	17.5	BD	BD	2210.0	N/A	22.0	339.0	938.0	4290.0	18.1
GDH04*	44.50	21	42	58	3.35E+23	3.05E+10	9.10E-14	5.50E-15	N/A	N/A	19700.0	66.8	BD	BD	4540.0	N/A	17.2	1260.0	2360.0	8510.0	30.6
GDH04*	58.30	23	80	20	2.70E+23	1.94E+10	7.20E-14	5.00E-15	N/A	N/A	15900.0	41.4	6.3	BD	3560.0	N/A	7.9	1100.0	1630.0	7050.0	39.8
GDH04*	64.50	20	25	75	2.31E+23	1.88E+10	6.93E-14	4.85E-15	N/A	N/A	13600.0	44.3	8.4	BD	3020.0	N/A	10.8	1060.0	1920.0	6910.0	22.0
GDH04*	71.30	13	95	5	1.95E+23	1.59E+10	7.55E-14	5.37E-15	N/A	N/A	11480.0	33.1	8.1	BD	2830.0	N/A	5.4	414.9	1200.0	5240.0	31.5
GDH04*	73.00	21	95	5	2.58E+23	2.19E+10	8.50E-14	5.60E-15	N/A	N/A	15200.0	46.4	8.3	BD	3350.0	N/A	6.6	525.0	1550.0	6900.0	45.7
GRB10	28.37	N/A	N/A	N/A	2.23E+23	2.62E+10	1.18E-13	5.85E-15	-4.53	-30.00	13155.7	38.0	2.0	BD	4058.0	610.7	26.1	249.6	1552.4	7245.8	48.9
GAC14	25.50	N/A	N/A	N/A	1.82E+23	1.83E+10	9.96E-14	5.07E-15	-4.19	-30.19	10691.3	34.2	1.6	BD	2705.7	413.2	22.1	318.3	1057.4	5742.8	40.6
GDH03_1	10.50	N/A	N/A	N/A	1.03E+23	1.30E+10	1.30E-13	8.31E-15	-4.70	-29.52	6063.8	23.9	BD	BD	1085.6	262.3	74.8	118.6	438.5	3297.2	3.7
GDH03_2	25.60	N/A	N/A	N/A	9.33E+22	1.27E+10	1.36E-13	8.00E-15	-4.70	-26.92	5491.5	22.4	8.4	BD	955.7	526.5	66.8	123.3	411.9	3049.5	5.7
GDH03_3	31.00	N/A	N/A	N/A	9.93E+22	1.21E+10	1.22E-13	7.74E-15	-4.65	-30.00	5848.7	21.8	7.2	BD	951.6	612.2	57.1	154.9	448.9	3261.4	9.2
GAC18_2	24.00	N/A	N/A	N/A	9.21E+22	1.35E+10	1.47E-13	9.00E-15	-4.33	-32.23	5424.5	24.8	13.5	BD	499.0	N/A	N/A	N/A	N/A	N/A	N/A
GAC17_3	62.00	N/A	N/A	N/A	1.64E+23	2.01E+10	1.23E-13	5.60E-15	-4.61	-33.50	9636.0	35.5	3.2	10.6	1683.3	590.5	41.7	774.5	1172.0	4150.0	50.5
GAC16_2	31.05	N/A	N/A	N/A	1.98E+23	2.10E+10	1.06E-13	5.17E-15	-4.20	-29.20	11654.9	41.5	0.9	BD	2451.0	518.6	11.4	468.5	1270.7	5488.5	35.2
GAC22	23.36	N/A	N/A	N/A	2.51E+23	2.08E+10	8.28E-14	4.24E-15	-4.31	-29.77	14787.3	50.1	3.4	BD	3291.0	160.8	65.0	686.1	1843.2	6820.8	48.0
GRB14	17.10	N/A	N/A	N/A	2.25E+23	1.96E+10	8.72E-14	4.39E-15	-5.01	-30.40	13225.0	42.5	N/A	1.2	2850.9	280.9	66.0	801.5	1353.1	6508.0	20.3
GAC28	36.00	N/A	N/A	N/A	2.69E+23	2.31E+10	8.60E-14	4.51E-15	-4.01	-31.17	15810.3	58.5	3.4	4.3	4159.3	372.1	28.6	1182.0	1549.8	7442.5	36.5
GAC26_1	43.00	N/A	N/A	N/A	2.67E+23	2.11E+10	7.90E-14	6.00E-15	-4.20	-31.92	15728.7	52.1	8.2	1.0	3195.8	N/A	N/A	N/A	N/A	N/A	N/A
GAC26_2	63.00	N/A	N/A	N/A	2.72E+23	2.01E+10	7.39E-14	4.22E-15	-4.36	-29.42	16003.6	55.5	1.6	BD	3510.0	248.9	11.7	1233.3	1770.2	6993.9	42.2
GRB19	14.50	N/A	N/A	N/A	2.52E+23	2.35E+10	9.31E-14	5.00E-15	-3.98	-30.84	14839.6	48.4	0.5	BD	3367.1	331.6	37.0	1439.8	1435.2	6949.9	21.7
GAC23_1	16.08	N/A	N/A	N/A	2.81E+23	2.16E+10	7.70E-14	6.00E-15	-4.10	-31.20	16513.7	55.2	0.9	BD	4126.7	631.1	33.8	1204.2	1713.9	8201.0	58.3
GA23_2	23.50	N/A	N/A	N/A	2.79E+23	2.20E+10	7.88E-14	4.28E-15	-4.06	-31.22	16415.3	54.5	0.5	BD	4037.2	676.7	29.1	1210.7	1743.4	8149.1	61.1
Seawater	0.00	N/A	N/A	N/A	3.23E+23	N/A	N/A	N/A	N/A	N/A	19000.0	67.0	0.7	0.1	2700.0	142.0	6.4	410.0	1350.0	10500.0	390.0

* Pore Water Samples (otherwise groundwater sample)
Seawater solute concentrations from Hem, 1992
N/A = non applicable or not measured
BD = below detection limit

Table 3.2: Barmedman Creek catchment sampling locations, sediment grain sizes and geochemical results. Geochemical results are reported as raw data values and accurated to 3 significant figures. Sampling locations reported in GDA94 geographical coordinates (metres). Sampling elevations reported in metres and were measured from the top of the piezometer casings. Sampling depths are reported in metres below the top of the casings. Groundwater solute concentrations are reported in mg/l. δ^2H and $\delta^{18}O$ are reported relative to V-SMOW.

3.3.2 Groundwater Geochemical Results

Groundwater Solutes

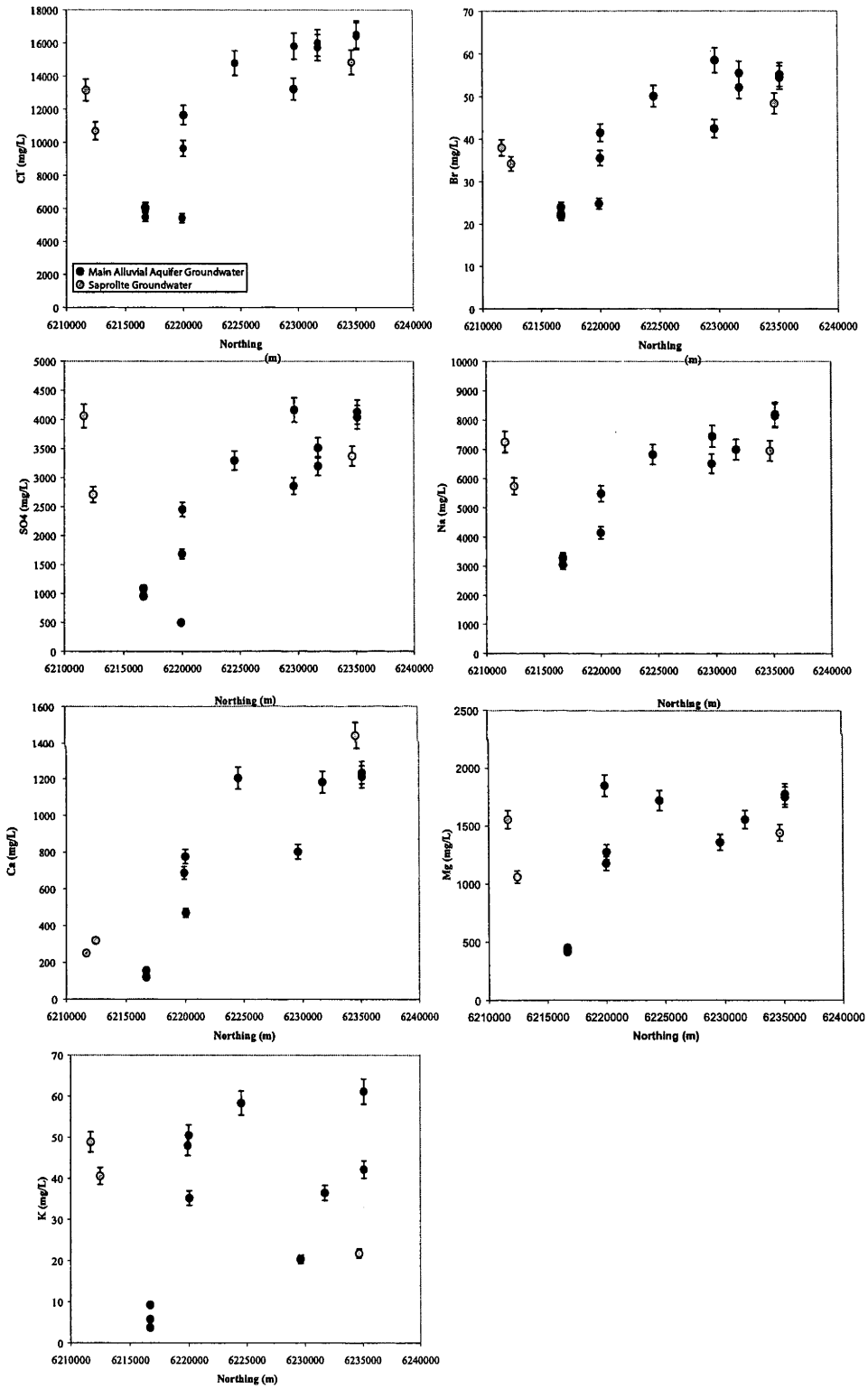

Figure 3.4: Groundwater solute concentrations vs. geographical northing. Analytical error estimated from replicate analyses and reported as +/- 5 % of measured concentration.

In general, all major ion concentrations in groundwater increase down the hydraulic gradient (Figure 3.4). Conservative ions Cl^- and Br^-, as well as SO_4^{2-}, Na^+ and Ca^{2+} exhibit the most systematic increases in concentration along the flow path (Figure 3.4). Groundwater samples exhibit Cl^- concentrations ranging from approximately 5,400 to 16,500 mg/l, Br^- concentrations from 22 to 58 mg/l, SO_4^{2-} from 500 to 4200

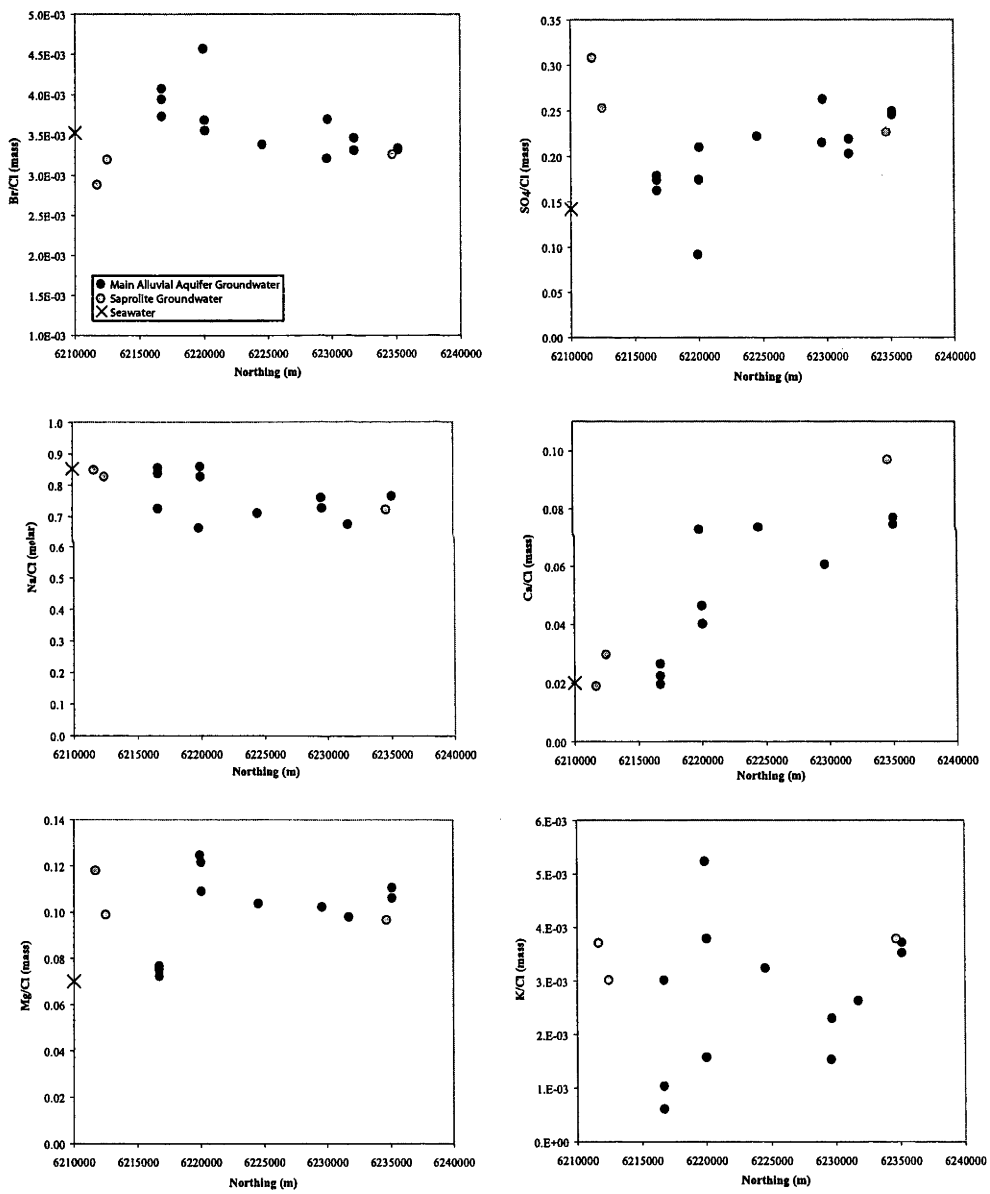

Figure 3.5: Spatial variations in major ion concentrations relative to chloride for groundwater samples collected from the main alluvial aquifer and from within clay-rich saprolite units. Seawater ratios are plotted for reference, with the exception of K/Cl, which is an order of magnitude greater than in groundwater samples.

mg/l, Na^+ concentrations from 3050 to 8150 mg/l and Ca^{2+} concentrations ranging from 123 to 1230 mg/l.

Br/Cl ratios and major element / chloride ratios exhibit distinct correlations to flow path position (Figure 3.5). Br/Cl and Na/Cl ratios decrease and SO_4/Cl and Ca/Cl ratios increase along the flow path. Mg/Cl ratios are relatively constant along the flow path and K/Cl ratios exhibit too much variability to discern trends. For the purposes of this paper only the elements that reflect trends along flow path (Cl^-, Br^-, $SO4^{2-}$, Na^+ and Ca^{2+}) will be discussed.

Stable Isotopes ^2H and ^{18}O

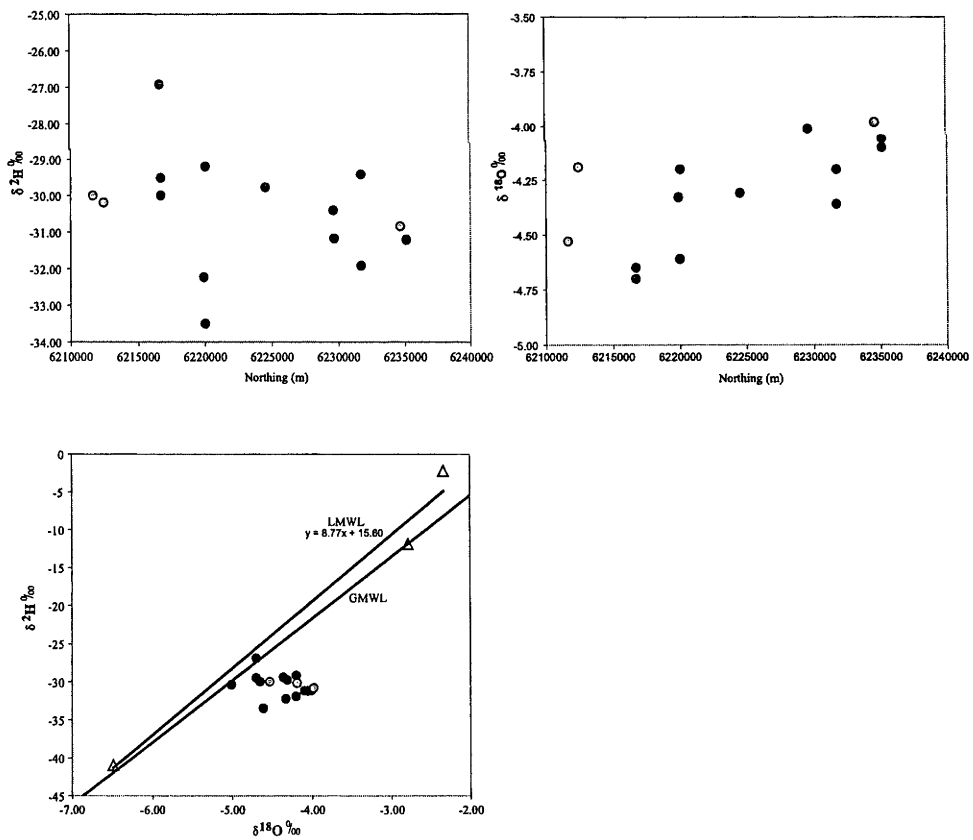

Figure 3.6: δ^2H and $\delta^{18}O$ for groundwater samples collected from the main alluvial aquifer system and from clay-rich saprolite units. Local meteoric water line (LMWL) was established from 3 rainwater samples (triangle symbols) and global meteoric water line as reported by Clark and Fritz (1997).

The δ^2H and $\delta^{18}O$ composition of water molecules in groundwater samples range from -33.50 to -26.92 and -4.70 to -3.98 ‰ respectively (Table 3.2). δ^2H distribution is variable; however, in general the data exhibit a decreasing trend along the flow path (Figure 3.6). $\delta^{18}O$ composition of groundwater increases along the flow path.

Radiogenic isotope ^{36}Cl

$^{36}Cl/Cl$ ratios in groundwater samples range from $74x10^{-15}$ to $147x10^{-15}$ and, in general, exhibit a decreasing trend along the south to north flow path (Figure 3.7). Meteoric water in this area has a Cl^- concentration of ~2 mg/l and $^{36}Cl/Cl$ ratio of approximately 380 x 10^{-15} (Chapter 5).

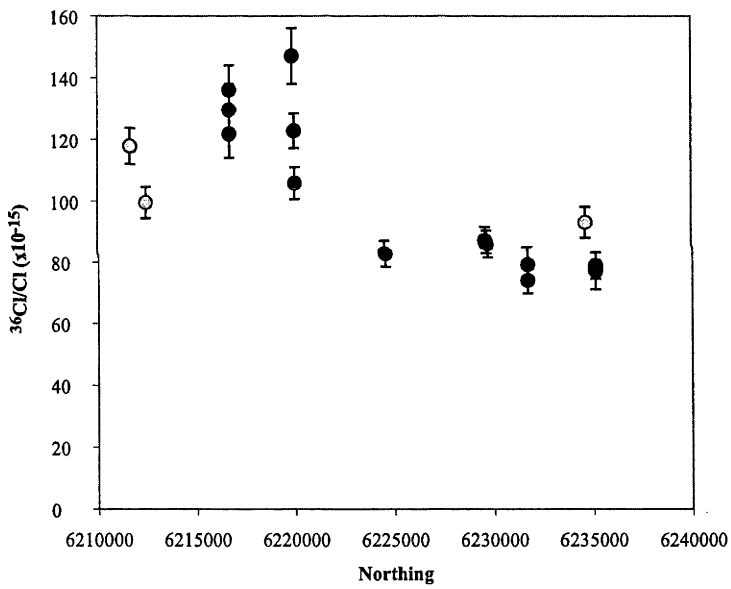

Figure 3.7: Spatial variations in $^{36}Cl/Cl$ ratios for groundwater collected from the main alluvial aquifer (black) and fine grained saprolite units (gray).

3.3.3 Pore Water Geochemical Results

Pore Water Solutes

Pore water solute concentrations in GDH03 and GDH04 exhibit considerable vertical variability at both diamond core locations (Table 3.2). Conservative anions Cl^- and

Br^-, as well as $SO4^{2-}$, also exhibit large variations throughout the two vertical profiles (Figure 3.8). However, SO_4/Cl and Br/Cl ratios are constant (Figure 3.9) throughout

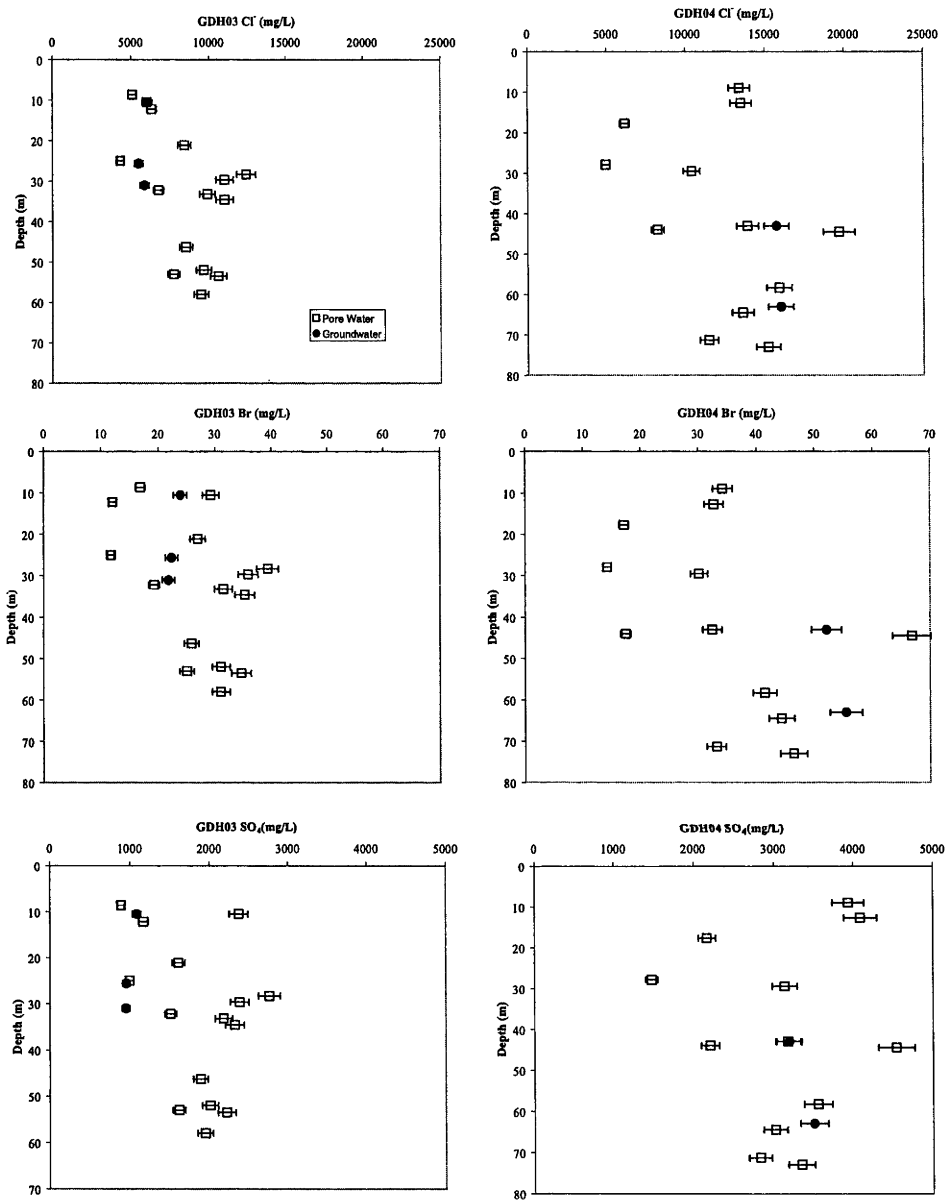

Figure 3.8: Solute concentration depth profiles for pore water extracted from diamond core materials at locations GDH03 (proximal to recharge zone) and GDH04 (distal to recharge zone, Figure 3.3). Solute concentrations in groundwater sampled from nested piezometers at both diamond core locations are plotted in the middle of the slotted interval depths.

the profiles yet differ from regional groundwater. For the purposes of this paper, only the Cl^-, Br^- and SO_4^{2-} concentrations are considered in detail. Other element concentrations are considered briefly to understand flow related geochemical reactions between groundwater and host geologic media.

Pore water Cl^-, Br^- and SO_4^{2-} concentrations, and $^{36}Cl/Cl$ ratios, are unique to each diamond core location and results are presented separately below.

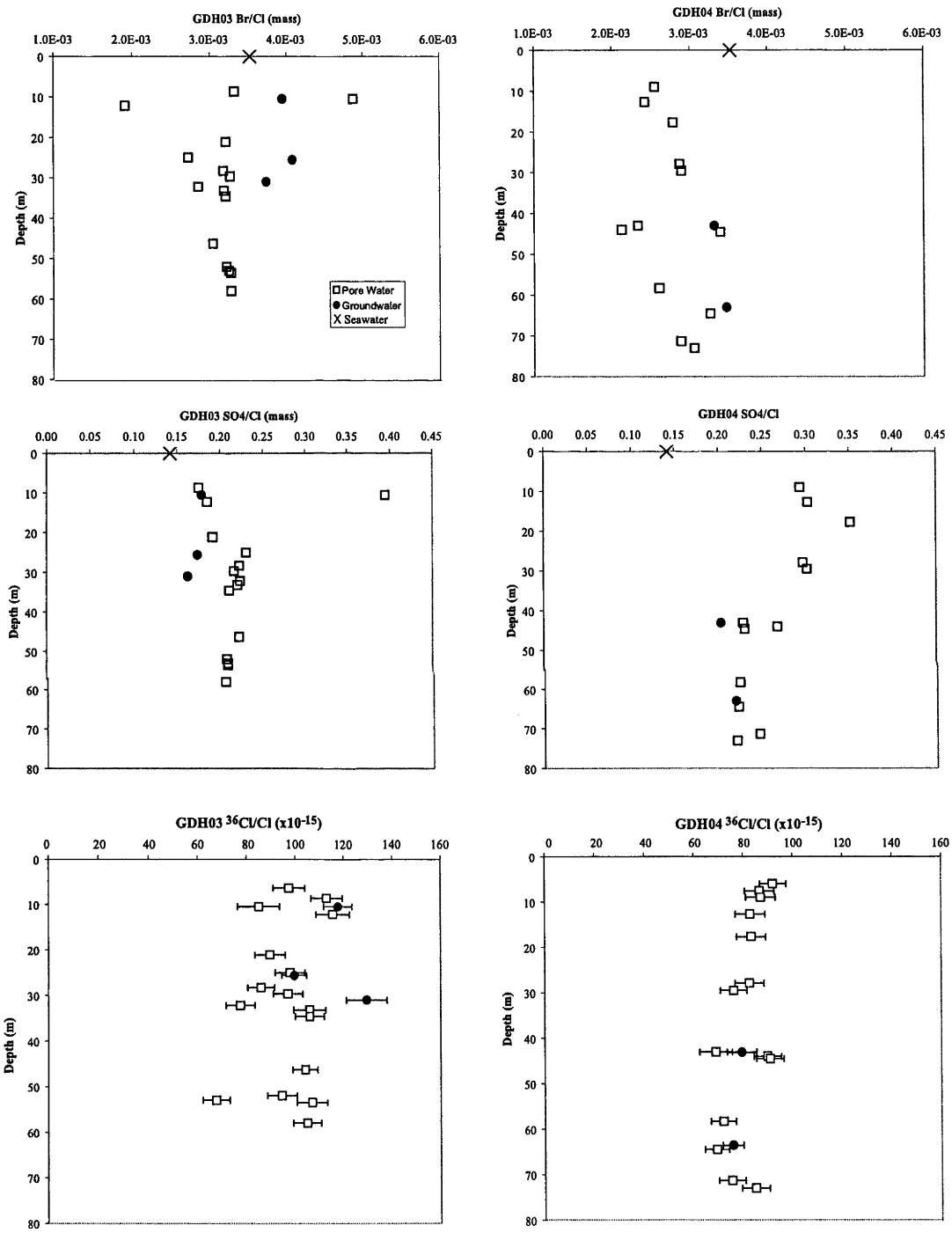

Figure 3.9: Depth profiles for selected ion ratios and $^{36}Cl/Cl$ ratios for pore water extracted from diamond core materials at locations GDH03 and GDH04. Ion ratios and $^{36}Cl/Cl$ ratios for groundwater sampled from nested piezometers at both diamond core locations are depicted as solid circles.

GDH03

Morphology and Lithology

This sampling location is situated on a present day alluvial fan, consisting of sandy alluvium sourced from granite (Gibson and Chan, 2000). This sampling location is located proximal to the suspected groundwater recharge zone in the southern portion of Barmedman Creek catchment. At this location, approximately 52 metres of sediments overlie saprolite derived from Silurian-Devonian clastic sediments (sandstone and siltstone). Vertical grainsize distribution is highly variable at this location (Figure 3.10). Groundwater was sampled from 3 nested piezometers, GDH03_1, GDH03_2 and GDH03_3 with water levels at 7.94 m, 18.16 m, and 18.86 m below the ground surface, respectively. The slotted interval at nest GDH03_1 is situated from 9-12 metres in a goethite mottled plastic grey clay unit with variable amounts of sand. The slotted intervals of GDH03_2 and GDH03_2 are both located within a coarse sand and gravel unit at 24-28 m and 28-32 m. The deepest piezometer (GDH03_3) partially extends from the coarse sand unit into a hematite mottled heavy grey clay unit at 30 m. This clay unit dominates the remainder of the profile to a depth of 50 m. A 3 metre goethite stained coarse sand unit is present at the base of the transported sediment sequence (49-52 m), which overlies a weathered siltstone and sandstone saprolite unit present to the bore termination depth of 59 metres.

Solute Profiles

Saturated zone pore water Cl^- concentrations are highly variable, but exhibit a general increasing trend from ~ 5,000 mg/l at 8.65 m to ~12,500 mg/l at 28 m, below which they fluctuate between ~ 8,000 and 11,000 mg/l (Figure 3.8). Cl^- concentrations of pore water is related to host sediment grain sizes (Figure 3.11). Coarse-grained

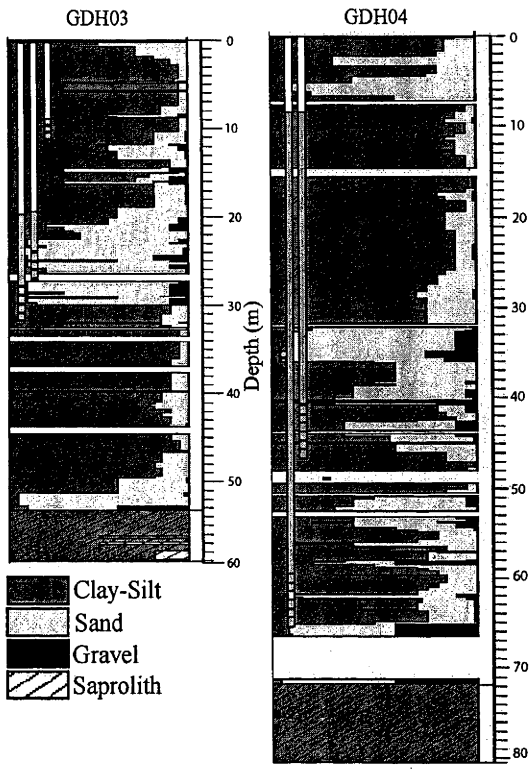

Figure 3.10: Grainsize distribution and piezometer locations for GDH03 and GDH04. Slotted interval depicted as dashed lines in lower portion of nested piezometers. Shaded portion of piezometers represents the water level measured at time of sampling (2004). Figure courtesy of Geoscience Australia.

materials (>65% sand) host pore waters with a wide range of Cl^- concentrations (4330-12400 mg/l). Clay and silt dominant (>50%) sediments appear to correlate well with pore water Cl^- > 6000 mg/l concentrations where an increase in clay/silt proportion corresponds to an increase in Cl^- concentration in pore water. Br^- and SO_4^{2-} concentrations are also highly variable throughout the depth profile with values ranging from 11.8 to 28.3 mg/l and 892 to 2760 mg/l respectively (Figure 3.8). Br/Cl and SO_4/Cl ratios are less variable, especially at depths greater than 20-30 m, than their respective element concentrations (Figure 3.9).

$^{36}Cl/Cl$ profile

$^{36}Cl/Cl$ ratios fluctuate between $76x10^{-15}$ and $116x10^{-15}$ with the greatest values located in the shallow portion of the saturated zone profile (Figure 3.9). The $^{36}Cl/Cl$ profile exhibits large variations over small depth intervals that appear unrelated to variations in sediment grain sizes (Figure 3.11).

Groundwater vs pore water

Cl^-, Br^-, and SO_4^{2-} concentrations in pore waters from diamond core GDH03 are greater, in general, than those measured in groundwater sampled from nested piezometers intersecting similar depth intervals (Figure 3.8). Pore water samples exhibit lower Br/Cl ratios and higher SO_4/Cl ratios than groundwater (Figure 3.9). $^{36}Cl/Cl$ ratios of pore waters are lower than that measured in groundwater from similar depth intervals (Figure 3.9).

GDH04 / GAC26

Morphology and Lithology

This sampling location is situated on a present day low angle alluvial fan (Gibson and Chan, 2000). Approximately 72 metres of sediments overlie saprolite derived from Late Ordovician clastic sediments and intermediate volcanics (andesite, tuff, breccia, sandstone and siltstone). Similar to diamond core GDH03, vertical grain size distribution is highly variable at this location (Figure 3.10) (Tan et al., 2002). Groundwater was sampled from two nested piezometers, GAC26_1 and GAC26_2, which were installed adjacent to the diamond core location. The slotted intervals for both nests are situated in a fine to coarse sandy unit with variable mottled clay content

at 40-46 m (GAC26_1) and 60-66 m (GAC26_2). A coarse sand and gravel unit is present at the base of the transported sediment sequence (65-72 m), which overlies weathered interbedded sand and siltstone saprolite unit present to the bore termination depth of 80 m. Groundwater levels for GDH04_1 and GDH04_2 are at 8.34 metres and 8.10 m below the ground surface, respectively.

Solute Profile

Similar to location GDH03, solute concentrations in pore water sampled at GDH04 are highly variable (Figure 3.8). Cl^-, Br^- and SO_4^{2-} concentrations range from 4980 to 19700 mg/l, 14.3 to 44.5 mg/l, and 1480 to 4540 mg/l, respectively. Samples extracted from shallow saturated zone sediments (9.0 and 12.7 m) exhibit more than twice the Cl^-, Br^- and SO_4^{2-} concentrations of samples collected at between 15-30 m (Figure 3.8). This interval is characterized by clay-rich sediments that are interpreted to be of lacustrine origin (Gibson et al., 2002). Below 30 m, Cl^-, Br^- and SO_4^{2-} concentrations are significantly greater than in the lacustrine sediments but exhibit considerable variability (Figure 3.8). In general, Cl^- and SO_4^{2-} concentrations are significantly greater than at GDH03 and Cl^- concentrations correlate poorly to sediment grain sizes (Figure 3.11). However, Br^- concentrations at both locations GDH03 and GDH04 exhibit similar ranges in values. Br/Cl ratios are lower and SO_4/Cl ratios are higher at GDH04 relative to GDH03 (Figure 3.9).

$^{36}Cl/Cl$ Profile

$^{36}Cl/Cl$ ratios fluctuate between $69x10^{-15}$ and $91x10^{-15}$ and exhibit a slight decreasing trend with increasing depth (Figure 3.9). $^{36}Cl/Cl$ ratios at GDH04 are lower and less

variable than at GDH03. The variation in $^{36}Cl/Cl$ ratios correlate poorly to variations in sediment grainsizes (Figure 3.11).

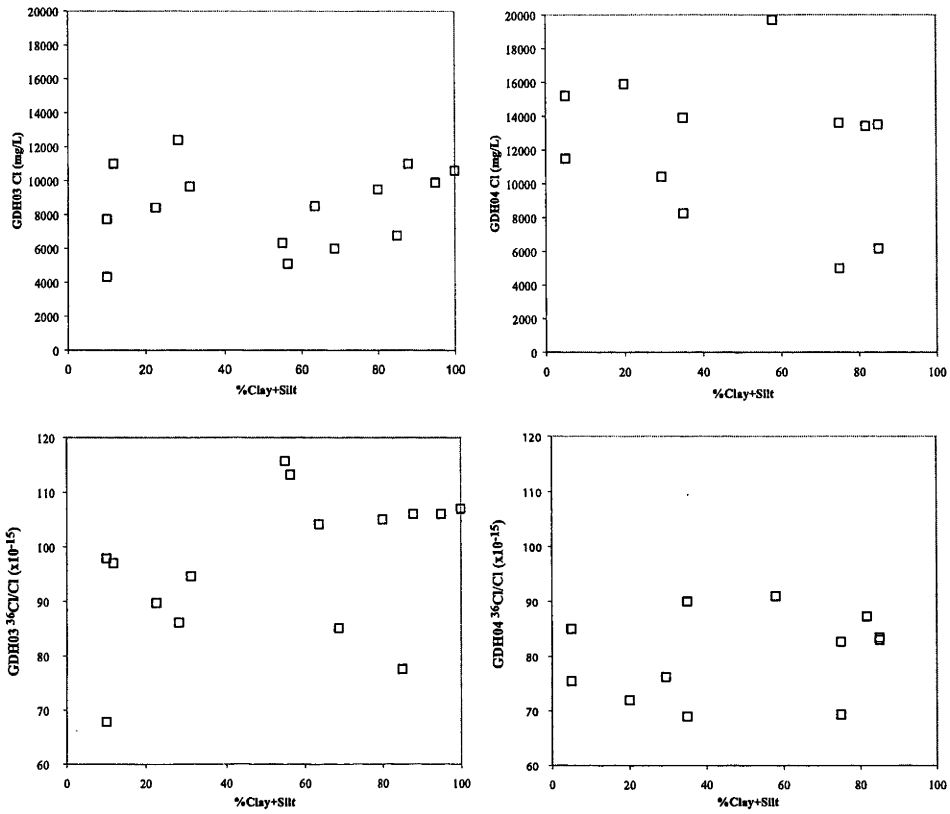

Figures 3.11: Pore water Cl^- concentrations and $^{36}Cl/Cl$ ratios as a function of sediment grain size for GDH03 (proximal to recharge zone) and GDH04 (distal to recharge zone).

Groundwater vs Pore water

Cl^-, Br^-, and SO_4^{2-} concentration in groundwater sampled from two nested piezometers located adjacent to GDH04 are within the range of values measured in pore waters extracted from sediments collected at similar depth (Figure 3.8). Cl/Br, SO_4/Cl, and $^{36}Cl/Cl$ ratios of groundwater and pore water are also similar (Figure 3.9).

3.4 Discussion

All major element data from groundwater and pore water samples were used in order to understand the geochemical processes occurring along the south to north flow path. Based on unsaturated zone Cl^- and ^{36}Cl profiles, groundwater recharge is known to

occur in the southern portion of the study location (GDH03) while a lack of recharge is apparent in the northern portion of the catchment (GDH04). This is inferred from bob-pulse ^{36}Cl at over 4 metres depth at GDH03 and a ^{36}Cl isotopic decay profile in the unsaturated zone at GDH04. Furthermore, one-dimensional piston-like flow along the hydraulic gradient (south to north) is assumed for interpreting ion mobility and solute distributions in this heterogeneous aquifer system. The groundwater samples have been categorized into two main hydrogeologic groups; the main alluvial aquifer group are those sampled from the transported middle sand unit described by Wilford et al. (2002), and the shallow (<30m) fine grained saprolite group for groundwater sampled from piezometers that intersect in-situ, highly weathered bedrock. Hydraulic heads of the saprolite unit are typically lower than in the main alluvial aquifer.

3.4.1 Ion Distribution in Groundwater

Shallow Saprolite Group

Groundwater samples, GRB10, GAC14 and GRB19 (Figure 3.3) were collected from piezometers intersecting shallow, fine-grained saprolite materials in the southern and northern portions of the study area. The two samples from the southern-most portion of the study area (GRB10 and GAC14) exhibit greater solute concentrations than groundwater sampled further along the flow path in the main alluvial aquifer (Figure 3.4). These samples also exhibit element ratios that differ from each other and from samples collected from the alluvial aquifer (Figure 3.5), which indicates a lack of connectivity between the two hydrogeologic units in the southern portion of the study area. The sample collected from the northern portion of the study (GRB19) area exhibits similar TDS and element ratios to groundwater sampled in the vicinity from the alluvial aquifer (Figures 3.4 & 3.5). The major element data from this location

suggests some degree of connectivity between the fine grained saprolite unit and the coarser grained alluvial aquifer.

Main Alluvial Aquifer

Cl concentrations and $^{36}Cl/Cl$ ratios in groundwater sampled from the main alluvial aquifer range from 5,400 to 16,500 mg/l and $74x10^{-15}$ to $147x10^{-15}$, respectively. This is in contrast to groundwater in the Bland Basin that has Cl ranging from 7 to 17,100 mg/l with the majority of the samples having Cl < 1,000 mg/l (Carrara, 2005). $^{36}Cl/Cl$ ratios range from 122 to 179 x 10^{-15} (Carrara et al., 2004).All major element concentrations increase along the inferred flow path (Figure 3.4), which suggests a subsurface source of solutes to the system. However, only conservative anions Cl^- and Br^-, as well as $SO4^{2-}$, Na^+ and Ca^{2+} concentrations increase systematically along the flow path. Cl^- and Br^- are the most chemically conservative, and the only subsurface sources for these element are mixing between the different hydrogeologic units and evaporative mineral dissolution/precipitation.

Na/Cl molar ratios and Br/Cl mass ratios decrease slightly along the flow path (Figure 3.5) suggesting either addition of Cl^- or removal of Na^+ and Br^- from solution. If the increase in Cl^- along the flow path were caused by halite dissolution, the Na/Cl molar ratio would increase towards a value of 1. Instead the ratio decreases with increasing Cl^- (Figure 3.12), which suggests either an additional source for Cl^- or a subsurface sink for Na^+. Na/Ca mass ratios decrease with increasing Cl^- (Figure 3.12), and Ca/Cl mass ratios increase along the flow path and with increasing salinity (Figure 3.4). Carrara (2005) also noted a decrease in Na/Ca ratios with increasing salinity and attributed this to cation exchange. Due to a preference for Na^+ over Ca^{2+} on the

exchange sites of 2:1 clays as the ionic strength of a solution increases (Arad and Evans, 1987), these data trends indicate that ion exchange, rather than halite dissolution, is influencing the Na/Cl and Na/Ca ratios of groundwater. Cartwright et al., 2007b discussed the relative importance of cation exchange in groundwater systems in the southeast Murray basin. The authors concluded that although cation exchange appeared to control 87Sr/86Sr ratios in groundwater, it had little affect on the major element chemistry. Based on Na/Cl and Cl/Br ratios of groundwater of the greater Bland basin, Carrara et al., 2005, concluded that halite dissolution was insignificant and the observed variations in Na/Cl ratios were the result of water-rock interations. Further water rock interactions are indicated from the ^{2}H and ^{18}O data (Figure 3.6). The enrichment in ^{18}O along the flow path, as well as relative to ^{2}H suggests potential silicate weathering along the flow path. Carrarar et al., 2005 noted

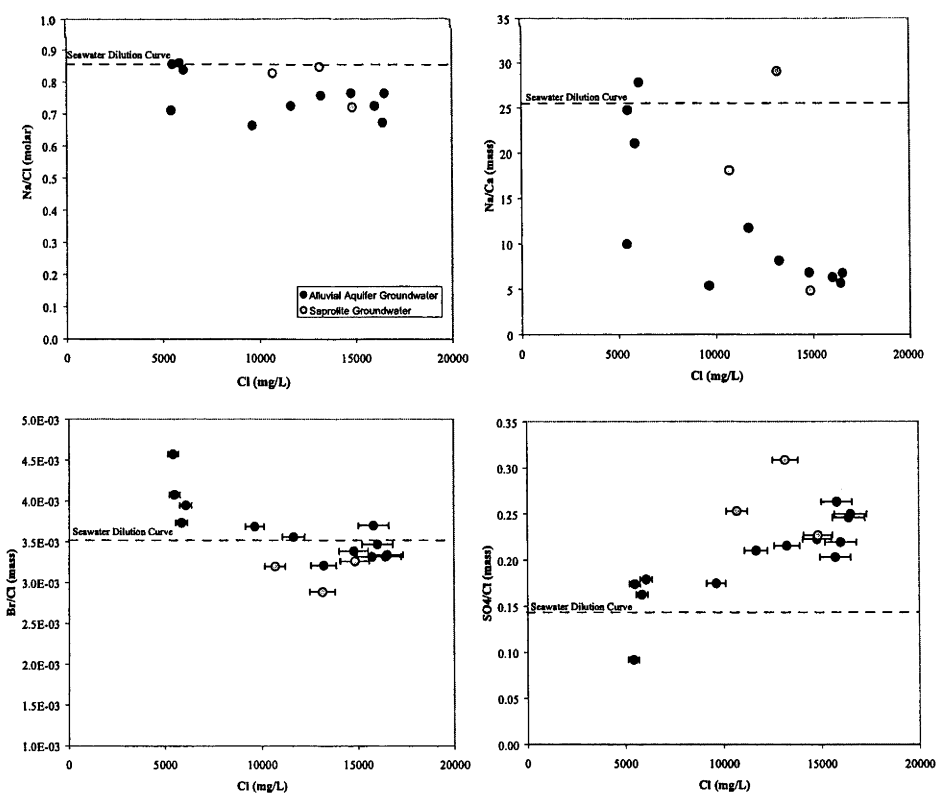

Figure 3.12: Ion ratios relative to chloride concentrations for groundwater samples collected from the

main alluvial aquifer and from fine grained saprolite units. Seawater dilution curves are depicted on plots for reference.

3.4.2 Groundwater Mixing

The decrease in Br/Cl mass ratio along the flow path (Figure 3.4), and decrease in ratio with increasing Cl^- (Figure 3.12) suggest an additional subsurface source of Cl^-, which is slowly being added to groundwater along the south to north flow path. SO_4/Cl ratios increase slightly along the flow path (Figure 3.5) and also increase with increasing Cl^- (Figure 3.12). Similar to the previously discussed trends in Na/Cl ratios, the SO_4/Cl trends are also contrary to dissolution of Cl^- bearing solutes. The most probable explanation appears to be mixing between less saline groundwater and a more saline endmember water with a composition more enriched in Cl^- and SO_4^{2-}. This is in contrast to the finding of Carrara (2005) for the groundwater systems in the Bland Basin where increases in salinity and constant Cl/Br and $^{36}Cl/Cl$ ratios were attributed to evapotranspiration.

The mixing endmember water responsible for the increasing salinity in the Barmedman Creek Aquifer is potentially residing within lower permeable units within the aquifer and surrounding aquitards. Similar occurrences were discussed by Domenico and Robbins (1985), who suggested that connate waters within sandstone units of the Milk River aquifer system in Canada were being displaced by meteoric recharge water. Based on numerical modelling, they estimated that displacement/mixing processes needed to occur over timescales of several millions of years to achieve a steady state, uniform solute distribution. Within a portion of the Milk River aquifer system, Fabryka-Martin et al. (1991) also encountered subsurface

sources of Cl^- and attributed the physical heterogeneity of the aquifer materials to a greater displacement of connate waters in more permeable sandstone than from less permeable shale. The authors concluded that the heterogeneous solute distribution resulted in the diffusion of higher concentration waters from less permeable to more permeable portions of the aquifer. The observed changes in chemical composition along the flow path, as well as decrease in $^{36}Cl/Cl$ ratios, in this study area supports the theory of "connate" pore waters slowly being displaced by, or mixed with younger, meteoric sourced water. The availability of vertical geochemical profiles from diamond cores GDH03 and GDH04 provide a means for assessing potential endmember compositions and subsequent modelling of the effects of incremental mixing on solute concentrations and $^{36}Cl/Cl$ ratios in groundwater.

3.4.3 Subsurface Solute Sources:

GDH03

At borehole GDH03, located proximal to the recharge zone (Figure 3.3), pore water within the unconsolidated aquifer sediments contain significantly higher solute concentrations than groundwater sampled from piezometers at similar depth intervals (Figure 3.8). Pore waters from within the aquifer also exhibit lower Br/Cl ratios and greater SO_4/Cl ratios than groundwater and Ca/Cl and Na/Cl ratios of pore waters are similar to those in groundwater (Figure 3.9). $^{36}Cl/Cl$ ratios of pore water are significantly less than the ratios of groundwater (Figure 3.9). Sampling of groundwater may preferentially sample water from the higher porosity portions of the aquifer that may have lower salinity. Groundwater samples may be a mixture if all pore waters within the screened interval. Conversely, groundwater may flow through higher porosity sediments thereby not flushing solutes from lower permeability

sediments therefore groundwater samples reflect the mobile fraction of water in the saturated zone. The difference in chemical composition between groundwater and pore water suggests that waters residing within the lower porosity sediments could reflect palaeo-hydrogeochemical conditions.

Similar Ca/Cl and Na/Cl ratios suggest similar geochemical processes have influenced both groundwater and pore water. Because Br/Cl ratios and SO_4/Cl ratios differ between groundwater and pore water ratios, it is unlikely that dissolution or precipitation of minerals such as halite or gypsum has produced the similar Na/Cl and Ca/Cl ratios. An alternative explanation is that similar cation exchange reactions have influenced both pore waters and groundwater, and the difference between Br/Cl and SO_4/Cl ratios of groundwater and pore water may reflect palaeo-climatic or paleao-hydrogeological conditions. Pore waters may also represent connate water deposited with sediments under dramatically different climatic conditions than present. This later possibility will be discussed with relation to ^{36}Cl in a later section. However, this explanation is unlikely considering that saturated zone sediments are presumably much older than the maximum ^{36}Cl dateable age (~1.5 mya,) and if the pore water were isolated at the time of deposition they would exhibit $^{36}Cl/Cl$ ratios closer to secular equilibrium ratios ($<12.5 \times 10^{-15}$) with sedimentary mineralogies (Bentley et al., 1986a). Instead, pore waters exhibit much higher ratios ($76\text{-}115 \times 10^{-15}$) and probably reflect a mixture of ancient and more modern water.

At borehole GDH04, located distally to the recharge area (Figure 3.3), pore waters sampled from aquifer materials exhibit similar solute concentrations and major element ratios to groundwater (Figures 3.8 & 3.9). $^{36}Cl/Cl$ ratios of pore water and groundwater are also similar (Figure 3.9). Other groundwater samples collected at the distal portion of the study area exhibit similar ion ratios and $^{36}C/Cl$ ratios as pore water from this location (Figures 3.5 & 3.7). This suggests that, along the flow path from GDH03 to GDH04, groundwater has equilibrated with the pore waters, and that mixing between lower and higher permeability units is less significant in the distal portion of this flow system.

3.4.4 Solute Mobility and Mixing

In the Milk River aquifer system in Canada, Fabryka-Martin et al. (1991) described pore water groundwater mixing processes as a function of proximity to recharge areas. Near the recharge areas, they observed large concentration gradients between groundwater in sandstone and pore water within shale units. This resulted in diffusion from the shale into the more conductive sandstone portion of the aquifer. As diffusion continued, groundwater Cl^- concentrations increased along the flow path and resulted in smaller concentration gradients between pore water and groundwater. This resulted in a decrease in diffusion in the distal portion of the aquifer system. Data from this study are consistent with their mixing model; particularly from the evidence of disequilibrium between aquifer pore water and groundwater at GDH03, and the increase in groundwater salinity along the flow path. The non-linear increase in Cl^- along the flow path (Figure 3.4) suggests that as groundwater Cl^- concentrations increase, mixing between pore water and groundwater decrease. Considering that halite dissolution does not appear to be a Cl^- source to this aquifer system, and

assuming Cl^- concentration as a proxy for quantity of mixing, the rate of mixing can be estimated from the position along the flow path. The rapid increase in groundwater Cl^- concentrations proximal to the recharge area suggests that mixing rates are greater in this portion of the study area than in the distal portion of the system. This further supports the theory that diffusive rather than advective transport of solutes from low permeability to higher permeability units is the dominant mixing process. Alternatively, the non-linear increase in Cl^- (Figure 3.4) could also be the result of a constant Cl^- flux from the lower permeability units into the aquifer. However, considering the complex nature of this aquifer system and the uncertainties associated with calculations of linear flow velocities and poorly constrained subsurface architecture, assuming constant advective transport rates from low permeability units in to the aquifer does not seem logical. Instead, a more simplified approach to understand the quantity of mixing at any given point along the flow path is employed based on Cl^- as a function of northing.

Cl^- as a proxy for mixing

In general, the Cl^- concentration in groundwater increases systematically along the flow path. However, three bores (GAC16, GAC17 and GAC18) located at similar geographical northings exhibit a large range in Cl^- concentrations (Figure 3.4). At this location there is a slight west-east hydraulic gradient. The Cl^- concentration of groundwater from these bores is greatest in the west (GAC16) and the lowest in the east (GAC18). GAC18 is located on the slopes of sandy alluvium sourced from the adjacent Barmedman Granite hills (Figure 3.3). Based on the Cl^- distribution in this area, it is possible that groundwater recharge is occurring in the vicinity of the granite

outcroppings and associated sandy alluvium. As such, two different mixing models based on the location of the recharge zone will be considered.

Model boundaries

This 1st model is based on the assumption that no groundwater recharge occurs north of borehole GDH03, and that only mixing is responsible for the increase in Cl^- concentration along the flow path (Figure 3.13). The 2nd model assumes the same except starting from borehole GAC17 (Figure 3.13). These models will be referred to as Model 1 and Model 2 respectively. From the measured Cl^- concentrations in groundwater, the amount of Cl^- being added to the main alluvial aquifer system per metre of flow along the south to north hydraulic gradient was calculated based on the slope of the best fit polynomial trend lines in Figure 3.13. If these functions represent the actual mixing fraction, changes in chemical composition along the flow path could be modelled if appropriate mixing endmember compositions can be determined. The starting endmember composition for Model 1 is assumed to be the composition of groundwater at location GDH03 and Model 2 assumes a starting endmember composition of groundwater sampled at GAC17. Selection of saline endmember compositions is discussed below.

Mixing endmember compositions

Similar Br/Cl and SO_4/Cl ratios are present in pore waters from both GDH03 and GDH04. If we assume these ratios represent endmember compositions then the effects

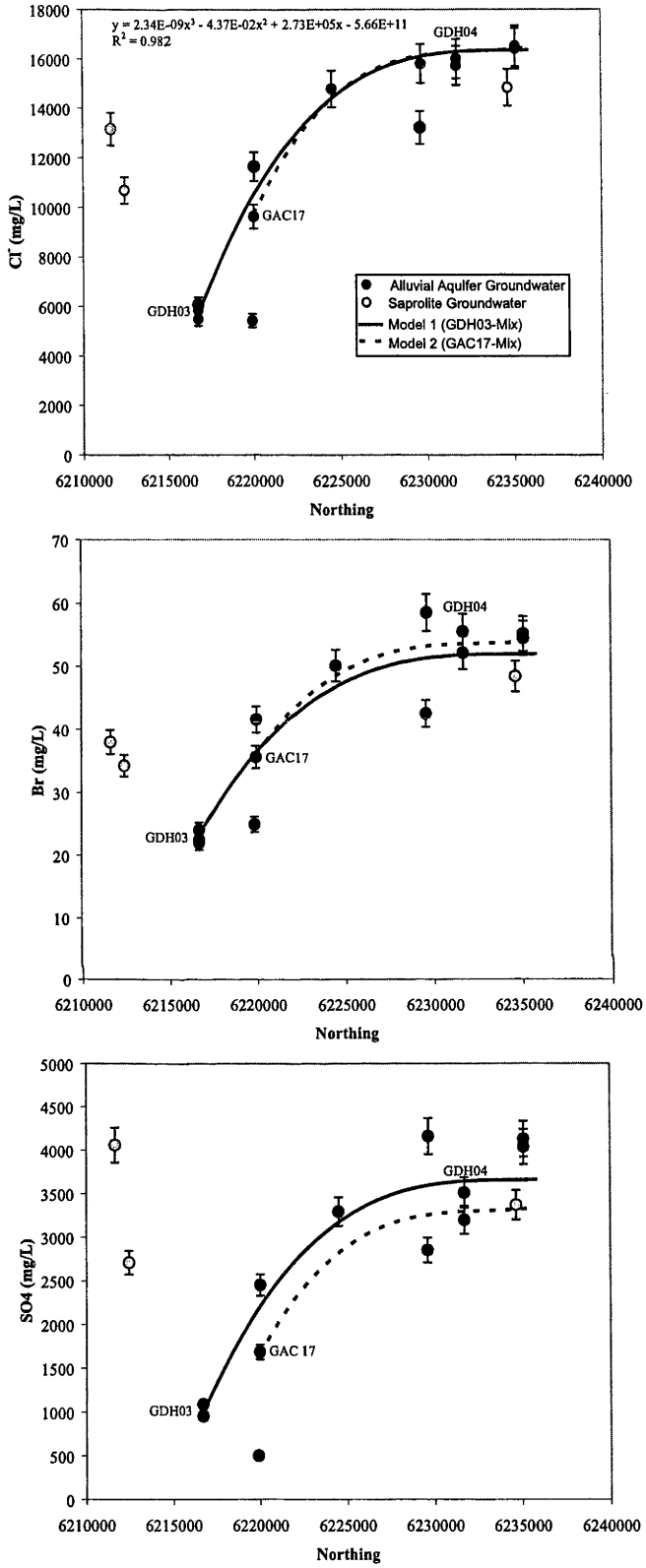

Figure 3.13: Modelled trends for Cl, Br and SO_4 concentrations in groundwater as a function of geographical northing. Mixing established from spatial distribution of Cl concentration in groundwater (Figure 3.4), and mixing endmember compositions established from pore water compositions at diamond cores GDH03 and GDH04 (Figures 3.8). Models assumes south to north, one dimensional south to north piston-like flow. Model 1 assumes no recharge is occurring beyond piezometer GDH03 (Figure 3.3), and Model 2 assumes no recharge is occurring beyond piezometer GAC 17 (Figure 3.3).

of mixing along the flow path can be predicted based on the slope of trend lines for Cl^- concentration vs geographical northing. Because trends in major cation concentrations indicate processes other than simple mixing, only trends for Cl^-, Br^- and SO_4^{2-} are considered in the models.

Modelled solute mixing trends

Figure 3.13 depicts the predicted trend lines for Br^- and SO_4^{2-} as a function of northing. The saline pore water endmember values were chosen from pore waters at GDH03 that exhibited higher Cl^- concentrations than groundwater and that also exhibited similar Br/Cl ratios and SO_4/Cl ratios to pore waters at GDH04. Br/Cl mass ratio of 2.7×10^{-3} and SO_4/Cl mass ratio 0.25 were used as endmember compositions to calculate their respective increases in concentration along the flow path from the Cl^- verses northing trend line in Figure 3.13. Both the predicted trends in Br^- and SO_4^{2-} concentrations relative to inferred flow path position agree relatively well with the observed data (Figure 3.14).

Figure 3.14 depicts the modelled trend for Br/Cl and SO_4/Cl ratios versus geographical northing and their ratios relative to Cl^-. The modelled trends qualitatively describe the general trend in data, but fail to accurately quantify the observed changes in chemical composition of groundwater with respect to flow path position and Cl^- concentration. The models better described the trends in Br/Cl ratios than trends in SO_4^{2-} suggesting that either SO_4^{2-} is not chemically conservative in this system or that inappropriate endmember compositions were chosen for the models.

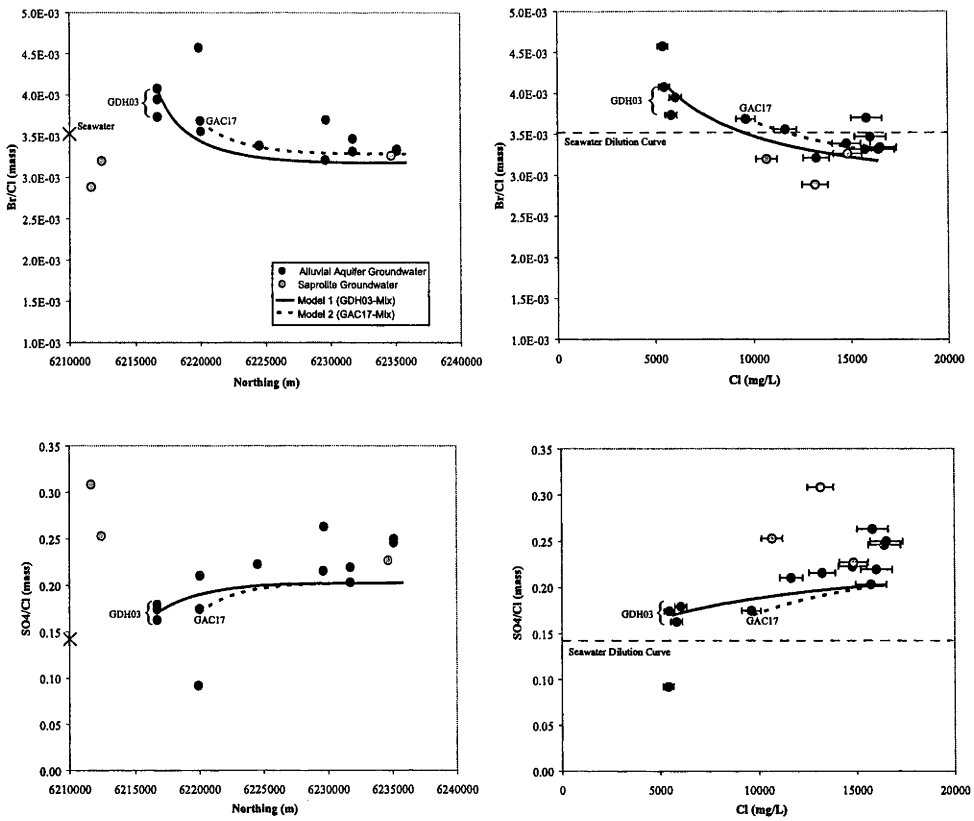

Figure 3.14: Modelled trends for ion ratios in groundwater as a function of northing and chloride concentration. Mixing established from spatial distribution of chloride concentration in groundwater (Figure 3.4), and mixing endmember compositions established from pore water compositions and ion ratios at diamond cores GDH03 and GDH04 (Figures 3.8 & 3.9). Models assumes south to north, one dimensional south to north piston-like flow. Model 1 assumes no recharge is occurring beyond piezometer GDH03 (Figure 3.3), and Model 2 assumes no recharge is occurring beyond piezometer GAC 17 (Figure 3.3).

Model 1 appears to best match the measured trends in groundwater samples. This suggests that mixing between groundwater and pore waters are the dominant process resulting in the observed increase in solutes along the flow path. Furthermore, the better correlation with Model 1 suggests that groundwater recharge is not occurring beyond borehole GDH03. The occurrence of low TDS water from borehole GAC18 contradicts this theory; however, the modelled and measured trends for Cl^-, Br^-, and SO_4^{2-} concentrations and their respective ion ratios suggest this is not the case. One possible explanation is that the west to southwest flow may be preventing any significant mixing of the lower salinity water in the east, with the more saline groundwater to the west.

3.4.5 Implications of Mixing on $^{36}Cl/Cl$ Ratios in Groundwater:

Similar to the solute mixing models discussed above, the saturated zone $^{36}Cl/Cl$ profiles allow for consideration of potential endmember ratios for modelling the effects of mixing on the measured $^{36}Cl/Cl$ ratios in groundwater. At both GDH03 and GDH04, numerous pore water extracts from aquifer materials exhibit $^{36}Cl/Cl$ ratios ranging from 70 $x10^{-15}$ to $80x10^{-15}$ (Figure 3.9). At GDH03 pore waters with similar $^{36}Cl/Cl$ ratios to pore waters at GDH04 exhibit higher Cl^- concentrations and lower $^{36}Cl/Cl$ ratios than groundwater, and are chosen as endmember mixing values for entering into the numerical mixing models established above.

Modelled $^{36}Cl/Cl$ mixing trends

Figure 3.15 depicts modelled $^{36}Cl/Cl$ trends as a function of northing for the mixing of groundwater from GDH03 (Model 1) and GAC17 (Model 2) with saline endmember ratios of $70x10^{-15}$ and $80x10^{-15}$. As discussed above, the mixing proportion was established from the trend in Cl^- vs. geographical northing. Figure 3.15 also depicts the modelled $^{36}Cl/Cl$ trends as a function of Cl^- concentration. With the exception of GRB14 and GAC28, all curves fall above the ratios measured in groundwater sampled from the distal portion of this study area. This suggests that either the parameters used in this model are inaccurate, or that isotopic decay accounts for the discrepancy between the modelled and measured trends. Considering the relative success of these models for interpreting solute distributions above, and a lack of evidence for $^{36}Cl/Cl$ ratios lower than $70x10^{-15}$, the parameters used in this model appear to be the most accurate available for this study. As such, isotopic decay seems the most probable explanation for the discrepancy between modelled mixing trends and measured ratios

in groundwater samples. Therefore, determining the actual flow ages of groundwater is only limited by which endmember ratios and which mixing models are chosen to quantify the effects of mixing on the measured $^{36}Cl/Cl$ ratios in groundwater.

Model validity

$^{36}Cl/Cl$ based groundwater ages can be calculated from the standard decay equation (Bentley et al., 1986a):

$$t = -1/\lambda \ln(R_s/R_r) \quad (1)$$

where $1/\lambda$ is the mean life of ^{36}Cl (434,251 years), R_s is the $^{36}Cl/Cl$ ratio of the groundwater sample and R_r is the initial $^{36}Cl/Cl$ ratio of groundwater recharge. For the purpose of this paper, R_r is considered the predicted $^{36}Cl/Cl$ ratio value of mixed groundwater at the equivalent geographic northing and Cl^- concentration as the actual groundwater sample (R_s). The groundwater ratios in the distal portion of the study area exhibit ranges in $^{36}Cl/Cl$ ratios that are within the analytical error of the measurements. Assuming the sample collected from furthest along the hydraulic gradient (GAC23) is the oldest, the flow ages corrected for "age-mixing" range depending on the model parameters are as follows: For mixing from GDH03 with $^{36}Cl/Cl$ endmember ratios of $70x10^{-15}$ and $80x10^{-15}$, the corrected ages are 58,000 and 89,000 yrs respectively. For mixing from GAC17 with $^{36}Cl/Cl$ endmember ratios of $70x10^{-15}$ and $80x10^{-15}$, the corrected ages are 119,000 and 136,000 yrs respectively.

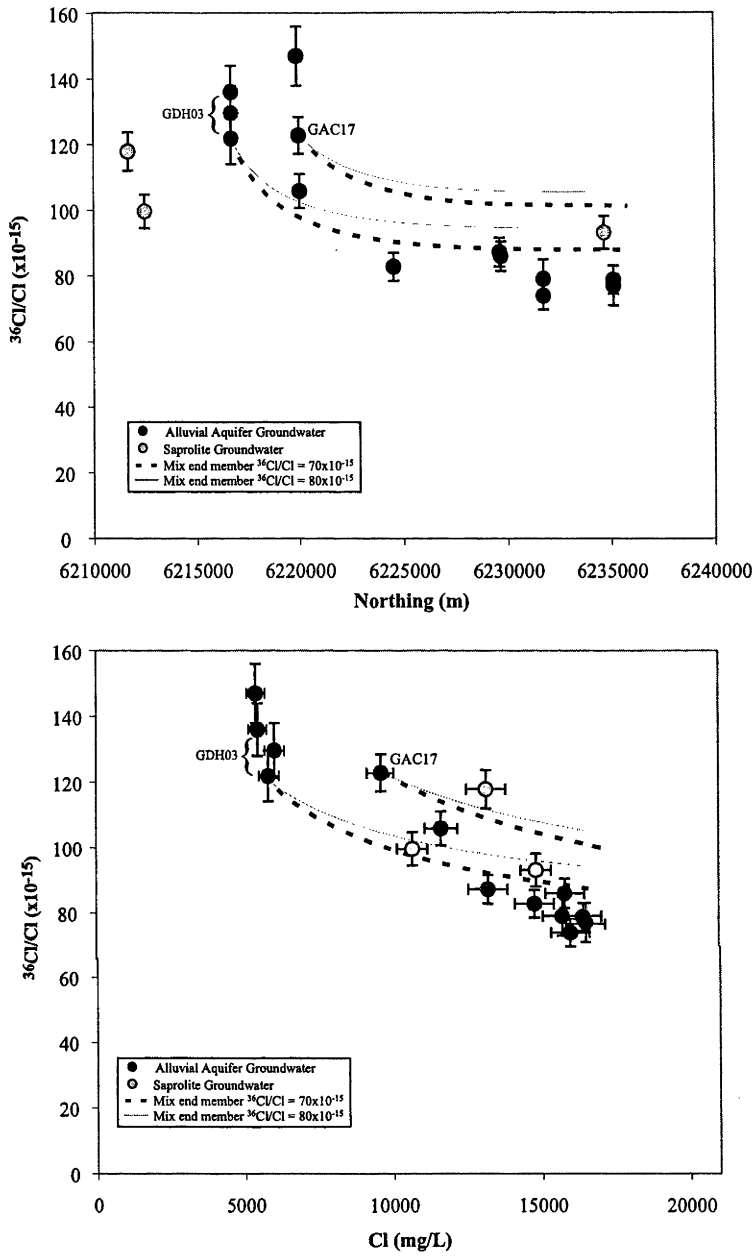

Figure 3.15: Modelled trends for ^{36}Cl/Cl ratios in groundwater as a function of northing and chloride concentration. Mixing rates established from spatial distribution of chloride concentration in groundwater (Figure 3.4), and mixing endmember ratios established from ^{36}Cl/Cl ratios in pore water at diamond cores GDH03 and GDH04 (Figures 3.9). Mixing endmembers ratios of $70x10^{-15}$ and $80x10^{-15}$ are used in this model. Models assume south to north, one dimensional piston-like flow. Model 1 assumes no recharge is occurring beyond piezometer GDH03 (Figure 3.3), and that mixing between pore water and groundwater is the only process influencing the decrease in ^{36}Cl/Cl ratios along the flow path. Model 2 assumes no recharge is occurring beyond piezometer GAC 17 (Figure 3.3) and, similar to Model 1, that mixing is the only process influencing the ^{36}Cl/Cl ratios along the flow path.

Modelled mixing and "aging" trends

From the corrected ages calculated above, the amount of isotopic decay occurring along the flow path can be incorporated into the numerical models (Figure 3.16).

Models that assume mixing and isotopic decay from GAC17 (Model 2) to GAC23 correlate less well with the measured data than for models that assume mixing and isotopic decay from GDH03 (Model 1) to GAC23. Relatively poor correlations were also obtained from the solute mixing trends calculated with this Model 2 (Figures 3.13 & 3.14). The model which best describes the measured trend in groundwater data is one which assumes mixing of groundwater from borehole GDH03 to borehole GAC23 (model 1) with an endmember ratio of $70x10^{-15}$. Reasonable correlations were also obtained from the solute mixing trends calculated with this model. This further supports that groundwater recharge is not occurring down gradient of borehole GDH03 and that mixing is the dominant process influencing Cl^-, Br^-, SO_4^{2-} concentrations, as well as $^{36}Cl/Cl$ ratios in groundwater.

Corrected flow ages

Corrected flow ages for groundwater samples in the distal portion of the study area are calculated from the differences between modelled $^{36}Cl/Cl$ ratios of mixing Model 1 and the actual ratios measured in groundwater samples. The corrected ages for samples collected from the distal portion of this study area are variable, but generally range from 50,000 to 75,000 yrs. Uncorrected flow ages for these samples, calculated from the differences in $^{36}Cl/Cl$ ratios from groundwater in the proximal portion of the study area (GDH03) and groundwater in the distal portion of the study area (GAC23) range from 237,000 – 265,000 yrs. The corrected flow ages are in far better agreement with the piston flow age calculated from the southernmost (GDH03) to the northernmost bore hole (GAC23) of 65,000 yrs.

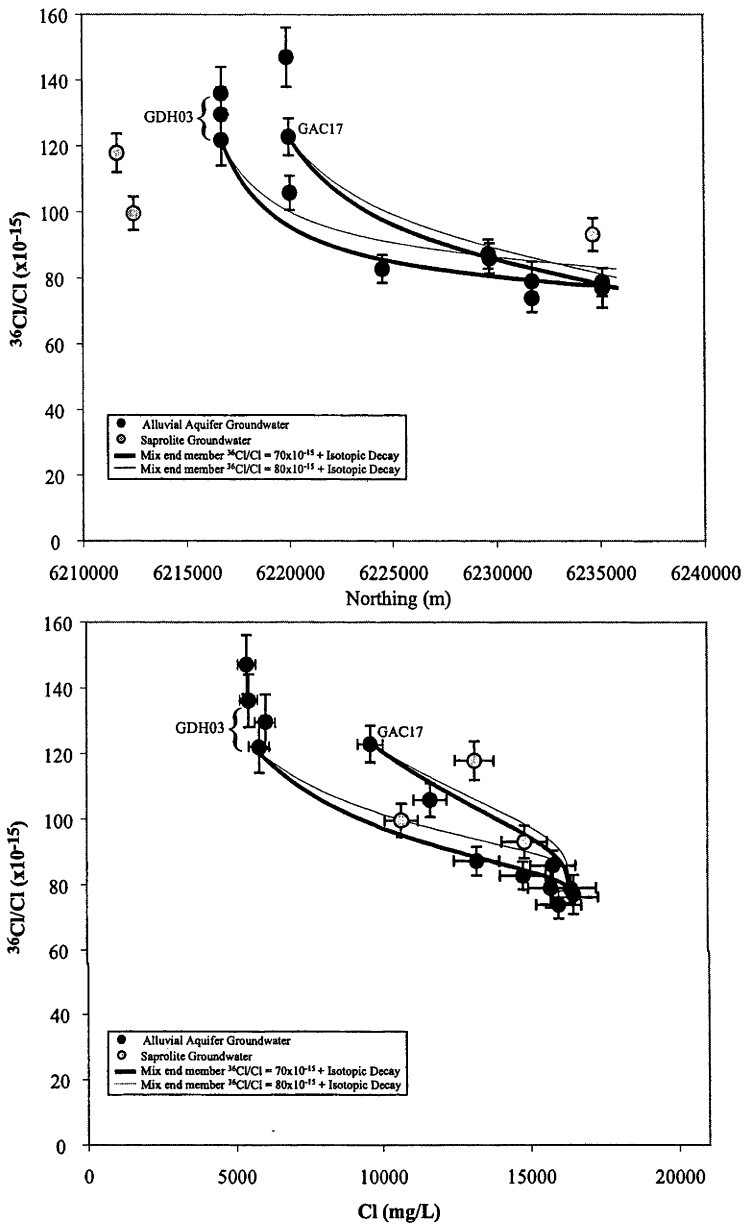

Figure 3.16: Modelled mixing and decay trends for $^{36}Cl/Cl$ ratios in groundwater as a function of northing and chloride concentration. Mixing amounts established from spatial distribution of chloride concentration in groundwater (Figure 3.4), and mixing end member ratios established from $^{36}Cl/Cl$ ratios in pore water at diamond cores GDH03 and GDH04 (Figures 3.9). The models incorporated isotopic decay into the numerical mixing models in Figure 3.15.

3.5 Conclusion

Barmedman Creek catchment is a low-lying alluvial basin that contains a heterogenous aquifer system hosting highly saline groundwater (Cl^- > 16,000 mg/l). Solute concentrations in groundwater exhibit systematic increases along the inferred

flow path. The sources for these solutes are low permeability portions of the aquifers and aquitards which host highly saline pore waters enriched in Cl^- and SO_4^{2-} relative to groundwater in the aquifer. Spatial variations in Cl^- concentration in groundwater function as a useful proxy for quantifying mixing between pore water and groundwater.

The availability of saturated zone pore water geochemical data has allowed for establishing geochemical endmember concentrations for inclusion into the Cl^- based mixing models. Modelled mixing trends for the conservative anion Br^-, as well as for less conservative SO_4^{2-}, correlated well with the measured trends in solute concentrations and element ratios. The model which best described the trend in measured data was one which assumed one-dimensional piston-like flow along a south to north hydraulic gradient. This model assumed no significant groundwater recharge occurring north of borehole GDH03 and that mixing with saturated zone pore waters was the dominant source of solutes to the system.

This model was also applied to help understand the effects of age mixing on the measured $^{36}Cl/Cl$ ratios in groundwater. Mixing endmembers were also selected from pre-existing pore water geochemical data and were incorporated into the Cl-based mixing models. The calculated mixing trends failed to describe the observed decrease in $^{36}C/Cl$ ratios along the flow path. The discrepancy between modelled and measured trends is the result of isotopic decay. Incorporating isotopic decay into the mixing model produced trends that correlated well with the measured data. However, mixing was still the dominant process resulting in the observed decrease in ratios along the flow path.

Uncorrected flow ages for these groundwaters range from 237,000 – 265,000 yrs. Corrected age calculations which account for the affects of "age-mixing" along the flow path suggest a much younger range of 50,000 and 75,000 yrs. This range in flow ages for groundwater sampled at the distal end of the system agrees well with the hydrodynamic age of 65,000 yrs.

4 GEOCHEMICAL EVOLUTION OF SALINE GROUNDWATER IN THE UNSATURATED ZONE

4.0 Introduction

Numerous hydrogeochemical studies throughout the world have recognized large discrepancies between chemical compositions of meteoric water, surface water and groundwater (i.e., Gibbs, 1970; Lundstrom and Olin, 1986; Herczeg et al., 1993; Davis et al., 1998b). However, less attention has been focused on understanding the geochemical processes and their implications on water resources, in particular groundwater salinity. Widely accepted conceptual models of the hydrologic cycle depict rainwater, derived from evaporation of seawater, as the atmospheric input to the continental fresh water cycle. Atmospheric precipitation generally has distinctive compositions that vary considerably from seawater due to incorporation of continental dust, biomass burning, anthropogenic pollution, and oxidation of organic matter (Blackburn and McLeod, 1983; Lundstrom and Olin, 1986; Chivas et al., 1991; Mano and Andreau, 1994; Sander et al., 2003). Groundwater and surface water are often sourced from meteoric water, yet can exhibit "marine" like chemical signatures that are regularly ascribed to hydrogeochemical processes such as evapotranspiration, mineral dissolution and precipitation, and cation exchange (i.e., Herczeg et al., 1993; Love et al., 2000; Herczeg et al., 2001; Davis et al., 2004; Cartwright et al., 2006). Commonly, these processes are assumed to occur during groundwater recharge in the unsaturated zone; however, very few groundwater studies have incorporated unsaturated zone solute dynamics into their interpretations of groundwater chemistry. Numerous studies have utilized Cl^- concentrations of soil water in the unsaturated zone to estimate infiltration rates (i.e., Eriksson and Khunakasem, 1969; Allison and

Hughes, 1978; Peck et al., 1981; Allison and Hughes, 1983; Scanlon, 1991; Wood, 1999), the timeframes of solute accumulation (Allison et al., 1985; Cook et al., 1992; Zhu et al., 2003), and to determine flow characteristics (matrix and/or preferential flow) and the effects of evapotranspiration (i.e., Peck et al., 1981; Ullman, 1985; Johnston, 1987; Cartwright et al., 2006). However, due to the typically chemically conservative nature of the Cl^- ion, reactions with sediments, plants and microbial biomass during groundwater recharge are often overlooked by hydrogeochemical studies that utilize only Cl^- profiles to understand processes in the unsaturated zone. Interpretations of other solute distributions may help develop a greater understanding of all unsaturated zone geochemical and biogeochemical reactions.

The influences of both biotic and abiotic processes in near surface sedimentary environments have been well documented. For example, nutrient cycling can have a significant effect on K^+,Ca^{2+},Mg^{2+},NO_3^-, and PO_4^{3-} distributions in near surface soils (i.e., Johnson, 1984; Foulds, 1993; Jobaggy and Jackson, 2001). In addition, processes such as organic adsorption and bioassimilation of solutes in rainwater during infiltration of near surface soils can significantly influence solute dynamics in the unsaturated zone (i.e., Gerritse and George, 1988; Mayer et al., 1995a; Mayer et al., 2001; Novak et al., 2003; Giesler et al., 2005). The effects of these processes on the chemical composition of groundwater have been considered to a far lesser extent (Kreitler and Jones, 1975; Mayer et al., 1995b; Walvoord et al., 2003; White et al., 2006). In addition to Cl^-, high resolution vertical profiles of all major elements in solution could provide valuable information towards understanding the physical and biogeochemical processes during groundwater recharge and contribute towards more quantitative interpretations of chemical compositions of regional groundwaters.

Saturated zone geochemical processes were discussed in Chapter 3; however, large differences between rainwater chemistry and groundwater chemistry were not highlighted or discussed. The purpose of this study is to determine the influence of various geochemical and biogeochemical processes in the unsaturated zone and their relation to groundwater salinity. This study presents major element concentrations of soil pore waters from four unsaturated zone profiles. The influences of vegetation type, soil texture, and soil mineralogy are considered to help understand spatial and vertical variations in solute concentrations. Element/chloride ratios are utilized to understand the dominant geochemical and biogeochemical processes occurring during groundwater recharge through the unsaturated zone.

4.1 Regional Setting

The study focuses on Barmedman Creek catchment, which is located in the southwest portion of the Bland basin in central New South Wales, Australia (Figure 4.1). The Bland basin is a former tributary system of the Lachlan River and is located within the Murray-Darling Basin. During the Cenozoic, deposition of alluvial sediments from the Lachlan River Catchment prevented northward drainage from the Bland Basin and produced the present day closed basin morphology (Anderson et al., 1993). The majority of Barmedman creek catchment is characterized by low topographic relief (<0.7 m/km) which grades from south to north. The exception is an area of low relief granite outcroppings (<50 m) and associated alluvium in the south-eastern portion of the study area.

4.1.1 Geology and Morphology

Bedrock geology within the basin consists of Cambro-Ordovician metasediments and granites, Ordovician intermediate volcanics and metasediments, and Silurian-Devonian clastic sediments (Warren et al., 1995). Cenozoic weathering resulted in the

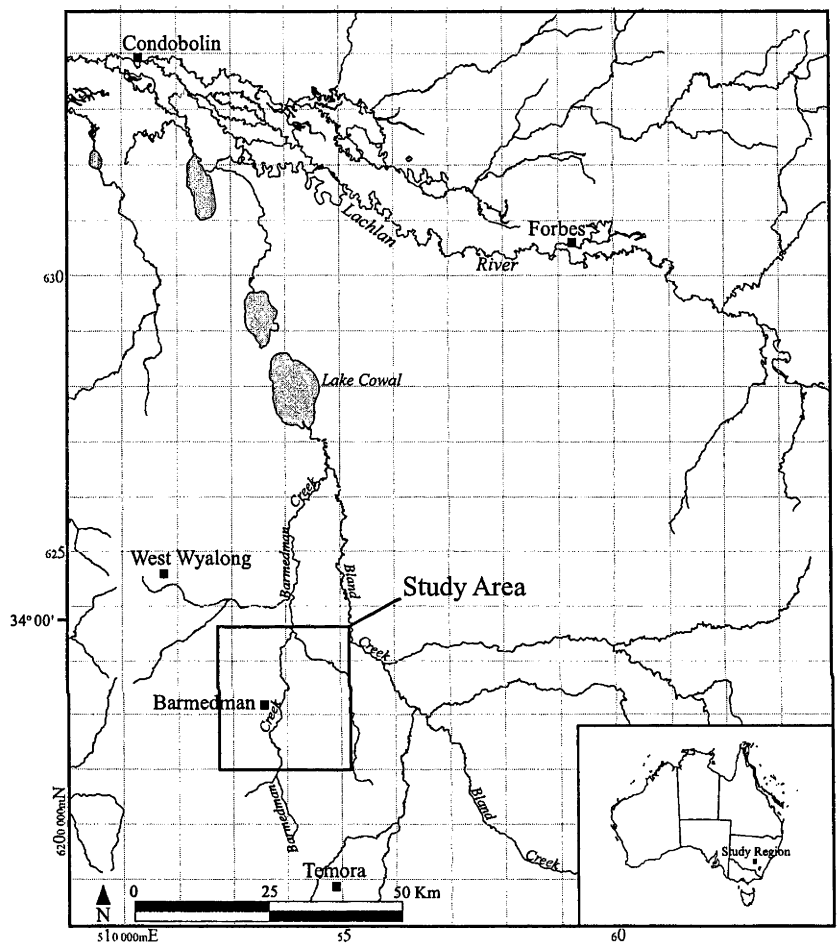

Figure 4.1: Location of study area within the Bland Basin, central New South Wales (NSW), Australia. Adapted from Forbes, NSW and Cootamundra, NSW 1:250 000 map sheets (courtesy Geoscience Australia).

formation of thick saprolite sequences (Wilford et al., 2002) followed by deposition of up to 80 metres of sediments (Gibson et al., 2002). Stratigraphic palynology of Lachlan River alluvium (~60 km northeast of the study area) suggests that regional sedimentation occurred during the Miocene and Pliocene with the most significant deposition of sediments occurring during the Pliocene (Martin, 1991). Wilford et al. (2002) identified lithofacies in the sedimentary sequence and related them to erosional

and depositional processes. Basal sands and gravels were attributed to erosion of bedrock and deposition along palaeo-drainage lines. An overlying clay/silt unit was explained as alluvial and colluvial transport of highly weathered bedrock within the palaeo-valleys. A mid to upper sandy unit represents distally sourced sandy sediments deposited by fluvial systems. The uppermost clay and silt unit is believed to represent modern sheet flow alluvium/colluvium and potentially aeolian material (Gibson and Chan, 2000; Wilford et al., 2002). Groundwater recharge presumably occurs through this near surface unit in the southern portion of the study area where coarser grained colluvial material is sourced from the granite outcropping areas (Gibson and Chan, 2000). A general south to north hydraulic gradient is present within this aquifer system (Chapter 3).

4.1.2 Climate

Historic rainfall records collected from the Barmedman Post Office were obtained from the Australian Bureau of Meteorology. Monthly rainfall (mm) data from 1887 to 2006 indicate average annual rainfall of 480 mm/yr. Average summer and winter rainfall are 157 mm and 160 mm respectively. Average summer and winter maximum temperatures recorded over a 45 year period at West Wyalong are 31°C and 16°C respectively. According to mean monthly pan evaporation rates collected at the Temora Agricultural Research Station (~ 40 km south of study area) evaporation exceeds rainfall except for the winter months of June and July.

4.1.3 Sampling Locations

The four core locations discussed in this paper are from within the near surface alluvial/colluvial unit. The locations of cores GDH03, BGMR and BGSF were chosen because of their proximity to the presumed groundwater recharge zone and because they are located within uncultivated areas containing native vegetation (Figure 4.2). The presumably undisturbed near surface soils should provide information regarding the long-term geochemical processes that have influenced the chemical composition of groundwater recharge in the unsaturated zone. For comparison, borehole GDH04 is located in the distal portion of the study area (Figure 4.2) within an area historically cultivated with canola and wheat. At the time of sampling, the ground surface at all sampling locations was vegetated with low-lying grasses.

Sampling locations GDH03, BGMR and BGSF are situated on a present day alluvial/colluvial fan (Figure 4.2), consisting of sandy material sourced from granite (Gibson and Chan, 2000). GDH04 is situated on a very low angle, coalescing alluvial fan consisting of fine grained transported material (Gibson and Chan, 2000). Cores GDH03 and GDH04 extend into the saturated zone. Water depths measured in piezometers at these locations are at 7.45 and 7.9 metres, respectively; indicating an unsaturated zone depth greater than 7 m. The physical characteristics of sediments sampled at each location will be presented and discussed in greater detail in following sections.

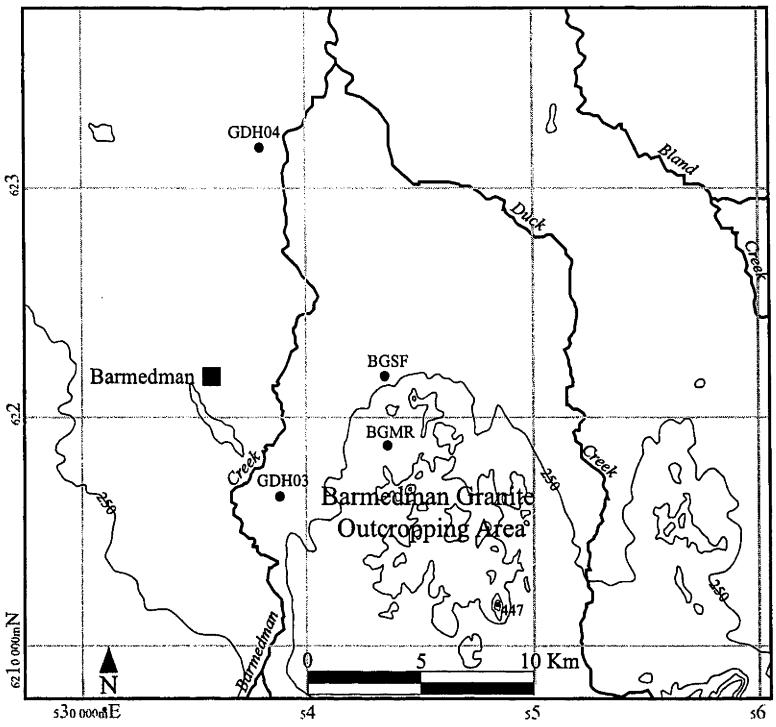

Figure 4.2: Sediment core locations locations within the Barmedman Creek subcatchment of the Bland Basin. Adapted from Cootamundra, NSW 1:250 000 map sheet (50 metre contour interval). Grids represent geographical easting and northing and depicted as 10,000 metre intervals.

Boreholes GDH03, BGMR and BGSF are located within mature stands (> 10 m height) of *Casuarina cristata* and *Casuarina luehmanniana* (common names Belah Oak and Bull Oak) in the vicinity of the Barmedman Granite outcroppings (Figure 4.2) in the southern portion of the study area.

4.2 Methods

Regolith materials were sampled by the Australian Bureau of Rural Sciences (BRS) in 2001 via diamond coring at two locations within the Barmedman Creek catchment, GDH03 and GDH04 (Figure 4.2), to depths of 59 and 80 m respectively. In 2005, regolith materials were sampled adjacent to the diamond core locations via push coring. Duplicate push cores were collected at these two locations; one for establishing high resolution solute profiles and the other for ^{36}Cl measurements of soil

pore water (Chapter 5). Two additional push cores (BGMR and BGSF) were completed in other locations within the study catchment. Soil pore water was extracted from saturated zone regolith materials with a uniaxial compression device at BRS laboratories in Canberra, ACT. Pore water samples were collected in sterile 10 mL syringes then filtered through a 0.45μm filter into sterile viles. Groundwater was sampled from permanently installed piezometers in 2004 (Chapter 3: Figure 3.3). Five rainwater samples were collected from single rain events with a teflon funnel attached to a sterile polyethylene bottle. Rainwater collectors were positioned in forested areas, but away from tree canopies to avoid through fall contamination. In addition, sites were positioned more than 50 metres from the nearest sealed or unsealed road/track to limit contamination from road dust and other aerosols. Two rainwater samples were also collected from domestic rainwater tanks in the town of Barmedman. Groundwater and rainwater samples were filtered in the field through 0.45 μm filter paper. Rainwater and groundwater sampling containers were thoroughly rinsed with respective filtered sample prior to collection. Samples for cation analysis were acidified in the field with concentrated A.R. grade nitric acid (Chapter 3). Pore water and groundwater samples were stored at ~10° C. Cation concentrations were determined via ICP atomic emission spectrophotometry at the Australian National University (ANU) Department of Earth and Marine Sciences (DEMS) and Australian Bureau of Rural Sciences. Anion concentrations were measured with a Dionex DX4500i ion chromatograph using an AS14A column with $NaHCO_3/Na_2CO_3$ eluent and electrochemical detector in conductivity mode at The Australian National University (ANU) Department of Earth and Marine Sciences (DEMS). Anion data for groundwater and pore water samples were measured using a 50 μL sample loading loop on the ion chromatograph. Rainwater samples were measured using a 500 μL

sample loading loop to lower detection limits. Reproducible results were obtained for concentrations >0.01 mg/l except for PO_4^{3-} which yielded reproducible results for concentrations >0.05 mg/l. Results from major/minor ions analyses for groundwater and pore water yielded charge imbalances of less than 3% of total charge. Laser grain size analyses were performed by Geoscience Australia, Canberra. Gravimetric moisture content was determined at ANU-DEMS by drying to constant weight at 110°C and calculated as mass percent of water lost from total wet mass of soil.

4.3 Results

All results are reported in Appendix 1. Results from GDH03 and GDH04 are plotted as entire unsaturated zone profiles and also as shallow near surface depth profiles to allow for comparison with data collected from shallow (< 1.2m) cores BGMR and BGSF.

4.3.1 Sediment Grain Size and Moisture Content Profiles

Vertical distribution of grain sizes throughout the unsaturated zone (boreholes GDH03 and GDH04), is highly variable, and is generally characterized by a greater proportion of clay and silt sized sediments than sand (>50% clay + silt) (Figure 4.3). Grain sizes in two near surface (<1.2 m) cores (BGMR and BGSF) exhibit less variation with depth and a greater proportion of clay + silt than at cores GDH03 and GDH04. Location GDH03 exhibits a greater proportion of sand sized sediments in the near surface than at other core locations where near-surface grain size distributions are characterized by fine-grained materials (>75% clay + silt).

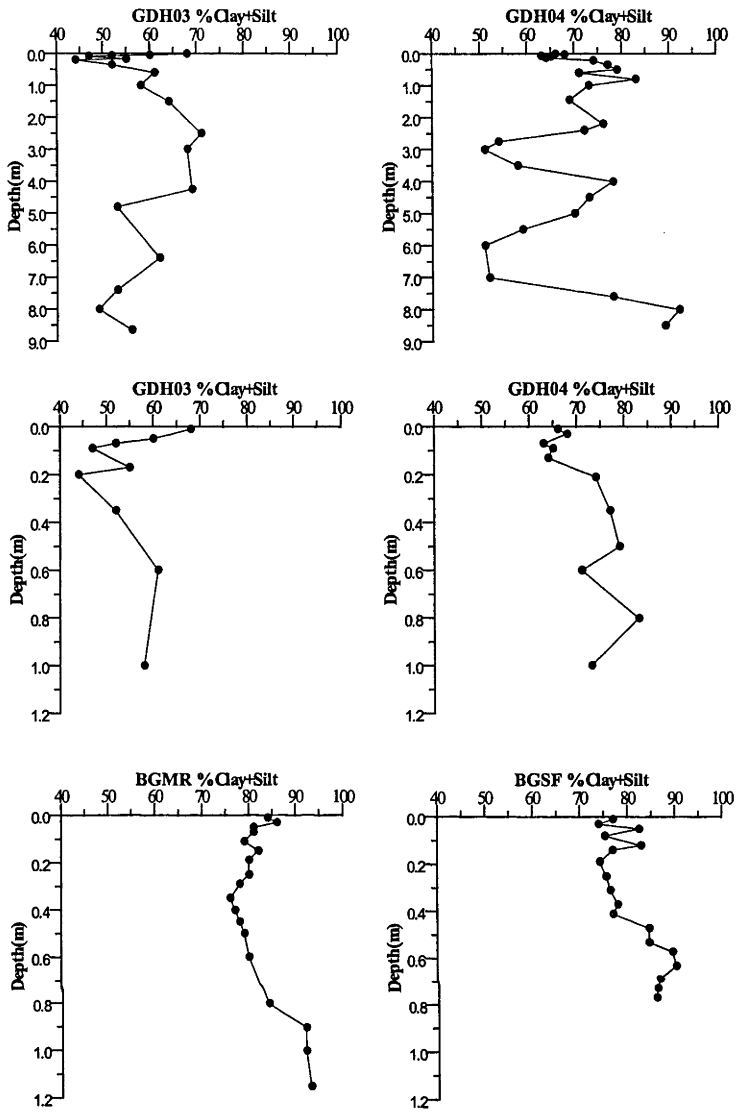

Figure 4.3: Sediment grain size distribution in the unsaturated zone at 4 locations within Barmedman Creek catchment (Figure 4.2). Water table is present at 7.45 metres at GDH03 and at 7.9 metres at GDH04.

Moisture contents vary between locations (4.9 wt. %-29.3 wt. %), but in general, are greatest in the near surface and decrease over the upper 20 cm (Figure 4.4). The exception is GDH04, which exhibits low near surface moisture contents that increase with increasing depth over the upper 10 cm. Moisture contents correlate poorly with the abundance of fine grained materials (clay + silt); however, they correlate positively with clay content. However, the limited correlation between sediment grain size and moisture content indicates that factors other than grain size, such as evapotranspiration, are strongly influencing the moisture content.

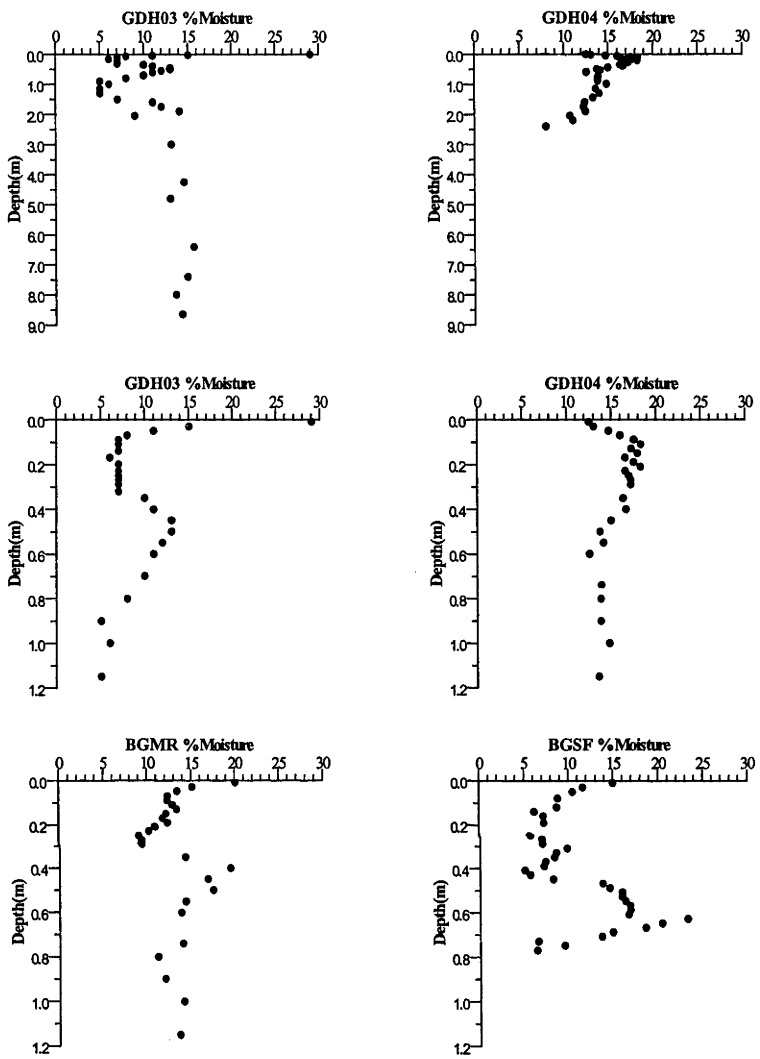

Figure 4.4: Gravimetric moisture content profiles from the four coring locations in Barmedman Creek catchment. Moisture contents calculated as ratio of mass water lost at 110° C to the wet mass of soil. Water table is present at 7.45 metres at GDH03 and at 7.9 metres at GDH04.

4.3.2 Pore Water Solute Profiles

Chloride and Bromide

Pore water Cl^- and Br^- concentrations increase with depth over the upper 1 metre at all four sampling locations (Figures 4.5 & 4.6). Values range from 8.9 mg/l to 12,658.6

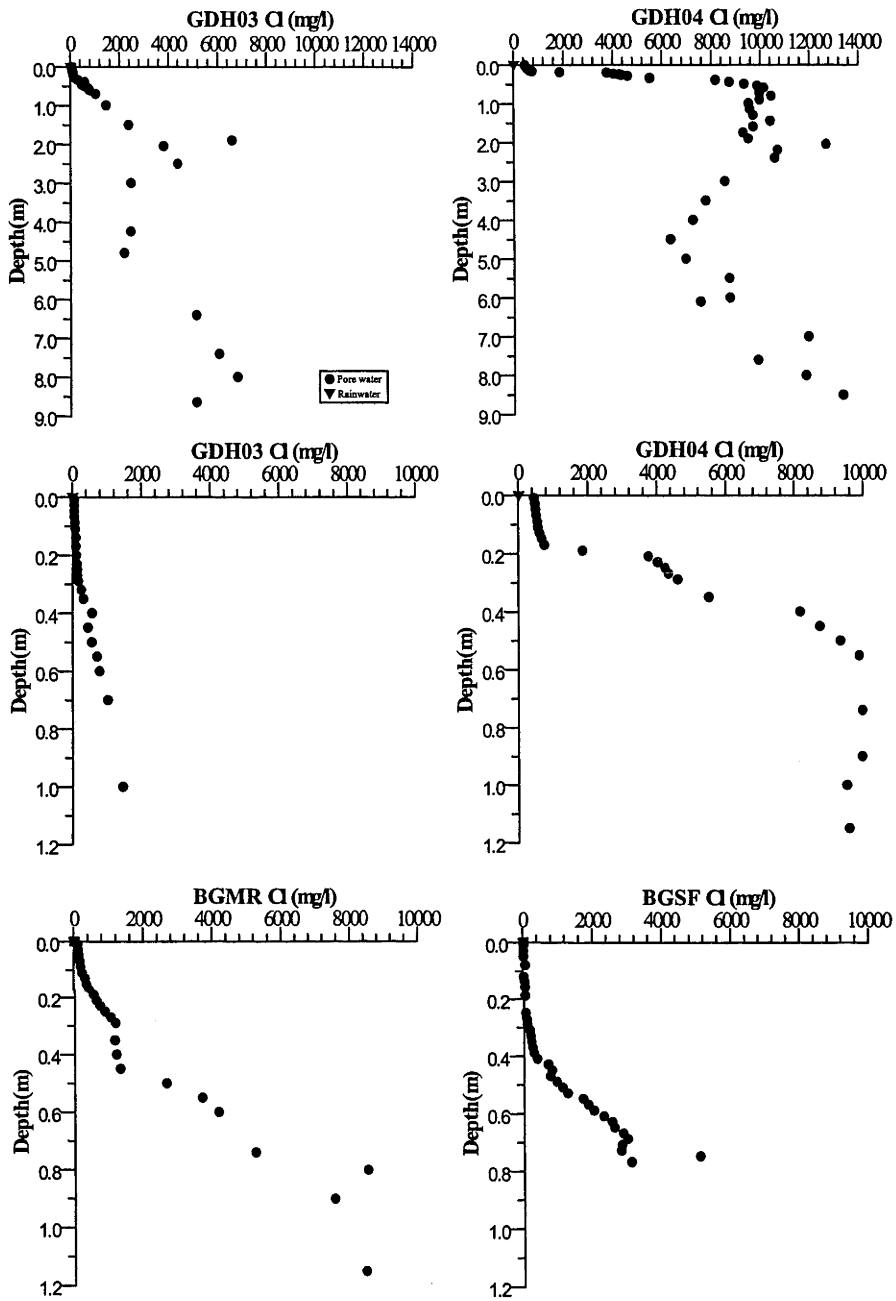

Figure 4.5: Variations in pore water Cl^- concentrations with depth at locations GDH03, GDH04, BGMR and BGSF. Water table is present at 7.45 metres at GDH03 and at 7.9 metres at GDH04.

mg/l for Cl^- and from below detection (<0.01 mg/l) to 40.5 mg/l for Br^-. Rainwater exhibits Cl^- concentrations ranging from 0.35 mg/l to 6.50 mg/l and Br^- concentrations ranging from below detection to 0.02 mg/l. Average global seawater exhibits Cl^- and Br^- concentrations of 19,000 mg/l and 67 mg/l (Hem, 1992). GDH03 and BGSF exhibit significantly lower Cl^- and Br^- concentrations than at GDH04 and BGMR, and

exhibit comparatively smaller increases in concentration over the upper 40 cm. This suggests a greater degree of evapotranspiration is occurring at GDH04 and BGMR than at GDH03 and BGSF. At cores GDH04 and

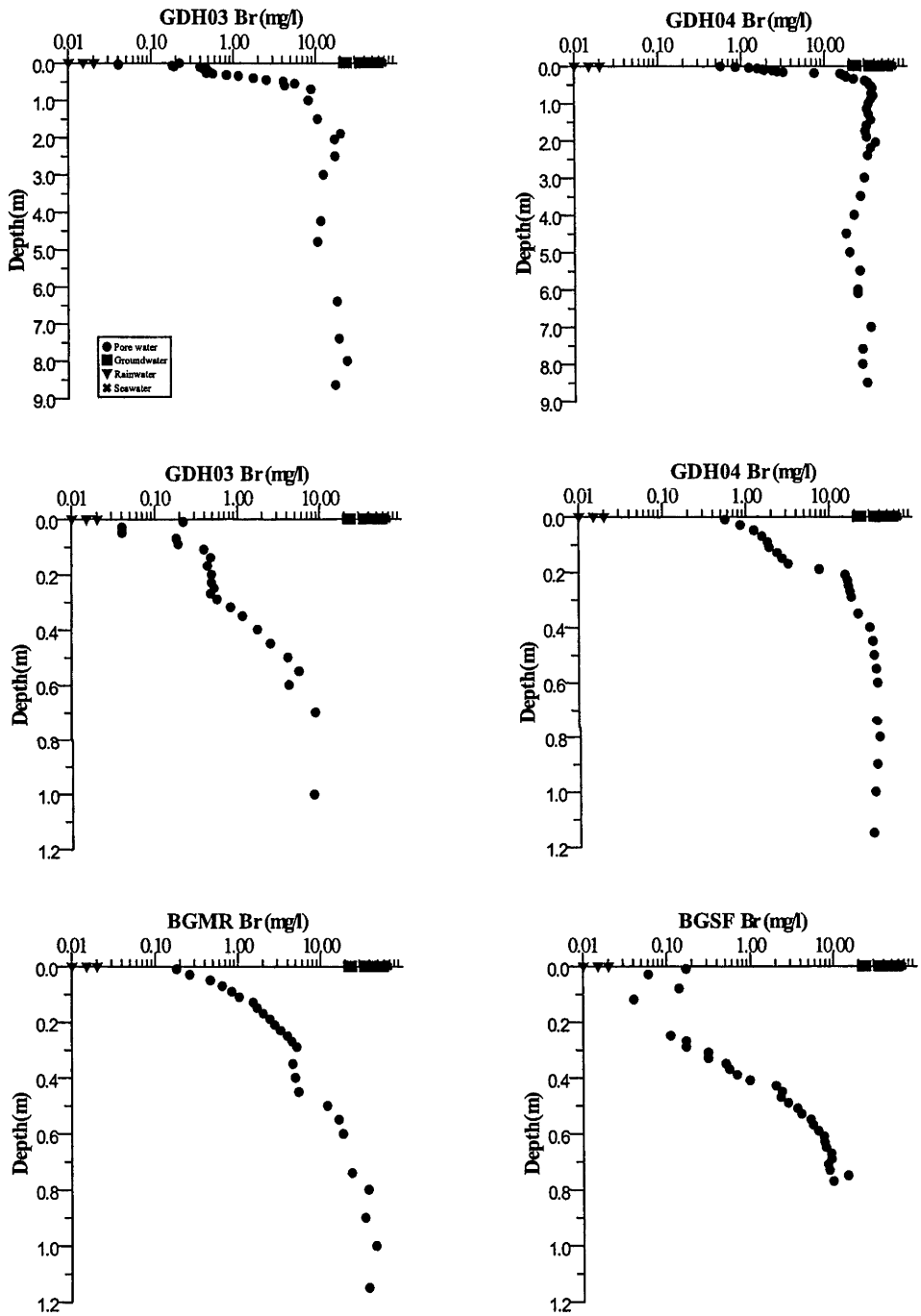

Figure 4.6: Variations in pore water Br^- concentrations with depth at locations GDH03, GDH04, BGMR and BGSF. Water table is present at 7.45 metres at GDH03 and at 7.9 metres at GDH04.

BGMR, pore water Cl^- and Br^- concentrations approach concentration ranges (5491.5-16513.7 mg/l Cl^- and 21.8-55.5 Br^-) measured in regional groundwater (See Chapter 3) within the upper 1 metre of the profile (Figures 4.5 & 4.6).

At the two complete unsaturated zone profiles (GDH03 and GDH04, see Figure 4.2) the increasing trends in near surface pore waters are interrupted by a zone of lower Cl^- and Br^- concentrations from approximately 2 to 5 metres depth. The composition of pore waters over this depth interval may reflect non-conservative behavior of Cl^- and Br^- (anion adsorption, vegetative uptake, mineral precipitation); preferential flow (vertical or horizontal) of modern meteoric water to this depth interval; or variations in palaeo-climatic or palaeo-hydrogeologic conditions during pore water deposition. These scenarios will be addressed in greater detail within the discussion section.

Sulfate

Near surface pore water SO_4^{2-} concentrations vary between each location, but similar to trends in Cl^- and Br^- concentrations, the SO_4^{2-} concentrations are greatest in cores GDH04 and BGMR (Figure 4.7). SO_4^{2-} concentrations range from 1.4 mg/l to 2,820 mg/l for pore waters, from 951.7 mg/l to 4,159.3 mg/l for groundwater and from 0.3 mg/l to 2.2 mg/l for rainwater. Average global seawater exhibits a SO_4^{2-} concentration of 2,700 mg/l (Hem, 1992).

All cores generally exhibit an increase with increasing depth. The exceptions are within near surface (<50 cm) samples collected from cores GDH03 and BGMR, which exhibit a decreasing trend with increasing depth. This indicates a near surface

sink for SO_4^{2-} at these two locations, and demonstrates spatial variations in near surface geochemical or biogeochemical processes. Processes such as vegetative

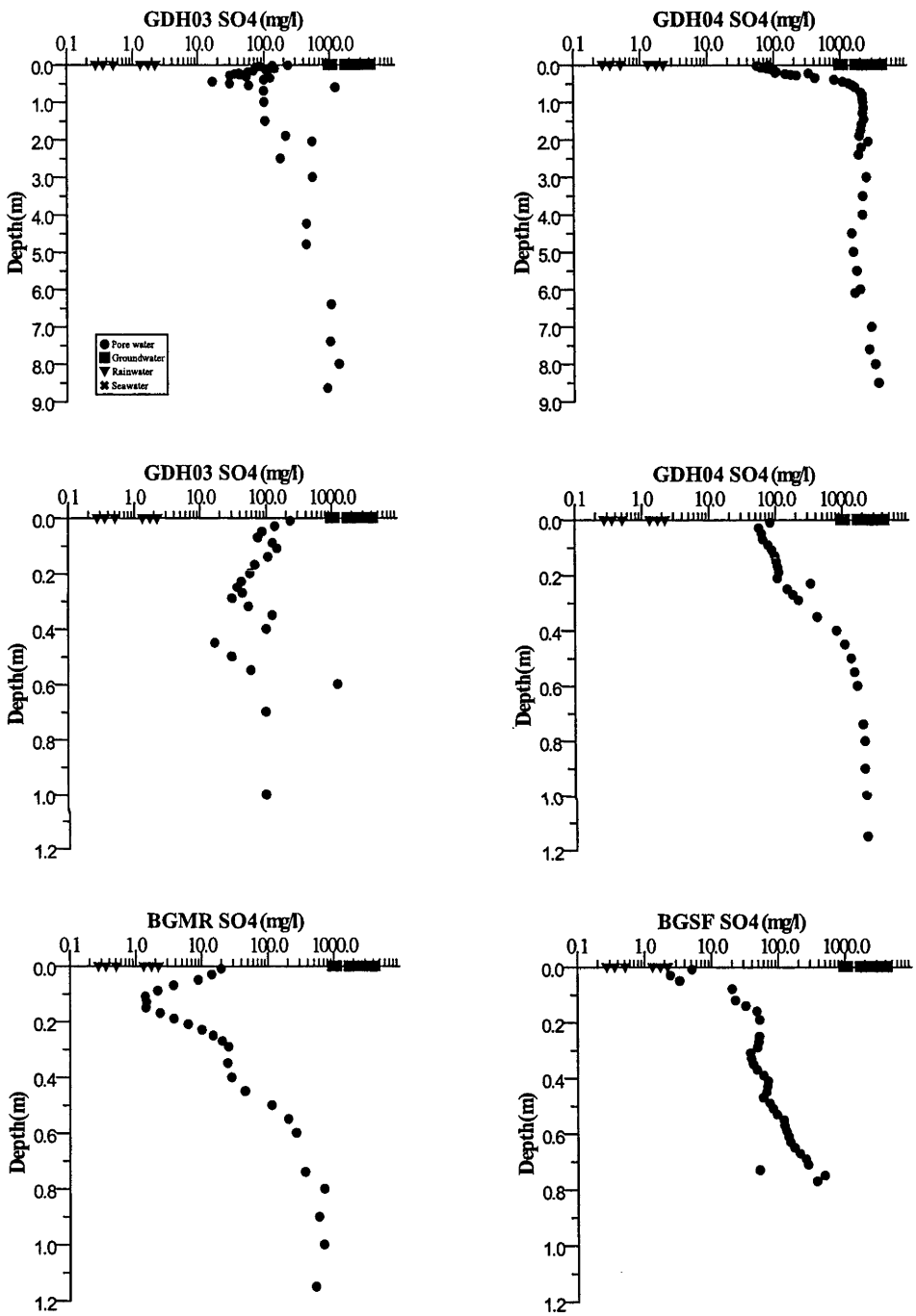

Figure 4.7: Variations in pore water SO_4^{2-} concentrations with depth at locations GDH03, GDH04, BGMR and BGSF. Water table is present at 7.45 metres at GDH03 and at 7.9 metres at GDH04. Groundwater and rainwater samples are depicted as black boxes and black triangles, respectively, and concentrations (mg/l) are plotted at zero metres depth.

uptake, bioassimilation, and SO_4^{2-} mineral precipitation/dissolution could potentially be occurring at these locations and will be considered in greater detail within the

discussion section. With the exception of core GDH03, pore water SO_4^{2-} concentrations within the upper one metre of the profile approach the concentration ranges measured in regional groundwater.

Nitrate

Near surface pore water NO_3^- concentrations are similar at locations GDH03, GDH04 and BGMR and are more than 2 orders of magnitude greater than those measured in regional groundwater and rainwater (Figure 4.8). Near surface pore water sampled from core BGSF has significantly lower NO_3^- concentrations than the other sampling locations, but are more than an order of magnitude greater than in groundwater and rainwater. NO_3^- concentrations range from 2.2 mg/l to 3,036.0 for pore waters, from below detection to 13.45 mg/l for groundwater and from 0.3 mg/l to 4.58 mg/l for rainwater. Average global seawater exhibits a NO_3^- concentration of 0.7 mg/l (Hem, 1992).

GDH03 and GDH04 exhibit decreasing trends with increasing depth, and approach concentrations similar to those measured in groundwater at the bottom of the unsaturated zone. At BGMR and BGSF, pore water NO_3^- concentrations decrease with depth at a more rapid rate than at GDH03 and GDH04, and approach values similar to groundwater within the upper 50 cm. However, at both locations the decreasing trends are followed by an increase in concentration with increasing depth.

The data from all profiles indicate a near surface enrichment in NO_3^- followed by a subsurface sink for this ion. The variations in total near surface enrichment and variations in profiles trends between the sampling locations demonstrate spatial

variations in near surface biogeochemical processes that may be related to the physical properties of near surface sediments or to vegetation type.

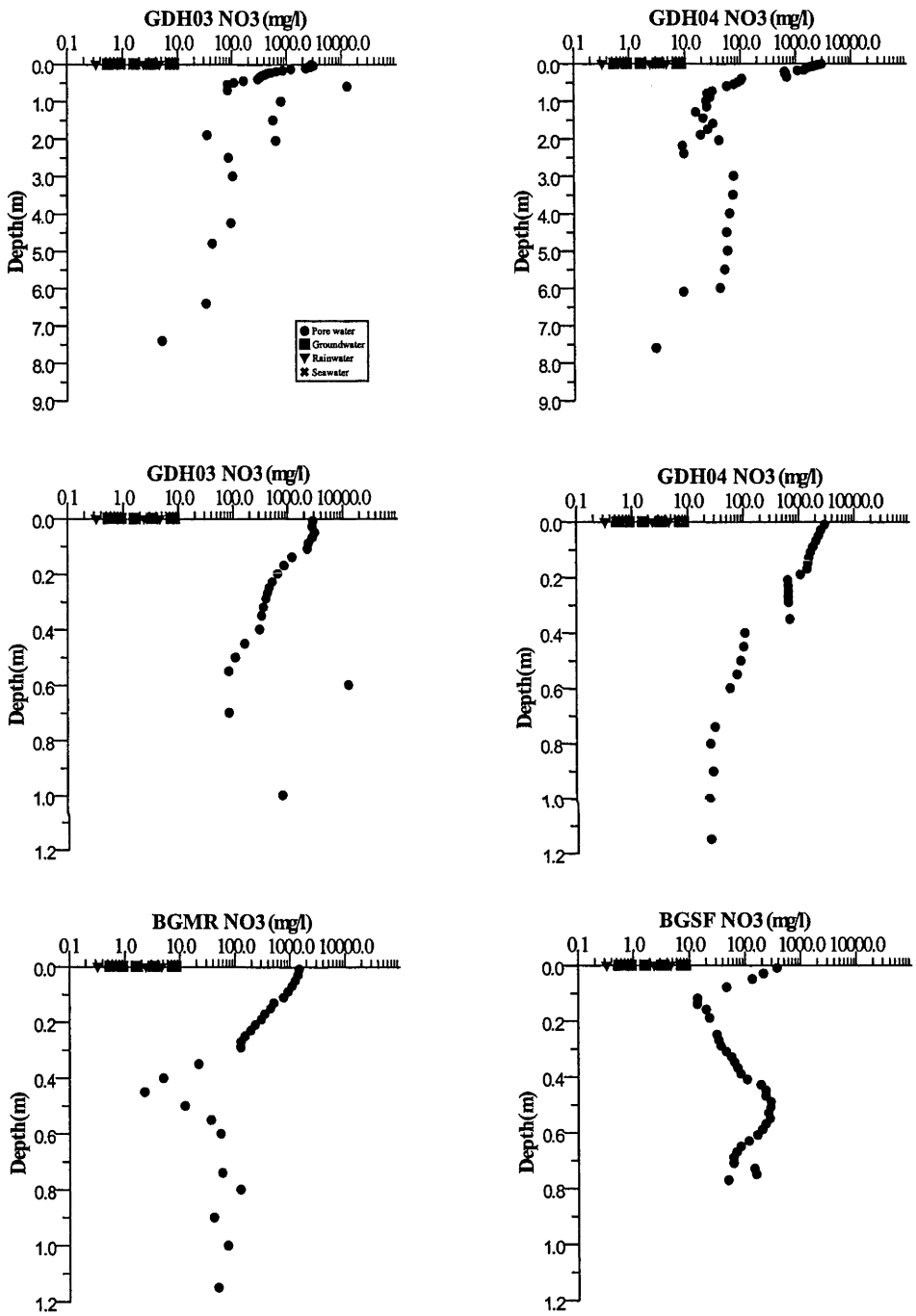

Figure 4.8: Variations in pore water NO_3^- concentrations with depth at locations GDH03, GDH04, BGMR and BGSF. Water table is present at 7.45 metres at GDH03 and at 7.9 metres at GDH04. Groundwater and rainwater samples are depicted as black boxes and black triangles, respectively, and concentrations (mg/l) are plotted at zero metres depth.

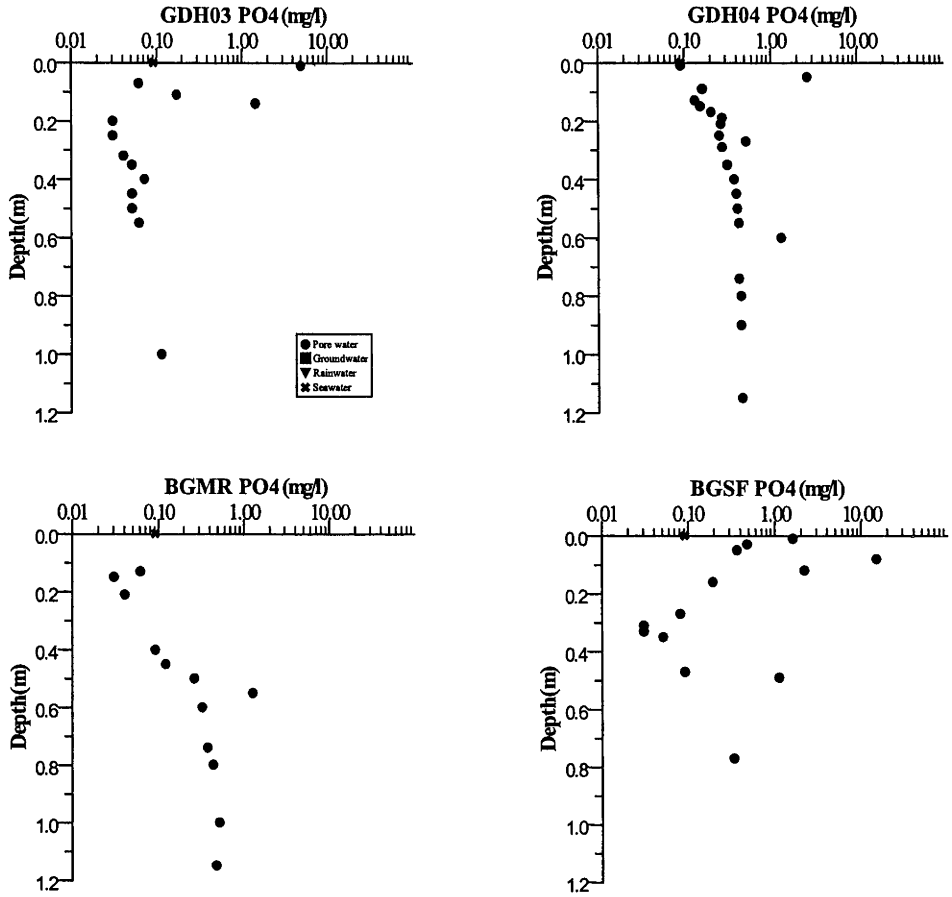

Figure 4.9: Variations in pore water PO_4^{3-} concentrations with depth at locations GDH03, GDH04, BGMR and BGSF. Water table is present at 7.45 metres at GDH03 and at 7.9 metres at GDH04.

Phosphate

Concentrations of PO_4^{3-} are highly variable with depth and vary between locations (Figure 4.9). PO_4^{3-} concentrations range from below detection to 14.8 mg/l for pore waters, from below detection to 10.65 mg/l for groundwater and below detection for rainwater. Average global seawater exhibits a PO_4^{3-} concentration of 0.09 mg/l (Hem, 1992). Concentrations increase with increasing depth at locations GDH04 and BGMR, but exhibit highly variable depth trends at GDH03 and BGSF. In most cases, PO_4^{3-}concentrations are less than 1 mg/l.

Sodium

Pore water Na concentrations increase with depth over the upper 1 metre at all four sampling locations (Figure 4.10). Na concentrations range from 5.0 mg/l to 5,800 mg/l for pore waters, from 3049 mg/l to 8,200 mg/l for groundwater and from 0.4

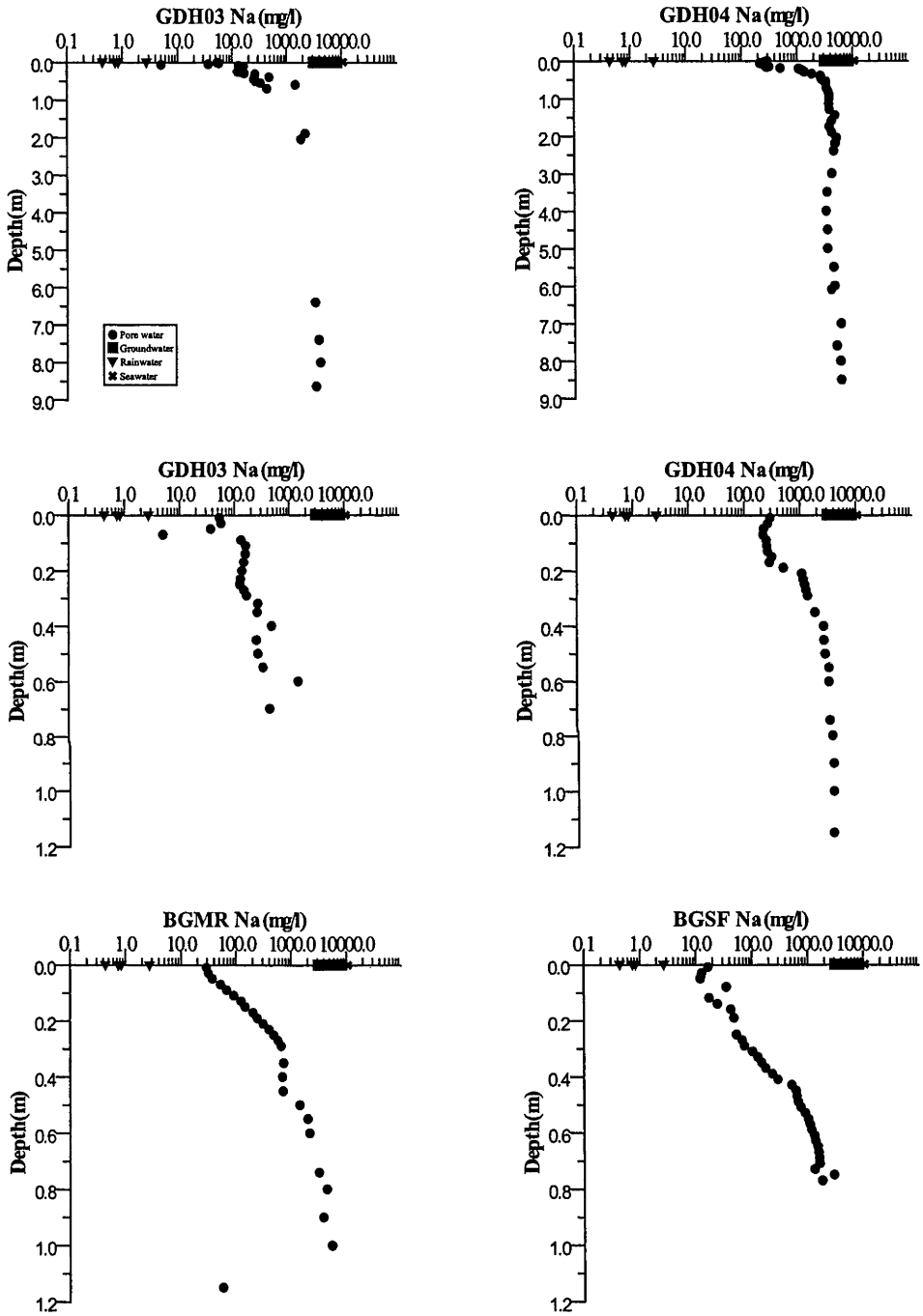

Figure 4.10: Variations in pore water Na concentrations with depth at locations GDH03, GDH04, BGMR and BGSF. Water table is present at 7.45 metres at GDH03 and at 7.9 metres at GDH04. Groundwater and rainwater samples are depicted as black boxes and black triangles, respectively, and concentrations (mg/l) are plotted at zero metres depth.

mg/l to 2.7 mg/l for rainwater. Average global seawater exhibits a Na concentration of 10,500 mg/l (Hem, 1992).

GDH03 pore waters exhibit significantly lower Na concentrations than at other sampling locations, and exhibit comparatively smaller increases in concentration over the upper 40 cm, which suggests less evapotranspiration occurring at this location. At cores GDH04, BGMR and BGSF, pore water Na concentrations approach concentration ranges measured in regional groundwater within the upper 1 metre of the profile (Figure 10). The progressive increase in Na with depth at each location suggests similar geochemical processes are influencing the concentrations of Na ions in pore water.

Potassium

K concentrations in pore water sampled in the upper 5 cm are similar between locations GDH03, GDH04 and BGMR (Figure 4.11). K concentrations range from 1.3 mg/l to 116.3 mg/l for pore water, from 3.7 mg/l to 72.4 mg/l for groundwater and from 0.05 mg/l to 0.74 mg/l for rainwater. Average global seawater exhibits a K concentration of 390 mg/l (Hem, 1992).

Pore water K concentrations are greater than those measured in regional groundwater and are approximately two orders of magnitude greater than rainwater. Within the upper 50 cm, concentrations decrease by more than an order of magnitude. This is in contrast with Na trends, which increase with increasing depth (Figure 4.10), suggesting that different geochemical processes are influencing the two monovalent

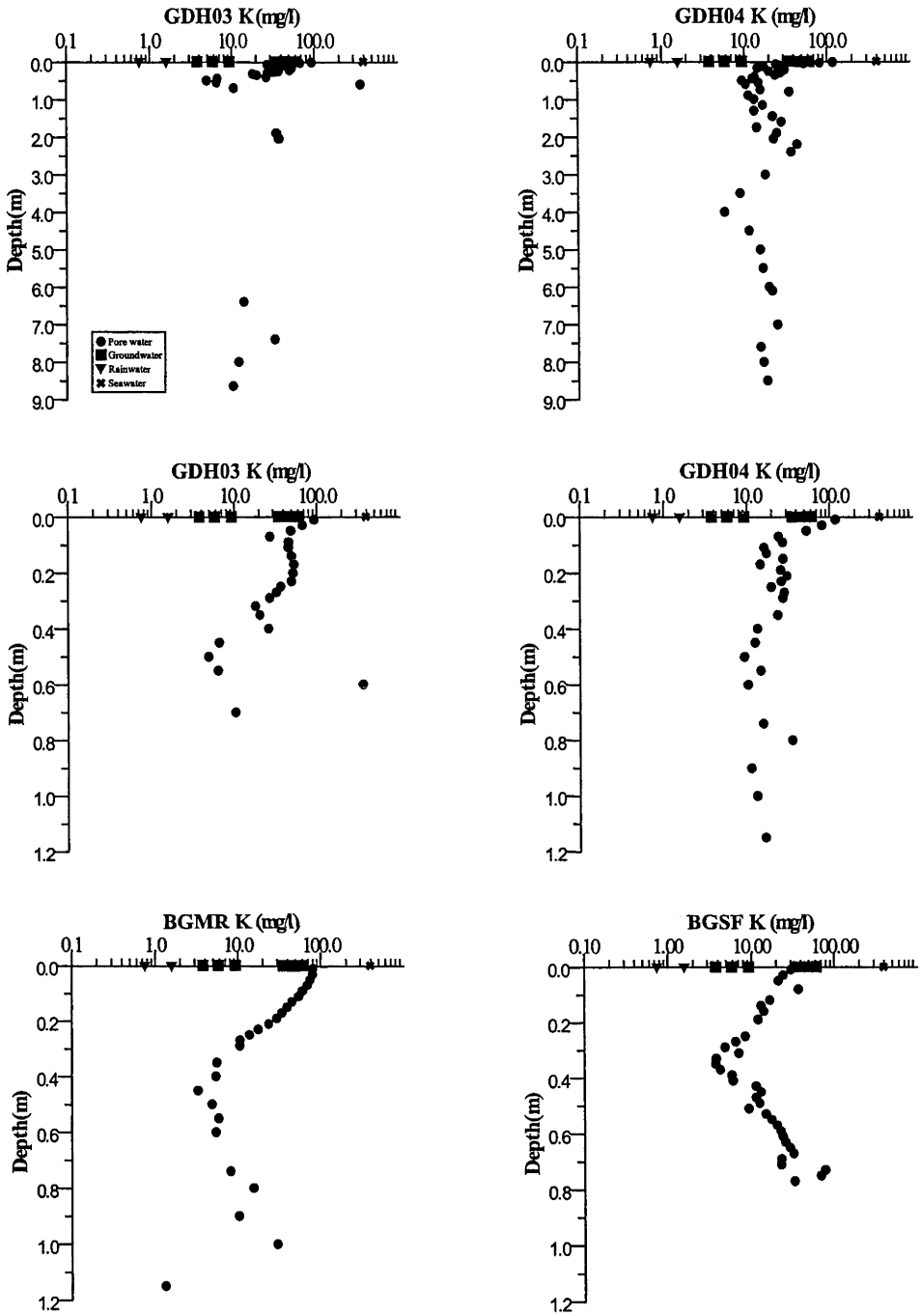

Figure 4.11: Variations in pore water K concentrations with depth at locations GDH03, GDH04, BGMR and BGSF. Water table is present at 7.45 metres at GDH03 and at 7.9 metres at GDH04. Groundwater and rainwater samples are depicted as black boxes and black triangles, respectively, and concentrations (mg/l) are plotted at zero metres depth.

cations. Similar trends are also observed for NO_3^- concentrations in near surface samples (Figure 8). K and NO_3^- concentrations in near surface (< 10 cm) pore waters from core BGSF have slightly lower concentrations than the other sampling locations.

The K concentrations in near surface pore waters at BGSF are similar to groundwater concentrations and NO_3^- concentrations are more than an order of magnitude greater than in groundwater. Both NO_3^- and K concentrations in the near surface are more than an order of magnitude greater than in rainwater and exhibit decreasing trends with increasing depth. Below the near surface, GDH03 and GDH04 exhibit variable trends with increasing depth, and samples collected from the bottom of the unsaturated zone exhibit K concentrations nearly an order of magnitude less than in the near surface. The samples at the base of the unsaturated zone approach concentrations similar to those measured in groundwater. At BGMR and BGSF, K concentrations decrease with depth to approximately 40 cm, followed by an increase with increasing depth for the remainder of the profiles. A similar trend was observed for NO3 concentrations at these locations. The data from the upper 40 cm of all profiles indicate a near surface enrichment in K and NO_3^- underlain by a zone of steady depletion. K and NO_3^- are limiting nutrients to plants (Jobaggy and Jackson, 2001) and the profiles of these elements suggest that vegetation is influencing their mobility within the unsaturated zone.

Calcium

Ca concentrations of pore water sampled in the upper 10 cm are similar between locations GDH03, and GDH04 and have slightly lower concentrations at BGMR (Figure 4.12). Ca concentrations range from 4.9 mg/l to 1517.1 mg/l for pore water, from 118.6 mg/l to 1439.8 mg/l for groundwater and from 0.03 mg/l to 1.30 mg/l for rainwater. Average global seawater exhibits a Ca concentration of 410 mg/l (Hem, 1992).

The concentrations are similar to those measured in regional groundwater and are more than two orders of magnitude greater than rainwater. Ca concentrations in near surface (< 10 cm) pore waters from core BGSF are significantly lower than at other sampling locations and are less than regional groundwater. At all locations, Ca

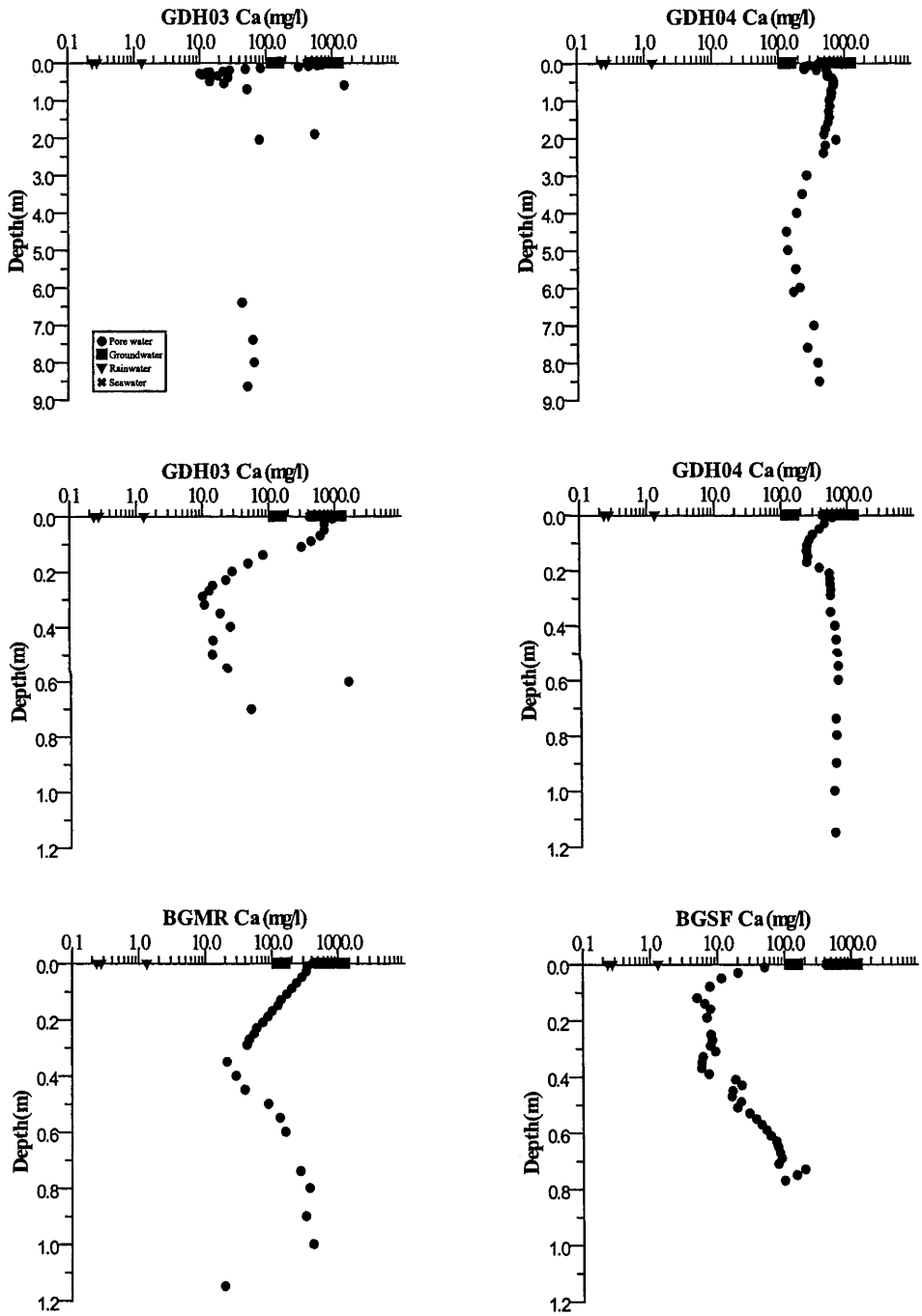

Figure 4.12: Variations in pore water Ca concentrations with depth at locations GDH03, GDH04, BGMR and BGSF. Water table is present at 7.45 metres at GDH03 and at 7.9 metres at GDH04. Groundwater and rainwater samples are depicted as black boxes and black triangles, respectively, and concentrations (mg/l) are plotted at zero metres depth.

concentrations of the near surface samples decrease significantly with depth to values appreciably less than in regional groundwater. However, the decreasing trend only occurs within the upper 40 cm. The largest decrease occurs at locations GDH03 and BGMR, and occurs over the upper 40 cm. Below this depth, the Ca concentrations increase with increasing depth. Locations GDH04 and BGSF exhibit relatively small decreases in Ca concentrations that occur over the upper 10 cm. Below this depth, they increase with increasing depth at BGSF, but remain relatively constant at GDH04. Throughout the remainder of the unsaturated zone, GDH03 and GDH04 exhibit variable trends with increasing depth.

Samples collected from the base of the unsaturated zone at GDH03 exhibit Ca concentrations less than regional groundwater, while GDH04 exhibits Ca concentrations similar to regional groundwater. Groundwater Ca concentrations exhibit a large range in concentrations. This suggests that geochemical processes occurring in the unsaturated zone significantly alter the Ca concentrations of meteoric input, but are not the dominant processes controlling the geochemical evolution of regional groundwater. Saturated zone geochemical processes may be responsible for the observed discrepancy between pore waters at the base of the unsaturated zone and regional groundwater.

Magnesium

Mg concentrations of pore water sampled in the upper 10 cm vary considerably between each location (Figure 4.13). Mg concentrations range from 4.0 mg/l to 1845.6 mg/l for pore water, from 411.9 mg/l to 1847.4 mg/l for groundwater and from

0.04 mg/l to 0.7 mg/l for rainwater. Average global seawater exhibits a Mg concentration of 1350 mg/l (Hem, 1992).

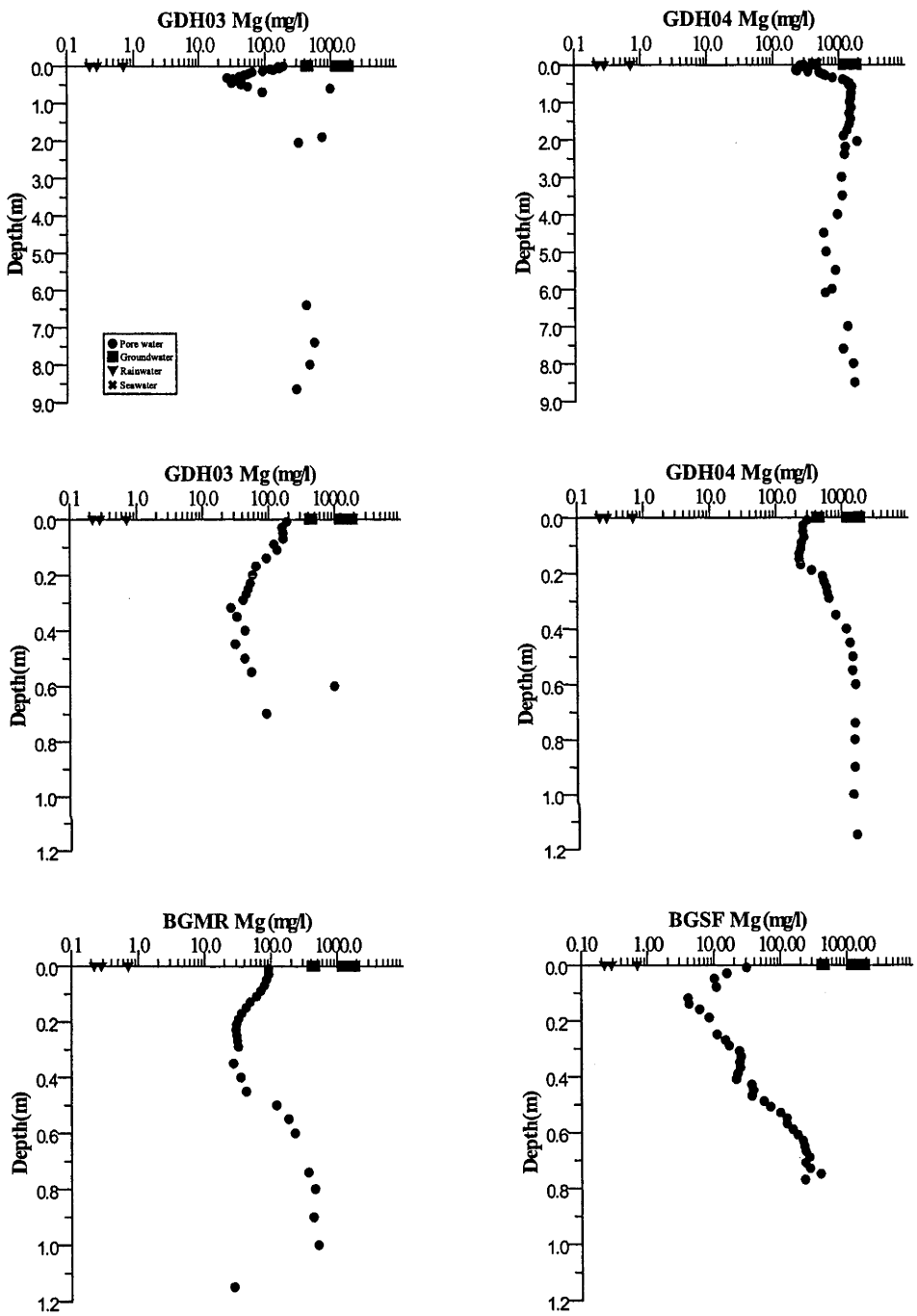

Figure 4.13: Variations in pore water Mg concentrations with depth at locations GDH03, GDH04, BGMR and BGSF. Water table is present at 7.45 metres at GDH03 and at 7.9 metres at GDH04. Groundwater and rainwater samples are depicted as black boxes and black triangles, respectively, and concentrations (mg/l) are plotted at zero metres depth.

Pore water Mg concentrations are less than in regional groundwater and are more than two orders of magnitude greater than rainwater. Mg concentrations in near surface (<

10 cm) pore waters from core BGSF have significantly lower concentrations than the other sampling locations. At all locations, Mg concentrations of the near surface samples decrease with depth to values appreciably less than in regional groundwater. However, the decreasing trend only occurs within the upper 40 cm. The largest decrease occurs at locations GDH03 and BGMR, and occurs over the upper 40 cm. Below this depth, the Mg concentrations increase with increasing depth to values similar to regional groundwater. Similar depth trends are observed for Ca suggesting similar geochemical processes are influencing the two divalent cations. Locations GDH04 and BGSF exhibit relatively small decreases in Mg concentrations that occur over the upper 10 cm. Below this depth, Mg concentrations increase with increasing depth to values similar to regional groundwater. Throughout the remainder of the unsaturated zone, GDH03 and GDH04 exhibit variable trends with increasing depth, and samples collected from the base of the unsaturated zone exhibit Mg concentrations similar to regional groundwater. This suggests that geochemical processes occurring in the unsaturated zone are the dominant processes controlling the geochemical evolution of regional groundwater.

4.4 Discussion

The complete unsaturated zone solute profiles available for cores GDH03 and GDH04 reveal large fluctuations in composition occurring within the upper metre of the profiles. Only minor variations in solute concentrations are observed over the remainder of the unsaturated zone (~8 m depth). At all four locations, solute concentrations in the upper 1 metre trend towards concentration ranges measured in regional groundwater. The data suggest that near surface processes are largely responsible for the geochemical evolution of groundwater in this study area.

4.4.1 Cl and Br Dynamics:

Conservative vs Nonconservative Anion Behaviour

Cl^- and Br^- are chemically conservative ions in natural waters and are often used as inorganic tracers in hydrogeochemical field studies (i.e., Ullman, 1985; Desaulniers et al., 1986; Fabryka-Martin et al., 1991; Herczeg et al., 1991). Relatively few sources and sinks for these elements allow them to be utilized for estimating the effects of evapotranspiration (i.e. Peck et al., 1981; Ullman, 1985; Johnston, 1987; Cartwright et al., 2006), vertical infiltration rates (i.e., Eriksson and Khunakasem, 1969; Allison and Hughes, 1978; Peck et al., 1981; Allison and Hughes, 1983; Scanlon, 1991; Wood, 1999), and timeframes of solute accumulation in the unsaturated zone (i.e., Allison et al., 1985; Cook et al., 1992; Zhu et al., 2003). However, bacterial and vegetative uptake (Shorter et al., 1995; Milton et al., 2003), organic adsorption (Gerritse and George, 1988), and mineral dissolution (Ullman, 1995; Davis et al., 1998b; Davis et al., 2001; Davis et al., 2004) can function as sources and sinks for these elements and compromise their use as chemically conservative tracers in hydrogeochemical field studies.

In this study, progressive increases in both Cl^- and Br^- concentrations with increasing depth suggest a high degree of evapotranspiration occurring in the upper 1 m of the unsaturated zone. However, if evapotranspiration were the only process influencing Br^- and Cl^- dynamics, both ions would accumulate at equivalent rates. Data from within the upper 0.5 metres reveal large fluctuations in Br/Cl ratios, below which the ratios remain relatively constant and are within the range of regional groundwater and seawater (Figure 4.14). Near surface (<5 cm) pore waters pore waters exhibit

significantly lower Br/Cl ratios than in meteoric water and groundwater (Figure 14). Furthermore, Br/Cl ratios increase over the upper 50 cm indicating a greater rate of accumulation of Br^- than Cl^-.

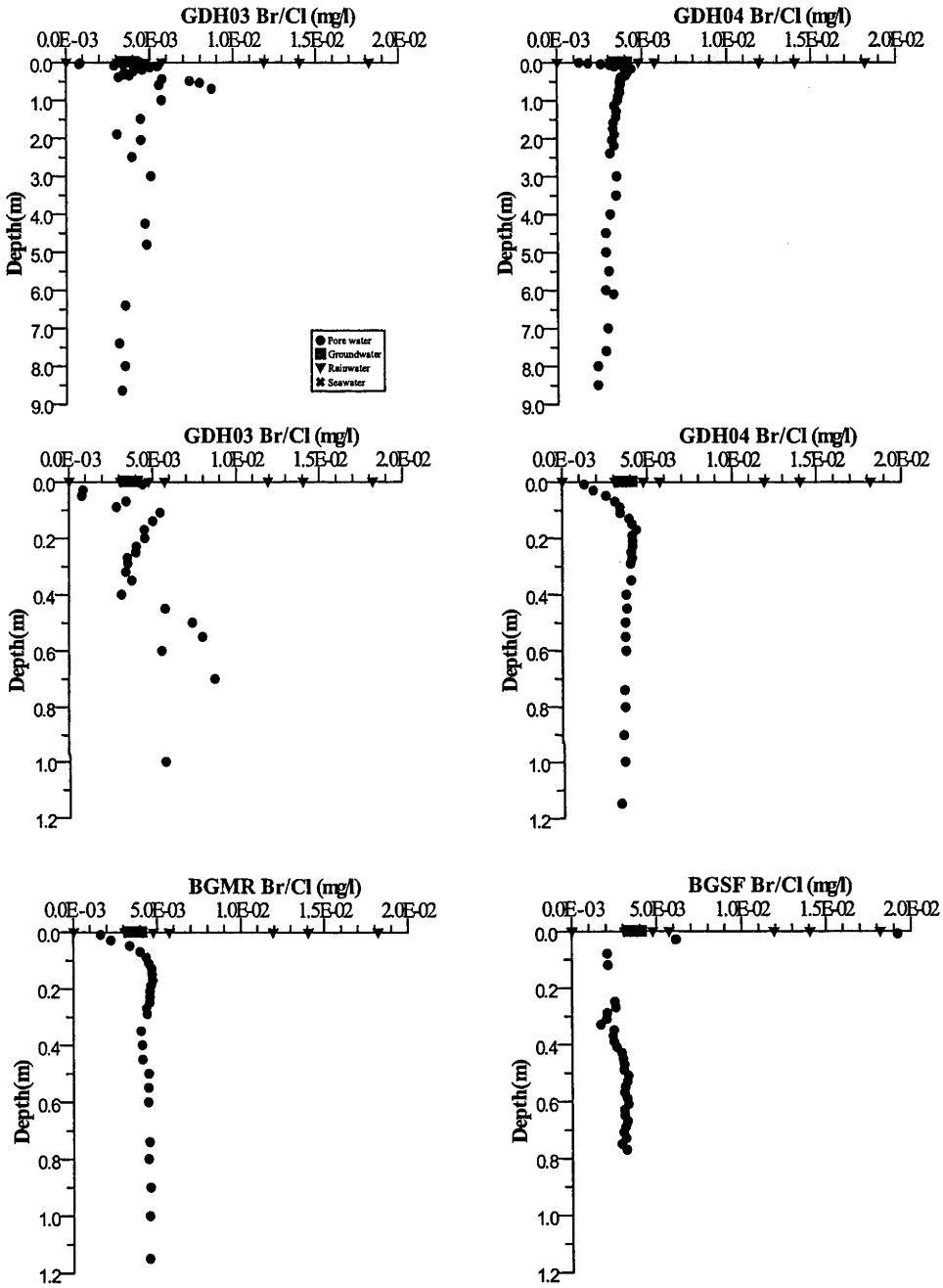

Figure 4.14: Variations in pore water Br/Cl (mass) ratios with depth at locations GDH03, GDH04, BGMR and BGSF. Water table is present at 7.45 metres at GDH03 and at 7.9 metres at GDH04.

Halite dissolution

Halite contains only trace amounts of bromine, and exhibits Br/Cl ratios ranging from approximately $1x10^{-5}$ to $1x10^{-4}$ (Ullman, 1995). A typical seawater Br/Cl ratio is approximately $3.5x10^{-5}$ (Hem, 1992). Studies in North America have reported Br/Cl ratios ranging from $6x10^{-3}$ to $2x10^{-2}$ for rainwater, from $3.5x10^{-3}$ to $2.3x10^{-2}$ for fresh groundwater (Cl<10mg/l), and 1x10-4 to $1x10^{-3}$ for water affected by halite dissolution (Davis et al., 1998b; Davis et al., 2004). Five rainwater samples collected from this study area exhibit Br/Cl ratios ranging from $2.9x10^{-3}$ to $1.9x10^{-2}$ with an average value of $1.1x10^{-2}$. Rainwater composition can vary dramatically between seasons, between rainfall events, and also vary with time in a single rain event (Warburton, 1982; Seymour and Stout, 1983; Lehmann et al., 2005). Large variations in Br/Cl ratios in rainwater have been well documented (Davis et al., 1998a; Sander et al., 2003) and has been attributed to plant emission and biomass burning (Mano and Andreau, 1994; Gan et al., 1998) sea salt aerosols (Guelle et al., 2001; Sander et al., 2003) agricultural fertilizers and pollution (Reeves and Penkett, 1993). The variations in rainwater Br/Cl ratios within Barmedman Creek catchment appear to reflect the variable trends observed in other studies throughout the world. Variations in Br/Cl ratios did not correlate with rainfall intensity, duration of rain events, season or wind directions. At this time the variations cannot be explained.

Two rainwater samples were collected from domestic rainwater tanks. These water samples are the product of multiple rain events, and the chemical composition of these samples are thus representative of average local meteoric water. Therefore, if rainwater has reacted with halite minerals during vertical infiltration of near surface sediments, the soil pore water should exhibit Br/Cl ratios that are significantly lower than measured in samples collected from the domestic rainwater tanks, and display a

progressive decrease in ratios with increasing Cl^- concentration. Near surface pore waters do exhibit Br/Cl ratios that are significantly lower than meteoric water (Figure 4.14). Dissolution of halite could possibly explain these low near surface values. Na/Cl molar ratios trend towards 1 with increasing depth at three of the four locations, which further supports the possibility of halite dissolution (Figure 4.15). However,

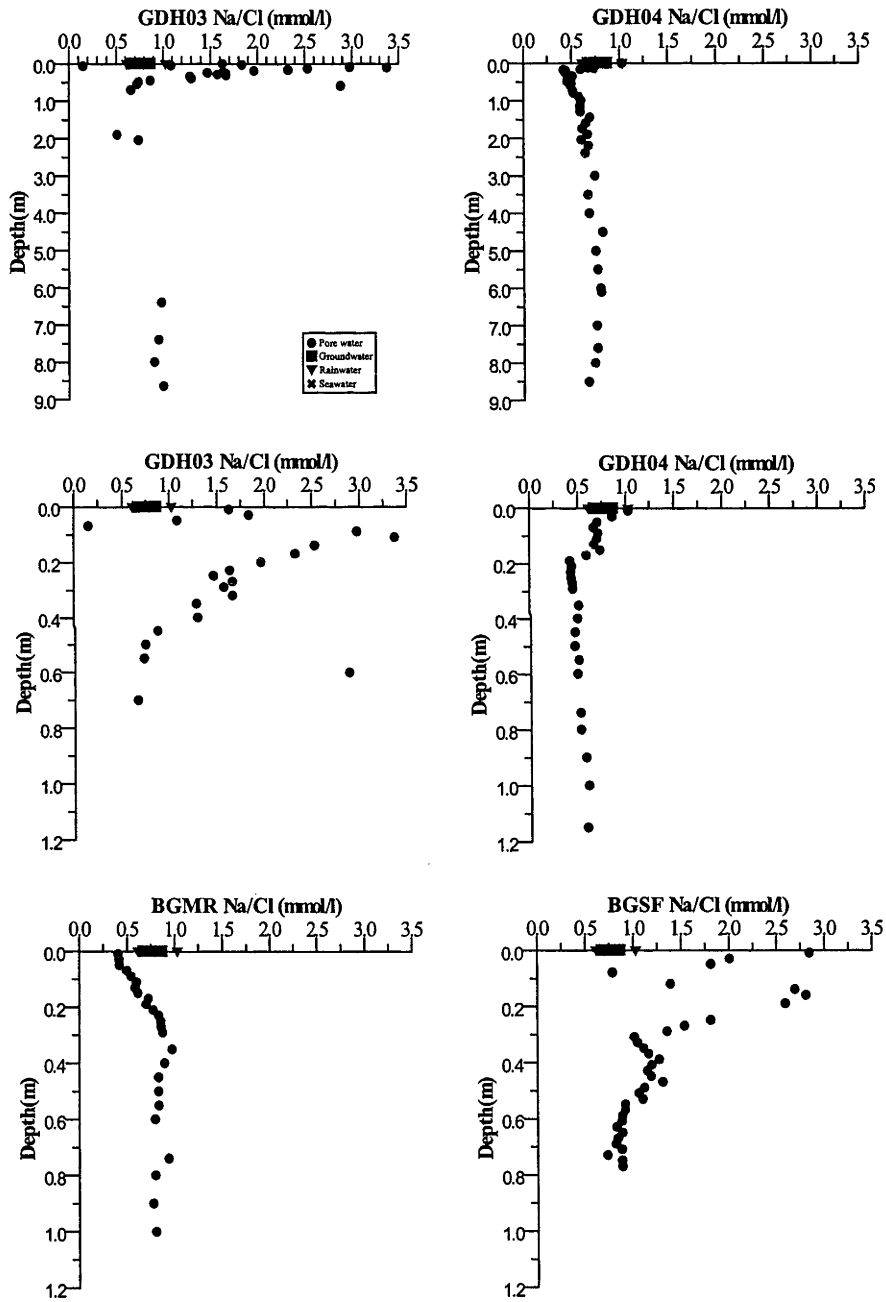

Figure 4.15: Variations in pore water Na/Cl (molar) ratios with depth at locations GDH03, GDH04, BGMR and BGSF. Water table is present at 7.45 metres at GDH03 and at 7.9 metres at GDH04.

because Na concentrations can be affected by cation-exchange reactions, particularly with increasing ionic strength (Arad and Evans, 1987), Br/Cl ratios are probably a more reliable indicator of halite dissolution. Ion exchange could explain the variations in Na/Cl ratios and will be discussed in a later section.

In order to understand if the observed Cl^-, Br^- and Br/Cl values are a result of evapotranspiration and/or halite dissolution/precipitation, a numerical model was constructed. The model is similar to Love et al. (2000) who modelled Br^- and Cl^- trends for dissolution of halite to understand Cl^- sources for groundwater in the Great Artesian Basin in South Australia. Their models and the ones presented below incorporate varying degrees of evapotranspiration of meteoric water and depict Br/Cl ratios and Cl^- concentration trends from progressive halite dissolution.

Figure 4.16 depicts predicted trends for halite dissolution and data trends for Cl^- concentrations and Br/Cl ratios. Only data from pore waters sampled from the upper 1 m exhibit large variations in Br/Cl ratios, which suggest non-conservative behavior of Cl^- and/or Br^-. Therefore only these values were compared with modelled halite dissolution trends. The model assumes meteoric input of Cl^- containing 2 mg/l Cl^- and Br/Cl ratio of $7x10^{-3}$, and depicts trends for rainwater dissolving halite during infiltration of the upper 1 metre of the unsaturated zone. Numerical models depict increases in Cl^- concentrations and decreases in Br/Cl ratios resulting from dissolution of halite only. 1 mg increments of Cl^- are added from initial concentration 2 mg/l to final concentration of 20,000 mg/l (greater than highest pore water Cl^- concentrations). Furthermore, predicted trends are depicted for evapotranspiration of rainwater to 50 mg/l and 500 mg/l, followed by dissolution of halite during

infiltration. This range in Cl^- concentrations is similar to those used by Love et al. (2000) and are within the range of pore waters from the upper 20 cm in Barmedman Creek catchment, where variation in Br/Cl ratios occur.

Comparisons of modelled trends to measured Cl^- and Br^- concentrations in soil pore water suggest that processes other than halite dissolution are occurring in the near surface of the unsaturated zone. This is supported by Na/Cl molar ratios greater than or less than 1 in near surface pore waters (Figure 4.15); a value expected if halite dissolution were a significant process influencing Na and Cl^- concentrations. Furthermore, the discrepancy between the modelled trends and measured trends suggest that the near surface depletions in Br/Cl relative to meteoric input are due to removal of Br from solution rather than addition of Cl.

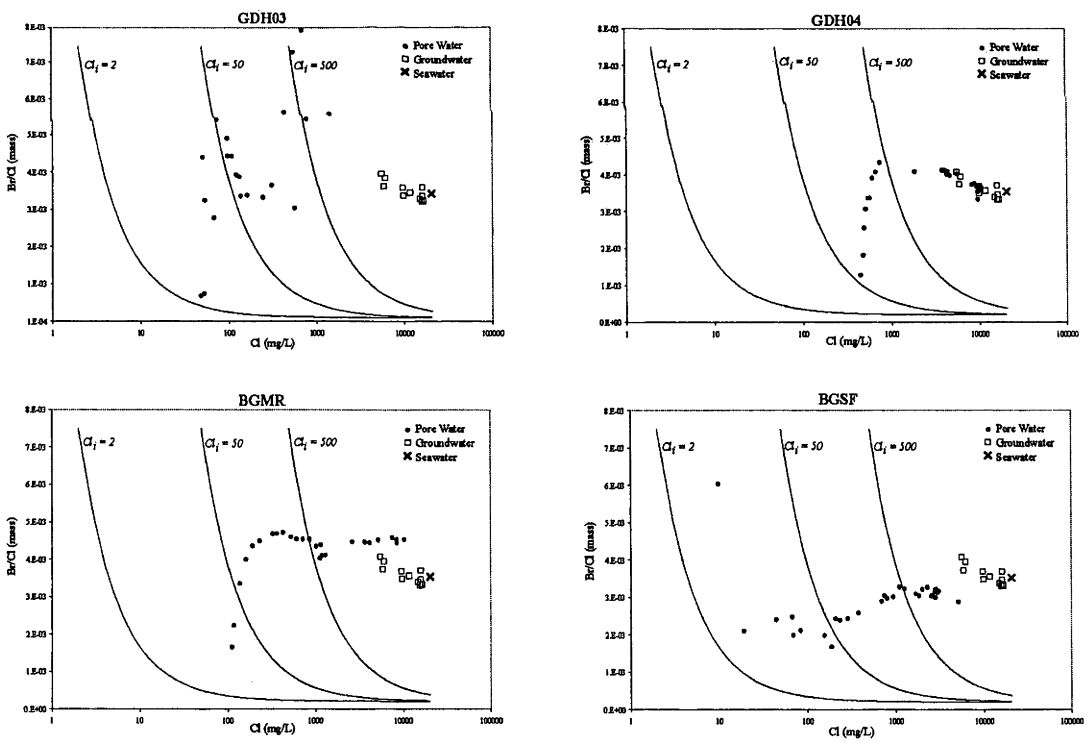

Figure 4.16: Br/Cl (mass) ratios and Cl concentrations for pore waters within the upper 1 m at locations GDH03, GDH04, BGMR and BGSF. Curves depict modelled trends for rainwater dissolving halite during infiltration of the upper 1 metre of the unsaturated zone. Different curves simulate evapotranspiration of rainwater to 50 and 500 mg/l Cl prior to dissolution of halite.

Non conservative bromide dynamics

Seaman et al. (1996) experimentally demonstrated the anion sorption capacity of highly weathered iron oxide coated sediments. The experiments consisted of eluting columns of predominantly sandy materials with a range of Br^- solutions under different pH conditions and found the degree of Br^- retardation correlated well with iron oxide content of sediments. In these experiments, Br^- retention correlated poorly with the pH of solutions; therefore, the authors concluded anion sorption capacity of sediments was not a pH dependent reaction. Although the pH of pore waters were not measured in this study, the sediment samples appeared to be coated with Fe oxyhydroxides and therefore adsorption of Br^- onto the grain surfaces could possibly explain the low Br/Cl ratios in near surface sediments.

An additional sink for Br^- could be due to cycling of bromine through soil organic mater and uptake by plants. Gerritse and George (1988) attributed low Br/Cl ratios relative to meteoric input in near surface soil water to biogeochemical processes and the preferential uptake of Br^- by vegetation. The authors experimentally demonstrated the sorption capacity of organic materials in sediments containing relatively low (2-7 %) organic carbon. The experiments consisted of leaching a soil columns packed with sandy near surface soils, followed by 30 days incubation and subsequent final leaching. The authors noted nearly 3 orders of magnitude increase in the Br/Cl ratios ($3x10^{-3}$ to $1x10^{-1}$) in the leachate that was attributed to decomposition and dissolution of organic material containing elevated Br^- relative to Cl^-. These processes were related to field studies where discrepancies between Br/Cl ratios in near surface soil water and groundwater relative to meteoric input were attributed to adsorption of Br^- onto organic materials and vegetative uptake (produced low dissolved Br/Cl ratios)

and oxidation of organic material (produced high dissolved Br/Cl ratios). Near surface sediments (<10 cm) from this study appear to be organic-rich and the low Br/Cl ratios in soil water extracted from this zone may be due to organic adsorption of Br^-. This theory is more likely than Br^- sorption onto iron oxyhydroxides because the depletion in Br/Cl only occurs in the organic-rich near surface horizon. This organic zone is underlain by highly ferruginous materials and the depletion in Br/Cl ratios should extend to greater depth if sorption of Br^- onto sediment surfaces were occurring.

An explanation for the increasing Br/Cl depth trend from depleted near surface values to values closer to meteoric input, is that near surface pore waters have significantly lower Br^- concentrations than samples at greater depth. In the near surface, a small loss of Br from solution would have a larger impact on the Br/Cl ratio than would occur for deeper pore waters exposed to a greater degree of evapotranspiration. As the Br^- concentration increases, the effects of minor removal of Br^- from solution become less evident. However, if vertical piston flow conditions are occurring in the unsaturated zone at these locations, the preferential removal of Br^- and decrease in Br/Cl ratios in the upper 10 cm should be preserved within the water as it slowly infiltrates and is subjected to greater degrees of evapotranspiration. The discrepancy between near surface Br/Cl ratios and those measured in deeper (>10cm) samples could be the result of preferential flow through the near surface organic rich horizon and subsequent lack of Br^- adsorption. Plants rely on only minor amounts of Cl^- for growth (Ozanne, 1958), however considering the high background levels of Cl^- at all four locations, vegetative uptake of Cl^- would have no measurable impact on the Br/Cl ratios. Oxidation of near surface organic materials is an alternative explanation for the increasing Br/Cl trend in the upper 10 cm (Gerritse and George, 1988). At

three of the four profiles in this study, moisture content decreases rapidly over the upper 10 cm indicating a greater degree of water removal below the surface, presumably due to uptake of water by roots (Figure 4.4). Over this interval the Br/Cl ratios increase suggesting that during evapotranspiration, organic material is oxidized and releases Br into solution causing the observed increase in Br/Cl ratios in the upper 10 cm.

Based on the available data from this study, Br^- appears to be exhibiting non-conservative behaviour in the near surface of the unsaturated zone. Following atmospheric deposition, Br^- is subjected to biogeochemical processes during vertical infiltration, particularly within the organic horizon. Cl^- appears to behave more conservatively than Br^-, and is therefore the more suitable geochemical tracer for this system. The following discussion sections assume Cl^- is sourced from the atmosphere and is behaving conservatively in the near surface.

Spatial variation in evapotranspiration

Pore waters sampled at 1 cm depth exhibit large variations in Cl^- concentrations between the four locations (Figure 4.5) indicating spatial variations in evapotranspiration. The highest degree evapotranspiration, as indicated by Cl^- concentrations of pore waters in the upper 10 cm, occurs at location GDH04 followed by BGMR>GDH03>BGSF. Rainfall evaporation factors, expressed as the ratio of Cl^- concentration of pore water at 1 cm to the Cl^- concentration of rainwater, indicate evaporation factors ranging from 4.4 at BGSF to 220 at GDH04. The greatest proportion of fine grained sediments (%clay + silt) in the upper 10 cm occurs at location BGMR followed by BGSF>GDH04>GDH03 (Figure 4.3). However, fined

grained materials are dominated by silt sized fractions at all locations. The proportion of clay in the upper 10 cm, although generally less than 20%, is greatest at location GDH04 followed by BGMR>GDH03>BGSF. Although near sediments at each location are dominated by clay and silt sized fractions, the proportion of clay appears to control the degree of evapotranspiration.

Comparisons of Cl^- concentrations at ~ 75 cm indicate total evapotranspiration over the upper 1 m was greatest at GDH04 followed by BGMR>BGSF>GDH03. However the greatest overall enrichment in Cl^-, determined by the ratio of Cl^- concentrations at the base of the profile to Cl^- concentrations at 1 cm, occurred at location BGSF followed by BGMR>GDH03>GHH04. Location BGSF had the lowest near surface (<10 cm) Cl^- concentrations yet greatest enrichment, while GDH04 exhibited the highest near surface Cl^- concentrations and lowest total enrichment over the upper 1 metre. This indicates variation in evapotranspiration with depth between the sampling locations. Greater near surface solute enrichments suggest a greater degree of evaporation while subsurface enrichments imply greater degrees of transpiration. At BGSF the greatest enrichment in Cl^- occurred below 10 cm while at GDH04 it occurred within the near surface. The greater near surface enrichment at GDH04 and lack of subsurface enrichment suggests that evaporation is more significant than transpiration at GDH04. The opposite occurs at the cores located proximal to the recharge area (GDH03, BGMR and BGSF), indicating transpiration as a significant process responsible for concentrating solutes during groundwater recharge. This theory is supported by δ^2H trends in regional groundwater, which display relatively constant δ^2H values with increasing Cl^- (Figure 4.17). Similar isotope trends were observed by Zimmerman et al. (1967), Arad and Evans (1987), Turner et al. (1987),

Turner et al. (1991) and Love et al. (1993) and were attributed to ion exclusion and lack of isotopic fractionation during uptake of water by plant roots.

Infiltration flow regimes

Atmospheric deposition of Cl^- appears to be the only source for Cl^- in this study, and evapotranspiration is responsible for the observed increase with increasing depth. At all near surface (>1 m) profiles the Cl^- concentration increases monotonically with depth. Johnston (1987) related the vertical distribution of Cl^- to subsurface hydrology and described the monotonically increasing profiles as the result of piston like flow in well drained soils. Allison et al. (1985) described the shape of these profiles as a result of progressive transpiration of infiltrating water under piston flow through the

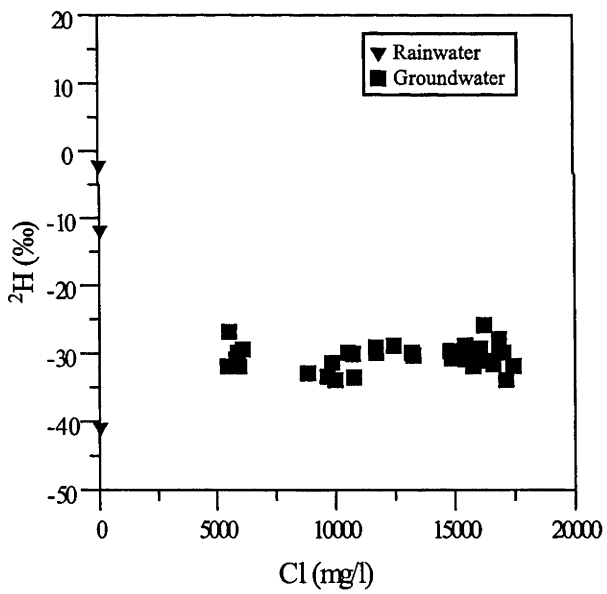

Figure 4.17: δ^2H‰ values as a function of Cl^- concentration for all groundwater samples collected from permanently installed piezometers in Barmedman Creek catchment.

root zone. Under these conditions, the maximum Cl^- concentration is reached within the root zone, beneath which the chloride concentration is constant with increasing depth. The conditions responsible for monotonically increasing profiles contrast to those that produce bulge type profiles (Johnston et al., 1980), which are the result of

bimodal flow regimes in the unsaturated zone (Allison et al., 1985). Under these conditions water infiltrates under piston-like flow conditions and is subjected to a high degree of evapotranspiration in the root zone. Lower Cl^- concentrations located beneath the root zone have been attributed to bypass flow along preferential flow paths (Peck et al., 1981; Allison et al., 1985).

All near surface (< 1 m) profiles from this study display progressive increases in Cl^- concentration with increasing depth (Figure 4.5), suggesting piston-like flow conditions. The depth interval over which the increase occurs has been attributed to the vertical extent of the root zone (Phillips, 1994; Tyler and Walker, 1994). GDH03 is located within a stand of mature Casuarinas whereas GDH04 is located in an area cultivated with canola and wheat. The differences in vegetation and root depth are reflected in the Cl profiles. At GDH03 the Cl^- concentration increases with increasing depth to 2.5 metres while GDH04 Cl^-concentrations increase to 50 cm.

Below the root zone, GDH03 exhibits a zone of lower Cl^- concentrations from 3 to 4.8 metres indicating preferential flow through the root zone (Figure 4.5). At GDH04, the Cl^- concentration increases only to 50 cm, below which the Cl^- concentration is reasonably constant. This suggests a much shallower root zone at GDH04 and a lack of preferential flow.

At cores BGSF and BGMR the Cl^- concentration increases with increasing depth to the base of the profiles (0.77 and 1.15 metres), which indicates piston-like flow over these depth intervals. Both locations are within stands of mature Casuarinas. At these locations the rate of Cl^-accumulation decreases with increasing depth indicating a lack

of evapotranspiration at the base of each profile. This indicates that despite the shallow coring depths at these locations, the profiles have penetrated most of the root zone.

Chloride Mass Balance: Infiltration rates

Numerous studies have used Cl^- concentrations in the unsaturated zone and in shallow unconfined groundwater as the means for quantifying vertical recharge rates (Eriksson and Khunakasem, 1969; Allison and Hughes, 1978; Peck et al., 1981; Allison and Hughes, 1983; Scanlon, 1991; Wood, 1999). In the absence of preferential flow and significant surface runoff, the following equation can be used to estimate vertical recharge rates from average annual precipitation, Cl^- concentration in precipitation and unsaturated zone soil pore water Cl^- concentrations (Wood, 1999):

$$q = (P)(Cl_p)/Cl_u \qquad (1)$$

where q is the vertical recharge flux (LT^{-1}), P is average annual precipitation (LT^{-1}), Cl_p (ML^{-3}) is the Cl concentration in precipitation and Cl_{uz} (ML^{-3}) is the Cl^- concentration of unsaturated zone pore water. Applying eqn. (1) to average Cl^- concentrations beneath the root zone at GDH03 (>2.5 m) and GDH04 (>0.5 m) yields vertical recharge rates of 2.6×10^{-4} and 1.2×10^{-4} m/yr. However, because the presence of lower Cl^- concentrations at 3-4.8 m at GDH03, the vertical recharge rate calculated from eqn. (1) is likely an underestimate due to the evidence for vertical preferential flow at this location. To understand vertical infiltrations rates in the upper 1 metre, eqn (1) was applied to Cl^- concentrations at similar depth intervals (70-75 cm) at the four locations. The calculated vertical rates (m/yr) ordered from greatest to least are:

GDH03 (0.7 m) = $9.5x10^{-4}$, BGSF (0.73 m) = 3.5×10^{-4}, BGMR (0.74 m) = 1.8×10^{-4}, GDH04 0 (0.74 m) = 9.6×10^{-5}. CMB based infiltration rates calculated from rainwater and groundwater Cl concentrations for the Bland Basin (0.2 and 5 mm/yr) are consistent with the CMB rates calculate here (Carrara 2005). The calculated values indicate an order of magnitude difference in vertical infiltration rates between the 4 locations and suggest a lack of groundwater recharge in the distal portions of the catchment area. This is consistent with the groundwater hydrogeochemistry results discussed in Chapter 3.

4.4.2 Biogeochemical Processes and Nutrient Cycling

The influences biogeochemical processes have on solute distributions in the near surface of the unsaturated zone have been well documented throughout the world. Bioassimilation of inorganic carbon, nitrogen, sulphur and phosphorus in rainwater during infiltration can act as a significant sinks for these elements (McGill and Cole, 1981; Johnson, 1984; Boring et al., 1988; Mayer et al., 1995a; Mayer et al., 1995b; Mayer et al., 2001; Novak et al., 2003; Walvoord et al., 2003). The influences of nutrient cycling by plants can also play an important role in unsaturated zone solute dynamics (Foulds, 1993; Jobaggy and Jackson, 2001; White et al., 2006). However, far less attention has been focused on the effects of biogeochemical processes and nutrient cycling on the chemical composition of regional groundwater. Kreitler and Jones (1975) and Walvoord et al. (2003) discussed the importance of these processes with regard to nitrogen while Mayer et al. (1995b) suggested the need for consideration of soil microbial processes for interpretation of groundwater stable isotopic ratios of sulphur and oxygen. The influences of nutrient cycling on the cation composition of groundwater were briefly discussed by White et al. (2006).

The results from this study suggest that biotic processes and nutrient cycling in the near surface of the unsaturated play a significant role in the geochemical evolution of major ion concentrations in regional groundwater.

Biotic vs abiotic sulphate retention

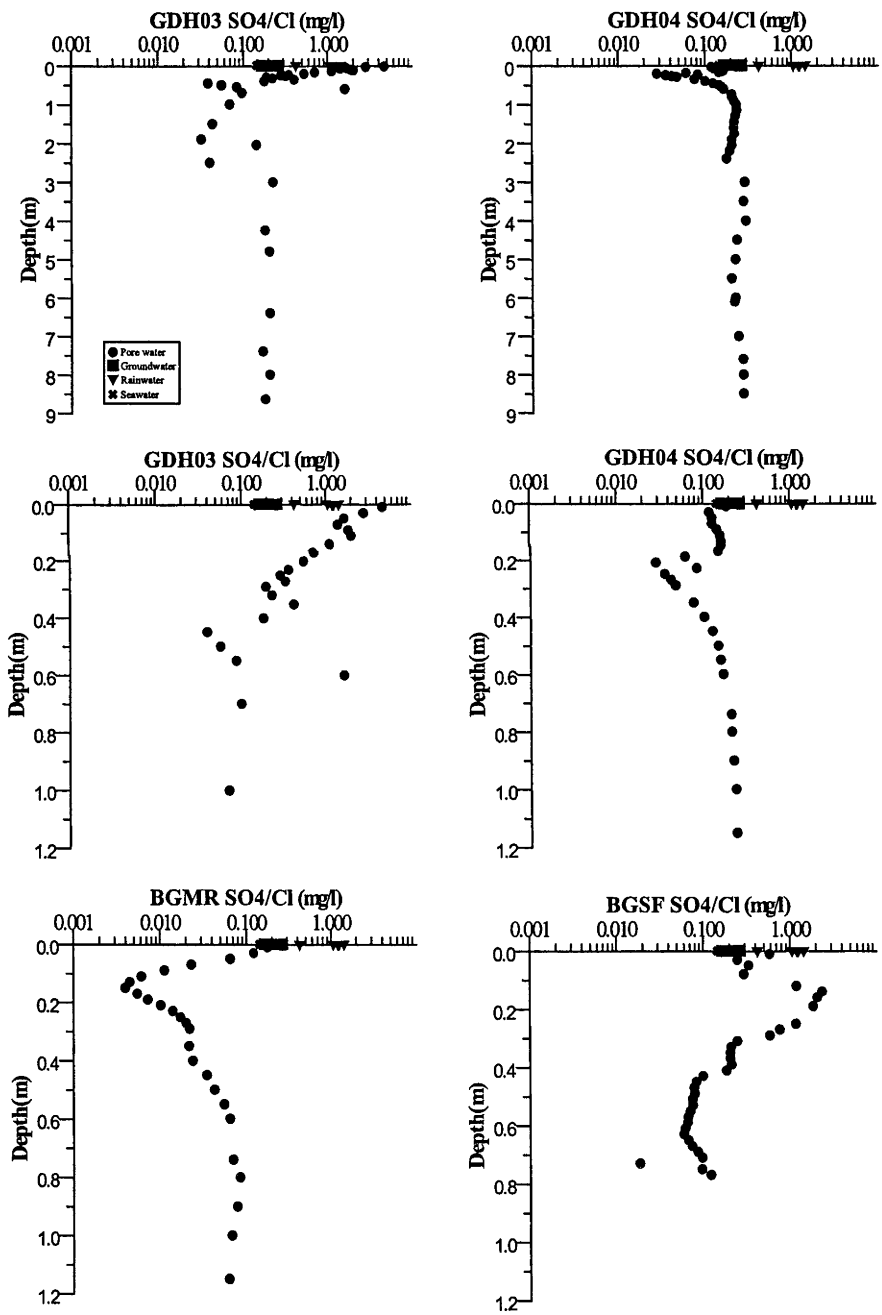

Figure 4.18: Variations in pore water SO_4/Cl (mass) ratios with depth at locations GDH03, GDH04, BGMR and BGSF. Water table is present at 7.45 metres at GDH03 and at 7.9 metres at GDH04.

The three solute profiles from within the proximal portion of the study area (GDH03, BGMR and BGSF) exhibit near surface decreases in SO_4/Cl ratios with increasing depth (Figure 4.18). At locations GDH03 and BGMR, the SO_4^{2-} concentrations decrease by an order of magnitude within the upper 50 cm. These trends indicate an active SO_4^{2-} sink within the near surface of the recharge zone. Ca concentrations also decrease over the upper 50 cm (Figure 4.12), suggesting that gypsum precipitation is occurring in the near surface. However, pore waters are significantly undersaturated with respect to gypsum (and anhydrite) indicating processes other than SO_4^{2-} mineral precipitation are responsible for the decreasing SO_4/Cl ratios. Biological assimilation of sulphate to carbon bounded sulphur or ester-bound sulphate have been found to be a significant near surface sinks for atmospherically derived SO_4^{2-} (Johnson, 1984; Mayer et al., 1995a; Giesler et al., 2005). Preferential retention of SO_4 relative to Cl^- was demonstrated experimentally by Yaalon (1965) and was attributed to interactions with the soil materials. Mayer et al. (2001) conducted field experiments which irrigated various soil types with applied SO_4 tracers and found that more than 80 % of applied SO_4^{2-} was retained within the soil matter. The total SO_4^{2-} retention was found to increase with increasing sesquioxides content of soils and the authors concluded that adsorption onto mineral surfaces was the dominant sink for inorganic sulphate. Nutrient cycling has also been shown to be an important process for SO_4^{2-} distributions and mobility in soils (Johnson, 1984; Jobaggy and Jackson, 2001).

Within this study area, XRF results from previous studies (unpublished data, courtesy Geoscience Australia and Australian Bureau of Rural Sciences) indicate high relative abundances of Al_2O_3 (<22 wt. %) and Fe_2O_3 (<20 wt. %) within sediments sampled

from various depth intervals at several locations. All sediments sampled by this study exhibited red to brown, highly oxidized appearance, and ferruginous precipitates were visibly identified at various depths at each location suggesting that adsorption onto sesquioxide mineral surfaces is a probable explanation for the observed near surface SO_4^{2-} depletion. However, these minerals are ubiquitous throughout this study area (Gibson et al., 2002; Tan et al., 2002) and degree of adsorption would presumably be

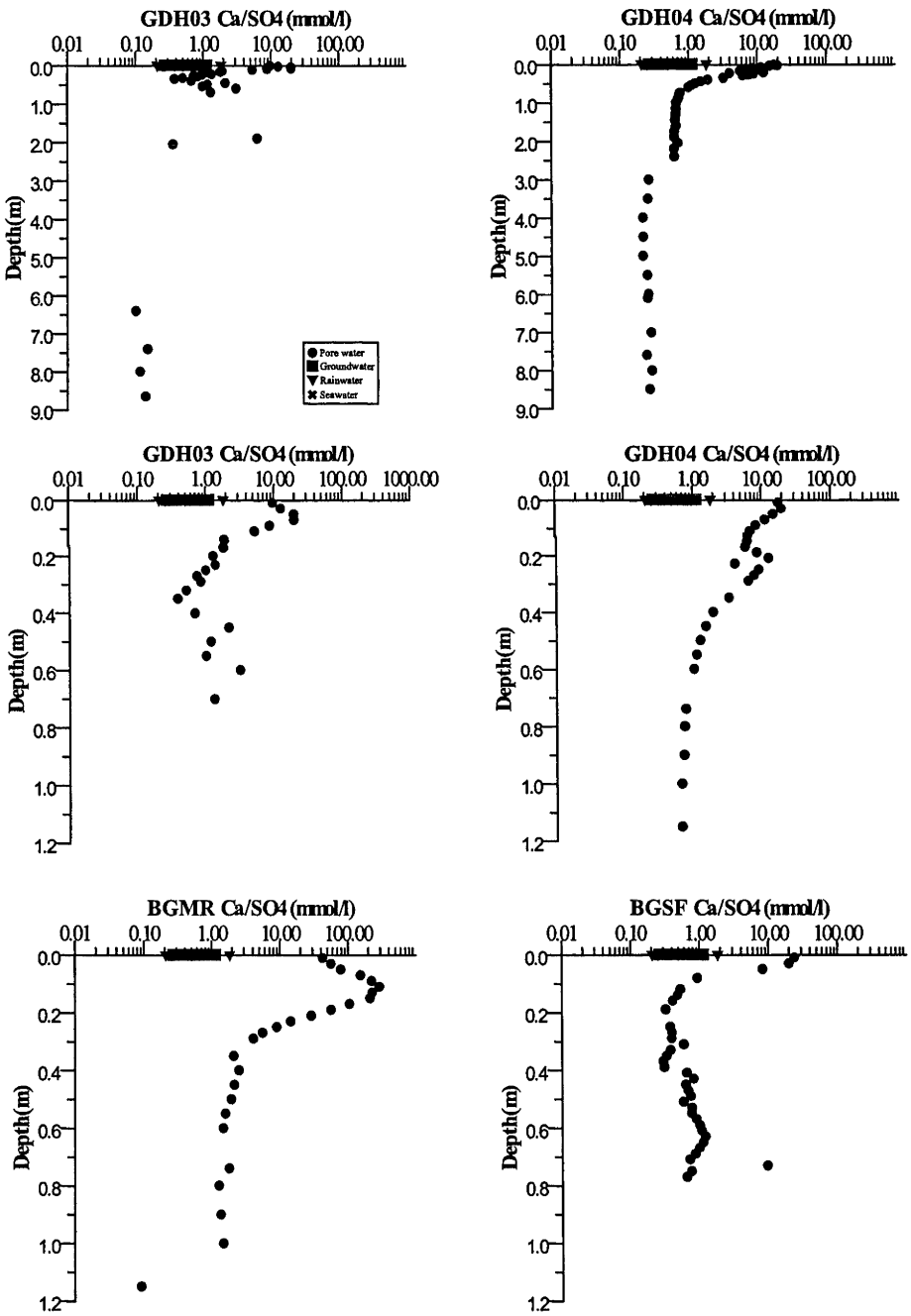

Figure 4.19: Variations in pore water Ca/SO_4 (molar) ratios with depth at locations GDH03, GDH04,

BGMR and BGSF. Water table is present at 7.45 metres at GDH03 and at 7.9 metres at GDH04.

independent of depth, and occur throughout the entire study area rather than within only the organic rich near surface horizon at three of the four locations. This suggests that other processes, such as bioassimilation of sulfur or sulphate reduction are responsible for the observed SO_4^{2-} trends. However, in the absence of pH measurements of pore water samples, and more comprehensive assessment of host sediment mineralogy, the possibility of abiotic retention of SO_4^{2-} on mineral surfaces cannot be discounted.

Nutrient cycling

The influences of nutrient cycling on solute distributions in the unsaturated zone were discussed in detail by Jobaggy and Jackson (2001). The authors described near surface solute distributions as dominated by two main processes, leaching and nutrient cycling. Leaching was described to result in a downward solute flux, and in combination with evapotranspiration, produces solute profiles that increase in concentration with increasing depth. Nutrient cycling results in a net upward solute flux and produces decreasing solute concentrations with increasing depth. The authors attributed the characteristic near surface enrichment as the result of nutrient uptake by plants and subsequent redistribution to the soil surface by litter fall and through fall. Elements such as Cl, Mg and Na have been found to be less limiting nutrients to plant growth compared to N, P, K and Ca (Zinke, 1962; Foulds, 1993; Schlesinger et al., 1996; Schlesinger and Pilmanis, 1998). Jobaggy and Jackson (2001) noted global distributions trends of growth limiting nutrients that were characterized by enrichment relative to non-limiting elements in the topsoil. Furthermore, they noticed in well leached soils, limiting nutrients (N,P,K,Ca) were retained within the profile while

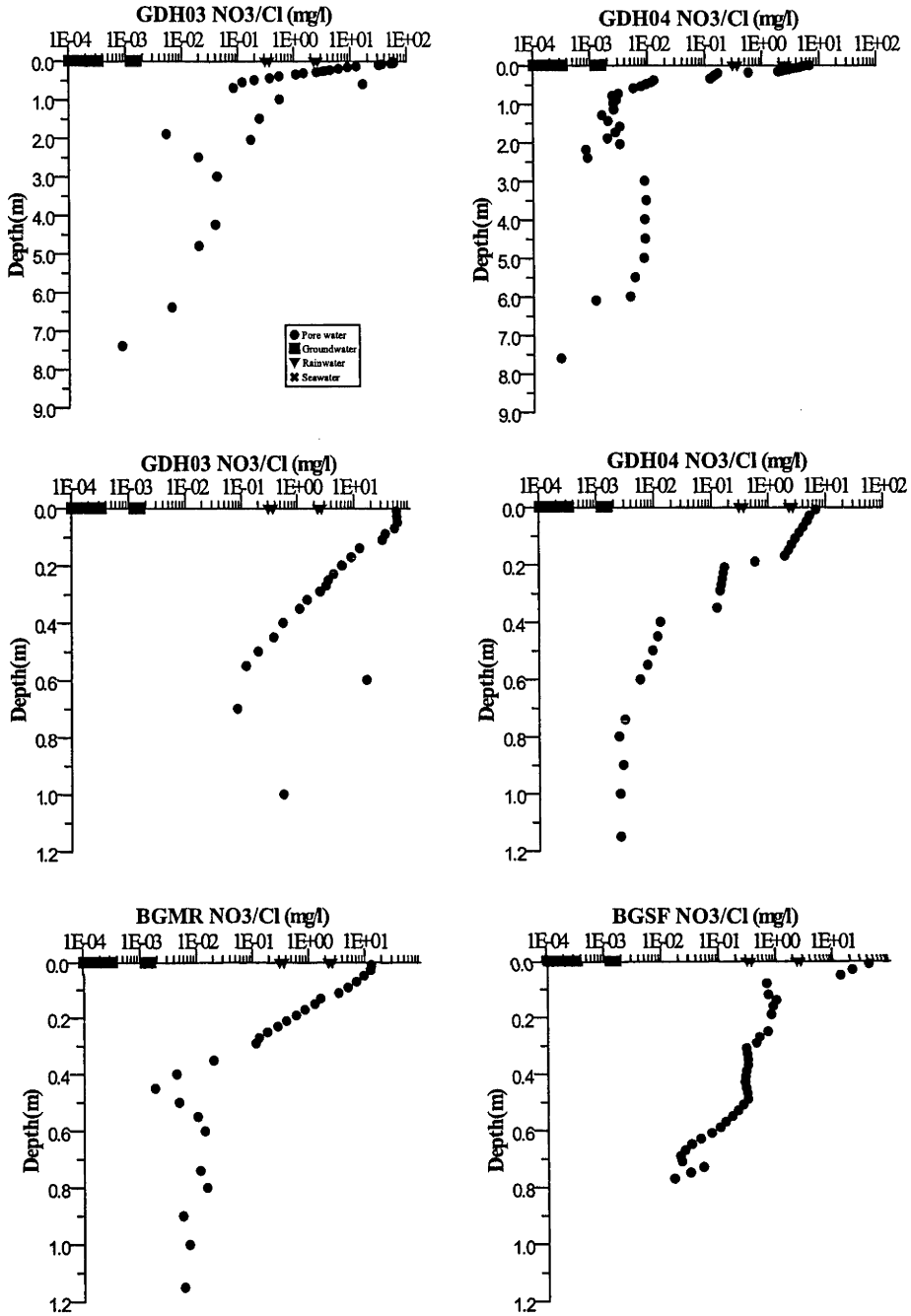

Figure 4.20: Variations in pore water NO_3/Cl (mass) ratios with depth at locations GDH03, GDH04, BGMR and BGSF. Water table is present at 7.45 metres at GDH03 and at 7.9 metres at GDH04.

non-limiting elements (Cl, Br, Na, Mg) were removed from the root zone. Solute distributions at the four sampling locations suggest that nutrient cycling is a significant process in the near surface of the unsaturated zone. The effects of this process on the observed profile trends and effects on groundwater composition are discussed below.

Limiting Nutrient Trends

Within the upper 5 to 10 cm at all locations, pore waters are enriched in NO_3^-, K, Ca and Mg relative to Cl^- compared to meteoric input (Figures 4.20-4.23). The greatest relative enrichment occurs with Ca followed by NO_3^- > K > Mg. When comparing nutrient concentrations in native plants to underlying soil, Foulds (1993) found that the *Casuarinaceae* family favoured the uptake of Ca>N> K> Mg>P, the same relative order of significance observed in near surface pore waters from this study. Location GDH04 is within an area cultivated with canola and wheat, and soil pore water sampled from the upper 10 cm exhibits slightly lower NO_3/Cl, K/Cl, Ca/Cl and Mg/Cl ratios than the sampling locations from within Casuarina stands. However, the relative enrichment is similar to the other locations within native Casuarina stands. The lack of relative enrichment at GDH04 can be explained by annual harvesting, which would remove the nutrients stored within plants rather than returning them to the surface. The similarities in relative element enrichment between the two vegetation types suggest that similar nutrient requirements exist between the species, or that pore waters at GDH04 reflect nutrient cycling trends established prior to clearing of native vegetation. Considering the findings of Foulds (1993), the near surface enrichment in specific elements reflects the net accumulation of limiting nutrients by the native Casuarina trees present at three of the four locations. The vegetation retains limiting nutrients within the root zone by scavenging the necessary elements from soil solutions and redistributing them to the soil surface by litter fall (Schlesinger et al., 1996; Schlesinger and Pilmanis, 1998; Jobaggy and Jackson, 2001). Non-limiting nutrients such as Na, Cl and Br are leached from the root zone which results in increasing concentrations with increasing depth. Limiting nutrients display near surface enrichments relative to Cl^-, and decrease relative to Cl^- throughout the root

zone (Jobaggy and Jackson, 2001; Walvoord et al., 2003). The depths to which the nutrient decreases occur are related to the depth intervals over which Cl^- concentrations increase at each location. This confirms that the peak in Cl^- concentrations correspond to the maximum depth of the root zone (Allison et al., 1985; Phillips, 1994; Tyler and Walker, 1994) and that transpiration is responsible for

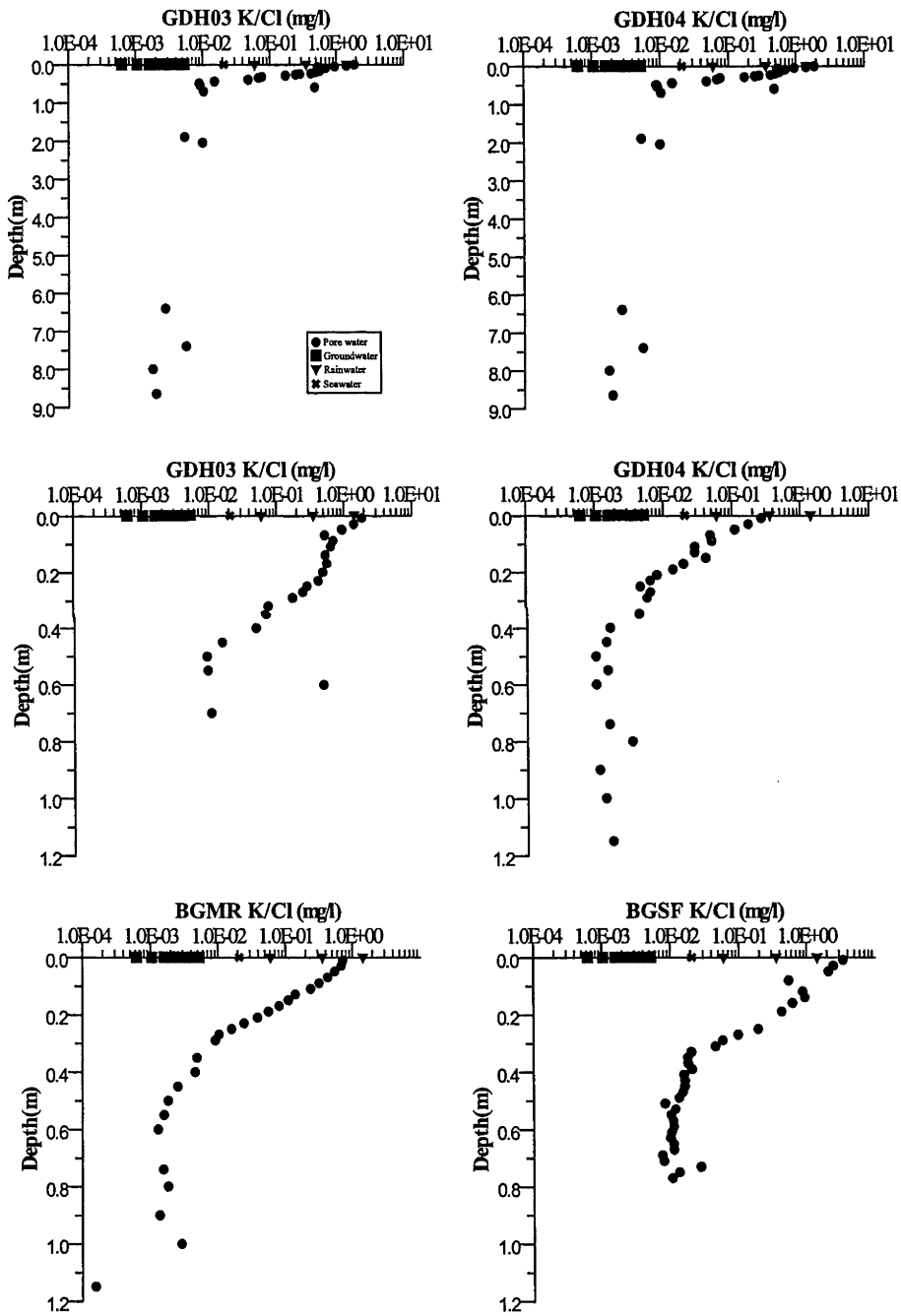

Figure 4.21: Variations in pore water K/Cl (mass) ratios with depth at locations GDH03, GDH04, BGMR and BGSF. Water table is present at 7.45 metres at GDH03 and at 7.9 metres at GDH04.

the observed increase in Cl^- concentrations. Water and nutrient uptake by vegetation appears to be as significant control on solute dynamics in the unsaturated zone. These processes are also reflected in cation/chloride ratios and stable isotopic compositions of groundwater indicating that vegetation is a dominant control on the relative solute proportions in groundwater.

Up-take of solutes in rainwater by the vegetation acts as a significant solute sink in the unsaturated zone. Comparing Cl concentrations of rainwater (~ 2mg/L) to average Cl concentrations of groundwater in the recharge zone (i.e. GDH03_1, 2, 3, GAC16, GAC17, GAC18) provide an estimate of the total evapotranspiration that has occurred during recharge. Average Cl concentrations of groundwater in the recharge zone is ~ 8,000 mg/L indicating an enrichment factor of ~ 4,000. In other words, assuming no other sources for Cl other than evapotranspiration, to produce the Cl concentrations measured in groundwater would require 4,000 times evapotranspiration of rainwater. Multiplying solute concentrations of rainwater by a factor 4,000 results in salinity values two times greater than were measured in groundwater in the recharge zone. This indicates that the vegetation removes up to half the solutes deposited in landscapes by rainwater.

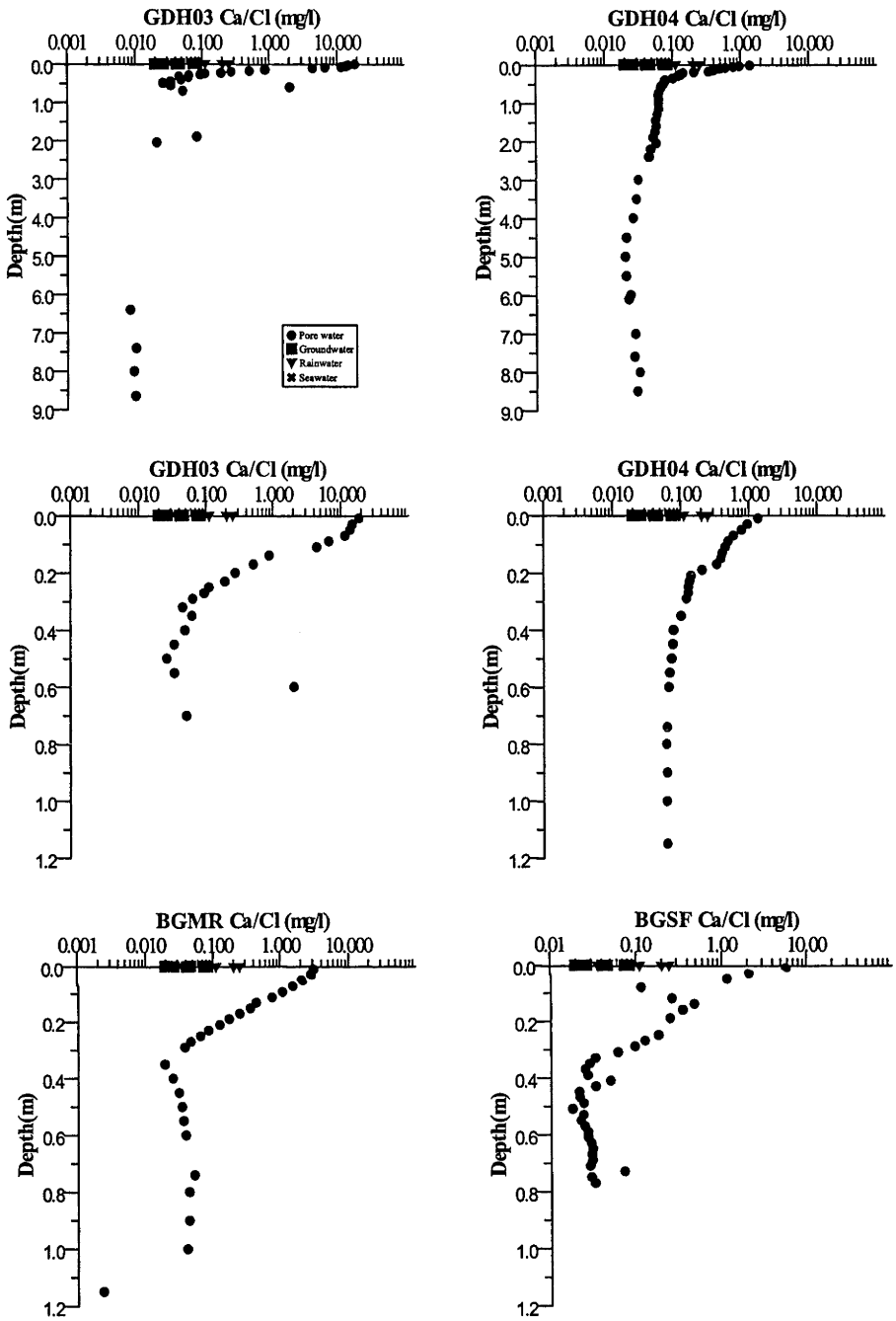

Figure 4.22: Variations in pore water Ca/Cl (mass) ratios with depth at locations GDH03, GDH04, BGMR and BGSF. Water table is present at 7.45 metres at GDH03 and at 7.9 metres at GDH04.

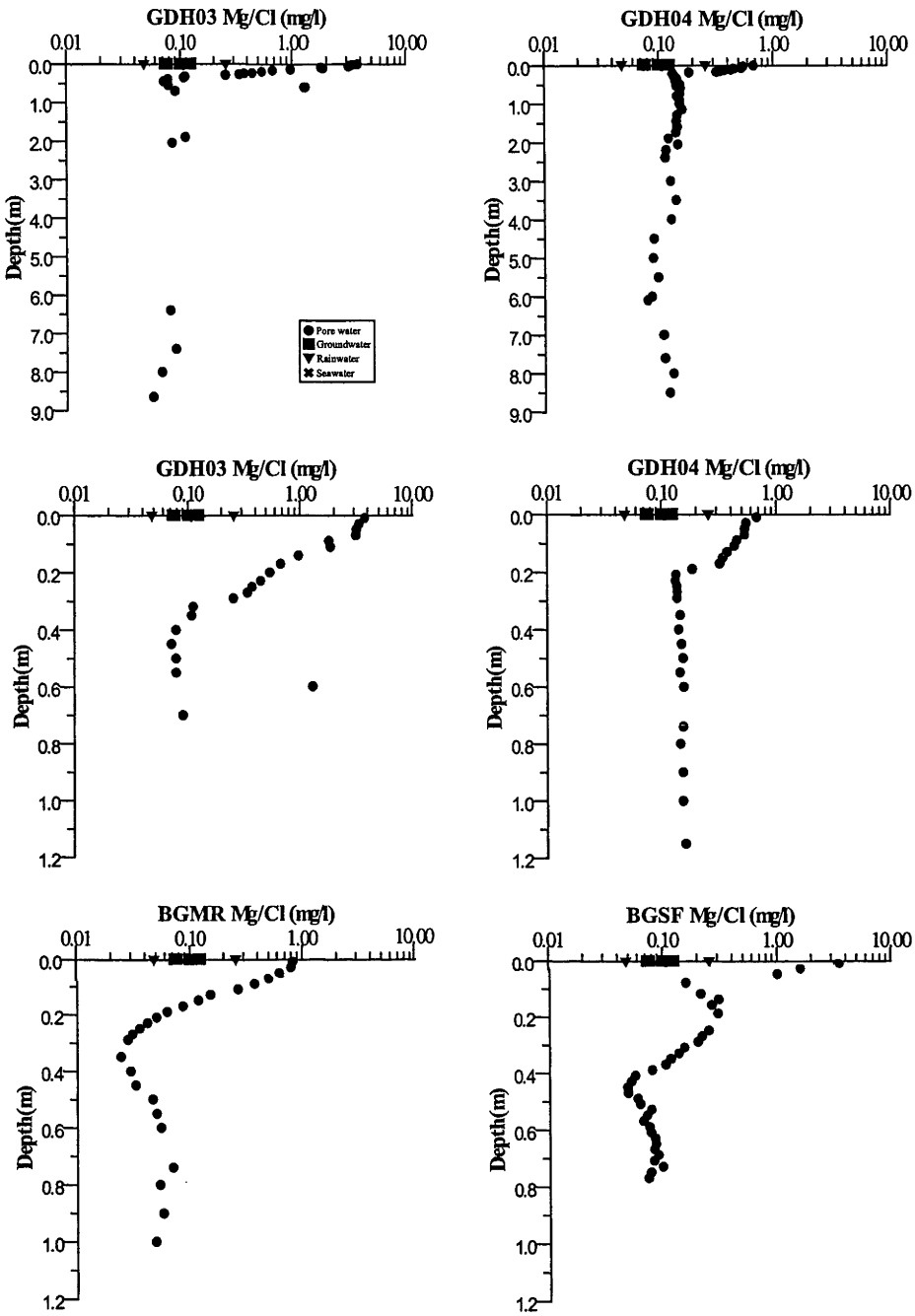

Figure 4.23: Variations in pore water Mg/Cl (mass) ratios with depth at locations GDH03, GDH04, BGMR and BGSF. Water table is present at 7.45 metres at GDH03 and at 7.9 metres at GDH04.

4.4.3 Water-sediment interactions

Mineral weathering and cation exchange reactions have been recognized as solute sources and sinks in hydrogeochemical studios from other semi-arid areas of Australia (i.e., Arad and Evans, 1987; Herczeg et al., 1991; Herczeg et al., 1993; Love et al.,

1993; Salama et al., 1999; Cartwright et al., 2004). As discussed above, biogeochemical processes and nutrient cycling can explain the observed cation/Cl trends; however, an alternative explanation is that mineral weathering or cation exchange reactions are also contributing to the chemical composition of pore water samples. In general, the cation/chloride ratios decrease over the upper 50 cm to values similar to those measured in regional groundwater (Figures 4.21-4.23). Evapotranspiration alone would have no affect on the cation/chloride ratios therefore the variations suggest that in addition to biogeochemical reactions, water-sediment reactions may also be influencing the chemical composition of recharge water in the unsaturated zone. The observed decreases in cation/chloride ratios indicate that silicate mineral weathering is not a significant process in the unsaturated zone. As discussed above, halite and gypsum dissolution/precipitation are unlikely influencing the observed Na/Cl or Ca/Cl ratios. An alternative explanation to the observed trends is cation exchange. Arad and Evans (1987) demonstrated that Ca^{2+} is preferentially exchanged for Na^{+} in clay minerals interacting with lower salinity waters. In addition, they noted a change in preference for Na^{+} over Ca^{2+} that occurred at Na^{+} concentrations greater than 30 meq/L. If large quantities of fresh rainwater were to infiltrate the clay-rich near-surface materials, the fresh water would transport solutes in solution and potentially leach those adsorbed to mineral surfaces. Prior to recharge events, the pore waters within the near surface would be subjected to high degrees of evapotranspiration and the subsequent increases in solute concentrations. Based on the findings of Arad and Evans (1987) and theory of displacement chromatography, the greater selectivity of Na^{+} at higher ionic strength would result in the preferential exchange of Na^{+} in solution for Ca^{2+} on the exchange sites of 2:1 clays. During a large recharge event, the displacement of saline pore water by rainwater would result in

exchange of Ca^{2+} for Na^{+} due to the greater affinity for Ca^{2+}on the exchange sites at lower salinity (Appelo and Postma, 1993) and explain the near-surface (<1 m) trends in Na/Cl and Ca/Cl ratios in Barmedman Creek Catchment.

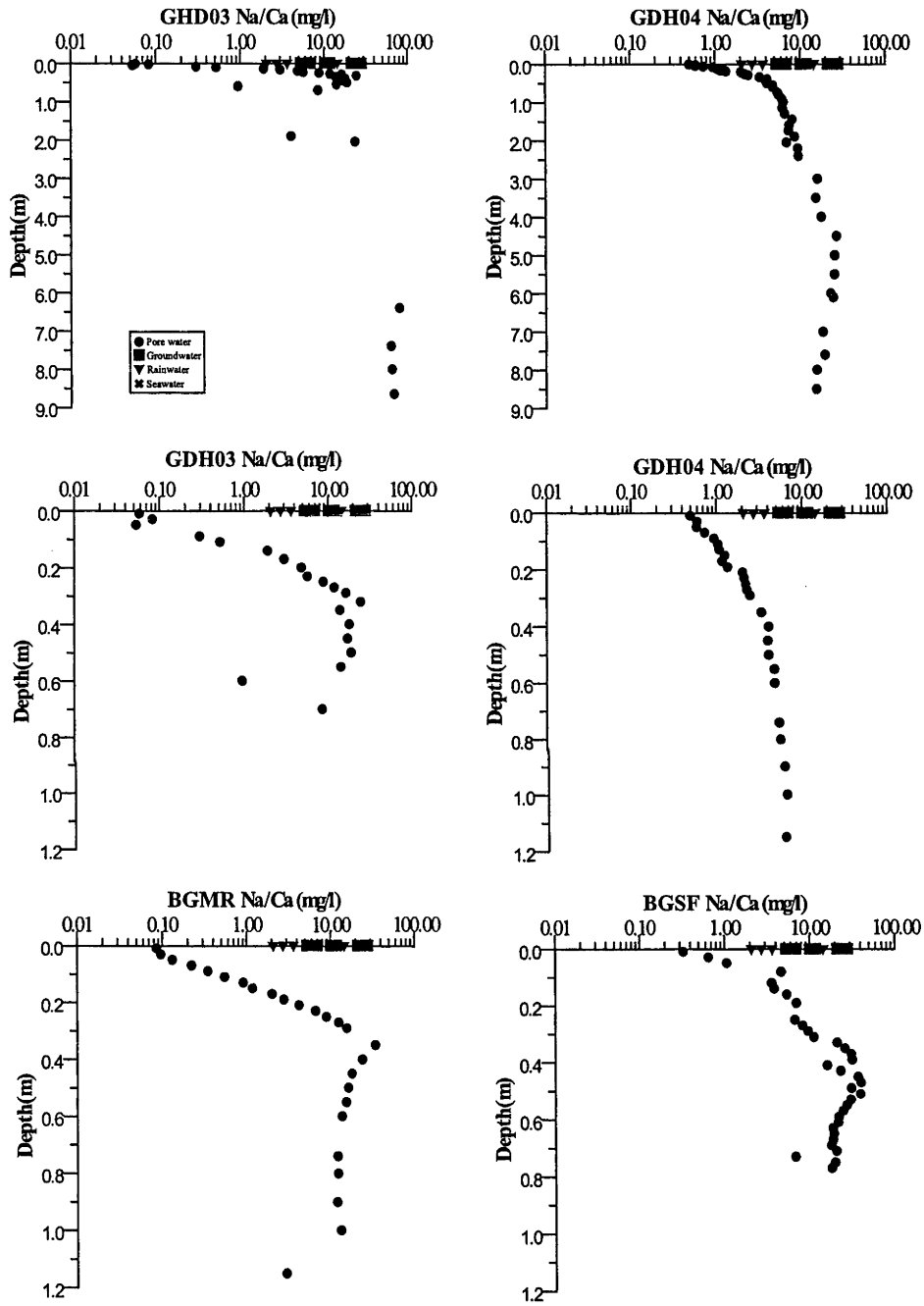

Figure 4.24: Variations in pore water Na/Ca (mass) ratios with depth at locations GDH03, GDH04, BGMR and BGSF. Water table is present at 7.45 metres at GDH03 and at 7.9 metres at GDH04.

Near surface (<5 cm) pore water samples exhibit Na/Ca ratios that are significantly less than rainwater and groundwater (Figure 4.24). At the three locations in the

proximal portion of the study area (GDH03, BGMR, BGSF), The Na/Ca ratio increases with depth through the upper 50 cm, below which it decreases slightly with increasing depth. Location GDH04 also exhibits increasing Na/Ca ratios over the upper 50 cm; however, the ratios continue to increase slightly throughout the remainder of the profile. At locations BGMR and BGSF, the depth at which the abrupt change in slope of Na/Ca vs. depth coincides with a change in the amount of increase in Na with depth (Figure 4.10). Ca/Cl ratios continue to decrease over this interval; however, Ca appears to be an important limiting nutrient to plants and variations in composition cannot be attributed solely to cation exchange. The change in slope of Na vs. depth occurs at Na concentrations of approximately 30 meq/L. This coincides with the Na concentrations reported by Arad and Evans (1987) for which 2:1 clays preferentially exchange interlayer Ca for Na in solution. XRD results from previous studies (unpublished data courtesy Geoscience Australia) on sediments within the Barmedman Creek catchment highlighted the presence of 2:1 clays such as smectite and illite in the unsaturated zone. This suggests that cation exchange is influencing the composition of soil pore water within the near surface of the unsaturated zone. The Na/Ca ratios within the upper 1 m trend towards regional groundwater suggesting that cation exchange during groundwater recharge is contributing to the geochemical evolution of groundwater. However, the near surface pore water samples that exhibit depletions in Na/Ca ratios relative to meteoric water exhibit high Ca/Cl ratios (Figure 4.22). Furthermore, the depth intervals over which the Na/Ca ratios increase correspond to decreasing Ca/Cl ratios. Because Ca^{2+} is the dominant limiting nutrient for the vegetation in this area, nutrient cycling is likely dominating the observed trends in Ca/Cl and Na/Ca ratios. Na concentrations of pore waters appear the more effective tool for assessing cation exchange. The effects of

nutrient cycling on the chemical composition of groundwater recharge appear more dominant than cation exchange within the unsaturated zone and may have a more widespread influence on the chemical composition of groundwater than previously considered by traditional hydrogeochemical studies.

4.5 Summary and Conclusion

Trends in chemical composition of pore waters within the unsaturated zone indicate the major geochemical evolution of groundwater composition occurs during recharge. The high resolution soil pore water profiles demonstrate rapid changes in composition that trend towards groundwater having a seawater-like composition within the upper 1 m of the unsaturated zone Processes such as evapotranspiration, nutrient cycling, biogeochemical reactions with organic materials and microbial biomass, and cation exchange can account for the large discrepancies between the chemical compositions of meteoric water and groundwater.

Evapotranspiration

Cl^- is sourced from the atmosphere and concentrated within the root zone by evapotranspiration. No evidence of Cl^- mineral dissolution was apparent in any of the four profiles. In the proximal portion of the study area a greater proportion of native vegetation remains, and transpiration is the dominant salt concentrating mechanism. This is reflected by the peak in Cl^- concentrations occurring at greater depths in the proximal portion of the study, which is the result of water extraction and subsequent ion exclusion by deeper rooted plants. The "bulge type" Cl^- profile at GDH03, suggests that preferential flow is occurring at this location. In the distal portion of the study location, in an area cultivated with canola and wheat, the Cl^- concentrations

reach a maximum within the upper 50 cm, followed by relatively constant Cl^- concentrations throughout the remainder of the unsaturated zone. At this location, a greater proportion of clay sized sediments are present within the near surface. The Cl^- profile and grain size distribution indicate a high degree of evaporation occurring in the near surface and lack of preferential flow to greater depths. ^2H and ^{18}O results of regional groundwater samples indicate transpiration rather than evaporation as the dominant salt concentrating mechanism. The lack of evaporative signatures in ^2H and ^{18}O of regional groundwater and consistent Cl concentrations below a depth of 50 cm at location GDH04 suggest that groundwater recharge is not occurring through the clay rich sediments within this portion of the study area.

Biogeochemical processes

Near surface (< 1 m) pore waters exhibit trends in Br^- and SO_4^{2-} that reflect biogeochemical processes. Large fluctuations in Br/Cl ratios in the near surface pore water suggest non-conservative behaviour of this ion. Low ratios relative to meteoric water are present within the organic rich horizons at all locations. Br/Cl ratios increase over the upper 10 cm to values similar to regional groundwater, but are considerably less than meteoric water. Data indicate that dissolution of Cl^- bearing solutes (i.e. halite) during vertical infiltration is unlikely. The low Br/Cl ratios are more likely the result of removal of Br^- from solution. Evidence for Br^- removal is only present within the organic rich near surface horizons. Biogeochemical processes such as adsorption of Br^- onto organic materials or uptake by plants are the best possible explanations for the low Br/Cl ratios. Pore waters are significantly undersaturated with respect to halite and Cl^- is not a limiting nutrient to plants therefore removal of Cl^- from solution is not responsible for the increasing Br/Cl

trends. The increasing ratios correspond to decreasing moisture content and increasing Cl^- concentrations suggesting that evapotranspiration results in oxidation of organic materials and subsequent desorption of Br^-.

Several profiles indicate a SO_4^{2-} sink in the near surface of the unsaturated zone. All waters are undersaturated with respect to gypsum therefore SO_4^{2-} is removed from solution by processes other than mineral precipitation. SO_4^{2-} distribution in the unsaturated zone is known to be influenced by biogeochemical processes (i.e., Johnson, 1984; Mayer et al., 1995a; Mayer et al., 1995b; Giesler et al., 2005). SO_4/Cl ratios fluctuate within the upper 50 and are considerably less than meteoric water. Below 50 cm, the ratios trend towards values similar to regional groundwater. This suggests that near surface biogeochemical processes are influencing the SO_4^{2-} composition of groundwater recharge and can account for the differences between SO_4/Cl ratios in meteoric water relative to groundwater.

Nutrient Cycling and Cation Exchange

Large variations in element/Cl ratios occur within the upper 50 cm and trend towards groundwater ratios within the upper one metre at all four locations. Profiles are characterized by elevated near surface ratios that decrease significantly with depth over the upper 50 cm. The greatest near surface enrichment and subsequent depletion with depth occurs for Ca>N> K> Mg>PO4. The order of significance corresponds to growth limiting nutrients for *Casuarinaceae* family plants (Foulds, 1993) that are found throughout the study area. Soil pore waters in an area cultivated with canola and wheat also reflect nutrient cycling by *Casuarinaceae* family plants. This suggests that the clearing of native vegetation in the late 1800's has had little impact on the ion

ratios within the unsaturated zone, and that vertical infiltration of modern meteoric water is insignificant at this location. Long term nutrient cycling by native vegetation appears to be a significant control on the chemical composition of groundwater.

Evidence of cation exchange is present at all locations, indicated by variations in Na/Cl and Ca/Cl ratios. However, because Ca^{2+} is a predominant limiting nutrient to most plant species (i.e. Foulds, 1993; Jobaggy and Jackson, 2001), the Na/Cl ratios appear to be the best tool for assessing the effects of cation exchange. Differentiating between cation exchange and nutrient uptake can only be approximated because neither process can be accurately quantified with the available data. However, the effects of cation exchange appear to be minimum compared to nutrient cycling. Variations in Na/Ca appear to be the result of nutrient cycling rather than cation exchange. However, Na/Cl ratios do decrease over the upper 50 cm at three of the four locations suggesting that progressive evapotranspiration leads to preferential sorption of Na on the interlayer sites of 2:1 clays. The variations in Na/Cl ratios correlate poorly to clay content of sediments indicating either large variations in mineralogy or that processes other than cation exchange are responsible for the variations. At all locations Na/Cl ratios vary by less than an order of magnitude, compared to Ca/Cl ratios which vary by more than 2 orders of magnitude. As such, nutrient cycling appears to be the dominant process controlling cation dynamics within the unsaturated zone and can explain the discrepancy between the cation/chloride ratios of rainwater and groundwater.

5 UNSATURATED ZONE Cl^-, Br^- AND ^{36}Cl DYNAMICS

5.0 Introduction

Within Australia, clearing of native vegetation and subsequent alterations to the hydrogeologic budget has resulted in enhanced mobilization of unsaturated zone solutes, which has resulted in extensive secondary salinization of groundwater and surface water (i.e., Peck and Hurle, 1973; Dimmock et al., 1974; Peck, 1978; Allison et al., 1990) and poses a serious environmental threat to freshwater resources in semi-arid and arid regions of Australia. However, the understanding of unsaturated zone solute dynamics and groundwater recharge rates in salinized landscapes is limited. In addition, few investigations of unsaturated zone geochemical processes have been conducted in arid and semiarid regions throughout the world (i.e., Johnston, 1987; Cook et al., 1992a; Nativ et al., 1997; Green et al., 2002). Mixing, evapotranspiration, mineral dissolution/precipitation, and water rock interactions are processes that are often discussed in these studies, but too difficult to quantify. These studies have often utilized Cl^- to normalize other element concentrations or to estimate groundwater recharge rates, assuming that the Cl^- ion is chemically conservative in the unsaturated zone. Br/Cl ratios are commonly used for testing this; however, nonconservative chemical behaviour of Cl^- and Br^- can result from processes such as mineral dissolution and mixing (Ullman, 1995; Davis et al., 2001; Davis et al., 2004), bacterial uptake (Shorter et al., 1995), adsorption by organic material (Gerritse and George, 1988), vegetative uptake (Milton et al., 2003), and adsorption onto mineral surfaces (Seaman et al., 1996). This demonstrates limitations toward assessing solute dynamics with Cl^- and Br^-, and their use as hydrogeochemical tracers.

Isotopes of chlorine and bromine can be useful for identifying non-conservative behaviour and for quantifying the respective hydrogeochemical processes. Chlorine isotopes (^{37}Cl and ^{36}Cl), and more recently $\delta\,^{81}Br$ (Shouakar-Stash et al., 2006; Stotler et al., 2006), have demonstrated this effectiveness in hydrogeologic studies. Stable ^{37}Cl has been utilized to discern diffusional transport of Cl^- (Desaulniers et al., 1986) and Cl^- sources (Clark and Fritz, 1997), whilst radiogenic ^{36}Cl has been used to investigate a greater host of hydrogeologic mechanisms, including their timeframes. ^{36}Cl has advantages over other radioisotopes isotopes commonly used in hydrogeologic studies due to the hydrophilic nature of the chloride ion and long half-life ($3.01 \pm 0.04 \times 10^5$ yrs) (Bentley et al., 1986a).

Numerous $^{36}Cl/Cl$ based groundwater dating studies have been conducted within Australia, most notable are those within the Great Artesian Basin (GAB) (Bentley et al., 1986b; Torgersen et al., 1991). In addition, fallout of elevated ^{36}Cl due to nuclear-weapons testing during the 1950's and early 1960's has allowed for the use of ^{36}Cl to identify modern recharge water in hydrogeologic studies (Bentley et al., 1982). This method has proved successful in understanding unsaturated zone flow rates in both the northern and southern hemispheres (i.e., Walker et al., 1992; Campbell et al., 2003). Thus, ^{36}Cl functions as a mean for estimating groundwater recharge rates, groundwater flow rates, and ultimately groundwater ages.

Determination of actual groundwater ages is complicated by chemical processes occurring in both the unsaturated and saturated zones. Processes such as mixing, filtration, and dilution can produce $^{36}Cl/Cl$ ratios not solely attributable to ^{36}Cl decay

(Bethke and Johnson, 2002). Selecting an appropriate input ratio for age determinations is equally as problematic, resulting in a large range in ^{36}Cl age calculations (Davis et al., 1998). Several studies in Australia (i.e., Bird et al., 1989; Turner et al., 1991; Cresswell et al., 1999a) have used $^{36}Cl/Cl$ ratios of shallow groundwater, rather than rainwater, as input values for assessing flow ages in regional systems. However; in Australia and other semi-arid regions, aquifers can be overlain by thick unsaturated zones consisting of highly weathered, low permeability materials (i.e., Cook et al., 1994; Hendry et al., 2000). If vertical infiltration of rainwater through these units represents the dominant recharge mechanism, the timeframes of this occurrence needs to be factored into the age calculation. In this case, $^{36}Cl/Cl$ of unsaturated zone pore waters may be the most appropriate input value for determining groundwater ages in regional systems.

Various geochemical mechanisms can influence the measured $^{36}Cl/Cl$ ratio during unsaturated zone flow (i.e., evapotranspiration, mineral dissolution, and mixing). These mechanisms have often been viewed as limitations to the application of ^{36}Cl in hydrogeologic studies because of the lack of understanding of geochemical processes in the unsaturated zone. Measurement of unsaturated zone Cl^- and Br^- concentrations in conjunction with $^{36}Cl/Cl$ ratios can allow for quantification of these processes, and to assess unsaturated zone flow dynamics. This application has gone largely underutilized in hydrogeological studies where $^{36}Cl/Cl$ has predominantly been used to estimate groundwater ages. This combination may prove useful to environmental studies interested in solute origin and mobility. In particular, to groundwater salinity studies which often rely on Cl^- as a hydrogeochemical tracer and mean for interpreting other solute dynamics.

In addition to the unsaturated zone results discussed in Chapter 4, this chapter presents an example of how soil pore water $^{36}Cl/Cl$ and Br/Cl ratios can be useful to identify and quantify unsaturated zone Cl^- dynamics, estimate groundwater recharge rates, and establish a reliable $^{36}Cl/Cl$ input value for age calculations of regional groundwater. The influence of evapotranspiration, halite dissolution, mixing, and infiltration rate on unsaturated zone pore water chemistry have been determined to help understand the chemical evolution and timeframes of groundwater recharge to a saline aquifer system in central New South Wales, Australia (Figure 5.1). This chapter

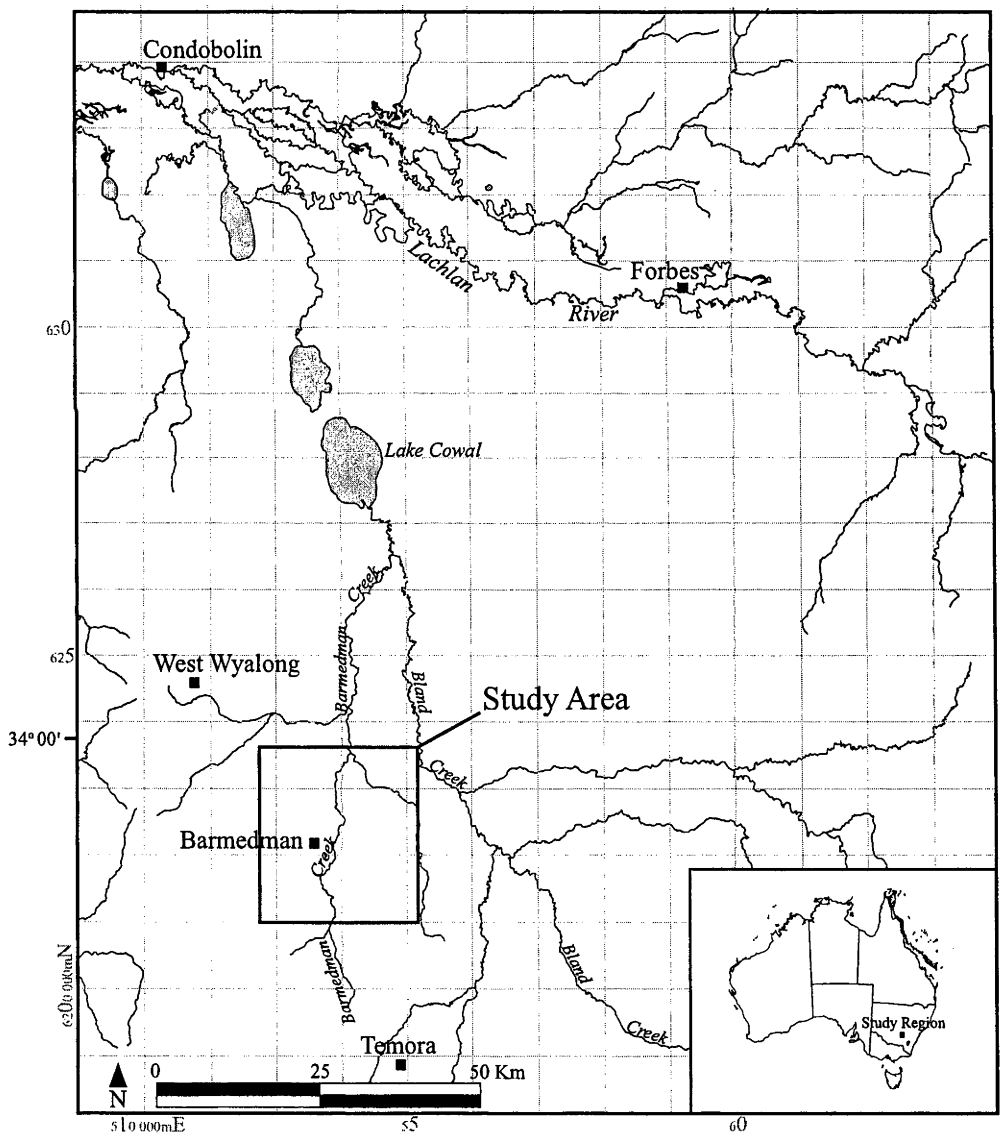

Figure 5.1: Location of study area within the Bland Basin, central New South Wales (NSW), Australia. Adapted from Forbes, NSW and Cootamundra, NSW 1:250 000 map sheets (courtesy Geoscience Australia).

aims to improve the application of ^{36}Cl to recharge studies in salinised landscapes. Furthermore, a better understanding of the timeframes of geochemical processes in the unsaturated zone is critical for managing secondary salinization in semi-arid environments.

5.1 Regional Setting and Local Hydrology

The study focuses the 25x25 km Barmedman Creek Catchment, which is a subcatchment of the low-lying alluvial Balnd Basin in central New South Wales, Australia (Figure 5.1). Up to 100 m of highly weathered, unconsolidated Cenozoic sediments comprise a heterogeneous hydrogeologic system (Wilford et al., 2002) and hosts highly saline groundwater (TDS> 30,000 mg/l). A low hydraulic gradient (< 0.2 m/km) and hydraulic conductivity values of 10^{-5} m/s result in an average linear velocity of ~15 cm/yr. Recharge to the main alluvial aquifer system in the Bland Basin (east of Barmedman Creek Catchment) occurs via vertical infiltration through sediments along the basin margins (Carrara, 2005). The upper reaches of Barmedman Creek Catchment represent the southwest margin of the Bland Basin. Groundwater recharge to the deeper confined/semiconfined aquifers is likely the result of vertical infiltration of rainwater at outcropping areas along the basin margins, and to the shallow unconfined/semiconfined aquifer through the near surface (<5 m) sandy-silt sediments present in the southern portion of the basin. Mean annual rainfall, calculated from monthly measurements from 1887-2005, is 48 cm/yr. The majority of the study area has been cleared of native *Eucalyptus* vegetation and is presently cultivated with canola and wheat. Barmedman Creek is an ephemeral tributary which flows from south to north after extended wet periods.

5.2 Methods

Regolith was sampled in 2001 via diamond coring at three locations, GDH03, GDH04, GDH05 (Figure 5.2), to depths of 59, 80 and 40 metres respectively. Soil pore water was extracted via uniaxial compression at the Bureau of Rural Sciences (BRS) laboratories in Canberra, Australian Capital Territory. Pore water samples were analysed by the BRS in 2001 via ion chromatography. In July 2005, shallow (~0-3m) regolith was samples via push coring at sites located adjacent to the two original diamond core holes. Two push cores were conducted at each site. One core was intended solely for chlorine-36, chloride and bromide measurement and will be discussed in this chapter. The second push core hole was intended for high resolution pore water solute profiles and results are discussed in Chapter 4. Soil pore water was extracted from the 2005 push cores via uniaxial compression from a variety of unsaturated materials at the Australian Bureau of Rural Sciences laboratory in. Soil pore water was extracted from 2-3 cm intervals throughout the unsaturated zone, with particular emphasis on the upper 1m of each of the two profiles. Samples were collected in sterile 10mL syringes then filtered through a 0.45μm filter into a 5 mL sterile vile. Samples for Cl^- analysis were diluted with 18 MΩ deionized water and stored at ~10°C. Cl^- and Br^- content was measured with a Dionex DX4500i ion chromatograph using an AS14A column with $NaHCO_3/Na_2CO_3$ eluent and electrochemical detector in conductivity mode at The Australian National University

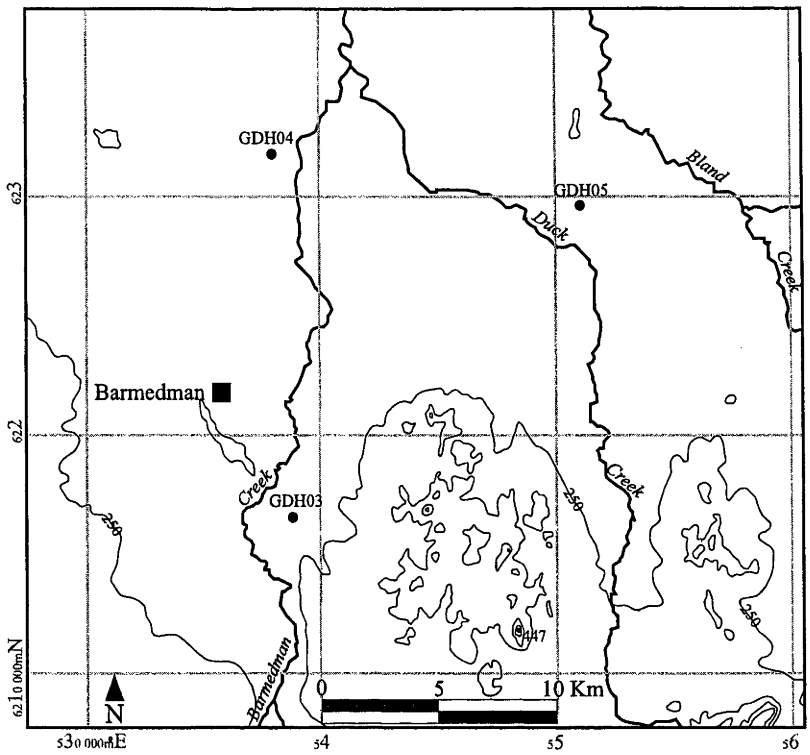

Figure 5.2: Sediment core locations within the Barmedman Creek subcatchment of the Bland Basin. Adapted from Cootamundra, NSW 1:250 000 map sheet (50 metre contour interval).

(ANU) Department of Earth and Marine Sciences (DEMS). Analytical error was estimated from replicate analyses of freshly prepared standard solutions and was found to be <5%.

Pore water samples from the 2001 diamond cores and the 2005 push cores were prepared for ^{36}Cl analysis using a similar method described by Conrad et al. (1986) in Cl^- free labs at ANU Department of Nuclear Physics and Research School of Earth Sciences. A solution of ^{36}Cl free carrier (Weeks Island Halite) was provided by T.T. Barrows of ANU Department of Nuclear Physics and was added to samples containing <1 mg total Cl^-. $^{36}Cl/Cl$ was determined by accelerator mass spectrometry at ANU Department of Nuclear Physics (Fifield et al., 1987). Cl^- and Br^- measurements were performed on all extracted pore waters from the 2001 diamond cores and 2005 push cores from locations GDH03, GDH04 and GDH05. In addition,

one creek water sample and one rainwater sample (collected from a domestic rainwater tank) were collected in 2005, field filtered and later analysed for Cl^- and Br^- at ANU DEMS. Selected samples from the diamond cores and push cores, as well as the creek water and rainwater samples were analysed for chlorine-36.

Comparison between pore water geochemical results from the 2001 diamond cores and corresponding duplicate push cores completed in 2005 indicate relatively good agreement between solute composition and distribution with depth. A slight disagreement between vertical solute distributions (<10 cm) is present between the two push cores (See Chapter 4, Figure 5) and is likely attributable to varying degrees of compaction of sediments during push coring. For the purposes of this study, comparison between solute profiles from adjacent sampling locations was only conducted to test for small scale (~1-2 m) spatial and temporal variability. Because some variations in solute concentrations with depth were present between the two push core locations, only the results from the holes intended for chlorine-36, chloride and bromide measurements are presented in this chapter. Full pore water geochemical results were presented and discussed in Chapter 4.

Laser scattering grain size analyses were performed by Geoscience Australia, Canberra on 2 cm vertical sections of regolith materials collected over regular depth intervals within the unsaturated zone profiles at GDH03, GDH04, GDH05 and adjacent push cores. Gravimetric moisture content was determined at ANU DEMS and is reported as percent mass ratio of water lost (after 24 hrs at 110° C) to total wet mass of soil.

5.3 Results

Geochemical results are presented in Table 5.1 and summarized below.

5.3.1 Rainwater and Creek Water

Local meteoric water, collected from a rainwater tank in the town of Barmedman, exhibits a Cl^- content of 2.75 mg/l, Br/Cl ratio of $7.14x10^{-3}$, and $^{36}Cl/Cl$ ratio of $250x10^{-15}$ (Table 5.1). Surface water collected from a stagnant pool in the ephemeral Barmedman Creek exhibits a Cl^- content of 17.2 mg/l, Br/Cl ratio of $7.59x10^{-3}$, and $^{36}Cl/Cl$ ratio of $374x10^{-15}$. For reference, average global seawater exhibits a Cl^- concentration of ~19,000 mg/l, Br/Cl ratio of ~ $3.5x10^{-3}$ (Hem, 1992) and $^{36}Cl/Cl$ ratio below the present detection limit of $1x10^{-15}$ (Cresswell et al., 1999b). Pore water Cl^- concentrations, Br/Cl ratios and $^{36}Cl/Cl$ ratios are unique to each diamond core location, and results are presented separately.

5.3.2 Diamond Core GDH03

Grain size and moisture content

Grain size distribution in the unsaturated zone is fairly uniform; comprised predominantly of silt (50%) and sand (40%) sized sediments (Figure 5.3). The upper 5 cm of the profile contains clay rich (40%) materials with some sand (32%) and silt (28%). Soil moisture content decreases from 29 wt. % at 0.01 m, to 7 wt. % at 1.5 m (Figure 5.3b). Below this depth, the moisture content remains at ~15 wt. % throughout the remainder of the unsaturated zone. In 2001, when the diamond core was completed through both the unsaturated and saturated zone and permanent piezometers were installed, the standing water level was located at 7.45 m below the ground surface. At this location, water levels decreased from 7.45 m in 2001 to 8.24 m below the ground surface in 2006 (Chapter 3).

Table 5.1: Sediment and soil pore water results from Barmedman Creek Catchment, New South Wales, Australia (exact locations presented in Chapter 3). Sediments sampled via diamond coring and push coring (*) in 2001 and 2005 respectively. Depth reported as metres below ground surface. Moisture content calculated as percent mass ratio of water lost at 110°C to total wet mass soil. ^{36}Cl and error reported as ratio of ^{36}Cl to total Cl ($x10^{-15}$).

Sample ID	Depth (m)	%Moisture	%Clay	%Silt	%Sand	%Clay+Silt	$^{36}Cl/Cl$	$^{36}Cl/Cl$ Error	Cl^-	Br^-
GDH03*	0.01	41.39	40.00	28.00	32.00	68.00	380	28	20.9	0.09
GDH03*	0.10	7.87	6.43	40.90	52.66	47.34	186	16	80.7	0.20
GDH03*	0.35	10.88	8.01	43.51	48.48	51.52	314	13	477.0	1.76
GDH03*	0.50	14.37	14.04	47.06	38.90	61.10	399	18	499.0	2.79
GDH03*	1.00	13.59	12.17	45.38	42.45	57.55	461	17	1430.0	8.13
GDH03*	1.50	12.34	13.42	50.43	36.15	63.85	323	13	2351.0	10.43
GDH03	2.05	8.67							3780.00	16.80
GDH03*	2.50		16.36	54.56	29.08	70.92	158	7	4348.0	17.06
GDH03	3.00	15.09	14.04	53.52	32.44	67.56	407	19	2440.0	12.30
GDH03	4.25	17.02	17.87	51.44	30.70	69.30	698	36	2430.0	11.40
GDH03	4.80	14.96	13.91	38.92	47.17	52.83	285	14	2150.0	10.30
GDH03	6.40	18.43	15.92	46.30	37.78	62.22	98	7	5090.0	17.90
GDH03	7.40	14.90							6010.00	18.90
GDH03	8.00	13.60							6760.00	23.60
GDH03	8.65	16.62	6.44	49.94	43.62	56.38	113	7	5090.0	16.90
GDH04*	0.02	14.29	21.11	44.40	34.49	65.51	152	8	184.8	0.25
GDH04*	0.05	17.25	14.46	53.44	32.10	67.90	157	8	322.0	0.69
GDH04*	0.11	22.31	19.69	45.38	34.93	65.07	159	7	595.0	1.47
GDH04*	0.14	21.81	22.61	41.72	35.67	64.33	142	8	748.0	2.23
GDH04*	0.17	19.84					157	8	1026.0	3.20
GDH04*	0.20	21.19	21.84	51.74	26.42	73.58	153	7	1417.0	4.96
GDH04*	0.23	19.82					167	8	2187.0	7.71
GDH04*	0.35	19.92	16.85	60.32	22.83	77.17	166	8	5331.0	19.08
GDH04*	0.50	16.40	13.94	64.62	21.44	78.56	173	8	8216.0	29.84
GDH04*	0.65	16.07	14.79	55.97	29.24	70.76	151	7	8780.0	32.21
GDH04*	0.80	15.99	11.11	71.60	17.29	82.71	141	8	8667.0	30.18
GDH04	1.40	14.09	16.58	52.00	31.42	68.58	131	7	8960.0	28.40
GDH04	2.15	16.64	14.40	61.80	23.81	76.19	118	6	8810.0	25.70
GDH04	3.00	16.73	10.38	40.29	49.34	50.66	106	6	8510.0	29.50
GDH04	3.50	22.58	15.68	42.69	41.62	58.38	99	6	7730.0	26.40
GDH04	4.50	23.46	29.70	43.68	26.61	73.39	96	5	6300.0	17.70
GDH04	5.00	19.08	10.62	59.54	29.83	70.17	94	4	6920.0	19.50
GDH04	6.00		5.25	45.59	49.16	50.84	95	4	8710.0	24.30
GDH04	7.60	34.79	28.64	48.91	22.46	77.54	94	5	9850.0	27.60
GDH04	9.00	29.51	46.53	35.23	18.25	81.75	95	5	13400.0	34.20
GDH05	0.25	24.92	42.09	57.91	0.00	100.00	157	8	834.4	3.10
GDH05	0.70	24.08	39.61	60.39	0.00	100.00	138	8	2456.3	8.72
GDH05	1.25	23.70	37.27	62.73	0.00	100.00			4351.1	14.73
GDH05	2.05	21.73	32.75	64.43	2.82	97.18			7199.5	23.79
GDH05	2.50	21.86	34.70	64.44	0.86	99.14			8127.9	25.64
GDH05	2.95	21.32	30.79	69.21	0.00	100.00			8760.1	27.84
GDH05	3.20	25.30							7048.6	21.70
GDH05	3.60	20.92	30.00	66.62	3.38	96.62			7576.0	22.33
GDH05	4.05	17.54	18.75	79.24	2.01	97.99			9150.3	26.02
GDH05	4.55	15.64	15.28	83.20	1.52	98.48			11213.7	33.38
GDH05	5.40	12.89	14.45	81.94	3.61	96.39				
GDH05	5.90	15.21	13.05	85.84	1.10	98.90			7198.7	21.05
GDH05	6.35	13.33	17.56	78.55	3.89	96.11			8097.8	23.25
GDH05	6.95	13.72	14.87	78.85	6.28	93.72			7625.2	21.88
GDH05	7.50	12.66	11.43	59.65	28.91	71.09			8337.8	24.23
GDH05	7.90	10.88	11.00	46.67	42.32	57.68			8236.8	23.53
GDH05	8.55	16.15	29.96	66.86	3.18	96.82			10895.5	31.65
GDH05	9.00	14.60	18.68	76.44	4.88	95.12				
GDH05	9.45	13.43	14.50	75.63	9.87	90.13			7808.0	23.58
Creek Water							374	16	17.2	0.13
Rainwater							250	18	1.8	0.01
Seawater							<1		19000.0	67.00

* Push core sample

Cl^- and Br^- Depth Profiles

Near surface pore water Cl^- concentrations increase linearly with increasing depth from approximately 20 mg/l at 0.01 m to 4,350 mg/l at 2.5 m (Figure 5.4a). Br^-

concentrations also increase linearly over this depth interval. This rapid near surface increase in Cl^- and Br^- concentrations was encountered at 3 other sampling locations within Barmedman Creek catchment and discussed in detail in Chapter 4. Br/Cl ratios over this interval are less than the meteoric input (~ $7.0x10^{-15}$) and exhibit a decreasing trend with increasing depth (Figure 5.4b).

Pore waters sampled from 3.0-4.8 m exhibit lower Cl^- concentrations (2150-2440 mg/l) and higher Br/Cl ratios (~$4.8x10^{-15}$) than overlying samples. Samples collected from the bottom portion of the unsaturated zone (6.4 m) and from within the saturated zone (8.65 m) exhibit Cl^- concentrations of approximately 5000 mg/l and similar Br/Cl ratios (~$3.4x10^{-15}$).

$^{36}Cl/Cl$ Depth Profile:

Pore water samples within the upper 0.5 m exhibit similar $^{36}Cl/Cl$ ratios to rainwater and creek water (Figure 5.5). The exception is a sample collected at 0.10 m which exhibits a $^{36}Cl/Cl$ ratio significantly lower than creek water and rainwater. Below 0.5 m, the pore water profile exhibits two zones of elevated $^{36}Cl/Cl$ ratios. The upper zone occurs between 1.0 m and 1.5 m where $^{36}Cl/Cl$ ratios increase from $399x10^{-15}$ at 0.5 m to $461x10^{-15}$ at 1.0 m, then decrease to 158 $x10^{-15}$ at 2.5 m. The lower peak occurs between 2.5 m and 6.4 m where $^{36}Cl/Cl$ ratios increase from $158x10^{-15}$ at 2.5 m to $698x10^{-15}$ at 4.25 m, then decrease to 98 $x10^{-15}$ at 6.4 m. A ratio of $113x10^{-15}$ is present at 8.65 m, which is within the saturated zone.

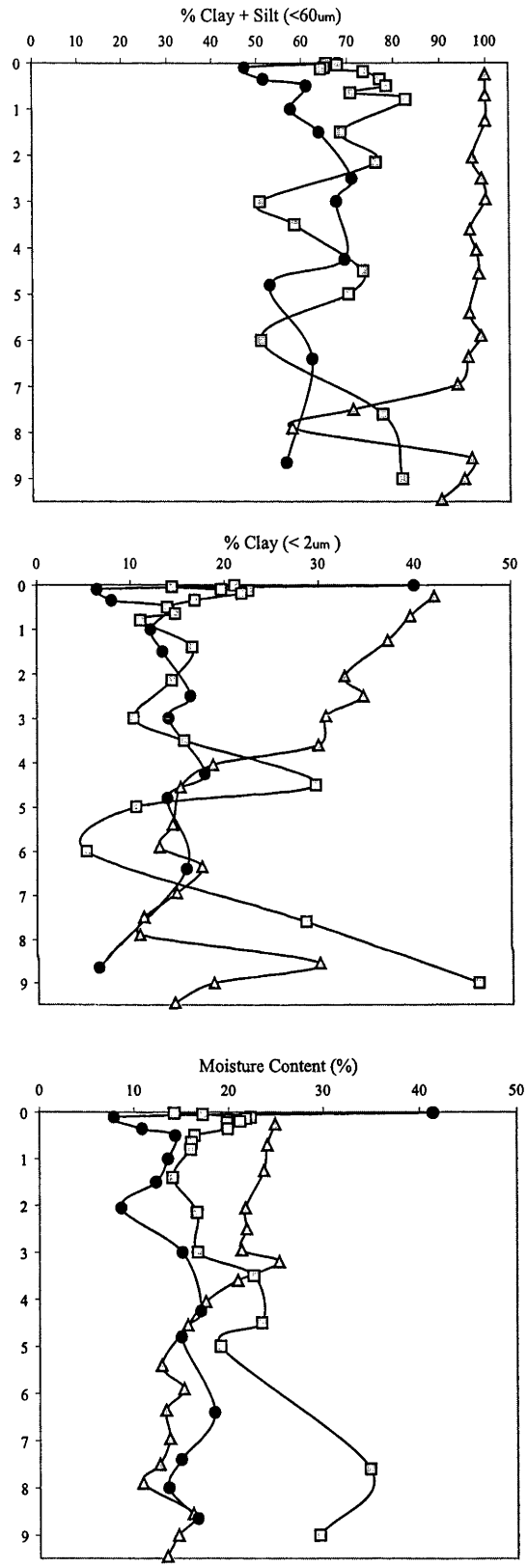

Figure 5.3: Results of laser grain size analyses of unsaturated and saturated zone sediments from diamond cores GDH03, GDH04 and GDH05.

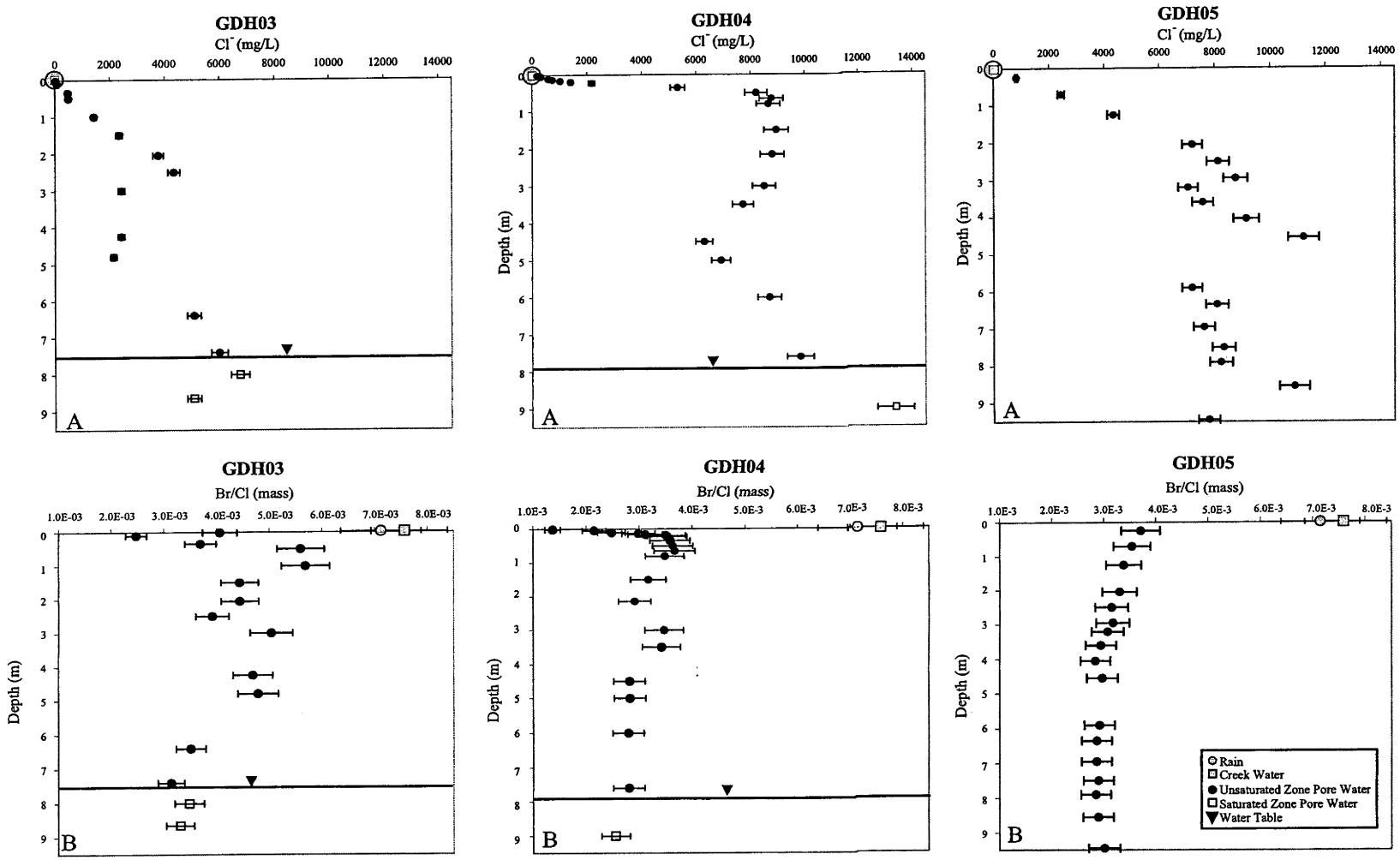

Figure 5.4: Unsaturated zone pore water Cl^- and Br/Cl profiles for GDH03, GDH04 and GDH05 pore waters. Ground water levels measured in permanently installed piezometers at locations GDH03 and GDH04 are also depicted. No piezometer is located at GDH05.

5.3.3 Diamond Core GDH04

Grain size and moisture content

Grain size distribution in the unsaturated zone is fairly uniform; comprised predominantly (75%) of clay and silt sized sediments (Figure 5.3). Moisture contents are highly variable at this location. Soil moisture content increases from 14 wt. % to 21 wt. % over the upper 15 cm, then decrease with increasing depth to1.4 metres. Below this depth, soil moisture contents increase with increasing depth to the base of the unsaturated zone. At the time the diamond core was completed through both the unsaturated and saturated zone and permanent piezometers were installed (2001), the standing water level was located at 7.88 m below the ground surface. At this location, water levels decreased from 7.88 m in 2001 to 8.35 m below the ground surface in 2006 (Chapter 3).

Cl^- and Br^- Depth Profile

Near surface pore water Cl^- concentration increases rapidly from ~185 mg/l at 0.02 m to ~8200 mg/l at 0.5 m (Figure 5.4a). Below this depth, pore water Cl^- concentrations are relatively constant to a depth of 3.5 m. A zone of slightly lower Cl^- concentrations (6300-7700 mg/l) is present from 4.5-5.0 m, followed by an increasing trend throughout the remainder of the unsaturated zone. Br^- concentrations exhibit a similar depth trend. Near surface (<10 cm) Br/Cl ratios are significantly less than meteoric input and exhibit an increasing trend with depth over the upper 0.2 m (Figure 5.4b). Below this depth, the Br/Cl ratios do not vary outside the analytical uncertainty and are similar to seawater.

$^{36}Cl/Cl$ Depth Profile:

$^{36}Cl/Cl$ ratio of pore water in the upper 0.20 m fluctuates between 142-159 $x10^{-15}$ followed by a slight increasing trend to a maximum of $173x10^{-15}$ at 0.50 m (Figure 5.5). $^{36}Cl/Cl$ ratios then decrease with increasing depth to a minimum of $93x10^{-15}$ at 4.5 m. Below a depth of 4.5 m, pore water $^{36}Cl/Cl$ ratios are constant within error throughout the remainder of the unsaturated zone.

5.3.4 Diamond Core GDH05

Grain size and moisture content

Grain size distribution in the unsaturated zone is fairly uniform; comprised predominantly (>90%) of clay and silt sized sediments (Figure 5.3). Soil moisture content decreases with increasing depth throughout the unsaturated zone. No piezometer is present at this location; however, based on the water table depths at GDH03 and GDH04 and moisture content profile at GDH05, this study assumes that the unsaturated zone extends to at least 8 metres depth.

At all three sampling locations, fluctuations in soil moisture content appear to correspond to fluctuations in sediment grain size. Furthermore, increases in clay and silt content correlate with increases in moisture content. This suggests that the decreases in grain size results in

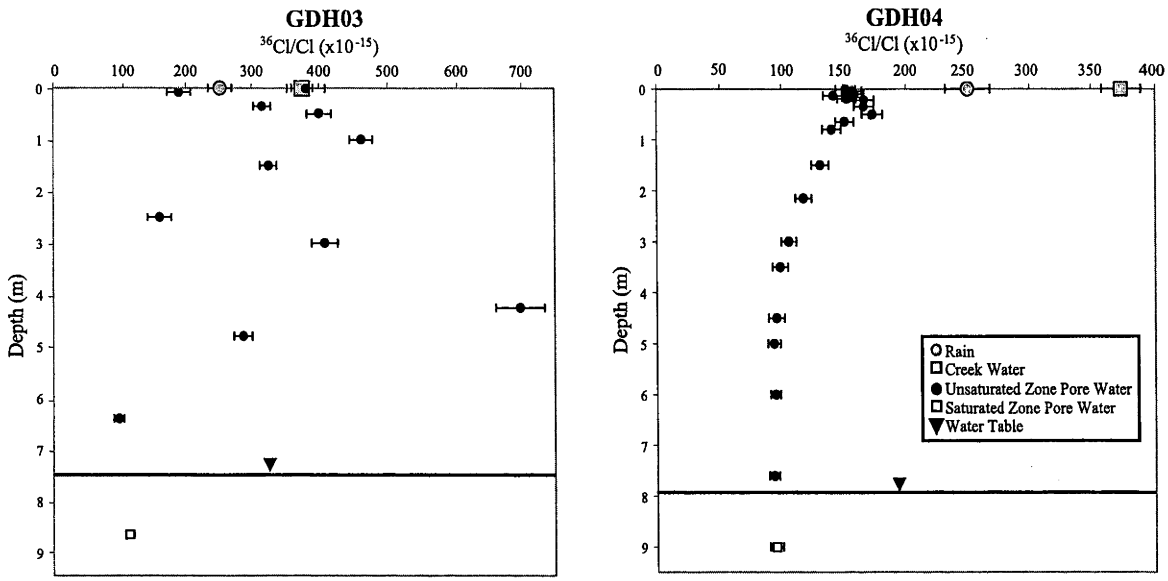

Figure 5.5: Unsaturated zone pore water ^{36}Cl/Cl profiles for GDH03 and GDH04 pore waters.

increased porosity and can account for the fluctuating moisture contents within the unsaturated zone.

Cl^- and Br^- Depth Profile

Near surface pore water Cl^- concentration increases rapidly from ~835 mg/l at 0.25 m to ~8760 mg/l at 2.95 m (Figure 5.4a). Below this depth, pore water Cl^- concentrations are relatively constant to a depth of 9.45 m. Near surface (<10 cm) Br/Cl ratios are significantly less than meteoric input but similar to seawater (5.4b). Br/Cl ratios decrease with increasing depth to 4.05 metres. Below this depth, pore water Br/Cl ratios are within the analytical uncertainty to a depth of 9.45 m.

^{36}Cl/Cl Depth Profile:

^{36}Cl/Cl analyses were conducted on two near surface pore water samples for comparison with results from profiles GDH03 and GDH04. Sampling depth are 0.25 and 0.70 m and Cl^- concentrations of approximately 830 mg/l and ~2500 mg/l

respectively. Br/Cl and $^{36}Cl/Cl$ ratios are less than meteoric ratios but are similar to those found in pore waters sampled from comparable depth intervals at GDH04 (Table 5.1)

5.4 Discussion

5.4.1 Meteoric Input

Rainwater can exhibit large fluctuations in Cl^- concentration and $^{36}Cl/Cl$ ratios due to wind direction, rainfall intensity, proximity to oceans or saline lakes, or time of year (Hingston and Gailitis, 1976; Blackburn and Mcleod, 1983; Simpson and Herczeg, 1994; Keywood et al., 1997; Davis et al., 1998; Keywood et al., 1998). Results from rainwater, creek water and near surface pore water are considered in this study to represent Br/Cl and $^{36}Cl/Cl$ ratios of local meteoric input. Furthermore, daily wind (1965-2006) and rainfall (1895-2006) information from several Australian Bureau of Meteorology weather monitoring sites in the vicinity (<40km) of the study area were reviewed to assess the potential contribution of marine aerosols or Cl^- solutes sourced from inland Australia to the measured $^{36}Cl/Cl$ and Br/Cl ratios of rainwater. Review of daily wind and rainfall data from 1965-2006 indicate the majority (>65%) of rainfall events were accompanied by westerly winds. In addition, rainfall intensity did not correlate with wind direction indicating that monsoonal rains do not reach this far south in Australia or this far inland from the coast. Furthermore, considering the study area's geographical location and predominant westerly winds, it is unlikely that marine aerosols regularly dilute ^{36}Cl concentrations in rainwater.

The observed discrepancy between the $^{36}Cl/Cl$ ratios of the rainwater sample and both the creek water and near surface pore water at GDH03 is likely due to seasonal variability of meteoric $^{36}Cl/Cl$ ratios. Keywood et al. (1998) sampled rainwater over a two year period from a west-east transect and south-north transect in Australia. The study found that experimental measurements of ^{36}Cl fallout in the southern hemisphere agreed with the predicted global fallout by Lal and Peters (1967). However, the study revealed large seasonal fallout fluctuations and poor correlation between rainfall amount and fallout rate. Review of daily climate data revealed several high rainfall events occurring just prior to sample collection from the domestic rainwater tank. The land holder confirmed that the tank had only been recently refilled by this brief period of high rainfall. This indicates that the chemical and isotopic composition of tank water represents a mixture of recent (weeks) rainwater rather than a mixture of longer term (months) rainfall chemistry. This could explain the lower $^{36}Cl/Cl$ ratio yet similar Br/Cl ratio compared to creek water and near surface pore water.

Several studies within Australia have considered the influence of cyclic solutes, in particular halite, on the chemical composition of groundwater (i.e. Simpson and Herczeg, 1994; Ullman, 1995; Love et al., 2000; Cartwright et al., 2004; Cartwright et al., 2006). These studies attribute low Br^- concentrations relative to Cl^- to dissolution of halite during groundwater recharge. In addition to low Br^- concentrations relative to Cl^-, Cartwright et al. (2006) also attributed low $^{36}Cl/Cl$ ratios to halite dissolution. Ullman (1995) reported extremely low Br/Cl ratios in halite minerals from Lake Frome, South Australia and Love et al. (2000) applied these values to model trends in

Br/Cl ratios and Cl^- concentrations resulting from evaporation and dissolution of halite minerals during groundwater recharge.

Cl^- bearing, Br^- depleted solutes sourced from further inland areas of Australia such as the Lake Frome region or other large playa lake regions, could potentially influence the Br/Cl ratios and $^{36}Cl/Cl$ ratios in the Barmedman Creek catchment. However, considering that unsaturated zone soil pore waters exhibit Br/Cl ratios only slightly lower than meteoric values, it is unlikely that solutes sourced from inland evaporative lakes are influencing meteoric input at this location. Near surface pore water at GDH03 exhibit the lowest Br/Cl ratios of all unsaturated zone samples collected from each location yet display $^{36}Cl/Cl$ ratios within the range of local meteoric values (Figure 5.5). This suggests that halite dissolution is not influencing the Br/Cl ratios of near surface pore waters.

As discussed previously, the ephemeral nature of Barmedman Creek is not the result of groundwater discharge, but rather prolonged wet periods. Similarly, near surface pore water, indicated by elevated Cl^- concentrations relative to rainwater, is also an accumulation of numerous rainfall events.

At location GDH03, $^{36}Cl/Cl$ ratios similar to the creek water sample are present within the upper 50 cm of the profile. The total Cl^- within this near surface zone can be estimated from the bulk density of the soil, moisture content and Cl^- concentration. Pore water sampled from 0-2 cm (depth reported as 0.01 m) exhibits a moisture content of 41% and bulk density data collected by Geoscience Australia indicate an average wet bulk density of unsaturated zone sediments of 2.1 g/cm^3. Considering a 1

m^2 by 2 cm deep soil column, and the pore water Cl^- concentration and moisture content at 0-2 cm depth, the total amount of Cl^- present is 360 mg Cl. Assuming an average local meteoric Cl^- concentration of 2mg/l and considering the average annual rainfall of 480 mm/yr, the total meteoric deposition of Cl^- is 960 mg/m^2/yr. Assuming no net loss of Cl^- and that rainwater is the sole source of Cl^-, the measured Cl^- concentration of 21 mg/l at 0.01 m represents nearly 5 months of Cl^- deposition.

Considering the meteoric-like $^{36}Cl/Cl$ ratio measured in a 3 of 4 pore water samples from within the upper 50 cm, the deposition timeframes can be estimated from the Cl^- concentrations by a method similar to the above example. Median Cl^- concentration and moisture content within the upper 50 cm is 280 mg/l and 12.6 % respectively. The calculated amount of Cl^- present within a 1x1x0.5 m soil column is ~ 9,000 mg which represents approximately 125 years of Cl^- deposition. As such, the $^{36}Cl/Cl$ ratios measured in the creek water sample and near surface pore waters samples from GDH03 appear to be representative of the average $^{36}Cl/Cl$ ratio for modern meteoric water.

Tank water sample and creek water samples exhibit Br/Cl ratios of $7.1x10^{-3}$ and $7.6x10^{-3}$ which are notably higher than the global mean seawater ratio and the measured ratios of near surface pore water within Barmedman Creek catchment. Within inland areas of Australia elevated Br concentrations relative to Cl^- have been reported for meteoric water, surface water and low salinity, modern groundwater (i.e., Arad and Evans, 1987; Love et al., 2000; Cartwright, 2003; Cartwright and Weaver, 2005; Cartwright et al., 2006). Data from these studies exhibited lower Br/Cl ratios in higher salinity waters that were attributed to Br uptake by organic material, mixing or

halite dissolution. Higher salinity pore water within the unsaturated zone in Barmedman Creek catchment also exhibit lower Br/Cl ratios and will be discussed in the context of mixing and evaporation during groundwater recharge in the following sections.

5.4.2 Unsaturated Zone Morphology and Solute Dynamics

The topography of Barmedman Creek Catchment is characterised by extremely low relief (0.7 m/km). The exception is a granite outcropping area in the southern portion of the catchment that rises a maximum 50 metres above the surrounding plains (Figure 5.2). Sediments within the unsaturated zone are characterized by fine grained transported materials deposited as low angle alluvial and colluvial fans (Gibson and Chan, 2000). Coarser grained unsaturated zone materials are present in the proximal portion of the catchment area, in the vicinity of Barmedman Creek and proximal to the granite outcropping areas. Flow within Barmedman Creek is ephemeral and creek water samples exhibit similar chemical and isotopic compositions to rainwater (Chapter 4). As such, the creek water appears to be sourced from meteoric water. Furthermore, based on differences in chemical and isotopic compositions of creek water compared to groundwater (See Chapter 3), Barmedman Creek does not appear to act as an area of localised groundwater recharge. Potential groundwater recharge likely occurs via diffuse recharge through the clay rich unsaturated zone materials. Variations in clay, silt and sand content of unsaturated zone sediments, as well as vegetation, appear to determine whether infiltrating rainwater recharges groundwater. Water movement in the unsaturated zone inferred from distribution of Cl^-, Br^- and ^{36}Cl at each of the three sampling locations will be discussed below.

5.4.2.1 Vertical Infiltration Rates

At all three sampling locations Cl^- contents of near surface (<2.5 m) pore waters suggest low infiltration rates and a high degree of evapotranspiration in the near surface. Vertical recharge rates to the unconfined/semiconfined aquifers can be estimated by the chloride-mass balance (CMB) technique presented by (Wood, 1999). This method can be applied if preferential flow and significant surface runoff are negligible. Vertical flux (Q) can be estimated from annual precipitation rate (P), from the Cl^- concentration in precipitation (Cl_p) and from the average Cl^- concentration unsaturated zone soil pore water:

$$q = (P)(Cl_p)/Cl_u \qquad (1)$$

Applying eqn. (1) to average Cl^- concentrations from beneath the root zone at GDH03 (>2.5 m), GDH04 (>0.5 m) and GDH05 (>2.5) yields vertical recharge rates of 2.6 x 10^{-4}, $1.2x10^{-4}$ and $1.1x10^{-4}$ m/yr respectively. Vertical infiltration rates are estimated for 2 other locations (BGMR and BGSF) within Barmedman Creek catchment and are discussed Chapter 4. The rates calculated for locations GDH03, GDH04 and GDH05 are similar to those calculated for locations BGMR and BGSF (Chapter 4). Figure 5.4 depicts vertical profiles of Cl^- concentrations and Br/Cl ratios from the three sampling locations. The following section will discuss Cl^- concentrations and Br/Cl of unsaturated zone pore water to assess the effects of evapotranspiration and mixing during groundwater recharge as well as potential halide sources and sinks in the unsaturated zone.

5.4.2.2 Evapotranspiration and Solute Mobility

At all three locations, Cl^- concentrations increase rapidly with increasing depth suggesting a high degree of evapotranspiration in the near surface. Vertical distribution of Cl^- in soil profiles the has been utilized to understand water movement in the unsaturated zone by Johnston et al. (1980), Peck et al. (1981), Allison et al. (1985) and Johnston (1987). Locations GDH04 and GDH05 can be described as monotonically increasing Cl^- profiles (Johnston et al., 1980), which suggests that matrix flow conditions are dominant in the unsaturated zone at these two locations. Location GDH03 exhibits a bulge type profile (Johnston et al., 1980; Peck et al., 1981; Allison et al., 1985) characterized by a zone of lower Cl^- concentration from 3.0-4.8 metres (Figure 5.4) which suggests that preferential flow, in addition to matrix flow, occurs at this location.

The depth of maximum Cl^- concentration is often attributed to the vertical extent of the root zone (Allison et al., 1985; Phillips, 1994; Tyler and Walker, 1994). Cores from within Barmedman Creek Catchment reveal maximum Cl^- concentrations occurring at depths 0.5 m at GDH04 and at 2.5 m for both GDH03 and GDH05. This suggests that deeper root zones are present at GDH03 and GDH05. Cl^- profiles at GDH04 and GDH05 from within areas cultivated with canola and wheat. Profile GDH03 is beneath mature stands of *Casuarina cristata and Casuarina luehmanniana*, which would presumably have greater rooting depths than the cultivated species at GDH04 and GDH05. The similar depths of maximum Cl^- concentrations occurring in areas of different vegetation types suggest that factors other than root depths are influencing the near surface solute dynamics.

Grainsize distributions at the three locations differ dramatically as well. Near surface sediments at GDH03 and GDH04 are dominated by silt sized particles (2-60μ) while GDH05 sediments are dominated by clay sized particles (<2μ). Cook et al. (1992b) proposed that under matrix flow conditions, soil texture was the dominant control on groundwater recharge rate. The authors noted a negative correlation between clay content and recharge rate in the upper 2 metres of the unsaturated zone in a study area in south eastern Australia. Despite variations in land management practices between sites, soil texture within the upper 2 metres was reported as the dominant control on recharge rate. The authors also presented unsaturated zone Cl^- profiles from beneath native vegetation and cultivated land and noted the peak in Cl^- concentration occurred at a greater depth at the cultivated site. They concluded that removal of native vegetation and replacement with cultivated species having lower water requirements resulted in increased infiltration and downward displacement of the chloride profile.

The three Cl^- profiles from within this study area seem to contradict both the vegetation soil texture models presented by Allison et al. (1985), Cook et al. (1992b) Phillips (1994) and Tyler and Walker (1994). Both GDH04 and GDH05 Cl^- profiles are beneath cultivated land and location GDH05 exhibits significantly greater proportions of clay sized sediments (Figure 5.3). According to the studies discussed above, near surface pore waters at GDH05 should theoretically exhibit greater Cl^- concentrations that occur at a shallower depth than at GDH04. Instead GDH05 Cl^- concentrations are lower within the upper 2 m and the peak Cl^- concentration occurs 2 metres deeper than at GDH04. Furthermore, profile GDH03 is beneath native vegetation and the upper 2 metres contain the lowest proportion of clay and silt sized sediments. The lower proportion of clay sized particles at GDH03 results in lower Cl^-

concentrations; however, despite the different vegetation types, the peak Cl^- concentrations occur at similar depths.

The conventional models describing the relationships between sediment texture, vegetation type and Cl^- distributions in the unsaturated zone do not adequately describe the results presented by this study. Factors such as variations in sediment mineralogy between the three sites and/or differences in historical land management practices may be a factor. Physical characteristics of clay-rich sediments of different mineralogy would behave differently during wetting and drying within the near surface of the unsaturated zone. In addition, the date of land clearance would also influence Cl distribution in the near surface. The deeper peak Cl^- concentration observed at location GDH05 compared to GDH04 may be the result of earlier cultivation of land in the vicinity of GDH05.

At all locations, near surface pore water samples exhibit lower Br/Cl ratios than rainwater which suggests non-conservative Cl^- and/or Br^- behaviour during infiltration of near surface sediments. Cartwright et al. (2006) attributed low Br/Cl and $^{36}Cl/Cl$ ratios in groundwater to dissolution of windblown halite containing $^{36}Cl/Cl$ ratios significantly lower than local meteoric values. However, mixing between different chemical and isotopic composition waters was not considered in detail in their study. In Barmedman Creek catchment, near surface pore waters at GDH03 exhibit lower Br/Cl ratios than rainwater, but similar $^{36}Cl/Cl$ ratios (Figures 5.4 & 5.5). Dissolution of locally sourced halite produced by evapotranspiration of local meteoric water would have meteoric-like $^{36}Cl/Cl$ ratios and could explain the observed Br/Cl and $^{36}Cl/Cl$ trend in near surface pore water at GDH03. However, if remobilization of

halite is a significant process, we would expect to also observe similar trends in near surface pore water composition at GDH04 and GDH05. Instead we see similar Br/Cl ratios to GDH03, but much lower $^{36}Cl/Cl$ ratios. As discussed in Chapter 4, organic rich material is present in the upper 0.15 m at both locations and removal of Br by biogeochemical processes such as anion adsorption onto organic material or by bacterial or vegetative uptake is a more likely explanation for the low near surface Br/Cl ratios than dissolution of halite.

Mixing between waters containing different Cl^- concentrations and Br/Cl ratios would also influence the Br/Cl ratios and potentially the $^{36}Cl/Cl$ ratios during groundwater recharge. To assess this process, numerical mixing models were constructed to simulate the effects of evapotranspiration and mixing on the measured Br/Cl and $^{36}Cl/Cl$ ratios of pore water samples. The resulting curves are depicted in Figures 5.6, 5.7 and 5.8 and the numerical models will be discussed in greater detail below. As discussed above, sediment texture and CMB calculated infiltration rates vary considerably between the sampling locations therefore the geochemical processes occurring at each location will be considered separately.

5.4.2.3 Diamond Core GDH04

At location GDH04 (distal to recharge zone), near surface Br/Cl ratios are also much lower than meteoric values, but exhibit an increasing trend within the upper 0.2 m to a consistent ratio comparable to seawater (Figure 5.4). Similar Br/Cl ratios were measured in pore water sampled from 0.25 m at GDH05, and are equivalent to the ratios measured in pore water from similar depth intervals at GDH04. As discussed earlier, it is unlikely that addition of Cl^- is responsible for the lower near surface Br/Cl

ratios encountered at all three locations, but rather removal of Br^- by biogeochemical processes (see also Chapter 4).

Pore water Cl^- concentrations increase rapidly with increasing depth over the upper 0.5 metres while $^{36}Cl/Cl$ ratios remain relatively constant at approximately 160 x 10^{-15} (Figures 5.4 & 5.5). Cl^- concentrations within the upper 0.5 metres are significantly higher than those encountered at locations GDH03 and GDH05 and can be attributed to a greater proportion of clay sized sediments and greater degree of evapotranspiration. Increasing Cl^- concentrations and constant $^{36}Cl/Cl$ ratios indicate that a high degree of evapotranspiration of meteoric water is occurring within the upper 0.5 metres. However, $^{36}Cl/Cl$ ratios are significantly lower than measured in rainwater and creek water samples suggesting that present day ^{36}Cl fallout may be greater than in the past.

The constant near surface $^{36}Cl/Cl$ ratio of ~ 160 x10^{-15} is similar to input values reported by numerous studies within arid and semi-arid regions of Australia (Bird et al., 1989; Turner et al., 1991; Cresswell et al., 1999a; Cresswell et al., 1999b). The $^{36}Cl/Cl$ ratios from these studies were measured in modern groundwaters, and were lower than measured $^{36}Cl/Cl$ ratios in rainwater or the predicted meteoric fallout based on the models presented by Lal and Peters (1967) and Keywood et al. (1998). Cornett et al. (1997) noted similar inconsistency between measured $^{36}Cl/Cl$ ratios in rainwater and shallow groundwater, and Blinov et al. (2000) found inconsistencies between predicted ^{36}Cl fallout and measured $^{36}Cl/Cl$ ratios in rainwater. Both studies attributed this excess to biotic cycling of bomb-pulse ^{36}Cl, in particular through burning of

biomass. Their interpretations were supported by measurements of elevated $^{36}Cl/Cl$ ratios in various plant materials by Milton et al. (1997).

Results from our study reveal a possible explanation to the commonly observed discrepancies between $^{36}Cl/Cl$ ratios of modern meteoric water and modern groundwater in arid and semi-arid regions of Australia. The near surface $^{36}Cl/Cl$ ratios significantly lower than meteoric input are likely the result of mixing of modern, low Cl^- meteoric water with older, high Cl^- pore water derived by extensive evapotranspiration in the upper 0.5 m. This process has likely occurred over extended periods of time and the consistent near surface $^{36}Cl/Cl$ ratios possibly represent average long-term meteoric input. Timeframe of near surface (> 0.5m) Cl^- accumulation calculated from modern Cl^- deposition rate and total pore water Cl^- content indicates a timeframe of ~500 yrs. The $^{36}Cl/Cl$ ratios measured in pore water samples from the upper 0.5 m at GDH04 and pore water from 0.20 m at GDH05 possibly represent an average of meteoric $^{36}Cl/Cl$ ratios over the past several hundred years. Modern meteoric water may be exhibiting unusually high ratios attributable to atmospheric recycling of bomb-pulse ^{36}Cl, or reflect short-term natural variations in ^{36}Cl fallout for this location.

Below 0.5 m, Cl^- content and Br/Cl ratios remains relatively constant while $^{36}Cl/Cl$ ratios steadily decrease to a depth of 3.5 m (Figures 5.6a-5.6c). This suggests that soil pore water below 0.5 m is no longer affected by present day Cl^- and ^{36}Cl deposition and evapotranspiration, and that the $^{36}Cl/Cl$ ratios of pore waters below 0.5 metres could only be influenced by processes such as halite dissolution, mixing and isotopic decay. However, the Br/Cl ratios of pore waters below 0.5 metres do not indicate any

influences of halite dissolution and all pore waters are undersaturated with respect to halite.

Numerical mixing models were constructed to simulate the effects of flow related mixing processes on Cl^- concentrations and $^{36}Cl/Cl$ ratios (Figure 5.6). The mixing processes is assumed to be mobilization of solutes stored in low porosity, low transmissivity sediments by water during infiltration through the insaturated zone. The model assumes one-dimensional piston flow mixing between water having similar chemical and isotopic composition as at 0.5 metres and at 7.6 metres. Poor correlation between the modelled mixing trend and data trends indicate a lack of mixing at this location. Furthermore, diffusional transport of Cl^- is also unlikely due to the lack in concentration gradient below 0.5 metres depth.

Within 0.5-3.5 m, the decreasing $^{36}Cl/Cl$ trend suggests that ^{36}Cl decay is the dominant mechanism influencing the $^{36}Cl/Cl$ ratios of pore water (Figure 5.6a). Assuming isotopic decay is responsible for the observed trend, the age difference between pore water sampled at 0.5 m and pore water sampled at 3.5 m is ~210,000 yrs, indicating a vertical flux of $1.4x10^{-5}$ m/yr. This value is in good agreement with the CMB calculated vertical flux of $1.2x10^{-5}$ m/yr indicating a lack of vertical flow at this location.

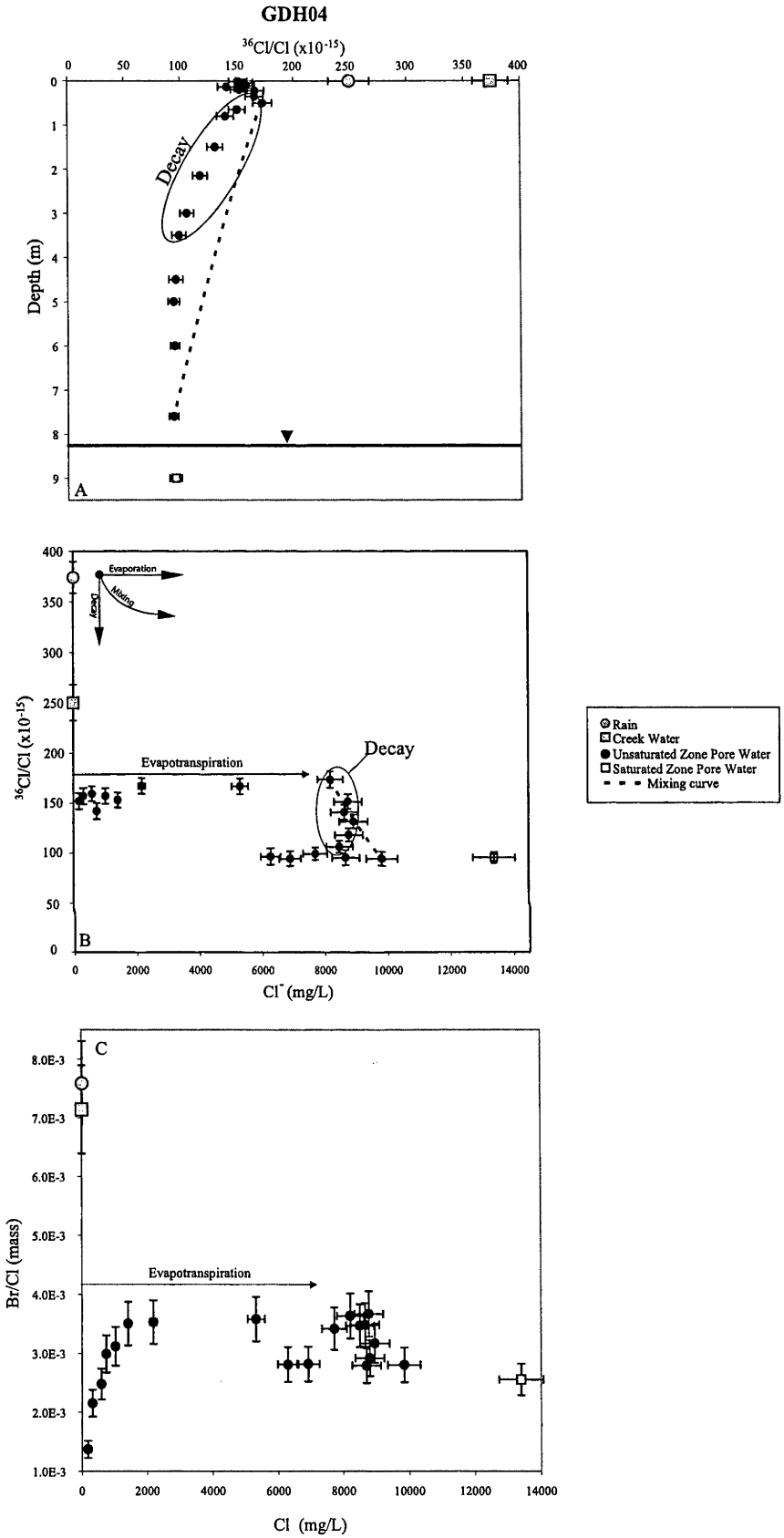

Figure 5.6: ^{36}Cl/Cl depth profile (a) and ^{36}Cl/Cl (b) and Br/Cl (c) ratios versus Cl^- concentration for rainwater, creek water and GDH04 pore waters. Curves represent numerical models of one-dimensional piston flow mixing between pore water at 0.5 metres at 7.6 metres.

Interestingly, the CMB calculation is based on modern Cl^- deposition rates. The agreement between these two calculations suggests that the Cl^- values of these pore waters are the product of meteoric deposition rates and near surface processes that are similar to present day, and that subsequent sedimentation of the catchment and lack of vertical water movement has preserved the Cl^- chemistry of these samples. Although Cl^- deposition may have fluctuated over time, the unsaturated zone pore water Cl^- concentrations at each sampling interval likely represent a cumulative average of meteoric deposition and evapotranspiration spanning timeframes of several thousands of years. The Cl^- concentrations and $^{36}Cl/Cl$ ratios at greater depths exhibit increasing Cl^- and relatively steady $^{36}Cl/Cl$ ratios. This could be due to variable palaeoclimatic conditions and/or sedimentation rates at the time of near surface Cl^- deposition.

5.4.2.4 Diamond Core GDH03

The Cl^-, Br/Cl and $^{36}Cl/Cl$ depth profiles at this location (proximal to recharge zone) exhibit a large range of values which reflect the complexity of unsaturated zone processes (Figures 5.4 and 5.5). The use of these three measured parameters has allowed for semi-quantitative assessments of both flow behaviour and the geochemical processes occurring during infiltration of the unsaturated zone. As discussed in Chapter 4, the sediments in this area are characterized by 2:1 clays, which are subjected to extensive shrinking and swelling. During dry periods, large cracks were observed at the surface and extend beneath the shallow root zone. Two types of flow likely occur at this location; rapid infiltration of rainwater along root

channels and through cracks in the sediments, and slow piston-like, porous flow through the silt and clay-rich sediments.

Unsaturated zone flow dynamics

As discussed above, the bulge type Cl^- profile is indicative of bimodal flow behaviour. The incremental increase in Cl^- with increasing depth within the upper 2.5 metres suggest that pore waters within this upper zone have been transported under piston-like flow conditions through the silt and clay rich materials. Within this zone the pore water has been subjected to a greater degree of evapotranspiration and mixing. This is indicated by steadily increasing Cl^- concentrations and decreasing Br/Cl ratios (Figure 5.4). Four pore waters samples from within the upper 1.5 metres exhibit meteoric like $^{36}Cl/Cl$ ratios and Cl^- concentrations from 20-2,250 mg/l. This indicates a high degree of evapotranspiration of modern meteoric water occured over this depth interval. Based on modern Cl^- fallout and assuming no net loss of Cl^-, Cl within the upper 1.5 metres presents approximately 200 years meteoric Cl^- deposition.

Evidence for preferential flow is also indicated by the geochemical profiles, in particular the $^{36}Cl/Cl$ profile which exhibits zones of $^{36}Cl/Cl$ ratios that are significantly greater than meteoric water (Figure 5.5). During this period ^{36}Cl was generated from thermal neutron activation of ^{35}Cl and the ^{36}Cl fallout "bomb-pulse" occurred over a relatively short period of time. Global atmospheric circulation of bomb-pulse ^{36}Cl was modelled by Bentley et al. (1982). The fallout pulse reportedly occurred from 1953-1964 with mid-latitude fallout maximum 1000 times greater than natural background. Therefore, bomb pulse ^{36}Cl in groundwater has likely originated from rainwater falling between the years 1953-1964. However, because of the lag

time in bomb-pulse tritium fallout between the northern hemisphere and southern hemisphere, and peak fallout two orders magnitude less than observed in the northern hemisphere (Allison and Hughes, 1977), this study assumes that atmospheric fallout of bomb ^{36}Cl ceased by 1966 and predict the magnitude of peak fallout was one to two orders of magnitude greater than present day meteoric water.

Bomb-pulse ^{36}Cl has been reported in water samples by numerous studies from within Australia, although often substantially diluted through mixing with non-bomb pulse waters (i.e., Bentley et al., 1986b; Fifield et al., 1987; Turner et al., 1987; Walker et al., 1992; Cook et al., 1994; Jacobson et al., 1998; Cartwright et al., 2006). At location GDH03, two zones of elevated $^{36}Cl/Cl$ ratios relative to meteoric water are present; one within the root zone (0-2.5 metres) and one at greater depth (Figure 5.5). Despite the strong evidence for evapotranspiration of present day meteoric water over the upper 1.5 metres, a sample extracted at 1 metre exhibits a significantly higher $^{36}Cl/Cl$ ratio suggesting the presence of "bomb-pulse" ^{36}Cl. The Cl^- concentration measured for this sample is 1,430 mg/l indicating that mixing with non bomb-pulse water has diluted the $^{36}Cl/Cl$. Furthermore, a region of elevated $^{36}Cl/Cl$ ratios is also present from 3.0 to 4.8 metres and corresponds to a zone of lower Cl^- and higher Br/Cl ratios than pore waters sampled at shallower depths (Figures 5.4 and 5.4). This suggests a lesser degree of evapotranspiration and mixing and supports the theory of groundwater recharge occurring via preferential flow in the unsaturated zone.

Because the lower $^{36}Cl/Cl$ peak is located beneath the root zone, the mean unsaturated zone recharge rate can therefore be estimated from the depth of bomb-pulse waters (Walker et al., 1992). At GDH03, bomb-pulse water is located at 4.8 m, which

corresponds to a vertical recharge rate of ~ 14 cm/yr. This is several orders of magnitude greater than was estimated from CMB calculations (< 1 mm/yr). Cartwright et al., 2007 presented the concept of dual porosity to explain differences between recharge rates calculated by CMB and those calculated based on ^{3}H and ^{14}C of groundwater. The authors argued that saline waters are trapped within low-permeability sediments in the unsaturated zone and are only slowly mobilized by enhanced groundwater recharge since clearing of native vegetation. CMB calculated groundwater recharge rates for the Cowra formation in the Bland Basin were more than an order of magnitude greater than estimated from ^{14}C ages of groundwater (Carrara, 2005). This was attributed to an underestimate with the CMB method due to evapotranspiration of groundwater following recharge. The main alluvial aquifer system in the Barmedman Creek Catchment is analogous to the Cowra Formation in the adjacent Bland Basin described by Williamson (1986). Groundwater recharge rates to the Cowra Formation aquifer are estimated to be 0.2 – 5.0 mm/yr (Carrara, 2005). The difference between CMB recharge rates and estimates based on bomb-pulse $^{36}Cl/Cl$ in the Barmedman Creek Catchment is most likely due to preferential flow.

Bomb pulse ^{36}Cl has already been detected in unsaturated soil profiles within Australia. Fifield et al. (1987) encountered it at 1-1.5m and Cook et al. (1994) at 4-6m. The presence of two distinct ^{36}Cl bomb pulses, one from within the root zone and one at greater depth, is the first known occurrence from within Australia. The discovery of bomb-pulse water at a depth of 4.8 m is also significant because it demonstrates two different unsaturated zone flow behaviours, and also a high degree of solute mobility. The upper bomb-pulse has likely resulted from piston-like flow

through the root zone while the lower bomb-pulse waters suggest that preferential flow via infiltration through cracks and along root channels is important at this location.

Evapotranspiration and Mixing

The presence of "bomb-pulse" ^{36}Cl at two different depth intervals indicates that modern meteoric water is infiltrating the unsaturated zone sediments at location GDH03. Evapotranspiration of modern meteoric water during groundwater recharge would produce Cl^- concentrations in the unsaturated zone that increased with increasing depth (Johnston et al., 1980; Allison et al., 1985; Johnston, 1987) and constant Br/Cl and $^{36}Cl/Cl$ ratios. At GDH03, the non-uniform Cl^- depth profile and variations in Br/Cl and $^{36}Cl/Cl$ ratios suggest that flow related geochemical processes are influencing the chemical composition of groundwater recharge.

As discussed in Chapter 4, biogeochemical processes appear to be influencing the Br^- concentrations of soil pore waters in the near surface organic horizon. Furthermore, results discussed in Chapter 4 indicate that halite dissolution during infiltration of near surface sediments is also unlikely. Mixing between different chemical composition waters during vertical infiltration of the unsaturated zone may explain the variations in Br/Cl and $^{36}Cl/Cl$ ratios beneath the organic horizon.

Mixing Effects on Br/Cl and $^{36}Cl/Cl$ Ratios

To better understand the effects of mixing on the measured Br/Cl and $^{36}Cl/Cl$ ratios, numerical models were constructed to simulate the effects of mixing between present day meteoric water and a saline unsaturated zone end member present at 7.4 m

(Figures 5.7a-5.7c). Based on Cl^- concentrations and $^{36}Cl/Cl$ ratios within the upper 1.0 metre the models incorporate evapotranspiration of meteoric water to 500-1000 mg/l followed by mixing under 1 dimensional piston-like flow conditions. The simple piston flow scenario was chosen due to the greater number of uncertainties associated with preferential flow, such as degree of evapotranspiration and variable flow rates.

Mixing endmember compositions were estimated from chemical and isotopic compositions of rainwater, creek water and pore waters sampled from the base of the unsaturated zone. Based on creek water, rainwater and near surface pore water results, average meteoric input is assumed to have a Br/Cl and $^{36}Cl/Cl$ ratios of approximately 7.15×10^{-3} and 380×10^{-15}. The saline endmember composition is based on soil pore water results from 6.4 and 7.4 metres depth and has a Cl^- concentration of 6010 mg/l, Br/Cl ratio of 3.15x10-3 and $^{36}Cl/Cl$ ratio of 98×10^{-15}.

Figure 5.7 depicts modelled trends for evapotranspiration and mixing of meteoric water during vertical infiltration under piston flow conditions at location GDH03. Cl^- concentrations and $^{36}Cl/Cl$ ratios in the upper 50 cm suggest that evapotranspiration of meteoric water is the dominant geochemical process within this zone. However, over this depth interval Br/Cl ratios are highly variable and are appreciably less than meteoric water. As discussed in Chapter 4, Br/Cl ratios near surface pore water samples from GDH03 as well as three other locations within the Barmedman Creek catchment, appear to reflect non-conservative geochemical behaviour of bromide within the upper 50 cm of the unsaturated zone. Processes such as Br^- adsorption onto organic material or nutrient up-take by plants could account for the lower Br/Cl ratios within the upper 35 cm at GDH03. However, differentiating between biogeochemical

processes and mixing between different chemical composition waters is not possible with the available data sets. Furthermore, because the $^{36}Cl/Cl$ ratios support evapotranspiration as the dominant process within the upper 50 cm, while Br/Cl ratios suggest that evapotranspiration and mixing are occurring over this depth interval, numerical models were constructed for mixing from 0.0 metres and from 0.5 metres depth (Figure 5.7). Resultant mixing curves are the products of numerical simulations of evapotranspiration of meteoric water to 500 and 1000 mg/l followed by mixing with a saline endmember present at 7.4 metres depth.

Comparison of modelled and measured trends for Br/Cl ratios as a function of depth and Cl^- concentration (Figure 5.7) suggest that evapotranspiration of modern meteoric water to 1000 mg/l Cl^- prior to mixing during downward piston flow through the unsaturated zone best describes the observed soil pore water trends. The exceptions are pore waters between 3 and 5 metres which exhibit bomb-pulse $^{36}Cl/Cl$ signatures. Modelled mixing trends for $^{36}Cl/Cl$ as a function of depth and Cl^- concentration (Figure 5.7) poorly describe those exhibiting bomb-pulse $^{36}Cl/Cl$ signatures. However, depth trends in non bomb-pulse pore water closely match the modelled trend in $^{36}Cl/Cl$ ratios for pore waters subjected to evapotranspiration to 1000mg/l followed by mixing. The failure of the one-dimensional piston-flow mixing models to describe the Br/Cl ratios of the bomb-pulse

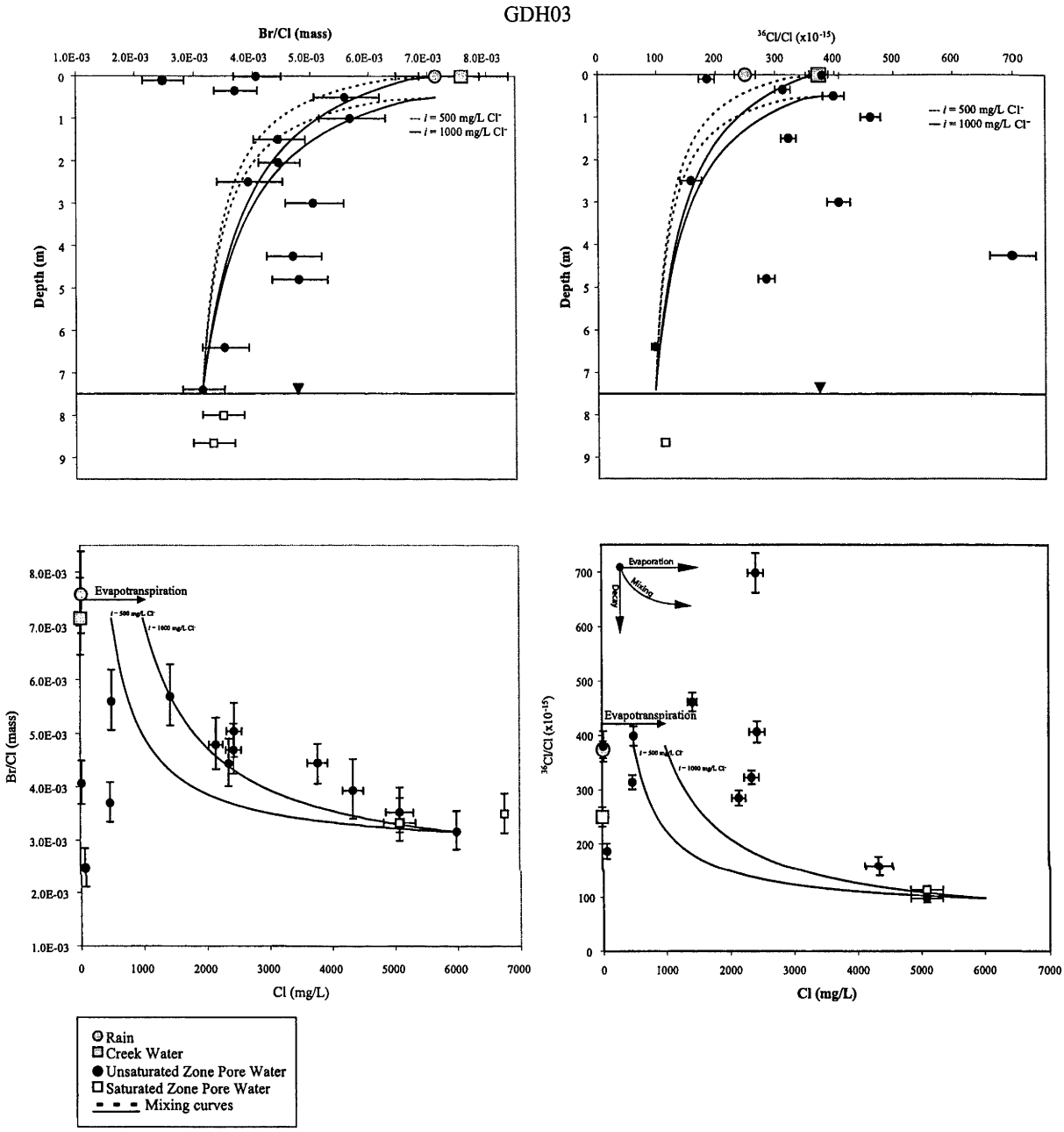

Figure 5.7: $^{36}Cl/Cl$ depth profile and $^{36}Cl/Cl$ and Br/Cl ratios versus Cl^- concentration for rainwater, creek water and GDH03 pore waters. Curves represent numerical models of evapotranspiration of rainwater to 500 mg/l and 1000mg/l Cl^- followed by one-dimensional piston flow mixing with pore water at 7.4 metres.

pore waters further support that these samples are subjected to lesser degrees of mixing which is most likely the result of preferential flow through the root zone. However, because the models reasonably succeed in describing the trends in Br/Cl and $^{36}Cl/Cl$ ratios of non bomb-pulse waters, one dimensional vertical piston-like flow also appears to be an important characteristic of unsaturated zone flow.

5.4.2.5 Diamond Core GDH05

At location GDH05 Cl^- concentrations increase over the upper the upper 3 metres and Br/Cl ratios decrease with increasing depth (Figure 5.4). This is similar to the Cl^- and Br/Cl trends observed at location GDH03 suggesting that similar near surface geochemical processes are occurring at both locations. The depth intervals over which unsaturated zone Cl^- concentrations increase have been attributed to the vertical extent of the root zone by Allison et al. (1985), Phillips (1994) and Tyler and Walker (1994) and described as the result of vertical infiltration under piston-like flow conditions (Johnston et al., 1980; Allison et al., 1985; Johnston, 1987). At locations GDH03 and GDH05, the similar depths of maximum Cl^- concentrations suggest similar root zone depths; however, Cl^- concentrations are much greater at GDH05 indicating greater degrees of evapotranspiration and/or mixing. The maximum Cl^- concentration at GDH04 is similar to location GDH05 indicating similar degrees of evapotranspiration; however, at location GDH04, pore water Cl^- concentrations increase over the upper 0.5 metres suggesting a shallower root zone than at locations GDH03 and GDH05.

The monotonically increasing Cl^- profiles present at both GDH04 and GDH05 suggest similar unsaturated zone flow characteristics. However, near surface Br/Cl ratios are lower at GDH04 and increase with increasing depth to 0.65 metres, although only one soil pore water sample was taken from the upper 0.65 metres at location GDH05, and comparison of near surface geochemical processes between the two locations is not possible. Below 0.65 metres, Br/Cl ratios at both GDH04 and GDH05 decrease slightly with increasing depth indicating similar unsaturated zone geochemical

processes. At GDH05, the decreasing trend is more pronounced suggesting that flow related geochemical processes may be important at this location. However, despite the consistent decrease in Br/Cl ratios with depth, almost all values are within the analytical uncertainty of the measurements.

Evapotranspiration and Mixing

Mixing models similar to those used for GDH03 were constructed to assess the roles of evapotranspiration and to test for potential flow related mixing processes on the observed Br/Cl depth profile (Figure 5.8). One dimensional piston flow conditions are assumed and mixing endmembers are meteoric water and GDH05 pore water sampled at 8.55 metres. Evapotranspiration of meteoric water to 500 and 1000 mg/l prior to vertical infiltration and mixing was incorporated into the numerical models (Figure 5.8). Both modelled trends fail to describe the near surface soil pore water Cl- concentrations and Br/Cl ratios indicating a lack of flow related mixing processes through this depth interval. The lack of data having Cl^- concentrations and Br/Cl ratios closer to meteoric water prevent any detailed assessment of geochemical processes occurring during infiltration through the near surface unsaturated zone at GDH05.

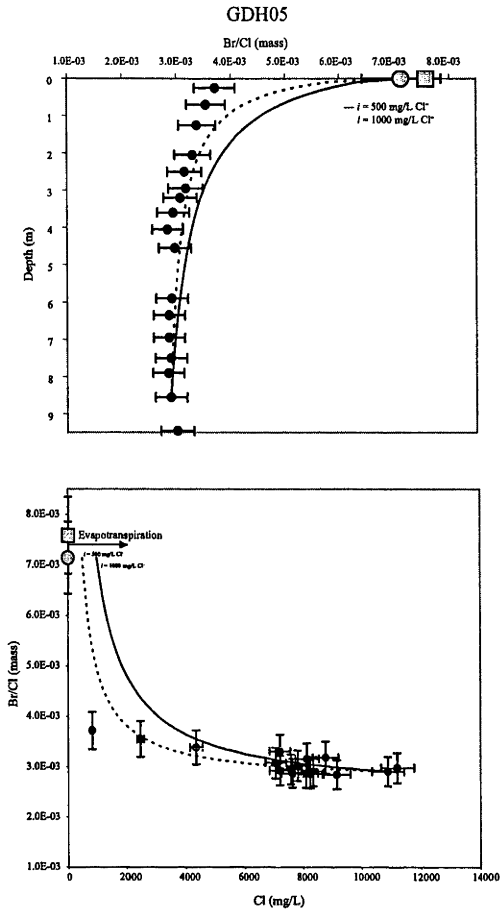

Figure 5.8: Br/Cl depth profile and Br/Cl ratios versus Cl^- concentration for rainwater, creek water and GDH05 pore waters. Curves represent numerical models of evapotranspiration of rainwater to 500 mg/l and 1000mg/l Cl^- followed by one-dimensional piston flow mixing with pore water at 8.55 metres.

Considering that Br/Cl ratios show no statistical variations and that Cl^- concentrations are fairly uniform beneath the monotonically increasing portions of this profile, location GDH05 appears to exhibit very similar unsaturated zone solute dynamics as location GDH04. The $^{36}Cl/Cl$ ratios measured in pore waters within the upper 1 metre are similar those measured at within the upper 1 metre at GDH04 and are significantly less than measured in rainwater, creek water and near surface pore waters at GDH03. This suggests that modern meteoric ^{36}Cl deposition is insignificant at this location and that $^{36}Cl/Cl$ ratios in the past may have been significantly lower than present.

5.5 Conclusion

The conjunctive use of ^{36}Cl, Cl and Br has improved the applications of ^{36}Cl for understanding groundwater recharge rates by allowing to quantify processes that can change the $^{36}Cl/Cl$ ratio other than isotopic decay (i.e. mixing and halite dissolution). Meteoric $^{36}Cl/Cl$ ratio in this region does not appear to be affected by addition of marine or terrestrial derived Cl^-. Cl^- concentrations of pore waters are the result of long term Cl^- and ^{36}Cl deposition and subsequent evapotranspiration in the near surface. Agreement between the chloride mass balance and ^{36}Cl calculated infiltration rates suggests that modern meteoric Cl^- concentrations are comparable to average Cl^- concentrations of rainwater over the last several hundred thousand years. In addition, the consistent $^{36}Cl/Cl$ ratios in the upper 0.5 m at GDH04 and GDH05 possibly represent a long term average meteoric $^{36}Cl/Cl$ ratio. This ratio is significantly less than present day values but similar to that reported for modern groundwaters in several studies within Australia. The discrepancy between modern meteoric $^{36}Cl/Cl$ ratios and potential long-term average is uncertain. Biosphere recycling of bomb-pulse ^{36}Cl has been proposed by studies in the northern hemisphere and could account for the elevated $^{36}Cl/Cl$ ratios of meteoric water relative to modern groundwater. However, due to the lack of long term monitoring of meteoric $^{36}Cl/Cl$ ratios in Australia, historical variability is not known. Results from this study suggest that $^{36}Cl/Cl$ measurements of unsaturated zone pore waters in arid and semi-arid areas of Australia may provide a mean for establishing an average long-term meteoric $^{36}Cl/Cl$ ratio, and provide an input value for age calculations of regional groundwater.

This study has also demonstrated that $^{36}Cl/Cl$, Cl^-, and Br^- measurements of unsaturated zone pore waters provide an accurate mean for assessing various

geochemical processes and flow characteristics in the unsaturated zone. The presence of bomb-pulse ^{36}Cl at two different depth intervals demonstrates two different unsaturated zone flow behaviours and variable solute mobility. The data suggest that rainwater slowly infiltrates the near surface under piston-like flow conditions and is exposed to a high degree of evapotranspiration. This results in long-term accumulation of solutes in the near surface, which are mobilized by rapid infiltration of modern water along preferential flow paths. This suggests that clearing of native vegetation has resulted in enhanced downward transport of unsaturated zone solutes and represents a significant mechanism of secondary salinization of groundwater.

6 FROM RAINWATER TO GROUNDWATER

6.0 Introduction

Approximately 30% of continental precipitation is sourced from the oceans (Garrels et al., 1975). The hydrologic cycle depicts rainwater, derived from evaporation of seawater, as the atmospheric input to the continental fresh water cycle. However, it is well documented that rainwater composition can vary dramatically between seasons, between rainfall events, and also vary with time in a single rain event (Warburton, 1982; Seymour and Stout, 1983; Lehmann et al., 2005). Large variations in the chemical composition have been attributed to plant emission and biomass burning (Mano and Andreau, 1994; Gan et al., 1998) sea salt aerosols (Guelle et al., 2001; Sander et al., 2003) agricultural fertilizers and pollution (Reeves and Penkett, 1993). Furthermore, within Australia, atmospheric precipitation can exhibit compositions that vary considerably from seawater due to incorporation of continental dust (Hingston and Gailitis, 1976; Blackburn and McLeod, 1983; Chivas et al., 1991).

Groundwater and surface water are often sourced from meteoric water, yet can exhibit "marine" like chemical signatures that are often attributed to hydrogeochemical processes such as evapotranspiration, cation exchange and mineral dissolution/precipitation (i.e., Herczeg et al., 1993; Love et al., 2000; Herczeg et al., 2001; Davis et al., 2004; Cartwright et al., 2006). These processes are often associated with the unsaturated zone; however, very few groundwater studies (Edwards and Webb, 2006; White et al., 2006) have incorporated unsaturated zone solute dynamics into their interpretations of groundwater chemistry.

Furthermore, numerous groundwater studies have noted variations in chemical composition and increases in salinity along the flow path that have been attributed to mixing between different hydrogeologic units (i.e., Domenico and Robbins, 1985; Bentley et al., 1986; Phillips et al., 1986; Love et al., 2000). However these studies often have little to no information on the chemical composition of mixing end member waters.

Chapters 3, 4 and 5 show the results of unsaturated and saturated zone pore water solute profiles for understand geochemical processes during groundwater recharge and groundwater flow through a highly heterogeneous aquifer system. Below is a general summary discussion of the finding from each of the chapters that comprise the main body of this thesis.

6.1 Evolution of Groundwater from Rainwater

5 rainwater samples collected from Barmedman Creek catchment exhibit ion ratios that differ from regional groundwater, which has a composition resembling diluted seawater. Rainwater exhibits elevated Br/Cl, SO_4/Cl, NO_3/Cl, Ca/Cl, and K/Cl ratios relative to groundwater and seawater. Na/Cl and Mg/Cl ratios are similar to regional groundwater.

Unsaturated zone pore water geochemical and isotopic results from 5 unsaturated zone profiles in Barmedman Creek catchment provide the missing link between rain water chemistry and groundwater chemistry. Cl^- and $^{36}Cl/Cl$ ratios from three complete unsaturated zone profiles provide a means for assessing solute mobility and

groundwater recharge rates. At all five locations, the trends in major ion concentrations indicate the geochemical evolution from rainwater to groundwater appears to occur in the upper 1 metre of the unsaturated zone and can be attributed to evapotranspiration, biogeochemical processes, nutrient cycling and cation exchange.

Less pronounced trends in groundwater chemistry are observed along the south to north flow path within the Barmedman Creek aquifer that can be attributed to mixing between more saline pore waters and less saline groundwater. Complete saturated zone pore water chemical and isotopic profiles at GDH03 and GDH04 provide a means for assessing flow related mixing processes in a complex heterogeneous aquifer system. Based on the results of this study, element concentrations and element ratios most useful for assessing unsaturated and saturated zone processes are presented in Table 6.1 and discussed below.

Table 6.1: Elements concentrations and elements ratios most useful for assessing the affects of various unsaturated and saturated zone processes

Evapotranspiration and Solute Mobility	Biogeochemical Processes (i.e. Bioassimilation and Organic Adsorption)	Nutrient Cycling	Cation Exchange	Mineral Dissolution/ Precipiration
Cl^-	SO_4^{2-}, SO_4/Cl	K, K/Cl	Na, Na/Cl	Br^-, Br/Cl
$^{36}Cl/Cl$	Br^-, Br/Cl	Ca, Ca/Cl	Ca, Ca/Cl	Na, Na/Cl
Br^-, Br/Cl		NO_3^-, NO_3/Cl	Na/Ca	SO_4^{2-}, SO_4/Cl
SO_4^{2-}, SO_4/Cl		Mg, Mg/Cl		Ca, Ca/SO_4^{2-}

6.1.1 Unsaturated Zone

Groundwater within the Barmedman Creek aquifer system exhibits Cl^- concentrations ranging from 5,492 mg/l to 16,514 mg/l that can be attributed to evapotranspiration and mixing during groundwater recharge and groundwater flow. Element to Cl^- ratios in groundwater are the result of biogeochemical processes, nutrient cycling and cation

exchange during vertical infiltration of rainwater through the upper 1 metre of the unsaturated zone. Minor variations in element to chloride ratios in groundwater can be attributed to mixing along the flow path.

Biogeochemical Processes

Near surface biogeochemical processes appear to influence the Br/Cl and SO_4/Cl ratios of rainwater and can account for ratios lower than meteoric water in pore water and groundwater. Low Br/Cl ratios and decreasing Na/Cl ratios with increasing Cl^- concentrations suggested halite dissolution; however, much lower Br/Cl ratios would occur if rainwater dissolved only a minor amount of halite during infiltration (Chapter 4). Decreasing SO_4/Cl and Ca/SO_4 ratios within the upper 40 cm suggest that progressive evaporation of meteoric water results in gypsum precipitation (Chapter 4). However, all pore waters are undersaturated with respect to gypsum. A more appropriate interpretation for the observed trends is that biotic processes are preferentially sequestering Br^- and SO_4^{2-} relative to Cl^-, as it is well documented that organic materials, vegetation and microorganisms can act as sinks for bromide and sulfate (Johnson, 1984; Gerritse and George, 1988; Mayer et al., 2001; Novak et al., 2003). The variations in Br/Cl and SO_4/Cl occur in the biologically active organic horizons at all locations therefore, adsorption of Br^- and bioassimilation of SO_4 during infiltration of rainwater through the organic soil horizon can explain the observed discrepancies between rainwater and groundwater chemistry.

Nutrient Cycling

Groundwater exhibits lower NO_3/Cl, Ca/Cl, and K/Cl than meteoric water (Chapter 4). Four near-surface (<1m) unsaturated zone profiles exhibit large variations in

NO_3/Cl, Ca/Cl, Mg/Cl and K/Cl ratios (Chapter 4). Within the upper 0.05 metres, these ratios are greater than meteoric water. At all four unsaturated zone profiles, the NO_3/Cl, Ca/Cl, Mg/Cl and K/Cl ratios in pore waters decrease with increasing depth, to ranges observed in regional groundwater (Chapter 4). It is well documented that vegetation retains limiting nutrients within the root zone by scavenging growth limiting elements from the soil and soil water and redistributing them to the near surface soils by litter fall and through fall (i.e., Schlesinger et al., 1996; Schlesinger and Pilmanis, 1998; Jobaggy and Jackson, 2001). This enrichment process results in near-surface accumulations of growth limiting solutes. In Texas, USA, agricultural practices have resulted in mobilization of limiting nutrient stores and were attributed to NO_3 contamination of groundwater (Kreitler and Jones, 1975). The near surface enrichment in pore water NO_3/Cl, Ca/Cl, and K/Cl ratios, and decreasing depth trends are the result of nutrient cycling by native vegetation and cultivated plant species. Different vegetation types have different limiting nutrient requirements (i.e., Foulds, 1993) and this is reflected as differences in cation/chloride ratios between the sampling locations under different vegetation types. At all locations, nutrient cycling appears to be a dominant control in the geochemical evolution from rainwater to groundwater. Near surface accumulations of limiting nutrients represent a significant solute store in Barmedman Creek catchment. Although not likely a threat to regional groundwater in this study location, solutes stored in the near surface by nutrient cycling may represent a significant solute source to regional groundwater in other agricultural catchments.

Cation Exchange

The variations in cation to chloride ratios in unsaturated and saturated zone pore waters and groundwater also suggest that cation exchange is influencing the chemical composition of groundwater recharge. Samples exhibit Na/Ca ratios that decrease with increasing salinity which is indicative of cation exchange (Arad and Evans, 1987). However the large near surface enrichment in cation to chloride ratios suggest that nutrient cycling is more dominant than cation exchange. The variations in Na/Ca ratios occur predominantly in the root zone at each location and can be explained by vegetative uptake of Ca. Because Ca is the most limiting nutrient to the native plant species (*Casuarina cristata* and *Casuarina luehmanniana*) found adjacent to three of four sampling locations (GDH03, BGMR, BGSF) (Foulds, 1993), the variations in Na/Ca ratios are likely dominated by nutrient cycling rather than cation exchange. Na is the least limiting nutrient for these plant species (Foulds, 1993) yet still exhibits minor variations in Na/Cl ratios that are most likely the result of cation exchange. This is further confirmed by Na/Cl trends that exhibit decreases with increasing salinity at Na concentrations >30meq/L. Similar Na concentration were reported by Arad and Evans (1987) for when a change in preference from Ca to Na occurs on exchange sites of 2:1 clays. In Barmedman Creek catchment, Na concentrations and Na/Cl ratios appear the best indicators of cation exchange. However, the effects of this process on the cation compositions of groundwater recharge are minor compared to nutrient cycling.

Evapotranspiration and Solute Mobility

Unsaturated zone pore water Cl^- concentrations increase with increasing depth at all 5 unsaturated zone profiles indicating a high degree of evapotranspiration of meteoric water during groundwater recharge. Cl^- concentration and moisture content correlated

positively with clay content in the upper 1 metre of the unsaturated zone. This indicates that increased clay content results in increased porosity, but also a decrease in permeability resulting in greater degrees of evaporation of rainwater during infiltration.

Complete unsaturated zone pore water solute profiles at two locations in the northern portion of the catchment (GDH04 and GDH05) exhibit monotonically increasing Cl^- profiles indicating similar solute dynamics. $^{36}Cl/Cl$ ratios of pore waters at location GDH04 exhibit an isotopic decay profile that indicates a lack of vertical infiltration of meteoric water and lack of solute mobility. Considering the similar Cl^- profiles and $^{36}Cl/Cl$ decay profile at GDH04, groundwater recharge does not appear to be occurring in the northern portion of Barmedman Creek catchment.

The complete unsaturated zone solute profile in the southern portion of the catchment (GDH03), exhibits a bulge-type Cl^- profile suggesting that preferential flow is occurring at this location. This location is characterized by lower proportions of clay and silt, and lower Cl^- concentrations than locations GDH04 and GDH05 indicating greater permeability and less evapotranspiration of meteoric water. Bomb-pulse $^{36}Cl/Cl$ ratios were also measured as deep as 4.8 indicating that groundwater recharge is occurring at this location. Bomb-pulse waters exhibit Cl^- concentrations from 1,430 mg/l to 2,440 mg/l indicating a high degree of solute mobility at this location. This demonstrates that unsaturated zone solute stores are a significant solute source to regional groundwater.

6.1.2 Saturated Zone

Major elements concentrations in groundwater increase along the south to north hydraulic gradient. Cl^-, Br^- and SO_4^{2-} exhibit the most systematic increases suggesting they are the more ideal hydrogeochemical tracers for assessing flow related processes. Cl^- concentrations in groundwater increase from 5,492 mg/l to 16,514 mg/l, Br^- from 21.8 mg/l to 58.5 mg/l and SO_4^{2-} from 499.0 mg/l to 4,159.3 mg/l. $^{36}Cl/Cl$ ratios decrease from $136x10^{-15}$ to $74x10^{-15}$. Saturated zone pore water profiles in the southern portion (GDH03) and northern portion (GDH04) of the study area exhibit Cl^- concentrations ranging from 4,330 mg/l to 19,700 mg/l, Br^- from 11.8 mg/l to 66.8 mg/l and SO_4^{2-} from 892.0 mg/l to 4540.0 mg/l. Pore waters at GDH03 exhibit Cl^- concentrations up to 6,900 mg/l greater than in groundwater sampled from the same hydrogeologic unit indicating a significant saturated zone solute store within the Barmedman Creek aquifer system. Pore waters exhibit Br^- concentrations up to 17.6 mg/l greater than groundwater. Pore water SO_4^{2-} concentrations are up to 2,261 mg/l greater than in groundwater. These pore waters also exhibit $^{36}Cl/Cl$ ratios as low as half that measured in groundwater. Pore waters at GDH04 exhibit similar Cl^-, Br^- and SO_4^{2-} concentrations, and similar $^{36}Cl/Cl$ ratios as groundwater.

The observed increase in Cl^-, Br^- and SO_4^{2-} concentrations and decrease in $^{36}Cl/Cl$ ratios along the flow path can be attributed to mixing between older more saline pore water residing in lower permeability units within the aquifer and younger less saline groundwater. The older more saline pore waters exhibit lower Br/Cl ratios and higher SO_4/Cl ratios than groundwater. This suggests that pore waters were subjected to different geochemical processes than modern groundwater and the different compositions possibly reflect palaeo-climate conditions different than present day.

Mixing between these pore waters and groundwater causes the Br/Cl ratios to decrease and SO_4/Cl ratios to increase along the flow path. Eventually this flow related process leads to a groundwater composition similar to pore water composition at the distal end of the aquifer system.

Isotopic decay accounts for only a minor decrease in the $^{36}Cl/Cl$ ratios along the flow path. "Age mixing" between pore water and groundwater accounts for most of the observed decrease. Numerical mixing models were constructed using end member compositions of pore waters and groundwater to simulate this affect. Mixing between the highest ratio groundwater and lowest ratio pore water could not account for the total observed decrease. The difference represents the fraction of isotopic decay that occurs along the flow path. Corrected flow ages for groundwater in the Barmedman Creek aquifer were between 50,000 and 70,000 years, compared to uncorrected flow ages of 237,000 to 265,000 years. The corrected flow ages are in better agreement with the Darcy flow age of 65,000 years. In this time, groundwater has evolved from a fresh rainwater source to a marine-like chemistry having TDS values of ~94% seawater.

7 CONCLUSIONS

Within semi-arid environments of Australia there is a fundamental lack of understanding of (a) the processes that change the relative solute proportions in rainwater to groundwater, (b) the timeframes of solute accumulation in the unsaturated zone and saturated zones, and (c) the nature and mobility of subsurface solute stores. Understanding the origin, distribution and mobility of solutes is fundamental for predicting and managing secondary salinization.

Combined hydrogeological and hydrogeochemical techniques were applied in a highly heterogeneous saline aquifer system in central New South Wales, Australia to address the current lack of understandings of salinised landscapes. The chemical composition, stable isotopic composition, and radiogenic isotopic composition of rainwater, pore waters, and groundwater, and their relationship to the physical and chemical characteristics of the regolith, were considered to understand the mechanisms controlling the evolution of groundwater from a fresh rainwater source to salinity values approaching that of seawater. Furthermore, the combined interpretations of major/minor element chemistry and stable/radiogenic isotope compositions of soil pore water and groundwater provided a means for quantitatively assessing accumulation timeframes and mobility of solutes in a highly variable regolith stratigraphy.

The chemical composition of pore waters extracted from two diamond cores dissecting an ~ 8 m unsaturated zone, as well as 4 shallow (< 3 m) push cores, allowed for interpretations of the geochemical and biogeochemical processes

controlling the chemical evolution of rainwater to groundwater during groundwater recharge. Meteoric water represents the dominant solute source to this system; however, local meteoric water exhibits unique chemical and isotopic compositions compared to groundwater. Evapotranspiration was found to be the dominant solute concentrating mechanism while nutrient cycling was the dominant processes responsible for changing the relative solute proportions of meteoric water to those measured in groundwater. Nutrient uptake by plants removes up to half the solutes deposited by rainwater, while non-growth limiting solutes pass through the root zone and eventually recharge groundwater. Evidence for biogeochemical processes such as organic adsorption of bromide and bioassimilation of sulfate were encountered within the upper 1 metre at all locations. Cation exchange and mineral weathering are only minor processes and no evidence was found for evaporative mineral dissolution (i.e., halite or gypsum). At all sampling locations unsaturated zone geochemical and biogeochemical processes account for the differences in element to chloride ratios of rainwater and groundwater. If evapotranspiration alone were controlling the chemical evolution of recharge waters, groundwater salinities would be twice as high as measured in groundwater in the recharge zone. Results from this study provide insight towards understanding the processes responsible for the commonly observed discrepancies between rainwater and groundwater compositions throughout the world.

Cl^-, Br^- and $^{36}Cl/Cl$ distributions in the unsaturated zone were measured at three locations to understand better the timeframes of solute accumulation and solute mobility. At all locations, Cl^- and Br/Cl data indicate that pore waters had not dissolved halite and that meteoric water is the principle source of Cl^- in the catchment study area. Cl^- and Br/Cl depth profiles indicate large variations in unsaturated zone

solute dynamics between the locations. Cl^- profiles indicate a high degree of solute mobility occurs proximal to the recharge zone while little to no vertical solute movement occurs in the distal portion of the study area. This is supported by the presence of "bomb-pulse" ^{36}Cl in saline ($Cl^- > 2{,}000$ mg/l) pore waters between 3 and 5 metres depth in the proximal portion of the study area and a $^{36}Cl/Cl$ decay profile representing over 200,000 yrs of isotopic decay in distal portion of the study area. The ^{36}Cl data confirm that the elevated Cl^- concentrations in the unsaturated zone at all locations represent extremely long-term (10^5 yrs) meteoric deposition. The data demonstrate low solute mobility (10^{-5} m/yr) and a lack of groundwater recharge occurring in the distal portion of the catchment area. Chloride mass balance calculated recharge rates based on present day Cl^- deposition rates and Cl^- concentrations of unsaturated zone pore waters are equivalent to those calculated from the $^{36}Cl/Cl$ decay profile. This suggests that average long-term Cl^- deposition rates are similar to present day. Furthermore, $^{36}Cl/Cl$ results of near surface (>1.0 m) unsaturated zone pore water suggest that present day $^{36}Cl/Cl$ ratios of meteoric water ($\sim 380 \times 10^{-15}$) are more than two times greater than meteoric ratios over the last several thousand years (~ 150 to 160×10^{-15}). Further research of unsaturated zone Cl^- and ^{36}Cl distribution may prove useful for understanding long-term Cl^- and ^{36}Cl deposition and prove a valuable tool for assessing palaeoclimatic conditions on a catchment scale.

Results of saturated zone pore fluid chemistry from two diamond cores allowed for determining subsurface solute and ^{36}Cl distributions in a highly heterogeneous aquifer system. This provided a means for determining mixing endmember compositions and quantitative assessment of mixing between different hydrogeological units. Observed increases in groundwater salinity, changes in major element to chloride ratios and

decreases in $^{36}Cl/Cl$ ratios along the flow path are the result of mixing between older more saline pore waters and younger less saline groundwater. The availability of saturated zone $^{36}Cl/Cl$ profiles allowed for the effects of age mixing to be reasonably well quantified and corrected flow ages were estimated for this system. Without this knowledge, the effects of age mixing would have produced overestimation of apparent flow ages by up to 180,000 yrs. Results from this study provide an example for future studies of how to overcome the limitations of using ^{36}Cl as a potential groundwater dating tool.

REFERENCES

Allibone, A. H., Cordery, G. R., Morrison, G. W., Jaireth, S., and Lindhorst, J. W., 1995. Synchronous Advanced Argillic Alteration and Deformation in the Shear Zone-Hosted Magmatic Hydrothermal Au-Ag Deposit at Temora (Gidginbung) Mine, New South Wales, Australia. *Economic Geology* **90**, 1570-1603.

Allison, G. B., Cook, P. G., Barnett, S. R., Walker, G. R., Jolly, I. D., and Hughes, M. W., 1990. Land clearance and river salinization in the western Murray Basin, Australia. *Journal of Hydrology* **119**, 1-20.

Allison, G. B., Holmes, J. W., and Hughes, M. W., 1971. Tritium fallout in Southern Australia and its hydrologic implications. *Journal of Hydrology* **14**, 307-321.

Allison, G. B. and Hughes, M. W., 1972. Comparison of recharge to groundwater under pasture and forest using environmental tritium. *Journal of Hydrology* **17**, 81-95.

Allison, G. B. and Hughes, M. W., 1974. Environmental tritium in the unsaturated zone: Estimation of Recharge to an unconfined aquifer. In: IAEA (Ed.),*Isotope Techniques in Groundwater Hydrology*. IAEA, Vienna.

Allison, G. B. and Hughes, M. W., 1977. The history of tritium fallout in southern Australia as inferred from rainfall and wine samples. *Earth and Planetary Science Letters* **36**, 334-340.

Allison, G. B. and Hughes, M. W., 1978. The use of environmental chloride and tritium to estimate total recharge to an unconfined aquifer. *Aust. J. Soil Res.* **16**, 181-195.

Allison, G. B. and Hughes, M. W., 1983. The use of natural tracers as indicators of soil-water movement in a temperate semi-arid region. *Journal of Hydrology* **60**, 157-173.

Allison, G. B., Stone, W. J., and Hughes, M. W., 1985. Recharge in karst and dune elements of semi-arid landscapes as indicated by natural isotopes and chloride. *Journal of Hydrology* **76**, 1-25.

Anderson, J., Gates, G., and Mount, T. J., 1993. Hydrogeology of the Jemalong and Wyldes Plains Irrigation Districts. Technical Services Division: New South Wales Department of Water Resources.

Appelo, C. A. J. and Postma, D., 1993. *Geochemistry, groundwater and pollution.* A.A. Balkema, Rotterdam.

Arad, A. and Evans, R., 1987. The Hydrogeology, Hydrochemistry and Environmental Isotopes of the Campaspe River Aquifer System, North Central Victoria, Australia. *Journal of Hydrology* **95**, 63-86.

Back, W., 1986. Role of aquitards in hydrogeochemical systems: a synopsis. *Applied Geochemistry* **1**, 427-437.

Begemann, F. and Libby, W. F., 1957. Continental water balance, ground water inventory and storage times, surface ocean mixing rates and world-wide water circulation patterns from cosmic-ray and bomb tritium. *Geochemica et Cosmochemica Acta* **12**, 277-296.

Bentley, H. W., Phillips, F. M., and Davis, S. N., 1986a. Chlorine-36 In The Terrestrial Environment. In: Fritz, P. and Fontes, J. C. Eds.), *Handbook of Environmental Isotope Geochemistry*. Elsevier Science Publishers, Amsterdam.

Bentley, H. W., Phillips, F. M., Davis, S. N., Gifford, S., Elmore, D., Tubbs, L. E., and Gove, H. E., 1982. Thermonuclear 36Cl pulse in natural water. *Letters to Nature* **300**, 737-740.

Bentley, H. W., Phillips, F. M., Davis, S. N., Habermehl, M. A., Airey, P. L., Calf, G. E., Elmore, D., Gove, H. E., and Torgersen, T., 1986b. Chlorine 36 Dating of Very Old Groundwater 1. The Great Artesian Basin, Australia. *Water Resources Research* **22**, 1991-2001.

Berry, F. A. F., 1969. Relative Factors Influencing Membrane Filtration Effects in Geologic Environments. *Chemical Geology* **4**, 295-299.

Bethke, C. M. and Johnson, T. M., 2002. Paradox of groundwater age. *Geological Society of America* **30**, 107-110.

Bird, J. R., Calf, G. E., Davie, R. F., Fifield, L. K., Ophel, T. R., Evans, W. R., Kellett, J. R., and Habermehl, M. A., 1989. The Role of 36Cl and 14C Measurements in Australian Groundwater Studies. *Radiocarbon* **31**, 877-883.

Blackburn, G. and McLeod, S., 1983. Salinity of Atmospheric Precipitation in the Murray-Darling Drainage Division, Australia. *Aust. J. Soil Res.* **21**, 411-34.

Blinov, A., Massonet, S., Sachsenhauser, H., Stan-Sion, C., Lazarev, V., Beer, J., Synal, H.-A., Kaba, M., Masarik, J., and Nolte, E., 2000. An excess of 36Cl in modern atmospheric precipitation. *Nuclear Instruments and Methods in Physics Research*, 537-544.

Boring, L. R., Swank, W. T., Waide, J. B., and Henderson, G. S., 1988. Sources, fates, and impacts of nitrogen to terrestrial ecosystems: review and synthesis. *Biogeochemistry* **6**, 119-159.

Campbell, K., Wolfsberg, A., Fabryka-Martin, J., and Sweetkind, D., 2003. Chlorine-36 at Yucca Mountain: statistical tests of conceptual models for unsaturated-zone flow. *Contaminant Hydrology* **62-63**, 43-61.

Carrara, E. A., 2005. Chemical and Physical Controls on Groundwater Evolution in the Semi-Arid Bland Region: an Integrated Approach for Sustainable Groundwater Management, *PhD Thesis* The University of Melbourne, Australia.

Carrara, E. A., Weaver, T. R., Cartwright, I. A., and Cresswell, R. G., 2004. 14C and 36Cl as indicators of groundwater flow, Bland Catchment, NSW. Proceedings of Water-Rock Interactions 11, 377-381.

Cartwright, I., 2003. Hydrogeochemical and isotopic constraints on the origins of dryland salinity, Murray Basin, Victoria, Australia, Clayton.

Cartwright, I. and Weaver, T. R., 2005. Hydrogeochemistry of the Goulburn Valley region of the Murray Basin, Australia: Implications for flow paths and resource vulnerability. *Hydrogeology Journal* **13**, 752-770.

Cartwright, I., Weaver, T. R., and Fifield, L. K., 2006. Cl/Br ratios and environmental isotopes as indicators of recharge variability and groundwater flow: An example from the southeast Murray Basin, Australia. *Chemical Geology* **231**, 38-56.

Cartwright, I., Weaver, T. R., Fulton, S., Nichol, C., Reid, M., and Cheng, X., 2004. Hydrogeochemical and isotopic constraints on the origin of dryland salinity, Murray Basin, Victoria, Australia. *Applied Geochemistry* **19**, 1233-1254.

Cartwright, I. A., Weaver, T. R., Stone, D., and Reid, M., 2007a. Constraining modern and historical recharge from bore hydrographs, 3H, 14C, and chloride concentrations: Applications to dual-porosity aquifers in dryland salinity areas, Murray Basin, Australia. *Journal of Hydrology* **332**, 69-92.

Cartwright, I. A., Weaver, T. R., and Petrides, B., 2007b. Controls on 87Sr/86Sr ratios of groundwater in silicate-dominated aquifers: SE Murray Basin, Australia. *Chemical Geology* **246**, 107-123.

Chivas, A. R., Andrew, A. S., Lyons, W. B., Bird, B. I., and Donnelly, T. H., 1991. Isotopic constraints on the origin of salts in Australian playas. 1. Sulfur. *Palaeogeography, Palaeoclimatology, Palaeoecology* **84**, 309-332.

Clark, I. D. and Fritz, P., 1997. *Environmental Isotopes in Hydrogeology*. Lewis Publishers, New York.

Conrad, N. J., Elmore, D., Kubik, P. W., Gove, H. E., Tubbs, L. E., Chrunyk, B. A., and Wahlen, M., 1986. The Chemical Preparation of AgCl for measuring 36Cl in Polar Ice with Accelerator Mass Spectrometry. *Radiocarbon* **28**, 556-560.

Cook, P. G., Edmunds, W. M., and Gaye, C. B., 1992a. Estimating Paleorecharge and Paleoclimate From Unsaturated Zone Profiles. *Water Resources Research* **28**, 2721-2731.

Cook, P. G., Jolly, I. D., Leaney, F. W., Walker, G. R., Allan, G. L., Fifield, L. K., and Allison, G. B., 1994. Unsaturated zone tritium and chlorine 36 profiles from southern Australia: Their use as tracers of soil water movement. *Water Resources Research* **30**, 1709-1719.

Cook, P. G., Love, A. J., Robinson, N. I., and Simmons, C. T., 2005. Groundwater ages in fractured rock aquifers. *Journal of Hydrology* **308**, 284-301.

Cook, P. G., Walker, G. B., Buselli, G., Potts, I., and Dodds, A. R., 1992b. The application of electrostatic techniques to groundwater recharge investigations. *Journal of Hydrology* **130**, 201-229.

Cook, P. G., Walker, G. R., and Jolly, I. D., 1989. Spatial Variability of Groundwater Recharge in a Semiarid Region. *Journal of Hydrology* **111**, 195-212.

Coplen, T.B., 1988. Normalization of oxygen and hydrogen isotopic data. *Chemical Geology* 72, 293-297.

Cornett, R. J., Andrews, H. R., Chant, L. A., Davies, W. G., Greiner, B. F., Imahori, Y., Koslowsky, V. T., Kotzer, T., Milton, J. C. D., and Milton, G. M., 1997. Is 36Cl from weapons' test fallout still cycling in the atmosphere. *Nuclear Instruments and Methods in Physics Research* **B 123**, 378-381.

Cresswell, R., Wischuesen, J., Jacobson, G., and Fifield, K., 1999a. Assessment of recharge to groundwater systems in arid Southwestern part of Northern Territory, Australia, using chlorine-36. *Hydrogeology Journal* **7**, 393-404.

Cresswell, R. G., Jacobson, G., Wishusen, J., and Fifield, L. K., 1999b. Ancient groundwaters in the Amadeus Basin, Central Australia: evidence from the radio-isotope 36Cl. *Journal of Hydrology* **223**, 212-220.

Davis, S. N., Cecil, D., Zreda, M., and Sharma, P., 1998a. Chlorine-36 and the initial value problem. *Hydrogeology Journal* **6**, 104-114.

Davis, S. N., Cecil, L. D., Zreda, M., and Moysey, S., 2001. Chlorine-36, bromide, and the origin of spring water. *Chemical Geology* **179**, 3-16.

Davis, S. N., Fabryka-Martin, J. T., and Wolfsberg, L. E., 2004. Variations of Bromide in Potable Groundwater in the United States. *Ground Water* **42**, 902-909.

Davis, S. N., Whittemore, D. O., and Fabryka-Martin, J., 1998b. Uses of Chloride/Bromide Ratios in Studies of Potable Water. *Ground Water* **36**, 338-350.

Degueldre, C., Scholtis, A., Laube, A., Turrero, M. J., and Thomas, B., 2003. Study of pore water chemistry through an argillaceous formation: a paleohydrochemical approach. *Applied Geochemistry* **18**, 55-73.

Desaulniers, D. E., Kaufmann, R. S., Cherry, J. A., and Bentley, H. W., 1986. 37Cl-35Cl variations in a diffusion-controlled groundwater system. *Geochemica et Cosmochemica Acta* **50**, 1757-1764.

Dimmock, G. M., Bettenay, E., and Mulcahy, M. J., 1974. Salt Content of Lateritic Profiles in the Darling Range, Western Australia. *Aust. J. Soil Res.* **12**, 63-69.

Domenico, P. A. and Robbins, G. A., 1985. The displacement of connate water from aquifers. *Geological Society of America* **96**, 328-335.

Drever, J. L., 1997. *The Geochemistry of Natural Waters*. Prentice-Hall, Inc., New Jersey.

Edmonds, W. M. and Wright, E. P., 1979. Groundwater recharge and palaeoclimate in the Sirte and Kufra basins, Libya *Journal of Hydrology* 40, 215-241.

Edwards, M. D. and Webb, J. A., 2006. Influence of soil processes on groundwater composition, southeastern Australia. *Geochemica et Cosmochemica Acta* **70**, A154-A162.

Elmore, D., Fulton, B. R., Clover, M. R., Marsden, J. R., Gove, H. E., Naylor, H., Purser, K. H., Kilius, L. R., Beukens, R. P., and Litherland, A. E., 1979. Analysis of 36Cl in environmental water samples using an electrostatic accelerator. *Nature* **277**, 22-25.

Eriksson, E. and Khunakasem, V., 1969. Chloride concentration in groundwater, recharge rate and rate of deposition of chloride in the Israel coastal plain. *Journal of Hydrology* **7**, 178-197.

Evans, W. R., 1994. Regional Salt Balances and Implications for Dryland Salinity Management. *Water Down Under*.

Ewing, S. A., Sutter, B., Owen, J., Nishiizumi, K., Sharp, W., Cliff, S. S., Perry, K., Dietrich, W., McKay, C., and Amundson, R., 2006. A threshold in soil formation at Earth's arid-hyperarid transition. *Geochimica et Cosmochimica* **70**, 5293-5322.

Fabryka-Martin, J., Whittemore, D. O., Davis, S. N., Kubik, P. W., and Sharma, P., 1991. Geochemistry of halogens in the Milk River aquifer, Alberta. Canada. *Applied Geochemistry* **6**, 447-464.

Fifield, L. K., Ophel, T. R., Bird, J. R., Calf, G. E., Allison, G. B., and Chivas, A. R., 1987. The Chlorine-36 Measurement Program At The Australian National University. *Nuclear Instruments and Methods in Physics Research* **B29**, 114-119.

Foulds, W., 1993. Nutrient concentrations of foliage and soil in South-western Australia. *New Phytologist* **125**, 529-546.

Gan, J., Yates, S. R., Ohr, H. D., and Sims, J. J., 1998. Production of methyl bromide by terrestrial higher plants. *Geophysical Research Letters* **25**, 3595-3598.

Garrels, R. M., Mackenzie, F. T., and Hunt, C., 1975. *Chemical cycles and the global environment*. W Kaufmann, Inc., Los Altos, California.

George, R. J., 1992. Hydraulic properties of groundwater systems in the saprolite and sediments of the wheatbelt, Western Australia. *Journal of Hydrology* **130**, 251-278.

Gerritse, R. G. and George, R. J., 1988. The Role of Soil and Organic Matter in the Geochemical Cycling of Chloride and Bromide. *Journal of Hydrology* **101**, 83-95.

Gibbs, R. J., 1970. Mechanisms controlling world water chemistry. *Science* **170**, 1088-1090.

Gibson, D., Tan, K., and Wilford, J., 2002. Sedimentary Systems in the 'Bland Basin', an Upstream Extension of the Murray Basin. In: Preiss, V. P. (Ed.),*Geoscience*

2002: Expanding Horizons. Abstracts of the 16th Australian Geological Convention. Geological Society of Australia Incorporated, Adelaide, S.A. Australia.

Gibson, D. L. and Chan, R. A., 2000. CRC LEME Open File Report 147: *GILMORE Regolith Landforms*. CRC LEME, GILMORE Study Area, Central NSW.

Giesler, R., Morth, C. M., Mellqvist, E., and Torssander, P., 2005. The humus layer determines SO4 isotope values in mineral soil. *Biogeochemistry* **74**, 3-20.

Green, A. T., McDaniel, P. A., and Boll, J., 2002. Chloride Distribution as Indicators of Vadose Zone Stratigraphy in Palouse Loess Deposits. *Vadose Zone Journal* **1**, 150-157.

Guelle, W., Schulz, M., and Balkanski, Y., 2001. Influence of the source formulation on modeling the atmospheric global distribution of sea salt aerosol. *Journal of Geophysical Research* **106**, 27,509-27,524.

Gunn, R. H., 1985. Shallow Groundwaters in Weathered Volcanic, Granitic and Sedimentary Rocks in Relation to Dryland Salinity in Southern New South Wales. *Aust. J. Soil Res.* **23**, 355-71.

Gunn, R. H. and Richardson, D. P., 1979. The Nature and Possible Origins of Soluble Salts in Deeply Weathered Landscapes of Eastern Australia. *Aust. J. Soil Res.*, 197-215.

Harrington, G. A. and Herczeg, A. L., 2003. The importance of silicated weathering of a sedimentary aquifer in arid Central Australia indicated by very high 87Sr/86Sr ratios. *Chemical Geology* **199**, 281-292.

Hem, J. D., 1992. *U.S. Geological Survey Water-Supply Paper 2254: Study and Interpretation of the Chemical Characteristics of Natual Water*. United States Government Printing Office, Washington, DC.

Hendry, M. J., Kelln, C. J., Wassenaar, L. I., and Shaw, J., 2004. Characterizing the hydrogeology of a complex clay-rich aquitard system using detailed vertical profiles of stable isotopes of water. *Journal of Hydrology* **293**, 47-56.

Hendry, M. J. and Schwartz, F. W., 1988. An alternative view on the origin of chemical and isotopic patterns in groundwater from the Milk River Aquifer in Canada. *Water Resources Research* **24**, 1747-1763.

Hendry, M. J. and Wassenaar, L. I., 1999. Implications of the distribution of δD in pore waters for groundwater flow and the timing of geologic events in a thick aquitard system. *Water Resources Research* **35**, 1751-1760.

Hendry, M. J. and Wassenaar, L. I., 2000. Controls on distribution of major ions in pore waters of a thick surficial aquitard. *Water Resources Research* **36**, 503-513.

Hendry, M. J., Wassenaar, L. I., and Kotzer, T., 2000. Chloride and chlorine isotopes (36Cl and 37Cl) as tracers of solute migration in a thick, clay-rich aquitard system. *Water Resources Research* **36**, 285-296.

Herczeg, A. L. and Edmonds, M. W., 2000. Inorganic ions as tracers. In: Cook, P. G. and Herczeg, A. L. Eds.), *Environmental tracers in subsurface hydrology*. Kluwer Academic Publishers Group, Dordrecht, The Netherlands, pp. 31-77

Herczeg, A. L., Dogramaci, S. S., and Leaney, F. W. J., 2001. Origin of dissolved salts in a large, semi-arid groundwater system: Murray Basin, Australia. *Mar. Freshwater Res.* **52**, 41-52.

Herczeg, A. L., Simpson, H. J., and Mazor, E., 1993. Transport of soluble salts in a large semiarid basin: River Murray, Australia. *Journal of Hydrology* **144**, 59-84.

Herczeg, A. L., Torgersen, T., Chivas, A. R., and Habermehl, M. A., 1991. Geochemistry of ground waters from the Great Artesian Basin, Australia. *Journal of Hydrology* **126**, 225-245.

Hingston, F. J. and Gailitis, V., 1976. The Geographic Variation of Salt Precipitated over Western Australia. *Aust. J. Soil Res.* **14**, 319-335.

Jacobson, G., Cresswell, R., Wischusen, J., and Fifield, K., 1998. Arid-zone groundwater recharge and palaeorecharge: insight from the radioisotope chlorine-36. *AGSO Research Newsletter* **29**.

Jobaggy, E. G. and Jackson, R. B., 2001. The distribution of soil nutrients with depth: Global patterns and the imprint of plants. *Biogeochemistry* **53**, 51-77.

Johnson, D. W., 1984. Sulfur cycling in forests. *Biogeochemistry* **1**, 29-43.

Johnston, C. D., 1981. Salt Content of Soil Profiles in Bauxite Mining Areas of the Darling Range, Western Australia. *CSIRO Australian Division of Land Resources Management. Technical Paper.* **8**, 1-25.

Johnston, C. D., 1987a. Distribution of Environmental Chloride in Relation to Subsurface Hydrology. *Journal of Hydrology* **94**, 67-88.

Johnston, C. D., 1987b. Preferred Water Flow and Localised Recharge in a Variable Regolith. *Journal of Hydrology* **94**, 129-142.

Johnston, C. D., Hurle, D. H., Hudson, D. R., and Height, M. I., 1983. Water Movement through Preferred Paths in Lateritic Profiles of the Darling Plateau, Western Australia. *CSIRO Australian Division of Land Resources Management. Technical Paper.* **1**, 1-34.

Johnston, C. D. and McArthur, W. M., 1981. Subsurface Salinity in Relation to Weathering Depth and Landform in the Eastern Part of the Murray River Catchment Area, Western Australia. *CSIRO Australian Division of Land Resources Management. Technical Paper.* **10**, 1-19.

Johnston, C. D., McArthur, W. M., and Peck, A. J., 1980. Distribution of Soluble Salts in Soils of the Manjimup Woodchip Licence Area, Western Australia. *CSIRO Australian Division of Land Resources Management. Technical Paper.*, 1-29.

Jolly, I. D., Dowling, T. I., Zhang, L., Williamson, D. R., and Walker, G. R., 1997. Water and salt balances of the Murray-Darling Basin. In: Water, C. L. a. (Ed.).

Jolly, I. D., Williamson, D. R., Gilfedder, M., Walker, G. R., Morton, R., Robinson, G., Jones, H., Zhang, L., Dowling, T. I., Dyce, P., Nathan, R. J., Nandakumar, N., Clarke, R., and McNeill, V., 2001. Historical stream salinity trends and catchment salt balances in the Murray-Darling Basin, Australia. *Marine and Freshwater Research* **52**, 53-63.

Jones, B. F., Hanor, J. S., and Evans, W. R., 1994. Sources of dissolved salts in the central Murray Basin, Australia. *Chemical Geology* **111**, 135-154.

Keywood, M. D., Chivas, A. R., Fifield, L. K., Cresswell, R. G., and Ayers, G. P., 1997. The accession of chloride to the western half of the Australian continent. *Aust. J. Soil Res.* **35**, 1177-1189.

Keywood, M. D., Fifield, L. K., Chivas, A. R., and Cresswell, R. G., 1998. Fallout of chlorine 36 to the Earth's surface in the southern hemisphere. *Journal of Geophysical Research* **103**, 8281-8286.

Kreitler, C. W. and Jones, D. C., 1975. Natural Soil Nitrate: The cause of contamination of groundwater in Runnels County, Texas. *Ground Water* **13**, 53-61.

Lal, D. and Peters, B., 1967. Cosmic Ray Produced Radioactivity on the Earth. In: Sitte, K. (Ed.), *Handbuch der Physick.* Springer-Verlag, New York.

Lawrie, K. C., Munday, T. J., Dent, D. L., Gibson, D. L., Brodie, R. C., Wilford, J., N.S. Reilly, Chan, R. A., and Baker, P., 2000. A geological systems approach to understanding the processes involved in land and water salinization. *AGSO Research Newsletter* **32**, 13-32.

Lehmann, C. M. B., Bowersox, V. C., and Larson, S. M., 2005. Spatial and temporal trends of precipitation in the United States, 1985-2002. *Environmental Pollution* **135**, 347-361.

Love, A. J., Herczeg, A. L., Armstrong, D., Stadler, F., and Mazor, E., 1993. Groundwater flow regime within the Gambier Embayment of the Otway Basin, Australia: evidence from hydraulics and hydrochemistry. *Journal of Hydrology* **143**, 297-338.

Love, A. J., Herczeg, A. L., Sampson, L., Cresswell, R. G., and Fifield, L. K., 2000. Sources of chloride and implications for 36Cl dating of old groundwater, southwestern Great Artesian Basin, Australia. *Water Resources Research* **36**, 1561-1574.

Lundstrom, U. and Olin, A., 1986. Bromide concentrations in Swedish precipitation, surface and ground waters. *Water Resources Research* **20**, 751-756.

Macumber, P. G., 1969. Interrelationship between physiography, hydrology, sedimentation, and salinization of the Loddon River Plains, Australia. *Journal of Hydrology* **7**, 39-57.

Mano, S. and Andreau, M. O., 1994. Emission of methyl bromide from biomass burning. *Science* **263**, 1255-1257.

Martin, H. A., 1991. Tertiary stratigraphic palynology and palaeoclimate of the inland river systems in New South Wales. *Geological Society of Australia Special Publication* **18**, 181-194.

Mayer, B., Feger, K. H., Giesemann, A., and H.J., J., 1995a. Interpretation of sulfur cycling in two catchments in the Black Forest (Germany) using stable sulfur and oxygen isotope data. *Biogeochemistry* **30**, 31-58.

Mayer, B., Fritz, P., Prietzel, J., and Krouse, H. R., 1995b. The use of stable sulfur and oxygen ratios for interpreting the mobility of sulfate in aerobic forest soils. *Applied Geochemistry* **10**, 161-173.

Mayer, B., Prietzel, J., and Krouse, H. R., 2001. The influence of sulfur deposition rates on sulfate retention patterns and mechanisms in aerated forest soils. *Applied Geochemistry* **16**, 1003-1019.

Mazor, E. and George, R., 1992. Marine airborne salts applied to trace evapotranspiration, local recharge and lateral groundwater flow in Western Australia. *Journal of Hydrology* **139**, 63-77.

McGill, W. B. and Cole, C. V., 1981. Comparative aspects of cycling organic C, N, S, P through soil organic matter. *Geoderma* **26**, 267-286.

Milton, G. M., Kramer, S. J., Kotzer, T. G., Milton, J. C. D., Andrews, H. R., Chant, L. A., Cornett, R. J., Davies, W. G., Greiner, B. F., Imahori, Y., Koslowsky, V. T., and Mckay, J. W., 1997. Cl36 - A potential paleodating tool. *Nuclear Instruments and Methods in Physics Research*, 371-377.

Milton, G. M., Milton, J. C. D., Schiff, S., Cook, P., Kotzer, T. G., and Cecil, L. D., 2003. Evidence for chlorine recycling-hydrosphere, biosphere, atmosphere-in a forested wet zone on the Canadian Shield. *Applied Geochemistry* **18**, 1027-1042.

Nativ, R., Adar, E., Dahan, O., and Nissim, I., 1997. Water salinization in arid regions-observations from the Negev desert, Israel. *Journal of Hydrology* **196**, 271-296.

Novak, M., Buzek, F., Harrision, A. F., Prechova, E., Jackova, I., and Fottova, D., 2003. Similarity between C, N and S stable isotope profiles in European spruce forest soils: implications for the use of 34S as a tracer. *Applied Geochemistry* **18**, 765-779.

Ortega-Guerrero, A., Cherry, J. A., and Aravena, R., 1997. Origin of pore water and salinity in the lacustrine aquitard overlying the regional aquifer of Mexico City. *Journal of Hydrology* **197**, 47-69.

Ozanne, P. G., 1958. Chlorine deficiency in Soils. *Nature* **182**, 1172-1173.

Peck, A. J., 1978. Salinization of non-irrigated soils and associated streams: A review. *Aust. J. Soil Res.* **16**, 157-168.

Peck, A. J. and Hatton, T., 2003. Salinity and the discharge of salts from catchments in Australia. *Journal of Hydrology* **272**, 191-202.

Peck, A. J. and Hurle, D. H., 1973. Chloride Balance of Some Farmed and Forested Catchments in Southwestern Australia. *Water Resources Research* **9**, 648-657.

Peck, A. J., Johnston, C. D., and Williamson, D. R., 1981. Analyses of Solute Distributions in Deeply Weathered Soils. *Agricultural Water Movement* **4**, 83-102.

Phillips, F. M., 1994. Environmental tracers for water movement in desert soils of the American Southwest. *Soil Sci. Soc. Am. J.* **58**, 15-23.

Phillips, F. M., Bentley, H. W., Davis, S. N., Elmore, D., and Swanick, G., 1986. Chlorine-36 dating of very old groundwater, 2. Milk River aquifer, Alberta, Canada. *Water Resources Research* **22**, 2003-2016.

Phillips, G. N., Hughes, M. J., and Lawrie, K. C., 2002. Victoria Undercover 2002, and the Victorian Geotraverse. In: Phillips, G. N. and Ely, K. S. Eds.)*Victoria undercover: Benalla 2002 Conference proceedings and field guide: collaborative geoscience in northern Victoria*. CSIRO Publishing, Benalla.

Reeves, C. E. and Penkett, S. A., 1993. An estimate of the anthropogenic contribution to atmospheric methyl bromide. *Geophysical Research Letters* **20**, 1563-1566.

Salama, R. B., Farrington, P., Bartle, G. A., and Watson, G. D., 1993. The chemical evolution of groundwater in a first-order catchment and the process of salt accumulation in the soil profile. *Journal of Hydrology* **143**, 233-258.

Salama, R. B., Otto, C. J., and Fitzpatrick, R. W., 1999. Contributions of groundwater conditions to soil and water salinization. *Hydrogeology Journal* **7**, 46-64.

Sander, R., Keene, W. C., Pszenny, A. A. P., Arimoto, R., Ayers, G. P., Babuokas, E., Cainey, J. M., Crutzen, P. J., Duce, R. A., Honninger, G., Huebert, B. J., Maenhaut, W., Mihalopoulos, N., Turekian, V. C., and Van Dingenen, R., 2003. Inorganic bromine in the marine boundary layer: a critical review. *Atmospheric Chemistry and Physics* **3**, 1301-1336.

Scanlon, B. R., 1991. Evaluation of moisture flux from chloride data in desert soils. *Journal of Hydrology* **128**, 137-156.

Schlesinger, W. H. and Pilmanis, A. M., 1998. Plant-soil interactions in deserts. *Biogeochemistry* **42**, 169-187.

Schlesinger, W. H., Raikes, J. A., Hartley, A. E., and Cross, A. F., 1996. On the spatial pattern of soil nutrients in desert ecosystems. *Ecology* **77**, 364-374.

Schmalz, B. L. and Polzer, W. L., 1969. Tritiated water distribution in unsaturated soils. *Soil Science* **108**, 43-47.

Seaman, J. C., Bertsch, P. M., Korom, S. F., and Miller, W. P., 1996. Physiochemical Controls on Nonconservative Anion Migration in Coarse-Textured Alluvial Sediments. *Ground Water* **34**, 778-783.

Seymour, M. D. and Stout, T., 1983. Observations on the chemical compoition of rain using short sampling timesduring a single event. *Atmospheric Environment* **17**, 1483-1487.

Shorter, J. H., Kolb, C. E., Crill, P. M., Kerwin, R. A., Talbot, R. W., Hines, M. E., and Harriss, R. C., 1995. Rapid degradation of atmospheric methyl bromide in soils. *Letters to Nature* **377**, 717-719.

Shouakar-Stash, O., Frape, S. K., Rostron, B. J., and Drimmie, R. J., 2006. Variation of the 81Br and 37Cl stable isotope signature for pre-Mississippian formation waters of Williston Basin*Goldschmidt*. Geochimica et Cosmochimica, Melbourne.

Simpson, H. J. and Herczeg, A. L., 1991. Salinity and Evaporation in the River Murray Basin, Australia. *Journal of Hydrology* **124**, 1-27.

Simpson, H. J. and Herczeg, A. L., 1994. Delivery of marine chloride in precipitation and removal by rivers in the Murray-Darling Basin, Australia. *Journal of Hydrology* **154**, 323-350.

Starr, B. J., 1999. *Soil erosion, phosphorus and dryland salinity in the upper Murrumbidgee : past change & current findings*. New South Wales: Upper Murrumbidgee Catchment Coordinating Committee, 1999.

Stotler, R. L., Frape, S. K., Shouakar-Stash, O., Ruskeeniemi, T., and Blomqvist, R., 2006. Methane-halide reactions in shield waters, inferred from 13C and 2H of methane and 81Br and 37Cl of dissolved ions*Goldschmidt*. Geochimica et Cosmochimica, Melbourne.

Tan, K. P., Kirste, D., Cresswell, R., Jones, G., and Gibson, D. L., 2002. Investigation into the association of groundwater chemistry and lithology from a bore-hole in the GILMORE project area, central New South Wales. In: Phillips, G. N. and Ely, K. S. Eds.)*Victoria undercover: Benalla 2002 Conference proceedings and field guide: collaborative geoscience in northern Victoria*. CSIRO Publishing, Benalla, Victoria.

Thompson, J. F. H., Lessman, J., and Thompson, A. J. B., 1986. The Temora Gold-Silver Deposit: A Newly recognized Style of High Sulfur Mineralization in the Lower Paleozoic of Australia. *Economic Geology* **81**, 732-738.

Timms, W., Acworth, R. I., and Jankowski, J., 2001. Quantifying leakage and mixing in an alluvial aquifer system: combined hydrochemical and hydrodynamic modelling approach constrained by isotopic evidence. In: Wohnlich, S. (Ed.),*XXXI International Association of Hydrogeologists Congress*. A.A. Balkema Publishers, Munich, Germany.

Torgersen, T., Habermehl, M. A., Phillips, F. M., Elmore, D., Kubik, P., Jones, B. G., Hemmick, T., and Gove, H. E., 1991. Chlorine 36 Dating of Very Old Groundwater 3. Further Studies in the Great Artesian Basin. *Water Resources Research* **27**, 3201-3213.

Turner, J. V., Arad, A., and Johnston, C. D., 1987. Environmental Isotope Hydrology of Salinized Experimental Catchments. *Journal of Hydrology* **94**, 89-107.

Turner, J. V., Waite, T. D., and Bradd, J. M., 1991. The Conjunctive Use of Isotope Techniques to Elucidate Solute Concentration and Flow Processes in Dryland Salinized Catchments*International Hydrology & Water Resources Symposium*, Perth, Australia.

Tyler, S. W. and Walker, G. B., 1994. Root zone effects on tracer migration in arid zones. *Soil Sci. Soc. Am. J.* **58**, 25-29.

Tyler, S. W., Chapman, J. B., Conrad, S. H., Hammermeister, D. P., Blout, D. O., Miller, J. J., Sully, M. J., and Ginanni, J. M., 1996. Soil-water flux in the

southern Great Basin, United States: Temporal and spatial variations over the last 120,000 years. *Water Resources Research* **32**, 1481-1499.

Ullman, W. J., 1985. Evaporation rate from a salt pan: estimates from chemical profiles in near-surface groundwater. *Journal of Hydrology* **79**, 365-373.

Ullman, W. J., 1995. The fate and accumulation of bromide during playa salt deposition: An example from Lake Frome, South Australia. *Geochemica et Cosmochemica Acta* **59**, 2175-2186.

Walker, G. B., Jolly, I. D., Stadter, M. H., Leaney, F. W., Davie, R. F., Fifield, L. K., Ophel, T. R., and Bird, J. R., 1992. Evaluation of the Use of 36Cl in Recharge Studies. In: IAEA (Ed.),*Isotope Techniques in Water Resource Development 1991: Proceedings of an International Symposium on Isotope Techniques in Water Resource Development*. IAEA, Vienna.

Walvoord, M. A., Phillips, F. M., Stonestrom, D. A., Evans, R. D., Hartsough, P. C., Newman, B. D., and Striegl, R. G., 2003. A resevoir of nitrate beneath desert soils. *Science* **302**, 1021-1024.

Warburton, J. A., 1982. The chemistry of precipitation in relation to precipitation type. *Science of the total environment* **23**, 379-386.

Warren, A. Y. E., Gilligan, L. B., and Raphael, N. M., 1995. *Explanatory Notes: Cootamundra 1:250 000 Geological Sheet*. Geological Survey of New South Wales, Sydney, New South Wales.

White, A. F., Schulz, M. S., Vivit, D. V., Blum, A. E., and Stonestrom, D. A., 2006. Controls of soil water solutes: An approach for distinguishing between biogenic and lithogenic processes. *Journal of Geochemical Exploration* **88**, 363-366.

Wilford, J., Gibson, D. L., Lawrie, K. C., and Tan, K. P., 2002. Extending regolith-landform maps into the third dimension - unravelling the palaeogeography story for mineral exploration and environmental applications. In: Ely, G. N. P. a. K. S. (Ed.),*Victoria undercover: Benalla 2002 Conference proceedings and field guide: collaborative geoscience in northern Victoria*. CSIRO Publishing, Benalla.

Williamson, W. H., 1986. Investigation of the groundwater resources of the Lachlan Valley alluvium. Part 1: Cowra to Jemalong Weir. Water Resources Commission of New South Wales.

Wood, W. W., 1999. Use and Misuse of the Chloride-Mass Balance Method in Estimating Ground Water Recharge. *Ground Water* **37**, 2-3.

Wood, W. W., Kraemer, T. F., and Hearn, P. P., 1990. Intragranular Diffusion: An important Mechanism Influencing Solute Transport in Clastic Aquifers. *Science* **247**, 1569-1572.

Wormald, R. J. and Price, R. C., 1988. Peralkaline granites near Temora, southern New South Wales: Tectonic and petrological implications. *Australian Journal of Earth Sciences* **35**, 209-221.

Yaalon, D. H., 1965. Downward movement and distributions of anions in soil profiles with limited wetting. In: Hallsworth, E. G. and Crawford, D. V. Eds.), *Experimental Pedology*. Butterworths, London.

Zhu, C., Winterle, J. R., and Love, E. I., 2003. Late Pleistocene and Holocene groundwater recharge from the chloride mass balance method and chlorine-36 data. *Water Resources Research* **39**, 1-15.

Zimmerman, U., Ehhalt, D., and Munnich, K. O., 1967. Soil water movement and evapotranspiration: changes in the isotopic composition of the water*Isotopes in Hydrology*. International Atomic Energy Agency, Vienna.

Zinke, P. J., 1962. The pattern of influence of individual forest trees on soil properties. *Ecology* **43**, 130-133.

APPENDIX 1: CHAPTER 4 RESULTS

Results of laser grain size analyses, moisture contents, and major element composition of soil pore water samples from four locations in Barmedman Creek catchment, central New South Wales, Australia. Results are discussed in Chapter 4. Depths reported in metres below ground surface. Raw data of element concentrations are reported in mg/l. Element data are accurate to 3 significant figures. Moisture content reported as percent water lost at 110° C from wet soil.

Sample ID	Depth	%Moisture	%Clay	%Silt	%Sand	Cl	Br	F	NO_3	PO_4	SO_4	Si	Ca	Mg	Na	K
GDH03	0.01	29	40.0	28.0	32.0	49.81	0.22	0.11	2815.86	4.88	228.80	49.67	914.82	185.66	52.35	91.78
GDH03	0.03	15	nm	nm	nm	47.52	0.04	0.48	2729.04	bd	131.74	46.05	691.78	157.12	56.33	66.63
GDH03	0.05	11	9.8	50.7	39.5	51.78	0.04	0.52	3036.03	bd	84.63	59.38	691.67	162.29	36.33	48.34
GDH03	0.07	8	9.2	43.0	47.8	52.69	0.18	0.47	2744.59	0.06	72.97	74.36	598.57	162.64	4.96	27.31
GDH03	0.09	7	6.4	40.9	52.7	66.67	0.19	1.03	2365.66	0.00	122.12	60.48	437.25	118.39	128.44	45.92
GDH03	0.11	7	nm	nm	nm	71.68	0.39	1.52	2242.59	0.17	142.41	83.71	309.32	132.16	156.75	45.40
GDH03	0.14	7	nm	nm	nm	94.07	0.47	1.41	1176.00	1.41	104.25	93.21	81.49	90.77	154.30	49.43
GDH03	0.17	6	9.8	45.4	44.7	95.61	0.43	1.33	842.92	bd	66.27	82.02	48.36	63.83	143.97	52.99
GDH03	0.20	7	6.2	38.1	55.7	106.13	0.48	1.05	645.23	0.03	55.38	68.31	28.20	56.68	134.76	51.64
GDH03	0.23	7	nm	nm	nm	119.46	0.48	0.83	517.85	bd	41.31	55.67	22.62	52.35	126.15	49.68
GDH03	0.25	7	nm	nm	nm	130.30	0.52	1.00	450.73	0.03	35.99	39.07	14.22	48.06	123.64	36.69
GDH03	0.27	7	nm	nm	nm	134.93	0.47	1.04	422.70	bd	42.72	37.63	12.53	45.06	145.06	32.70
GDH03	0.29	7	nm	nm	nm	159.66	0.56	1.29	395.35	bd	30.03	39.52	10.06	40.32	162.48	27.27
GDH03	0.32	7	nm	nm	nm	240.73	0.82	0.74	351.46	0.04	52.86	60.22	10.74	26.38	258.79	17.97
GDH03	0.35	10	8.0	43.5	48.5	303.69	1.14	1.45	326.53	0.05	120.79	73.23	18.58	32.33	252.70	20.31
GDH03	0.40	11	nm	nm	nm	555.52	1.74	1.34	300.80	0.07	97.19	53.50	26.46	43.05	466.95	26.35
GDH03	0.45	13	nm	nm	nm	434.76	2.49	bd	159.55	0.05	16.58	42.07	14.40	30.70	242.30	6.49
GDH03	0.50	13	nm	nm	nm	548.11	4.03	bd	107.04	0.05	29.84	33.28	14.04	42.34	260.53	4.83
GDH03	0.55	12	nm	nm	nm	693.99	5.51	bd	81.65	0.06	57.50	24.66	23.06	53.94	322.09	6.31
GDH03	0.60	11	14.0	47.1	38.9	759.03	4.20	7.48	12407.15	bd	1196.92	720.62	1517.05	971.63	1415.44	357.32
GDH03	0.70	10	nm	nm	nm	1005.38	8.72	0.00	81.85	bd	95.95	47.14	50.85	89.83	424.94	10.32
GDH03	0.80	8	nm	nm	nm	nm	nm	nm	nm	nm	nm	nm	nm	nm	nm	nm
GDH03	0.90	5	nm	nm	nm	nm	nm	nm	nm	nm	nm	nm	nm	nm	nm	nm
GDH03	1.00	6	12.2	45.4	42.5	1430.44	8.13	0.64	780.07	0.11	97.28	nm	nm	nm	nm	nm
GDH03	1.15	5	nm	nm	nm	nm	nm	nm	nm	nm	nm	nm	nm	nm	nm	nm
GDH03	1.30	5	nm	nm	nm	nm	nm	nm	nm	nm	nm	nm	nm	nm	nm	nm
GDH03	1.50	7	13.4	50.4	36.2	2351.02	10.43	1.07	558.93	0.13	100.73	nm	nm	nm	nm	nm
GDH03	1.60	11	nm	nm	nm	nm	nm	nm	nm	nm	nm	nm	nm	nm	nm	nm
GDH03	1.75	12	nm	nm	nm	nm	nm	nm	nm	nm	nm	nm	nm	nm	nm	nm
GDH03	1.90	14	nm	nm	nm	6568.05	20.00	0.45	33.63	0.00	208.15	28.58	535.60	718.84	2135.48	34.48
GDH03	2.05	9	nm	nm	nm	3780.00	16.80	bd	624.00	bd	533.00	13.10	77.50	318.00	1790.00	36.90
GDH03	2.25	nm	15.0	49.3	35.7	nm	nm	nm	nm	nm	nm	nm	nm	nm	nm	nm
GDH03	2.50	nm	16.4	54.6	29.1	4348.74	17.06	1.61	83.67	0.23	172.42	nm	nm	nm	nm	nm
GDH03	2.75	nm	7.8	38.7	53.5	nm	nm	nm	nm	nm	nm	nm	nm	nm	nm	nm
GDH03	3.00	13.1	14.0	53.5	32.4	2440.00	12.30	bd	100.00	bd	537.00	nm	nm	nm	nm	nm
GDH03	3.25	nm	10.1	62.7	27.2	nm	nm	nm	nm	nm	nm	nm	nm	nm	nm	nm
GDH03	3.50	nm	20.5	72.0	7.5	nm	nm	nm	nm	nm	nm	nm	nm	nm	nm	nm
GDH03	3.75	nm	17.3	66.5	16.1	nm	nm	nm	nm	nm	nm	nm	nm	nm	nm	nm
GDH03	4.00	nm	18.7	59.2	22.0	nm	nm	nm	nm	nm	nm	nm	nm	nm	nm	nm
GDH03	4.25	14.5	17.9	51.4	30.7	2430.00	11.40	bd	93.00	bd	431.00	nm	nm	nm	nm	nm
GDH03	4.50	nm	16.8	46.5	36.7	nm	nm	nm	nm	nm	nm	nm	nm	nm	nm	nm
GDH03	4.80	13	13.9	38.9	47.2	2150.00	10.30	bd	41.50	bd	427.00	nm	nm	nm	nm	nm
GDH03	5.00	nm	7.5	25.1	67.5	nm	nm	nm	nm	nm	nm	nm	nm	nm	nm	nm
GDH03	5.25	nm	17.2	55.5	27.2	nm	nm	nm	nm	nm	nm	nm	nm	nm	nm	nm
GDH03	5.50	nm	18.1	67.1	14.8	nm	nm	nm	nm	nm	nm	nm	nm	nm	nm	nm
GDH03	6.00	nm	15.1	56.7	28.2	nm	nm	nm	nm	nm	nm	nm	nm	nm	nm	nm
GDH03	6.40	15.6	15.9	46.3	37.8	5090.00	17.90	bd	32.00	bd	1020.00	32.50	41.70	407.00	3210.00	13.50
GDH03	7.00	nm	12.2	54.1	33.6	nm	nm	nm	nm	nm	nm	nm	nm	nm	nm	nm
GDH03	7.40	14.9	7.0	45.5	47.4	6010.00	18.90	bd	5.00	bd	997.00	24.40	60.10	538.00	3670.00	32.60
GDH03	8.00	13.6	8.9	40.3	50.8	6760.00	23.60	bd	0.00	bd	1340.00	35.70	63.00	453.00	3920.00	11.70
GDH03	8.65	14.3	6.4	49.9	43.6	5090.00	16.90	bd	0.00	bd	892.00	13.80	50.00	285.00	3280.00	9.92
GDH03	8.80	nm	nm	nm	nm	3740.00	11.90	bd	4.80	bd	544.00	12.70	41.50	266.00	2580.00	12.00
GDH03	9.00	nm	6.7	30.9	62.4	nm	nm	nm	nm	nm	nm	nm	nm	nm	nm	nm
GDH04	0.01	12.50	21.1	44.4	34.5	438.99	0.56	0.29	2896.84	0.09	81.34	64.00	590.80	293.11	290.87	116.30
GDH04	0.03	13.01	14.5	53.4	32.1	470.80	0.85	0.07	2454.49	bd	55.15	49.61	444.89	254.35	261.78	80.67
GDH04	0.05	14.71	nm	nm	nm	482.12	1.23	0.09	2244.51	2.60	60.76	43.69	374.99	252.19	218.88	52.45
GDH04	0.07	15.99	18.8	44.3	36.9	502.29	1.54	0.06	2007.90	bd	63.42	33.79	296.55	261.81	215.20	23.96
GDH04	0.09	17.50	19.7	45.4	34.9	532.25	1.79	bd	1798.67	0.16	75.97	25.96	262.35	239.07	245.73	26.89
GDH04	0.11	18.24	nm	nm	nm	557.38	1.88	0.10	1605.17	bd	87.04	21.75	245.37	237.02	252.31	16.02
GDH04	0.13	17.22	22.6	41.7	35.7	599.64	2.34	0.13	1506.79	0.13	95.91	18.52	240.34	221.46	259.04	17.10
GDH04	0.15	17.90	nm	nm	nm	657.17	2.68	0.15	1455.10	0.15	101.14	17.88	249.55	222.11	310.80	27.31
GDH04	0.17	16.56	nm	nm	nm	734.37	3.18	bd	1386.09	0.20	105.11	15.40	242.78	232.31	280.38	14.37
GDH04	0.19	17.48	nm	nm	nm	1837.77	7.51	bd	1055.75	0.27	109.65	11.92	372.22	339.32	496.16	25.60
GDH04	0.21	18.22	21.8	51.7	26.4	3749.57	15.45	bd	622.70	0.26	103.96	9.21	526.55	497.61	1056.71	30.57
GDH04	0.23	16.54	nm	nm	nm	4008.55	16.52	bd	633.44	bd	326.68	8.11	534.10	526.26	1110.90	25.94
GDH04	0.25	16.93	nm	nm	nm	4228.93	16.97	0.25	644.29	0.25	147.40	7.19	537.87	571.89	1175.18	19.65
GDH04	0.27	17.16	nm	nm	nm	4327.05	17.71	bd	634.58	0.51	178.41	8.13	552.66	590.09	1238.53	28.18
GDH04	0.29	17.16	nm	nm	nm	4587.37	18.24	bd	640.99	0.27	214.21	7.94	546.03	621.69	1332.23	26.95
GDH04	0.35	16.29	16.8	60.3	22.8	5492.12	22.04	0.62	676.39	0.31	410.36	7.51	545.61	793.26	1807.72	23.44
GDH04	0.40	16.61	nm	nm	nm	8151.07	30.35	0.37	104.58	0.37	807.72	6.88	634.22	1137.03	2556.99	13.16
GDH04	0.45	14.96	nm	nm	nm	8723.35	32.84	0.77	100.06	0.39	1071.63	6.44	659.32	1293.53	2585.40	12.32
GDH04	0.50	13.71	13.9	64.6	21.4	9323.19	34.18	0.79	87.85	0.40	1332.79	6.44	677.53	1420.92	2731.93	9.21
GDH04	0.55	14.09	nm	nm	nm	9864.31	36.16	1.26	75.26	0.42	1498.57	6.05	675.36	1412.83	3173.69	14.55
GDH04	0.60	12.53	14.8	56.0	29.2	10121.60	37.49	0.86	56.88	1.29	1653.90	7.00	673.71	1561.46	3172.52	10.18
GDH04	0.74	13.84	nm	nm	nm	9951.45	35.98	0.85	30.48	0.42	2002.31	8.54	619.02	1522.65	3293.65	15.52
GDH04	0.80	13.76	11.1	71.6	17.3	10429.27	38.03	0.87	24.92	0.44	2119.60	9.70	632.47	1508.29	3492.68	34.98
GDH04	0.90	13.79	nm	nm	nm	9944.57	35.52	1.33	27.97	0.44	2119.44	7.72	618.25	1507.62	3676.38	11.02
GDH04	1.00	14.75	8.5	64.0	27.5	9492.83	33.57	0.90	23.72	bd	2149.51	9.13	583.35	1433.93	3655.50	12.98
GDH04	1.15	13.54	nm	nm	nm	9555.50	31.78	0.90	24.17	0.45	2200.98	10.15	593.51	1522.83	3605.95	16.43
GDH04	1.30	13.94	nm	nm	nm	9681.34	33.52	0.91	15.40	0.45	2130.87	9.28	568.10	1409.39	3689.12	12.92
GDH04	1.45	13.25	16.6	52.0	31.4	10388.44	35.48	0.91	20.92	0.45	2223.88	16.00	582.97	1479.62	4601.06	21.71
GDH04	1.60	12.35	nm	nm	nm	9680.83	31.64	0.88	31.20	0.44	2048.22	11.46	552.55	1401.77	4048.28	27.83
GDH04	1.75	12.23	nm	nm	nm	9265.48	30.13	1.39	25.03	0.46	1994.36	11.55	505.52	1302.52	3645.47	13.83
GDH04	1.90	12.43	nm	nm	nm	9476.95	31.52	0.98	18.71	0.49	1902.98	11.55	482.08	1146.46	4058.35	24.42
GDH04	2.05	10.65	nm	nm	nm	12658.56	40.46	1.12	40.46	0.56	2553.40	17.39	723.82	1845.60	4911.09	22.19

bd = below detection limit (.01 mg/L)
nm = not measured

(Appendix 1 continued)

Sample ID	Depth	%Moisture	%Clay	%Silt	%Sand	Cl	Br	F	NO_3	PO_4	SO_4	Si	Ca	Mg	Na	K
GDH04	2.20	11.00	14.4	61.8	23.8	10672.34	35.37	bd	8.84	bd	2019.13	21.41	503.43	1221.81	4645.02	42.82
GDH04	2.40	7.95	6.0	66.0	28.0	10557.84	32.46	0.98	9.34	0.98	1842.43	40.49	468.52	1192.71	4366.95	36.24
GDH04	2.75	nm	5.1	49.0	46.0	nm	nm	nm	nm	nm	nm	nm	nm	nm	nm	nm
GDH04	3.00	nm	10.4	40.3	49.3	8510.00	29.50	bd	73.50	bd	2400.00	42.90	259.00	1070.00	4060.00	17.52
GDH04	3.50	nm	15.7	42.7	41.6	7730.00	26.40	bd	71.00	bd	2110.00	54.90	221.00	1090.00	3320.00	8.61
GDH04	4.00	nm	28.7	49.6	21.7	7220.00	22.20	bd	62.20	bd	2090.00	54.00	184.00	917.00	3170.00	5.62
GDH04	4.50	nm	29.7	43.7	26.6	6300.00	17.70	bd	54.80	bd	1440.00	39.05	128.00	568.00	3330.00	11.05
GDH04	5.00	nm	10.6	59.5	29.8	6920.00	19.50	bd	56.90	bd	1520.00	34.19	134.00	611.00	3330.00	15.04
GDH04	5.50	nm	5.3	53.4	41.2	8680.00	25.80	bd	50.10	bd	1710.00	46.61	175.00	848.00	4290.00	16.21
GDH04	6.00	nm	5.3	45.6	49.2	8710.00	24.30	bd	41.30	bd	1910.00	35.60	202.00	746.00	4470.00	19.30
GDH04	6.10	nm	nm	nm	nm	7510.00	24.30	bd	8.99	bd	1600.00	35.30	164.00	590.00	3890.00	20.99
GDH04	7.00	nm	4.6	47.4	48.0	11900.00	34.60	bd	bd	bd	2820.00	48.90	324.00	1280.00	5800.00	24.20
GDH04	7.60	nm	28.6	48.9	22.5	9850.00	27.60	bd	2.90	bd	2610.00	49.30	259.00	1090.00	4850.00	15.10
GDH04	8.00	nm	25.4	67.0	7.6	11800.00	27.40	bd	bd	bd	3170.00	47.60	373.00	1550.00	5620.00	16.40
GDH04	8.50	nm	34.4	54.6	11.1	13300.00	30.90	bd	bd	bd	3560.00	44.80	387.00	1620.00	5750.00	18.20
GDH04	9.00	nm	46.5	35.2	18.2	13400.00	34.20	bd	bd	bd	3940.00	35.80	447.00	1750.00	6010.00	13.20
BGMR	0.01	20.03	9.5	74.9	15.6	110.84	0.18	0.02	1452.43	bd	19.61	35.37	341.43	90.83	28.89	79.18
BGMR	0.03	15.08	12.0	74.2	13.8	116.25	0.26	0.05	1383.98	bd	14.05	31.17	325.35	92.09	31.03	78.52
BGMR	0.05	13.38	12.4	68.7	18.9	136.68	0.46	0.07	1231.27	bd	8.76	25.76	280.53	84.77	36.64	73.22
BGMR	0.07	12.29	6.2	75.0	18.8	161.37	0.64	0.03	1070.37	bd	3.69	21.94	233.62	78.30	51.39	68.24
BGMR	0.09	12.26	nm	nm	nm	191.18	0.83	0.03	904.41	bd	2.13	18.49	196.12	69.21	66.66	60.00
BGMR	0.11	12.85	10.2	69.3	20.6	229.77	1.03	0.03	750.46	bd	1.38	15.42	164.65	59.55	88.56	53.87
BGMR	0.13	13.36	nm	nm	nm	325.13	1.52	0.03	498.58	0.06	1.43	14.32	135.00	47.86	121.09	44.64
BGMR	0.15	12.15	10.8	71.4	17.9	360.15	1.69	0.09	434.51	0.03	1.41	13.46	121.92	41.50	141.67	39.02
BGMR	0.17	11.73	nm	nm	nm	426.10	2.01	0.03	343.82	bd	2.30	14.12	99.68	35.66	197.59	33.80
BGMR	0.19	12.32	9.2	71.1	19.7	523.34	2.41	0.04	293.96	bd	3.72	13.01	85.95	31.90	235.63	29.13
BGMR	0.21	10.90	nm	nm	nm	605.95	2.76	0.08	228.80	0.04	6.12	15.03	72.28	29.75	301.24	23.21
BGMR	0.23	10.20	nm	nm	nm	714.37	3.25	bd	187.77	bd	9.95	17.78	58.27	29.13	380.50	17.24
BGMR	0.25	9.07	9.3	71.0	19.7	856.89	3.89	0.06	147.96	bd	14.63	20.46	53.45	29.92	469.35	13.53
BGMR	0.27	9.44	nm	nm	nm	1015.73	4.42	0.06	125.61	bd	20.04	23.13	45.52	30.64	560.19	10.42
BGMR	0.29	9.28	8.4	69.9	21.7	1152.26	5.05	bd	123.73	bd	25.10	26.76	42.00	31.53	645.35	10.33
BGMR	0.35	14.20	10.2	65.8	24.0	1132.29	4.56	bd	21.52	bd	24.21	50.75	20.81	26.90	709.12	5.45
BGMR	0.40	19.34	16.7	60.1	23.2	1180.68	4.84	0.09	4.93	0.09	27.94	57.04	28.71	34.27	677.27	5.30
BGMR	0.45	16.75	15.5	62.7	21.8	1294.53	5.32	bd	2.23	0.12	44.28	15.79	38.83	41.59	690.32	3.21
BGMR	0.50	17.37	17.5	61.7	20.8	2631.69	11.78	bd	12.04	0.26	110.98	24.16	87.37	118.58	1401.54	4.75
BGMR	0.55	14.25	nm	nm	nm	3665.63	16.39	0.31	35.88	1.24	197.97	25.25	129.09	179.67	1959.12	5.75
BGMR	0.60	13.74	18.0	61.8	20.2	4141.12	18.43	0.65	53.99	0.32	261.89	21.54	156.89	222.50	2112.56	5.33
BGMR	0.74	13.92	nm	nm	nm	5215.59	23.61	0.37	56.95	0.37	357.45	20.09	263.44	354.81	3146.96	7.98
BGMR	0.80	11.09	17.7	66.3	16.1	8488.44	37.80	1.30	122.08	0.43	698.57	22.19	361.09	443.95	4337.32	15.18
BGMR	0.90	11.94	17.5	74.4	8.0	7517.12	34.45	0.44	40.12	bd	577.87	22.92	319.62	422.01	3739.41	10.09
BGMR	1.00	14.02	18.6	73.2	8.2	10351.74	46.91	0.51	71.89	0.51	686.27	33.37	411.03	497.99	5339.28	29.40
BGMR	1.15	13.56	19.2	74.1	6.7	8432.68	38.24	0.47	48.03	0.47	516.26	2.29	19.31	26.98	56.43	1.31
BGSF	0.01	14.94	6.2	70.7	23.1	8.85	0.17	0.02	368.20	1.59	5.07	nm	50.01	30.14	16.30	29.76
BGSF	0.03	11.60	8.3	65.6	26.1	9.81	0.06	0.14	207.36	0.47	2.41	nm	19.82	15.27	12.73	24.22
BGSF	0.05	10.44	8.9	73.6	17.5	10.15	0.00	0.13	132.51	0.36	3.33	nm	11.28	9.90	11.88	21.01
BGSF	0.08	8.74	8.5	66.8	24.7	68.21	0.14	0.20	45.89	14.83	19.76	nm	7.58	10.59	34.53	36.80
BGSF	0.12	8.66	9.9	73.0	17.1	19.06	0.04	bd	13.66	2.16	22.19	nm	4.86	3.99	17.13	16.52
BGSF	0.14	6.12	7.2	69.7	23.1	13.81	0.00	bd	13.52	0.00	31.90	nm	6.35	4.12	24.05	12.91
BGSF	0.16	7.12	nm	nm	nm	22.62	0.00	bd	19.39	0.19	46.20	nm	7.72	5.90	41.10	13.88
BGSF	0.19	7.18	7.2	67.0	25.8	28.06	0.00	bd	22.48	0.00	51.29	nm	6.84	8.25	47.04	11.87
BGSF	0.25	5.58	8.8	66.7	24.5	44.05	0.11	0.05	30.52	0.00	50.79	nm	7.82	10.80	51.51	8.33
BGSF	0.27	6.85	nm	nm	nm	66.53	0.17	0.08	32.85	0.08	49.77	nm	8.18	14.39	65.96	6.41
BGSF	0.29	6.89	nm	nm	nm	82.67	0.17	0.06	35.95	0.00	47.25	nm	7.70	16.39	72.22	4.76
BGSF	0.31	9.68	6.9	69.5	23.6	153.98	0.31	0.03	44.48	0.03	37.30	nm	9.10	23.14	100.37	6.94
BGSF	0.33	8.47	nm	nm	nm	184.85	0.31	bd	55.58	0.03	38.30	nm	5.98	24.82	124.64	3.72
BGSF	0.35	8.27	nm	nm	nm	204.51	0.50	bd	62.83	0.05	41.15	nm	5.68	23.46	146.20	3.66
BGSF	0.37	7.28	7.5	70.6	22.0	230.34	0.55	bd	71.18	0.00	46.20	nm	5.65	23.83	172.55	4.17
BGSF	0.39	7.10	nm	nm	nm	278.99	0.68	bd	81.03	0.00	58.13	nm	7.32	21.92	228.45	5.73
BGSF	0.41	4.94	9.2	67.8	23.0	373.86	0.97	bd	104.72	0.00	68.09	nm	18.12	20.82	287.64	5.92
BGSF	0.43	5.54	nm	nm	nm	685.76	1.99	bd	185.78	0.00	66.95	nm	22.31	35.29	508.47	11.18
BGSF	0.45	8.11	nm	nm	nm	790.84	2.36	bd	226.18	0.00	64.30	nm	16.53	37.61	606.89	12.80
BGSF	0.47	13.66	21.6	62.9	15.4	744.19	2.27	bd	225.25	0.09	57.28	nm	15.87	35.90	627.44	11.19
BGSF	0.49	14.46	nm	nm	nm	923.93	2.79	bd	280.50	1.10	72.07	nm	21.73	54.01	664.60	12.26
BGSF	0.51	15.84	nm	nm	nm	1094.48	3.59	bd	275.53	0.00	80.44	nm	19.29	67.37	746.29	9.09
BGSF	0.53	15.84	24.5	60.1	15.4	1247.48	4.03	bd	252.26	0.00	92.78	nm	29.20	95.89	883.24	14.63
BGSF	0.55	16.23	nm	nm	nm	1682.88	5.21	bd	270.35	0.00	117.25	nm	36.80	119.42	991.37	17.16
BGSF	0.57	16.72	33.9	55.6	10.5	1829.86	5.58	bd	225.96	0.00	120.22	nm	44.18	120.44	1077.38	19.94
BGSF	0.59	16.76	nm	nm	nm	1995.73	6.42	bd	195.75	0.00	128.47	nm	52.32	147.63	1138.86	22.15
BGSF	0.61	16.55	nm	nm	nm	2276.26	7.46	bd	160.26	0.00	138.41	nm	60.49	173.46	1286.93	23.63
BGSF	0.63	23.12	29.7	60.6	9.7	2518.55	7.65	bd	112.66	0.00	147.47	nm	72.43	209.05	1339.07	25.05
BGSF	0.65	20.24	nm	nm	nm	2590.09	7.92	bd	81.28	0.00	169.64	nm	77.67	219.55	1474.58	28.50
BGSF	0.67	18.44	nm	nm	nm	2830.73	9.14	bd	68.01	0.00	204.55	nm	82.75	231.66	1527.18	31.55
BGSF	0.69	14.79	23.8	62.9	13.3	2961.69	9.26	bd	59.47	0.00	249.93	nm	87.84	263.91	1562.19	22.45
BGSF	0.71	13.55	nm	nm	nm	2805.01	8.40	bd	59.38	0.00	267.60	nm	78.56	229.20	1589.22	22.28
BGSF	0.73	6.45	19.9	66.2	13.9	2780.21	8.75	bd	140.95	0.00	50.55	nm	195.73	269.97	1302.71	76.17
BGSF	0.75	9.39	nm	nm	nm	5062.06	14.60	bd	152.59	0.00	476.35	nm	147.11	387.37	2875.89	67.70
BGSF	0.77	6.30	15.7	70.2	14.1	3072.23	9.75	bd	48.12	0.33	365.42	nm	97.90	223.73	1752.00	32.54

bd = below detection limit (.01 mg/L)
nm = not measured